Experimental Evaluation of Surfactant Application to Improve Oil Recovery

By

Zhijun Liu

Submitted to the graduate degree program in Chemical and Petroleum Engineering and the Graduate Faculty of the University of Kansas in partial fulfillment of the requirement for the degree of Master of Science

Committee: _____

G. Paul Willhite

_____

Stan McCool

_____

Jenn-Tai Liang

Date defended: _____

Thesis Committee for Zhijun Liu certifies

that this is the approved version of the following thesis

Experimental Evaluation of Surfactant Application to Improve Oil Recovery

Committee: _____

G. Paul Willhite

_____

Stan McCool

_____

Jenn-Tai Liang

Date approved: _____

Dedication

To God and my family

ABSTRACT

The objective of this research was to identify high performance surfactant formulations and design efficient core floods for a limestone reservoir with high salinity formation brine. Microemulsion phase behavior experiments were conducted to identify best chemicals formulation (including surfactants, alcohol, alkali, polymer and electrolyte) for core flood test. A successful formulation should be one clear stable phase at reservoir conditions, fluid microemulsion phase, fast equilibration and high solubilization ratio. Formulations with glycol ether alcohols were easier to achieve one clear stable phase than formulations with sec-butanol. Primary surfactant-to-cosurfactant ratio and alcohol concentration were fine tuned to obtain fluid microemulsion phase and sufficiently high solubilization ratio. Core floods with optimized formulation validated its high oil recovery efficiency (95-99%) in Berea sandstone cores with synthetic formation brine. The effect of surfactant slug size, surfactant slug/polymer drive viscosity and formation brine composition was discussed to design more efficient core flood. The properties of the aqueous phase from chemical flood, e.g. total dissolved solids, viscosity and pH were measured to help understand oil displacement process in the core during the chemical flood. Core floods in Indiana limestone cores yielded low oil recovery (27-41%) suffering from large dispersion of the core. Recommendations were made to improve oil recovery on future limestone core floods and field application.

TABLE OF CONTENTS

LIST OF FIGURES

LIST OF TABLES

ACKNOWLEDGMENTS

I would like to express my gratitude to my advisors, Dr. G. Paul Willhite and Dr. Stan McCool for their guidance, support and encouragement throughout my graduate study at the University of Kansas. I appreciate their effort and patience for continuously challenging me to make progress during the research.

I would like to thank Dr. Jenn-Tai Liang for serving on my thesis committee and giving me insightful comments about research and course work. I would like to thank Mr. Scott Ramskill and Dr. Karen Peltier for their help on ordering and providing experimental materials, setting up equipment and troubleshooting various problems occurred during my research work.

I would like to thank my co-workers, Shahab Ahmed, Dr.Rondon Miguel, Dr. Kaixu Song for their constructive advices and friendly support. I would like to give special thanks to Kashif Naseem, Thora Whitmore and Ed Colson , who offered, assistance and collaboration with laboratory experiment and were very helpful to complete my research work.

I would like to thank the faculty and staff members of the University of Kansas Center for Research's Tertiary Oil Recovery Project (TORP), especially Dr. Jyun-Syung Tsau, Mr. Mark Ballard and Ms. Mayumi Crider. I would like to acknowledge the University of Kansas Center for Research's Tertiary Oil Recovery Project (TORP) for financial support. I would like to acknowledge TIORCO/Stepan, Sasol, Huntsman, Shell and SNF Floerger for providing surfactant and polymer samples.

Finally I want to express the deepest appreciation to my parents and my brother for their love and support.

Chapter 1 Introduction

The purpose of the research presented in this work is to identify high performance surfactant formulations for chemical enhanced oil recovery of a crude oil from a Kansas reservoir and provide guidance for future field application. Phase behavior experiments were conducted to select an effective surfactant formulation. Core floods were conducted to validate their oil recovery efficiency. In this chapter, research motivation and rationality are discussed in following sections.

1.1 Research Motivation

Currently, waterflood leaves more than half of the original oil in sandstone reservoirs, and even more in carbonate reservoirs. In order to recover the residual oil, the interfacial tension between water and oil needs to be reduced substantially to increase the capillary number to about ten thousand fold more than the capillary number of a waterflood. Surfactants could solubilize water and oil in a microemulsion phase, which could reduce interfacial tension between microemulsion and water/oil to an ultralow level. Other chemicals such as co-surfactant, co-solvent, alkali, and electrolyte are usually blended with primary surfactant to produce a clear, fluid, and stable surfactant formulation that has the highest solubilization ratio of water/oil, i.e. the lowest interfacial tension. In order to select the best surfactant formulation, a three stage method, developed by Levitt (2006), Jackson (2006) and Flaaten (2007) at the University of Texas at Austin, was adopted in my research. In the first stage, surfactants were selected based upon data and knowledge of surfactant structure, the target reservoir and crude oil properties. The second stage screens the surfactant formulations with crude oil in phase behavior experiments to evaluate phase behavior performance through solubilization ratio (which is inversely

proportional to interfacial tension), microemulsion viscosity, equilibration time, aqueous phase stability limit and optimal salinity among other characteristics. In the third stage, the surfactant formulations were tested in laboratory core flood experiments.

1.2 Research Rationality

This research was conducted for a crude oil in a limestone reservoir located in western Kansas. The reservoir has been water flooded for the last fifteen years and currently is at a stage of water flood with low oil cut. The formation brine has high salinity (121669 ppm) with moderate hardness. In order to select the right surfactant formulation, some commercially available and promising surfactants were selected based on studies of Levitt (2006), Jackson (2006) and Flaaten (2007) and tested with the crude oil. Then these surfactants were compared to and optimized with some other newly developed surfactants from other companies. After optimal surfactant formulation passes all criteria, core floods were conducted to validate the oil recovery efficiency. In order to understand the chemical flood process, soft brine with equivalent salinity to surfactant slug instead of high salinity hard formation brine was used to saturate and waterflood the core in the initial core flood experiments. Also, because chemical flooding in sandstone core is more extensively studied than in limestone, sandstone was used in initial core flood tests. Formation brine and limestone cores were used after core floods in sandstone validated the high oil recovery efficiency of the surfactant formulation to evaluate formulation performance to mimic actual reservoir conditions.

1.3 Summary of Chapters

Chapter 2 discusses background and literature information, chemical component structure and principles of chemical mixture and core flood design for EOR applications.

Chapter 3 describes the equipment, methodology and data calculations used in the phase behavior and core flood experiments in the research. Chapter 4 summarizes phase behavior screening results and the optimal formulation design process. Chapter 5 presents results of different core flood designs for a crude oil and analysis of core flood pressure data and effluent properties. Chapter 6 presents a summary and conclusion of all experimental results and proposes future work and direction for further research.

Chapter 2 Literature Review

2.1 Introduction

This chapter provides background and a literature review on the theory and methodology used in this research. It describes phase behavior screening experiments, including microemulsion characterization and its mechanism to mobilize oil, and the roles and effects of chemicals in phase behavior experiments. It then reviews the basic principles of core flood design and introduces the crude oil evaluated in this research.

2.2 Chemical Flood Oil Mobilization Mechanism

Residual oil in the reservoir is trapped by capillary forces and can be mobilized by increasing viscous forces and/or gravitational forces over capillary forces. The dimensionless terms referred to as capillary number Nc and Bond number N_B are the ratios of viscous forces to capillary forces and gravitational forces to capillary forces:

$$N_c = \frac{k \cdot \nabla\Phi}{\sigma} \quad ; \quad N_B = \frac{k \cdot g \cdot \Delta\rho}{\sigma}$$

Pope *et al.* (2000) defined the trapping number which was the combination of both capillary number and Bond number to characterize the mechanism to recover residual oil. Because we can do little to increase rock permeability (*k*), reducing interfacial tension is an effective way to increase capillary number under a normal pressure gradient ($\nabla\Phi$). Chemical flooding with surfactants could reduce interfacial tension to as low as 10^{-4} dyne/cm, which usually could increase capillary number low enough to mobilize residual oil the surfactant contacts.

Capillary number for normal water flood in sandstones are in the range of 10^{-6} to 10^{-7}. In order to mobilize the residual oil, capillary number usually needs to be increased by a factor of 100-1000 times above typical water flood (Abrams, 1975). Delshad *et al.* (1986)

showed capillary number needed to increase to be on the order of 10^{-5} before residual oil saturation will decrease for sandstone. Kamath (2001) showed that due to different pore structures and wettability, on the order of 10^{-7} was required to start mobilizing residual oil in carbonate.

2.3 Phase Behavior Screening

2.3.1 Microemulsion Characterization

Winsor (1954) described the phase behavior for the mixture of an oil/water/surfactant system. Bourrel and Schechlter (1988) described microemulsion phase as a thermodynamically stable phase under certain conditions and in theory it never separates into two phases unless conditions change. Microemulsion is different from "macroemulsion", which is thermodynamically unstable even though it may be kinetically stable. Winsor(1954) identified the three types of phase equilibria in microemulsion phase behavior as Type I, Type II and Type III. Type I microemulsion is an oil in water microemulsion with excess brine phase, also referred as Type II (-) because the phase diagram has a negative slope. Type II microemulsion is water in oil microemulsion with excess oil phase, also referred as Type II (+) as the phase diagram has positive slope. A Type III microemulsion phase exists as a distinct and bicontinuous third phase with excess oil and water phases. Type III is a transitional phase between Type I and Type II. The transition of phase behavior from Type I to Type III to Type II depends on surfactant type, electrolyte, temperature, oil properties etc. The surfactant structure could be characterized with hydrophilic-lipophilic balance (HLB), and the oil properties could be characterized by equivalent alkane carbon number (EACN), which could help to categorize the surfactants and select the right surfactants for target

reservoirs and crude oils. The most common phase behavior transition from Type I->Type III->Type II is accomplished by changing electrolytes.

2.3.2 Microemulsion and Interfacial Tension

A microemulsion can be characterized in several ways: the amount of water/oil solubilized in microemulsion, the time for microemulsion to coalesce, or microemulsion viscosity. Healy and Reed (1976) defined water/oil solubilization ratio by dividing the amount of water/oil solubilized in microemulsion by total surfactant volume (V_w/V_s, V_o/V_s). Water solubilization ratio decreases as salinity increases while oil solubilization ratio increases as salinity increases. The intersection where the water/oil solubilization ratio are equal was defined as the optimal salinity and optimal solubilization ratio. At this point, water/oil is solubilized the same amount and to the greatest degree for both the water and oil in the microemulsion phase. This happens to correspond to the lowest interfacial tension between oil/water and microemulsion. Healy and Reed also suggest a correlation between water/oil solubilization ratio and interfacial tension (IFT), which was theoretically derived by Chun Huh (1979). Chun Huh's equation shows that IFT is inversely proportional to the square of the water/oil solubilization ratio:

$$\gamma = \frac{C}{\sigma^2}$$

where C is approximately 0.3 dynes/cm for most crude oils. Interfacial tension can be reduced to 3×10^{-3} dyne/cm with solubilization ratio higher than 10. Because it is difficult and time consuming to measure the IFT between water/oil and microemulsion, by using this equation one could quickly screen out the surfactants giving low solubilization ratios. Surfactants forming complex phases, such as a liquid crystal phase and a gel phase, usually have lengthy equilibration time. It takes a very long time to

obtain stabilized solubilization ratio for these surfactants and they usually have problems in propagating in the core or reservoir, and therefore they are also screened out.

2.4 EOR Chemicals

A typical surfactant formulation usually contains primary surfactant, co-surfactant, co-solvent, alkali, polymers and electrolytes. The primary surfactant is the chemical mainly responsible for solubilizing oil in the microemulsion phase. The co-surfactant is used to improve the performance of primary surfactant (Nelson *et al*. 1984). The co-solvent is added to the surfactant formulation to reduce equilibration time and to prevent forming of the gel or crystal phases Another important role of co-solvent is to make surfactant formulation compatible with polymers (Pope *et al.* 1982) in order to maintain the surfactant slug as a stable one phase solution at reservoir conditions. Alkali could react with naphthenic components in crude oil and generate in-situ soap to improve the solubilizing of oil in the microemulsion phase. Alkali also can minimize surfactant adsorption in carbonate reservoir by changing surface charge from positive to negative. It could also accelerate microemulsion coalescence and reduce surfactant adsorption (Jackson 2006). Polymer is added to the surfactant formulations to increase its viscosity and maintain mobility control when displacing oil in reservoir. Electrolytes are adjusted to achieve optimal Type III phase to maximally reduce interfacial tension (increase capillary number) and therefore achieve high oil recovery.

2.4.1 Surfactants

Surfactants are the key components in the surfactant formulations used to solubilize oil and water in the microemulsion phase and hence reduce interfacial tension between the microemulsion and the oil/water phase. Surfactants contain a hydrophilic head, a

hydrophobic tail and possible intermediate neutral groups. The structures of surfactant head and tail could be tailored for each specific crude oil for the highest oil recovery efficiency and are discussed in the following paragraphs. Surfactants can be classified into anionic surfactants, cationic surfactants, nonionic surfactants and amphoteric surfactants according to charge of their hydrophilic head groups. Anionic and nonionic surfactants are more commonly used EOR surfactants than others, therefore they are described in following paragraphs.

2.4.1.1 Anionic surfactants

Anionic surfactants give rise to a negatively charged surfactant ion (hence anionic) and a positively charged counterion upon dissolution in water. They are the most commonly used and most promising surfactants in chemical EOR because of their excellent performance and low adsorption in rocks. Sandstone particles usually carry a net negative charge at reservoir conditions, which could prevent attracting anionic surfactants (Zhang and Hirasaki, 2004). The surface charge on carbonate rock particles is dependent on brine composition and pH (Churcher *et al*. 1991). Anionic surfactants adsorption on carbonates, however, can be reduced by increasing pH to above 8.5 to change the surface charge from positive to negative. Examples of common anionic surfactants in recent advances of chemical EOR are alkylbenzene sulfonates (ABS), alcohol ethoxy sulfates (AES), alcohol propoxy sulfates (APS), internal olefin sulfonates (IOS) and Guerbet alkoxy sulfates (GAS).

ABS surfactants were extensively used in the past. Their advantages are a high solubilization ratio of crude oil and low optimal salinity due to strong hydrophobicity from the benzene aromatic ring and alkyl chain. Their aqueous solubility, however, is low

and they tolerate only low hardness (Jackson, 2006). Therefore, they can only be injected into the formation with fresh water or low salinity brine, or used as a co-surfactant to increase the hydrophobicity with a co-solvent to improve its solubility.

IOS surfactants have proved to be excellent EOR surfactants (Levitt, 2006; Jackson, 2008; Flatten, 2008), particularly as co-surfactants that improve the compatibility between the primary surfactant and the aqueous phase through its structural heterogeneities of branched large carbon chains.

AES/APS are sulfates containing ethylene oxide (EO) or propylene oxide (PO) groups. EO and PO groups are intermediate function groups that attach to the carbon chain and have opposite effects. For example, increasing EO groups will increase surfactant aqueous solubility, calcium tolerance and optimal salinity while increasing PO groups has the reverse effect. The number of EO/PO groups determines the hydrophilicity and hydrophobicity of surfactants and they can be tailored specifically for different crude oils. This flexibility of surfactants widens the range of their application in chemical EOR.

GAS surfactants are anionic surfactants, which can be manufactured in a relatively inexpensive way that are produced by addition of ethylene oxide and/or propylene oxide to the blend of Guerbet alcohol and monomer alcohol rather than pure Guerbet alcohol. These molecules contain very large hydrophobes and branched structures which result in ultra-low interfacial tensions and low micro-emulsion viscosities (Liu *et al*. 2007), GAS can be used for crude oils with equivalent alkane carbon number higher than 12. The hydrolysis of GAS surfactants can be largely reduced at certain alkalinity range at high

temperatures, which could enhance surfactant stability, and therefore make GAS surfactants able to be used in high temperature reservoirs (Adkins, *et al*. 2010).

2.4.1.2 Nonionic surfactants

Nonionic surfactants do not ionize in aqueous solution because their hydrophilic group is of a non-dissociable type, such as alcohol, phenol, ether, ester or amide. The advantages of nonionic surfactants are that they are usually easily blended with other types of surfactants and are relatively insensitive to the salinity of the solution. A large proportion of these nonionic surfactants are alcohol ethoxylates, which are made by the polycondensation of ethylene oxide. Alcohol ethoxylates may be used as co-solvents that could replace conventional solvents in greatly diminished amounts (Sahni *et al.*, 2010). Nonionic surfactants, such as alcohol ethoxylates, however, usually have high optimal salinity and their usage is limited due to relatively low cloud point, i.e., aqueous solubility (Milton, 2004).

2.4.2 Co-solvents

Co-solvents are used in surfactant formulation to increase the compatibility between surfactants and the aqueous phase, and therefore increase its thermal stability. Achieving a clear and stable surfactant slug is important to ensure the injected solution will transport in the reservoir over long distances with low retention (Sahni *et al.*, 2010). Co-solvent also helps to reduce or eliminate the viscous phase and accelerate microemulsion equilibration (Sanz and Pope, 1995). Co-solvents are usually amphiles and have the ability to partition into aqueous phases, and oleic and microemulsion phases, which allows co-solvents to change phase behavior (Dwarakanath *et al.*, 2008). For example, a hydrophilic co-solvent increases optimal salinity and a lipophilic co-solvent reduces

optimal salinity while both increase aqueous stability. Alcohols are one of the widely used conventional solvents. Branched structure alcohols provide better hydrophilicity than linear structure alcohols for the same molecular weight (Hsieh and Shah, 1977). Common alcohols used in EOR include iso-propanol (IPA), iso-butanol (IBA), sec-butonal (SBA). Glycol ether alcohols are promising co-solvents because of their excellent ability to make surfactants compatible with the aqueous phase at high salinity (Sahni *et al.* 2010) and their higher flash point.

The disadvantage of using co-solvents is that they reduce the solubilization ratio of water/oil and consequently increase interfacial tension (Salter, 1977). It is possible to achieve high oil recovery with the alcohol free surfactant formulation (Sanz and Pope, 1995). Alcohol can also be replaced by other chemicals. For example alcohol ethoxylates can give better aqueous stability and higher optimum salinity at low concentrations. For active oil, which contains sufficient naphthenic acid to produce soap with alkali, a hydrophilic surfactant is sufficiently soluble in brine at optimal salinity without the need for any co-solvent or only a small amount of co-solvent. For inactive oil, surfactants with large hydrophobes are often needed to achieve a high oil solubilization ratio and low IFT. These surfactants are less soluble in brine, and hence they need a relatively large amount of co-solvents to obtain aqueously stable surfactant slug. In sum, alcohol concentration needs to be determined in such a way to balance the microemulsion viscosity, equilibration time and the solubilization ratio for maximum formulation performance and highest oil recovery.

2.4.3 Alkali

Alkali has been observed to improve surfactant phase behavior and oil recovery in core flood experiments (Nelson *et al*., 1984; Wellington and Richardson, 1997). The mechanisms contribute to improve oil recovery are:

(1) Alkali reacts with naphthenic acids in crude oil in-situ and produces natural surfactant. The amount of natural surfactant usually is not enough to reduce interfacial tension and needs to be compensated by synthetic surfactant in a chemical flood. Also, natural surfactant has relatively low optimal salinity (alkali concentration) and synthetic surfactant could be added to raise optimal salinity to adjust surfactant formulation to the appropriate alkali concentration needed to propagate in the reservoir (Nelson *et al.*, 1984). In phase behavior experiments, the natural surfactant from saponification naphthenic acid increases optimal solubilization ratio with even mildly or weakly reactive crude oils. Conventionally the total acid number, which is the amount of potassium hydroxide in milligrams that is needed to neutralize the acids in one gram of oil, is a good indicator of naphthenic acids that can be saponified. Saponification number, however, should be measured to determine the total amount of soap that could be generated by an alkali reaction (Yang *et al.*, 2010). Heavy oil tends to have higher total acid number than light oil and can benefit more from alkali.

(2) Elevating pH by adding alkali can reduce surfactant adsorption by increasing negative charges on sandstone rock (Nelson *et al.*, 1984; Wessen and Harwell 2000; Zhang and Somasundaran, 2006). Low surfactant adsorption promotes surfactant slug propagation (Nelson and Pope, 1977) and enables low surfactant concentration chemical flooding.

Alkali in surfactant formulation also improves the coalescence time of microemulsion in phase behavior experiments (Castor, 1981), which indicates low viscosity of the microemulsion phase (Nelson *et al*., 1984) and facilitates rapidly mobilizing oil and development of the oil bank in-situ. The reduction of microemulsion phase viscosity and consequent improvement of fluidity can reduce the amount of alcohol needed.

Sodium carbonate is a conventional alkali in chemical flood. In the presence of gypsum or anhydrite ($CaSO_4$), which is often the case with dolomite rocks, however, carbonate ions and calcium ions precipitate as calcium carbonate. Sodium metaborate is an alternative alkali that prevents precipitation of calcium carbonate by forming soluble complexes with dissolved calcium ions and borate ions (Flaaten *et al.*, 2006).Tetrasodium ethylenrdiamine tetraacetate (EDTA-4Na^+) is another promising alkali which acts as a chelating agent to sequester metal ions such as calcium and magnesium ions with its two amines and four carboxylates (Yang *et al.*, 2010).

2.4.4 Polymer

Polymer is used to increase the viscosity of surfactant slug and to therefore provide mobility control for stable displacement of the oil bank by surfactant slug in chemical flooding (Sorbie, 1991; Willhite and Green, 1998). Increasing the viscosity of the surfactant slug increases the sweep efficiency by reducing or eliminating fingering, particularly in heterogeneous reservoirs. Polymer is needed in both surfactant slug and polymer drive, which protects the integrity of surfactant slug. The viscosity of slug/drive (depends on amount/molecular weight of polymer) of stable displacement is determined in such a way that mobility ratio is maintained to be less than one (Gogarty *et al.*, 1968).

Partially hydrolyzed polyacrylamides (HPAMs) are conventional polymers which are susceptible to degradation by shearing as well as thermal degradation. The effects on stability of HPAM by various factors such as temperature, initial degree of hydrolysis, amount of divalent cations, pH, and dissolved oxygen are examined by Shupe (1981) and Moradi-Araghi (1987).

Xanthan gum, a bacterial polysaccharide, has a rigid structure, which yields significant resistance to shear degradation compared to HPAMs. It has the advantage of being insensitive to salinity and divalent cations due to its rigid structure and lack of an anionic group. It, however, is susceptible to bacterial degradation. Although xanthan gum was widely used in early chemical floods, HPAMs are more commonly used in recent chemical floods.

2.5 Core Flood Design

Laboratory core floods are used to validate the performance of surfactant formulation that shows good phase behavior results before field application. Residual oil trapped in the core after water flooding is the target of chemical flooding. The highest capillary number corresponds to the lowest IFT for both oil-microemulsion and water-emulsion phases, which is achieved at the optimal salinity of surfactant formulation. Therefore, surfactant slug with optimal salinity is usually injected into the core. A surfactant slug with over optimal salinity drives surfactant into the oil phase causing surfactant loss and leaves oil trapped again even though the oil is mobilized by microemulsion due to low oil-microemulsion IFT. A surfactant slug with under optimal salinity may have relatively high oil-microemulsion IFT and therefore cannot mobilize oil. For coreflooding, the brine salinity in the core can be well controlled to achieve optimal salinity in order to broaden

the surfactant Type III region with low IFT. In the field, however, reservoir salinity usually is not optimal salinity, and it is difficult to achieve optimal salinity everywhere because of (1) surfactant slug dispersion with reservoir brine; and (2) optimal salinity is a function of changing surfactant concentration. Pre-flush of optimal salinity brine is frequently un-necessary, and even detrimental to oil recovery (Pope *et al.*, 1979). A robust chemical flood design which uses a salinity gradient is proposed by Pope *et al.* (1979), where the salinity downstream of the slug is higher than optimal salinity, at the slug is equal to optimal salinity and upstream of the slug is lower than optimal salinity. This salinity gradient design greatly increases the chances of surfactant slug passing by optimal salinity and promoting low IFT at least somewhere in the mixing zone. Over optimal salinity downstream also helps mobilize oil and under-optimal salinity upstream helps prevent surfactant or mobilized-oil from being trapped.

2.6 Crude Oil Evaluated

The crude oil used in this study is Wahrman crude oil, produced from a limestone reservoir located in the northwest part of Kansas. Reservoir temperature is about 43.3 ℃ (110 ℉). It has low viscosity, 7.5 cP (filtered) at reservoir temperature and is light (API gravity: 37.9 at reservoir temperature). It has low acid number, about 0.014 g KOH/g; therefore there is little naphthenic acid in Wahrman crude oil to produce natural surfactants with reaction of sodium carbonate. The formation brine contains 12% TDS including 2500ppm divalent ions.

Chapter 3 Experimental Description

3.1 Introduction

The experimental equipment used in this research can be categorized for two main purposes: (1) to prepare solutions or crude oil and related hardware for phase behavior study, including mass balances, water deionizer, borosilicate pipettes, pipette dispensers, torches, convection ovens, viscometers, spinning drop interfacial tensiometers, filter membranes, vortex mixers, oil dispensers and polymer hydration mixers. (2) To prepare for core flood and analyze core flood effluent properties, including pumps, glass columns, pressure transducers and data acquisition system, tracer devices, a fraction collector, a rheometer, a pH meter, a conductivity meter and a hyamine titrator. The following sections describe the equipment and how it is set up for experiments.

3.2 Phase Behavior Screening Description

3.2.1 Equipment

3.2.1.1 Mass Balance

Three mass balances were used in this research. The primary mass balance was ALFIE Packers HM-202, with a capacity of 210 grams and a resolution of 0.0001 grams, and it was used to measure masses of chemicals such as surfactant, salt to make phase behavior bulk solution and surfactant slug and drive. The second balance was the ALFIE Packers HF-2000G, with a capacity of 2100 grams and resolution of 0.01 grams. This balance was used to weigh epoxy for casting cores and oil flood effluent etc. The third balance was an ALFIE Pacers Explorer OHAUS, with a capacity of 32000 grams and resolution of 0.1 grams, and it is used to weigh dry and saturated core mass for porosity calculation.

3.2.1.2 Water Deionizer

Ions in tap water will interfere with phase behavior results in phase behavior screening and core floods, therefore it is important to use deionized water. The water deionizer used is a Water PRO PS from LABCONCO.

3.2.1.3 Borosilicate Pipettes

Fisherbrand® standard 10mL borosilicate pipettes with 0.1mL markings were used to store the mixture of aqueous solution and crude oil in phase behavior study. After dispensing fluids into the pipettes, the end of pipettes was flame-sealed with a Benzomatic® torch. After cooling the end for several minutes, the pipettes were then inverted 20 times before housing in the oven at corresponding temperature.

3.2.1.4 Pipette Dispenser

The pipette dispenser used in phase behavior and core flood slug/drive preparation is an eppendorf Research PRO 100-5000uL. It can deliver between 100 microliters and 5000 microliters with 10 microliter increments at one time through disposable plastic tips.

3.2.1.5 Torch

Before dispensing fluids into borosilicate pipettes, the tip of each pipette was flame sealed by torch. After dispensing solutions into the borosilicate pipettes, the end of each pipette was flame-sealed by the same torch and was squeezed by a plier for fast seal. The torch used in this research is a BERNZOMATIC SUREFIRE TS8000, fueled by propylene.

3.2.1.6 Convection Oven

Temperature is critical in phase behavior studies. Phase behavior pipettes are housed and incubated in a THELCO Laboratory convection oven to be allowed to equilibrate at

reservoir temperature for each crude oil. A calibrated digital thermometer and an oven temperature gauge ensure a constant temperature in the oven.

3.2.1.7 Viscometer

The viscometer frequently used is a Brookfield LVDVI+CP viscometer. It can produce a shear rate as low as 3.75 $second^{-1}$ and as high as 7500 $second^{-1}$, however, the effective viscosity at that shear rate depends on the percentage of torque resulting from shear stresses. The advantage of this viscometer is that it requires relatively small sample, about 0.5mL. Because of this, this viscometer is used to measure viscosity of microemulsion, core flood effluent, crude oil and brine etc.

3.2.1.8 Rheometer

Bohlin CS Rheometer from ATS Rheosystems is used to measure the viscosity of surfactant slug and polymer drive at low shear rate beyond the range of the Brookfield viscometer. It can measure viscosity at a shear rate as low as 0.07 $second^{-1}$ and as high as 800 $second^{-1}$. The rheometer requires relatively large sample, about 30mL, therefore it was not used to measure the viscosity of core flood effluent samples.

3.2.1.9 Filter Membrane

Polymer solution was filtered through a specified membrane to remove un-hydrated polymer so it could be injected into the core without blocking the pores. Unfiltered polymer solution was stored in homemade plastic container and is filtered through 1.2 micron MicronSep Cellulosic membrane from GE Water & Process Technologies under a pressure of 15psi. The detailed polymer filtration process will be described later.

Brine used in the core flood was stored in a 1000-2000mL flask and filtered through a 0.45 micron MicronSep Cellulosic membrane from GE Water & Process Technologies under a vacuum to filter out impurities.

Crude oil filtration will be described later. The pre-filter membranes are 1.6um glass microfiber filters from Whatman upstream and 1.0 micron TefSep teflon Laminated filters from GE water & process technologies downstream.

3.2.1.10 Vortex Mixer

After solutions were added to borosilicate pipettes, the sealed pipettes were shaken by the Fisher Scientific VORTEX Mixer to fully mix the solution to one homogeneous phase before contacting the crude oil.

3.2.1.11 Oil Dispenser

Crude oil was added to each pipette by a Dispensette® III from Brand TECH Scientific Inc. into the pipettes. This approach can dispense oil in the range of 1-10mL with increments of 0.1mL.

3.2.1.12 Polymer Hydration Mixer

The mixer used in polymer hydration was Super-NUOVA^{TM} MULTI-Place from Barnsted Thermolyne. Its stirring range was 50-1200 RPM with stirring adjustable to 1 RPM to control the stirring rate well.

3.2.2 Chemical EOR Fluids

3.2.2.1 Primary and Co-surfactants

The primary surfactants used in this study are alcohol propoxy sulfates (APS). Surfactants with different carbon chain lengths and different numbers of proproxy groups were tested for best performance for the Wahrman crude oil. The most extensively

studied APS surfactants in phase behavior are C_{16-17}-7PO-SO^{4-} from Stepan with the trade name Petrostep S1, C_{12-13}-8PO-SO^{4-} from Sasol with trade name of Alfoterra 123-8S and C_{13}-n ÞO-SO_4^- from TIORCO with the trade name of Petrostep S13D.

The co-surfactants used in this study are mainly internal olefin sulfonates. The most extensively used were IOS_{15-18} from Stepan with the trade name of Petrostep S2. Other co-surfactants include IOS_{20-24}, alcohol ethoxylates.

The surfactants used in this research are listed in Table 3.1.

3.2.2.2 Co-solvents

Sec-butanol (SBA) was used extensively - initially based on the study of Levitt (2006) and Flatten (2007). Other similar alcohols such as iso-propanol (IPA) and other butanols are also evaluated. Surfactant formulations with these alcohols, however, all failed the aqueous phase test, which means that the surfactant formulation at optimal salinity and reservoir temperature will separate to two phases. Ether glycol alcohols such as ethylene glycol monobutyl ether (EGBE), di-ethylene glycol monobutyl ether (DGBE), tri-ethylene glycol monobutyl ether (TGBE) were found to help surfactant formulation pass the aqueous phase test with an aqueous phase stability limit higher than optimal salinity. Among all glycol ether alcohols, DGBE shows best performance for Wahrman crude oil and therefore was used in later phase behavior study.

3.2.2.3 Polymer

Hydrolyzed polyacrylamides (HPAM) were used in this study to increase aqueous phase viscosity. Flopaam polymer series from SNF Floerger® are available and tested. Flopaam 3530S was tested to be most suitable polymer for Wahrman oil and therefore was used both in phase behavior and core flood experiments.

3.2.2.4 Alkali

Sodium carbonate was used as the main alkali in this study. Sodium hydroxide was tested only to evaluate surfactant formulation performance at high pH, but was not used in later study.

3.2.2.5 Electrolyte

Sodium chloride is the main electrolyte for phase behavior experiments. Other electrolytes such as magnesium chloride, calcium chloride and sodium sulfate were used to provide additional ions to make synthetic formation brine. Alkali also contributes additional electrolyte to aqueous solutions and is taken into account in the optimal salinity calculation.

3.2.3 Bulk Solution and Crude Oil Preparation

This section describes the procedure for how to prepare bulk solution for phase behavior, crude oil filtration, aqueous phase stability tests and crude oil activity assessment. An initial microemulsion phase behavior experiment was conducted to estimate optimal salinity of certain surfactant formulations, and then another microemulsion phase behavior experiment was conducted to pinpoint optimal salinity. At the same time, aqueous phase stability limit of that surfactant formulation was evaluated. If surfactant formulation passes all four criteria, then core flood was conducted to further test its oil recovery efficiency.

3.2.3.1 Surfactant/Co-surfactant Bulk Solution

Surfactant/Co-Surfactant stock solutions provided by vendors have activities of 30-90% in weight percentage. Because they were so concentrated that the solutions were viscous and cause measurement errors when they were directly added to pipettes in volume with

dispenser. As a result, they were diluted into 10 wt% solution and then dispensed into pipettes with other bulk solutions.

3.2.3.2 Co-Solvent Bulk Solution

Co-Solvent/alcohol was initially diluted to 10-20% bulk solution before dispensing into pipettes. Because alcohols were easy to evaporate, therefore the concentration of the bulk solution changed during the frequent daily uses. Evaporation of the stock solution caused un-repeatable phase behavior results. Therefore pure alcohol (its concentration does not change due to evaporation because it's almost 100%) was added directly into pipettes with other bulk solutions. Slightly different amounts of alcohol did not cause significant error in phase behavior results.

3.2.3.3 Brine/Alkali Bulk Solution

Two brine solutions were prepared for phase behavior study. One brine solution was 20% NaCl and another brine solution was 10% NaCl. The 20% NaCl was used to prepare the base solution with surfactants, co-solvent, alkali and polymer, which are the same in each pipette. The same amount of base solution was added to each pipette. 10% NaCl is then added in various amounts to an array of pipettes to establish a salinity gradient. This method of preparing pipettes helps to reduce the error in adding different amount of surfactant/alcohol/alkali/polymer to each pipette.

3.2.3.4 Polymer Bulk Solution

Polymer received from the vendor was dried to determine its activity and then hydrated with sodium chloride to make polymer bulk solution. The detailed preparation is described as follows:

(1). Determine polymer activity: weigh and record e.g. about 10 grams (m_1) polymer in an aluminum cup; put the cup in a vacuum oven at 60 ^oC for about 7 days, record the weight every day; record the final polymer net weight(m2) and calculate polymer activity(m2/m1). Table 3.2 lists the activity of some common polymers available in our lab.

(2). Polymer bulk solution component weight calculation: in order to obtain repeatable results and simplify the calculation process, same polymer bulk solution is recommended to be prepared in the same way. Table 3.3 lists the weight of each component needed to make 500 grams in total, 5000ppm polymer concentration and 2% NaCl polymer bulk solution. A sodium chloride concentration of 2% was used to accelerate polymer hydration.

(3). Polymer hydration: For example, to make 500g, 2%NaCl, 5000ppm Flopaam 3330S, and 10 grams sodium chloride (NaCl) were added to 487.2253g of DI water and mixed on the magnetic stir plate. A container with a large section area and stirrer which is as big as possible while still fitting into the container is recommended for maximum polymer hydrolysis and lowest polymer aggregation. Cold water is also recommended to prevent polymer aggregation at the beginning of hydrolysis. Start stirring at 300-400 RPM; while stirring rate is stable, add polymer powder gradually in grain quantities to the shoulder of the vortex formed by the rotating of the stirrer. The addition of the polymer should be performed at a rate which is low enough to prevent clumping of the hydrate powder and high enough to prevent non-hydrated powder from floating on solution causing it to become too viscous to hydrate; typically it takes about 3-5 minutes. Maintain 300-400

RPM stirring rate for 1 hour then reduce the rate to 100-200 RPM. Usually at least 48 hours should be allowed to mix polymer solution for complete hydrolysis.

(4). Polymer filtration: after hydration, the polymer solution was filtered through a 1.2 micron hydrophilic cellulose filter membrane under 15 psi at a relatively constant rate. The filtration ratio is a measure of the time taken to filter the same volume of polymer solution at the beginning and end of the filtration process. It is expressed as:

$$F.R. = \frac{t_{200ml} - t_{180ml}}{t_{80ml} - t_{60ml}} \qquad \text{Eq. 3.1}$$

t_{200ml} –time to filter 200ml or corresponding volume of polymer

The filtration ratio (F.R) should be less than or equal to 1.2.

Even though filtration ratio calculation only requires the time to filter 60mL, 80mL, 180mL and 200mL, a continuous weight log of the filtered polymer (Figure 3.1) was recorded for further examination of the filtration process. When starting filtration, the filter valve is recommended to be open first before applying pressure to the filter in order to avoid building pressure in the filter and then to break the filter membrane. It is suggested that first several grams of filtered polymer solution be discarded for homogeneous polymer solution. Polymer solution with a filtration ratio of > 1.2 may require re-filtration.

(5) Bulk polymer solution viscosity: in order to examine polymer solution reproducibility, the viscosity of filtered bulk polymer solution was measured at 25 ^{o}C by the Bohlin CS rheometer. Low shear rate viscosities (e.g. at 1 second^{-1}) was compared for

the same polymer bulk solution prepared at a different time. This also helped us identify the viscosity difference in surfactant slug and polymer drive used in core floods.

3.2.3.5 Crude Oil Filtration

Crude oil received directly from the oil field contains certain impurities which will block pores in the core and may also affect phase behavior results. Therefore crude oil was filtered before use. The detailed filtration process is described below. The apparatus set-up is shown in Figure 3.2.

Set up a temperature controlled oven at reservoir temperature. Leave un-filtered crude oil, pump, filter and any related parts in the oven for a sufficient period of time, e.g. overnight to preheat to reservoir temperature. Prepare the filter inlet/out parts as shown in the right part of Figure 3.2 and Figure 3.3. Both inlet/outlet O-rings are crucial for sealing, and therefore they need to be checked carefully before assembling. After that, place two membranes between the filter caps. As shown in Figure 3.2, because oil will flow vertically upward, a 1.6 micron Teflon fiber glass filter membrane will be placed upstream, which is close to the inlet, and the 1.0 micron Teflon filter membrane will be placed downstream, which close to the outlet (smooth side of filter towards the inlet). Connect the parts as shown in the left part of Figure 3.2. Place the un-filtered crude oil source above the level of pump to reduce gravity effect on pumping crude oil; set up filter in a position where the crude oil flows vertically upwards. Start the pump at 0.25 mL/min for 15 minutes; monitor pressure gauge to ensure pressure is within 150 psig; flow rate can usually be increased gradually by 3 ml/min, however, the pressure gauge should be monitored within half an hour after increasing flow rate to ensure pressure is within range. High pressure filtration is not recommended because it may break the filter

membrane. A pressure of 20 psi when the flow rate is above 0.25 mL/min usually indicates the filter membranes are broken. In this case, filter membranes must be replaced with new membranes and the oil must be refilled.

3.2.4 Phase Behavior Methodology

3.2.4.1 Phase Behavior Description

Phase behavior experiments are a fast and efficient method to identify surfactant formulation given a crude oil compared to core flooding. Generally there are four criteria for a successful surfactant formulation that may then be used in core flooding to validate its efficiency.

(1). Surfactant solution must be clear and in one single phase at reservoir temperature. In order to achieve this, optimal salinity of the surfactant solution with specific crude oil must be below the aqueous phase stability limit, which will be described below. This criterion is critical and should never be compromised.

(2). Solubilization ratio should be higher than 10. Surfactant formulation with high solubilization ratio corresponds to low interfacial tension between microemulsion and water/oil. Surfactant formulations with a solubilization ratio lower than 10 could also achieve high oil recovery (Zhao *et al.* 2010). It is better to have the solubilization ratio as high as possible if that's possible while still meeting the other criteria, however, a solubilization ratio of higher than 10 is used to select certain formulations for further tests.

(3). The surfactant solution should be free of gel, liquid crystal and other viscous phases at any possible salinity the surfactant slug may encounter in core flood or reservoir condition. Viscous phases in microemulsion tend to retain surfactant in porous media and therefore deteriorate surfactant performance. Because we use a negative salinity gradient

to ensure passing through the Type III phase region, there should be no viscous phase - at least at a salinity level at or below optimal salinity, or below reservoir salinity if reservoir salinity is higher than optimal salinity.

(4). Equilibration time is the time when the volume of microemulsion phase at optimal salinity ceases changing. Phase behavior samples should have fast equilibration time, usually less than 7 days. The equilibration of microemulsion phase will decrease as the salinity deviates from optimal salinity. Fast equilibration of microemulsion is a good indicator of fluid interfaces and low microemulsion viscosity. The equilibration of microemulsion when surfactant slug meets crude oil at core flood or reservoir is understood to be faster than at lab because of more contacting area due to porous structure. Long equilibration time will reduce surfactant oil recovery efficiency and therefore is not recommended in chemical flooding design.

3.2.4.2 Aqueous Phase Stability Limit Test

The aqueous phase stability limit (APSL) of a surfactant formulation is the maximum salinity the surfactant formulation can have while remaining in a single phase solution. It is necessary to inject a single phase clear surfactant solution for chemical flooding at reservoir temperature. Chemical flooding with hazy surfactant solution was proven to contribute to low oil recovery (Sahni *et al.* 2010). A series of tubes with a specific surfactant formulation and the same salinity gradient as optimal solution tubes was prepared and placed in a water bath at reservoir temperature for about seven days. Tubes were checked visually for phase separation. The aqueous phase stability limit is the salinity above where the aqueous phase will separate into two phases. Below the APSL, the aqueous phase will remain a single phase.

Usually the aqueous phase will separate into two phases within a couple of hours; however, when the aqueous phase salinity is the APSL limit, one to two days may be required to separate into two phases completely. Polymer decelerates the phase separation, and therefore it is important to check the aqueous phase stability limit after sufficient time, e.g. seven days. No phase separation was observed after seven days. A water bath was used for the aqueous phase stability limit test for better temperature control.

3.2.4.3 Crude Oil Activity Assessment

Total Acid Number (TAN) is the amount of potassium hydroxide in milligrams that is needed to neutralize the acids in one gram of oil. The total acid number is a measure of the amounts of naphthenic acid in crude oil and usually is a good indicator of activity of crude oil. Therefore the total acid number was measured for Wahrman crude oil to evaluate its activity.

3.2.5 Phase Behavior Data Analysis

The equations used in data analysis of phase behavior are presented in this section. Solubilization ratio is an important parameter that could be used to estimate interfacial tension and hence evaluate surfactant performance.

3.2.5.1 Solubilization Ratio

The solubilization ratio of water/oil is the volume of water/oil present in a microemulsion phase per volume of total active surfactant in the microemulsion phase. The volume of water/oil is estimated by the interval between initial aqueous phase level and the bottom/top interface level of microemulsion. The total active surfactant is the total surfactant volume originally dispensed in the pipette assuming that all surfactants stay in the microemulsion phase.

$$\sigma_i = \frac{V_i}{V_s}$$ Eq. 3.2

σ_i –water/oil solubilization ratio

V_i –water/oil solubilized in microemulsion phase

V_s –volume of surfactant in microemulsion phase

Water solubilization ratio decreases and oil solubilization ratio increases as salinity increases. The salinity at which water solubilization ratio equals oil solubilization ratio is defined as the optimal salinity and the solubilization ratio is the optimal solubilization ratio. The lowest interfacial tension is achieved at optimal salinity and can be estimated by an equation developed by Huh (1979):

$$\gamma = \frac{C}{\left(\sigma^*\right)^2}$$ Eq. 3.3

γ=interfacial tension

σ*=solubilization ratio at optimal salinity

C=constant, about 0.3 dyne/cm

3.2.5.2 Activity Diagram

The salinity boundary of phase Type III and optimal salinity changes with oil concentration. If the crude oil is active (contains enough naphthenic acid), then the phase Type III salinity range increases as oil concentration increases - given sufficient alkali in surfactant formulation. The activity diagram is a plot of the salinity range of phase Type

I/III/II versus oil concentration. An activity diagram with a wide type III salinity range and negative slope is desirable because it will help to pass and maintain Type III phase in chemical flooding when the salinity gradient is applied. Generally, natural surfactant is more hydrophobic than synthetic surfactant therefore optimal salinity shifts to lower salinity as oil concentration increases. The activity diagram also helps to analyze the chemical flooding process in the core.

3.3 Core Flood Description

The equipment used in core flooding includes pumps for injecting fluid into the core; glass columns for storage of tracer fluid, surfactant slug and polymer drive; pressure transducers for measuring pressures; tracer devices for evaluating core dispersion characteristics; fraction collector for collecting chemical flood effluent and pH and conductivity meter for analyzing core flood effluent.

3.3.1 Equipment

3.3.1.1 Pumps

Quizix pumps were used to deliver fluid at a constant flow rate into the core during core flooding. Two pumps were used alternatively for the convenience of changing the brine reservoir. The main pump was a Quizix QX, which had a maximum flow rate of 200mL/min, and a minimum flow rate 0.002mL/min and could withstand a maximum pressure of 1500psi. The secondary pump was a Quizix QL-700, which had a maximum flow rate of 10mL/min and could withstand a maximum pressure of 5000psi. Both pumps were connected to and controlled by a computer.

3.3.1.2 Glass Columns

The glass columns used to store surfactant slug and polymer drive temporarily during core floods were Kontes Chromaflex glass columns. The columns had 300mL fluid storage capacity and were sealed air-tight through Viton O rings at the Teflon ends. They could withstand as high as 70psi and were tested prior to use for leakage at pressures corresponding to those that occurred in core floods.

3.3.1.3 Pressure Transducer/Data Acquisition Recorder

The pressure transducers used in measuring pressure during core floods are Validyne Model DP15 series with different ranges. One set of pressure transducers with range of 0-100 psi was used to measure overall pressure across the core. Another six sets of pressure transducers with range of 0-10 psi were used to measure pressure of each section of the core. The outputs of transducers are recorded using the data acquisition recorder from Validyne and managed by Labview software. Raw data are recorded at 5-30 seconds intervals according to specific needs and exported into files for subsequent data analysis. The transducers were calibrated by Mensor. The output pressures from the transducers were adjusted if the transducers gave pressure values more than 0.25% of the actual pressure provided by Mensor.

3.3.1.4 Tracer Devices

Tracer was injected into the core to determine core pore volume and mixing pattern in the core and residual oil saturation. Initially the non-tracer solution was sodium chloride, and the tracer solution was the corresponding sodium chloride solution plus 1% potassium nitrate. The Prostar 340/345 UV-VIS detector from Varian Analytical Instruments was used to measure absorbance of nitrate during the tracer test. The permeability of Berea sandstone cores was reduced by nitrate during the tracer test. Therefore a different tracer

test was developed. The Prostar 350 Refractive Index detector was used to measure the refractive index of different salinity brine used in tracer tests. The non-tracer solution using this device was certain salinity brine and the tracer was different salinity brine. The salinity difference between the refractive index of tracer and non-tracer solution were selected to be within instrument measuring range.

3.3.1.5 Fraction Collector

Effluent fluid samples from chemical flood were collected using a RETRIEVER IV fraction collector from Instrument Specialties Company (ISCO). The fraction collector used in chemical flood was set to collect 4.5mL effluent every 30 minutes.

3.3.1.6 pH meter

The pH of core flood effluent and aqueous samples was measured by HORIBA Compact pH meter B-213. It was used to measure the pH of solutions with pH>7 while it is only calibrated at pH=4 and pH=7. The advantage of this pH meter was that it required small samples - only about 0.1mL to cover three electrodes for measurement. Therefore, it was convenient to use for small sample core flood effluent samples.

3.3.1.7 Conductivity Meter

A conductivity meter - YSI 3200 Conductivity Instrument was used to measure the conductivity of the core flood effluent. The conductivity meter was first calibrated with standard solutions. The cell constant was adjusted to let the conductivity meter show the correct conductivity value of the standard solution. The conductivity was measured in mS and converted to equivalent concentration of sodium chloride through a calibration curve. Surfactants, alcohols and polymer reduce solution conductivity slightly but were not taken into account in the calibration curve.

3.3.2 Core Flood Methodology

Laboratory core floods were necessary to demonstrate oil recovery efficiency for each surfactant formulation. Berea sandstone and Indiana limestone as industry core standards were used in core floods to help examine surfactant formulation efficiency and understand chemical flood process in the core. Brine permeability measurement and tracer tests were conducted at room temperature (about 23^{o}C) while core floods (brine flood, oil flood, water flood and chemical flood) were conducted at Wahrman oil reservoir temperature (43^{o}C). Core orientation (vertical/horizontal) during core flood did not seem to affect oil recovery for Berea sandstone cores, therefore core floods for all Berea sandstones except the first Berea sandstone core flood were done horizontally for convenience. After observing what appeared to be gravity segregation during core flood in the first limestone core flood, core floods in limestone were done vertically to minimize the gravity effect.

Permeability reduction was often observed and increased with time for Berea sandstone - particularly for the inlet section. Therefore, after the core was saturated, brine flooding, oil flooding, water flooding and chemical flooding were done soon to avoid permeability variation. Core flood procedure includes a tracer test, brine flooding, oil flooding, water flooding, chemical flooding and also an effluent properties analysis and pressure analysis.

3.3.2.1 Tracer Test

After casting and saturating the core with 2% sodium chloride (NaCl), a tracer test was conducted to examine the dispersion characteristic of the core and the pore volume. During the tracer tests, the tracer (e.g. 1% KNO3) was injected into the core along with the carrier fluid (e.g. 2% NaCl brine) and was detected at the end of the core after some

period of time. The tracer curve was a curve showing how tracer concentration in the effluent changed with time/volume injected. The pore volume or residual oil saturation was determined from integration of the tracer curve. The tracer curve also showed how easily fluids could be dispersed when it flowed through the core. The dispersion property of the core was a very important factor in chemical flooding - especially in limestone since its pore structure and wettability was quite different, or worse to some degree, compared to sandstone. Cores with a large dispersion coefficient were discarded, or were used to interpret chemical flooding process even if it is used. Initially, tracer tests were conducted only before brine flooding, later tracer tests were also done after water flooding to understand the dispersion property during chemical flooding.

3.3.2.2 Brine Flooding

After the tracer test, the core was flushed with either brine of equivalent salinity to the surfactant formulation or synthetic formation brine. The objective of brine flooding was to prepare the core to be at the desired conditions - for example, at optimal salinity of surfactant formulation for best surfactant performance, or at formation brine condition to better mimic reservoir conditions in chemical flooding. It was necessary to recalculate the brine's absolute permeability as the latest core permeability due to the permeability reduction mentioned above.

3.3.2.3 Oil Flooding

The objective of oil flooding was to establish the initial oil saturation prior to water flooding. The detailed process of oil flooding is described below. Set up the apparatus as in **Figure 3.4**. Filled crude oil to the tubing up to the inlet valve; emptied the tubing from the outlet valve to the end so there was no need to calculate dead tubing volume in the

mass balance calculation of initial oil saturation. If the core was placed horizontally, put the core in a position so that the pressure ports on the core are facing upside down to minimize a capillary pressure effect during pressure logging. If the core was placed vertically, oil should be injected into the top end for consideration of the different gravity effects on water and oil. Inlet and outlet dead tubing length (the length between inlet valve and core, and the length between core and outlet) should be measured for dead volume calculation and so it could be taken into account in the mass balance calculation of initial oil saturation.

Oil flooding was done at an appropriate injection rate to ensure the pressure gauge was within limits. The effluent brine volume was recorded at certain intervals, particularly at the time when oil breaks out of the core. Thus, the oil/water production history can be examined and compared between each core. Oil injection was stopped when pressure stabilized and no brine was produced. Usually 3-4 pore volume injections of oil were needed. Collect the effluent brine in a burette; measure its weight and the density at room temperature and reservoir temperature to calculate brine volume at reservoir temperature. The oil volume in the core was the effluent brine volume after subtracting the dead tubing and dead valve volume at reservoir temperature. Initial oil/residual water saturations were calculated. The differential pressures for the entire core and each section during oil flooding were recorded so oil permeability and relative oil permeability could be calculated.

3.3.2.4 Water Flooding

Water flooding with filtered brine of equivalent salinity to the surfactant formulation or synthetic formation brine followed the oil flood. The detailed process of water flooding

is described below. Set up the apparatus as in Figure 3.5. Brine was filled in the tubing up to the inlet valve; the tubing from the outlet valve to the end was emptied for convenience of mass balance calculation. If the core was placed horizontally, put the core in a position such that the ports on the core are facing upside down to minimize a capillary pressure effects during pressure measurement. If the core was placed vertically, inject water from the bottom end for consideration of the different gravity effects on water and oil. Inlet and outlet dead tubing length (the length between the inlet valve and core, and the length between the core and the outlet) should be measured for dead volume calculation.

All water floods were conducted at 0.3 mL/min (~ 4 feet/day) to mimic an actual water flood situation. Effluent oil volume was recorded during a certain period of time - particularly at the time when water breaks through so the oil/water production history could be examined and compared among each core. The water flood was stopped when no oil was produced, or oil cut decreased to less than 1% and pressure stabilized. Usually it required about 0.4 pore volume of brine injection. Collect the effluent crude oil in a burette; measure the weight of the crude oil effluent and its density at 25^{o}C and reservoir temperature to calculate oil volume at reservoir temperature. The volume of brine remaining in the core was the crude oil effluent volume at reservoir temperature after subtracting the dead tubing and dead valve volume. Residual oil/water saturation were calculated.

The differential pressures for the entire core or each section were recorded to calculate water permeability and relative water permeability. After water flooding, it was necessary to flush each pressure port to eliminate the capillary pressure effect during pressure logging in chemical flooding; also check whether all the pressures at zero flow rates were

the same as before the water flood; repeat flushing the corresponding pressure ports until they are the same. For data consistency, after water flooding, flow rate was reduced to chemical flood flow rate, usually 0.15mL/min, and pressures of sections except section 1 were recorded and compared with the pressures at the beginning of chemical flooding.

3.3.2.5 Chemical Flooding

Chemical flooding was done after water flooding to determine the performance of surfactant formulation and recovery of residual oil in the core as tertiary recovery. Set up the apparatus as in **Figure 3.6**. It was necessary to prepare the surfactant slug and conduct phase behavior tests with crude oil prior to chemical flooding to ensure the surfactant slug was at optimal salinity. If phase behavior shows the surfactant slug was not at the desired salinity then another surfactant slug was made and tested until it was at the desired salinity. A 0.3-0.6PV surfactant slug was usually injected into the core followed by a 1.4-1.7PV polymer drive. About 30mL of extra surfactant slug and polymer drive should be prepared to measure their viscosities at low shear rate by Bohlin CS rheometer. The viscosities at low shear rate were used for mobility analysis and apparent viscosity calculation during chemical flooding. The actual viscosities were also compared with designed viscosity for mobility control; if the viscosity was lower than desired viscosity, then a new slug or drive was made. If the core was placed horizontally, put the core in a position such that the ports on the core are facing upside down to avoid a capillary pressure effect during pressure logging. If the core was placed vertically, inject surfactant slug and polymer from the bottom end for consideration of the different gravity effects of water and oil.

All chemical floods were done at a constant flow rate of 0.15mL/min (~2 feet/day) until no more oil was produced. It was important to record the time of crude oil breakthrough and surfactant breakthrough. The surfactant breakthrough time was when oil emulsion was observed in the tubing near the outlet of the core after a clean oil drop. Effluent fluids were collected by fraction collector every 30 minutes for further analysis. After the chemical flooding was completed, the polymer solution was injected at different flow rates, e.g. 0.05mL/min, 0.075mL/min, 0.1mL/min, 0.125mL/min, 0.15mL/min, 0.2 mL/min for 1 hour each, and the pressures were recorded for polymer in situ rheology analysis. The effluent from the polymer flow experiment was collected to measure its viscosity with the Bohlin CS rheometer. The effluent rheogram was compared to the measured rheogram of the polymer drive. Brine with equivalent salinity to the polymer drive was injected until there were no pressure changes. Permeability reduction factor was evaluated.

The effluent vials were set in oven at reservoir temperature to equilibrate for about 3-5 days to separate crude oil from the emulsion and aqueous phase. The oil cut and cumulative oil recovery were calculated in the manner described above. Effluent pH, conductivity and viscosity and surfactant concentration were measured to evaluate the performance of the surfactant formulation.

3.3.3 Core Flood Data Analysis

3.3.3.1 Bulk Volume

The bulk volume of a core was calculated from the dimensions of diameter and length before casting with epoxy according to the equation:

$$V_b = \frac{\pi D^2 L}{4}$$ Eq. 3.4

V_b –bulk volume,mL

D –core diameter,cm

L –core length,cm

3.3.3.2 Pore Volume

The pore volume (PV) was calculated by mass balance and a tracer test. For the tracer test, which will be described later, the pore volume was calculated by integrating the tracer curve. For the mass balance method, pore volume was the mass of saturated brine divided by density of brine:

$$V_p = \frac{m_{saturated} - m_{vacuumed}}{\rho_{brine}}$$ Eq. 3.5

Vp –pore volume,mL

$m_{saturated}$ –mass of brine saturated core,g

$m_{vacuumed}$ –mass of vacuumed core,g

ρ_{brine} --density of brine, g/mL

3.3.3.3 Porosity

Porosity of the core is pore volume divided by bulk volume as follows:

$$\phi = \frac{V_p}{V_b}$$ Eq. 3.6

ϕ --porosity

V_p –pore volume,mL

V_b –bulk volume,mL

3.3.3.4 Brine Permeability

After the core was saturated with brine, brine was injected into the core at different flow rates, and pressure was recorded to calculate absolute brine permeability. The brine permeability can be calculated by rearranged Darcy's law equation:

$$k_{brine} = \frac{q\mu L}{A\Delta p} \qquad \text{Eq. 3.7}$$

k_{brine} –absolute brine permeability,mD

q –flow rate,mL/min

Δp –overall pressure drop,psi

μ --brine viscosity,cP

L –core length,cm

A –core cross section area, cm^2

3.3.3.5 Effective Oil/Water Permeability

The effective oil permeability is the oil permeability at the end of the oil flood. The oil flow rate, oil viscosity and the overall pressure (oil pressure) at the end of the oil flood are used to calculate effective oil permeability. The effective water permeability is the water permeability at the end of the water flood. The water flow rate, water viscosity and

overall pressure (water pressure) at the end of the water flood are used to calculate effective water permeability. The equation is Darcy's Law, given as:

$$k_{o/w} = \frac{q_{o/w}\mu_{o/w}L}{A\Delta p_{o/w}} \qquad \text{Eq. 3.8}$$

$k_{o/w}$ –permeability to oil/water,mD

$q_{o/w}$ –oil flow rate,mL/min

μ_o –oil/water viscosity,cP

$\Delta p_{o/w}$ –overall pressure drop of oil phase at the end of oil flood, psi

or water phase at the end of water flood

3.3.3.6 End Point Relative Oil/Water Permeability

End point relative oil/water permeability is effective oil/water permeability dividing by brine permeability as shown:

$$k_{ro}^0 = \frac{k_o}{k_b} \qquad \text{Eq. 3.9}$$

k_{ro}^0 --end point oil relative permeability

k_o – effective oil phase permeability,mD

k_{brine} –brine permeability,mD

$$k_{rw}^0 = \frac{k_w}{k_b} \qquad \text{Eq. 3.10}$$

k_{rw}^0 --end point oil relative permeability

k_w –effective water permeability,mD

k_{brine} –brine permeability,mD

3.3.3.7 Initial Oil Saturation

After the core was saturated with brine, the core was oil flooded until no more water was produced and pressure stabilized. Initial oil saturation could be determined through mass balance:

$$S_{oi} = \frac{V_w}{V_p} \qquad \text{Eq. 3.11}$$

S_{oi} –initial oil saturation

V_w –volume of water displaced during oil flood,mL

V_p –pore volume,mL

3.3.3.8 Residual Oil Saturation

After oil flooding, the core was water flooded until no oil produces, where residual oil saturation is reached, and pressure stabilizes. Residual oil saturation is the remaining oil dividing by pore volume:

$$S_{orw} = \frac{V_w - V_o}{V_p} \qquad \text{Eq. 3.12}$$

S_{orw} –residual oil saturation after water flood

V_w –volume of water displaced during oil flood,mL

V_o –volume of oil displaced during water flood,mL

After chemical flooding, the residual oil saturation can be calculated as follows:

$$S_{roc} = \frac{S_{orw} \cdot V_p - V_{oc}}{V_p} \qquad \text{Eq. 3.13}$$

S_{orc} –residual oil saturation after chemical flood

V_{oc} –volume of oil displaced during chemical flood,mL

3.3.3.9 Mobility Ratio

The mobility and mobility ratio calculations are important to determine appropriate apparent viscosity for the injected fluid to achieve good mobility control during chemical flooding. They are based on viscosity and relative permeability and will determine the molecular weight and concentration of polymer in the surfactant slug and polymer drive. The mobility design of chemical flooding in this research was based on Gogarty's (1968) mobility control theory. The total mobility is the sum of water and oil mobility given as:

$$\lambda_t = k_{brine}\left(\frac{k_{rw}}{\mu_w} + \frac{k_{ro}}{\mu_o}\right) \qquad \text{Eq. 3.14}$$

The plot of total mobility versus water saturation yields minimum total mobility at some water saturation. According to Gogarty, mobility of surfactant slug and polymer drive should be lower than minimum total mobility of oil/water bank, which means the viscosity of slug and drive should be higher than the minimum apparent viscosity:

$$\mu_{slug/drive} > \mu_{app\_\max} = \frac{k_{brine}}{\lambda_{t\_\min}} = \frac{k_{brine}}{\left(k_w / u_w + k_o / u_o\right)_{\min}} \qquad \text{Eq. 3.15}$$

$\mu_{slug/drive}$ –surfactant slug or polymer drive viscosity,cP

$\mu_{app\_\max}$ –maximum apparent viscosity,cP

λ_{t_min}–minimum total relative mobility,mD/cP

3.3.3.10 Polymer Resistance Factor

The polymer resistance factor is the ratio of water mobility to polymer mobility.

$$R_f = \frac{\lambda_w}{\lambda_p} = \frac{k_w \mu_p}{k_p \mu_w} \quad \text{Eq. 3.16}$$

R_f –polymer resistance factor

μ_p –polymer viscosity,cP

μ_w –water viscosity,cP

k_p – effective polymer permeability,mD

k_w – effective brine permeability,mD

At the end of chemical flooding, if the residual oil saturation reaches zero, which means the main flow fluid is polymer solution, then the resistance factor can be calculated using this equation:

$$R_f = \left(\frac{\Delta P_p}{\Delta P_w} \right)\Big|_q \quad \text{Eq. 3.17}$$

3.3.3.11 Polymer Permeability Reduction Factor

The polymer permeability reduction factor is the ratio of the effective brine permeability to effective polymer permeability:

$$R_k = \frac{k_w}{k_p} \quad \text{Eq. 3.18}$$

R_k –polymer permeability reduction factor

k_p – effective polymer permeability,mD

k_w – effective brine permeability,mD

The effective polymer/brine permeability both assumes brine or polymer is the only flowing fluid in the core. Effective polymer permeability is usually lower than brine permeability because of polymer absorption on rock surfaces.

3.3.3.12 Oil Cut

The method to calculate oil cut was developed by Dr. Kaixu Song. It used height of oil phase to correlate volume of oil. Calibration curve of oil height and oil volume was developed to measure and calculate correct oil volume.

3.3.3.13 Cumulative Oil Recovery

The effluent of chemical flood was collected by a fraction collector and the cumulative oil volume was the sum of oil volume in each vial. The effluent with microemulsion phase was placed in the oven at reservoir temperature for 3 to 5 days to break the microemulsion. The cumulative oil recovery is calculated as below:

$$Cumulative\ oil\ recovery = \sum_{1}^{n}(V_{oi}) \Big/ (PV \cdot S_{or}) \qquad \text{Eq. 3.19}$$

V_{oi} –volume of free oil in vial (i),mD

S_{ro} –residual oil saturation

V_p –pore volume,mD

Table 3.1 The names, supplier and abbreviated chemical representation of the surfactants used in this research

Trade Name (Supplier)	**Common Chemical Name**	**Abbreviated Chemical Representation**
Alfoterra® 123-8S (Sasol)	Alcohol Propoxy Sulfate	C_{12-13}-$(PO)_8$-SO_4^-
Alfoterra® 145-4S (Sasol)	Alcohol Propoxy Sulfate	C_{14-15}-$(PO)_4$-SO_4^-
Alfoterra® 145-8S (Sasol)	Alcohol Propoxy Sulfate	C_{14-15}-$(PO)_8$-SO_4^-
Alfoterra® 167-4S (Sasol)	Alcohol Propoxy Sulfate	C_{16-17}-$(PO)_4$-SO_4^-
Alfoterra® 167-7S (Sasol)	Alcohol Propoxy Sulfate	C_{16-17}-$(PO)_7$-SO_4^-
Petrostep® S-1 (Stepan/TIORCO)	Alcohol Propoxy Sulfate	C_{16-17}-$(PO)_7$-$SO4^-$
Petrostep® S-3 (Stepan/TIORCO)	Internal Olefin Sulfonate	C_{20-24} IOS
Petrostep® S-2 (Stepan/TIORCO)	Internal Olefin Sulfonate	C_{15-18} IOS
Petrostep® C-1 (Stepan/TIORCO)	Alpha Olefin Sulfonate	Not Available
Petrostep® C-5 (Stepan/TIORCO)	Alpha Olefin Sulfonate	Not Available
Petrostep® S-8B (Stepan/TIORCO)	Alcohol Propoxy Sulfate	Not Available
Petrostep® S-8C (Stepan/TIORCO)	Alcohol Propoxy Sulfate	Not Available
Petrostep® S-13B (Stepan/TIORCO)	Alcohol Propoxy Sulfate	Not Available
Petrostep® S-13C (Stepan/TIORCO)	Alcohol Propoxy Sulfate	Not Available
Petrostep® S-13D (Stepan/TIORCO)	Alcohol Propoxy Sulfate	C_{16-17}-$(PO)_n$-$SO4^-$
Neodol® 25-12 (Shell)	Alcohol Ethoxylate	Not Available
Neodol® 25-9 (Shell)	Alcohol Ethoxylate	Not Available

Table 3.2 Polymer activity information

Polymer	Molecular Weight (MM Dalton)	Hydrolysis in Mole (%)	Activity (%)
Flopaam 3330S	~8	25-30	90.1
Flopaam 3430S	~12	25-30	92.2
Flopaam 3530S	~16	25-30	88.9
Flopaam 3630S	~20	25-30	89.0

Table 3.3 Polymer bulk solution (5000ppm polymer +2% NaCl) weight

Polymer	Activity	Total weight	Polymer	NaCl	DI Water
	(%)	(g)	(g)	(g)	(g)
Flopaam 3330S	90.1	500	2.7747	10	487.2253
Flopaam 3430S	92.2	500	2.7115	10	487.2885
Flopaam 3530S	88.9	500	2.8121	10	487.1879
Flopaam 3630S	89	500	2.8090	10	487.1910

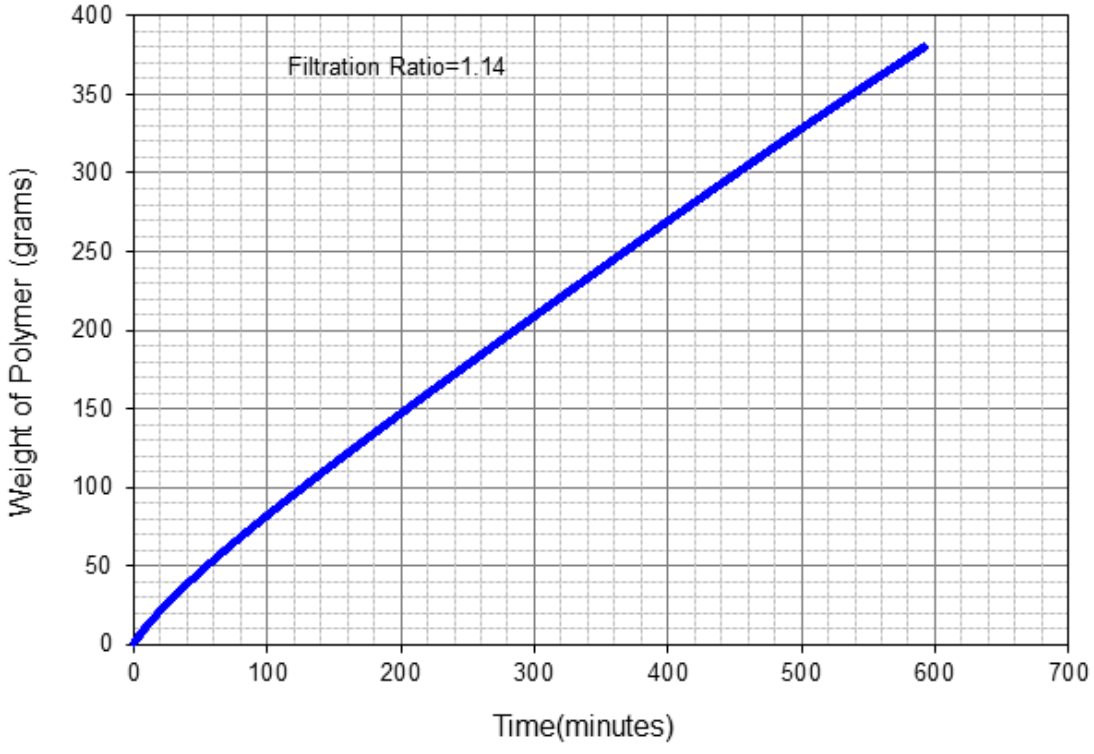

Figure 3.1 An example of a weight log of polymer filtration (filtration ratio=1.14).

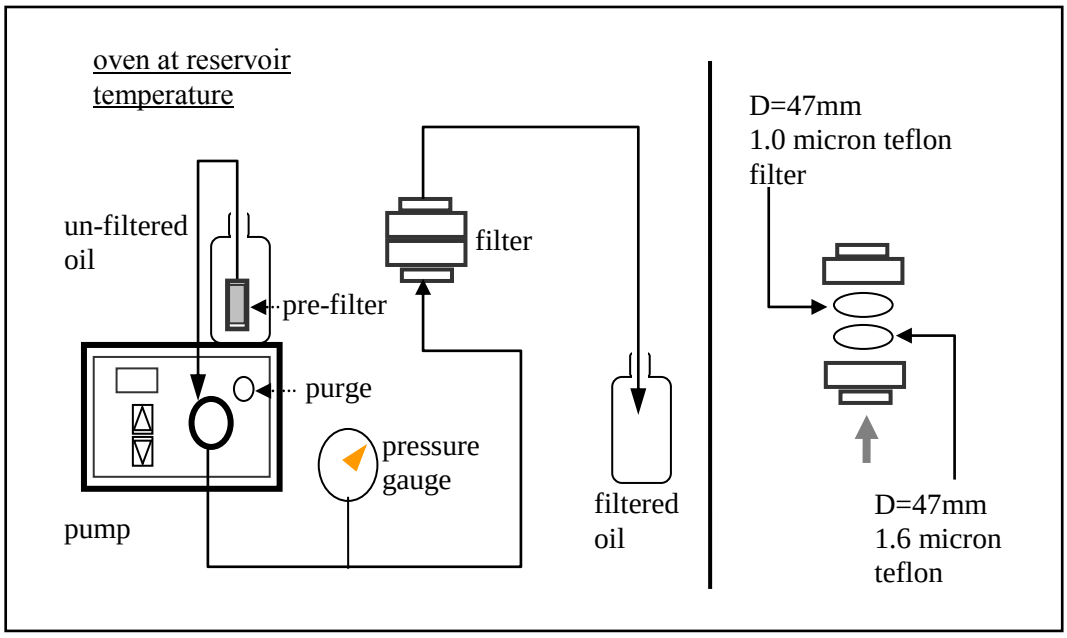

Figure 3.2 Crude Oil Filtration Apparatus Setup

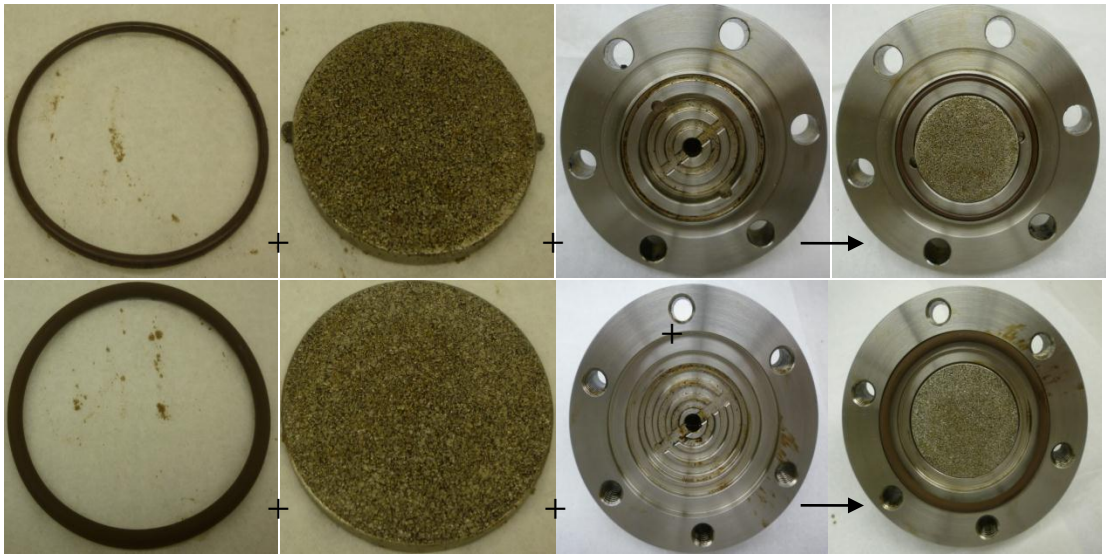

Figure 3.3 Photo of filter parts. Top: inlet O-ring, inlet steel filter, inlet cap, inlet filter assembly; Bottom: outlet O-ring, outlet steel filter, outlet cap, outlet filter assembly.

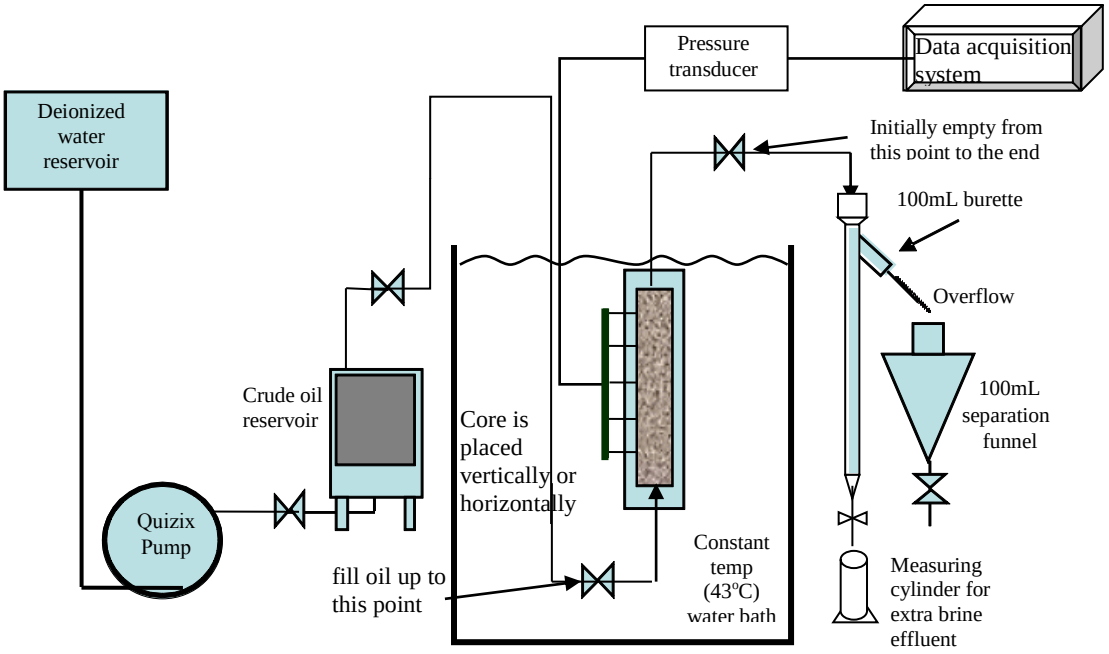

Figure 3.4 Oil flood apparatus setup

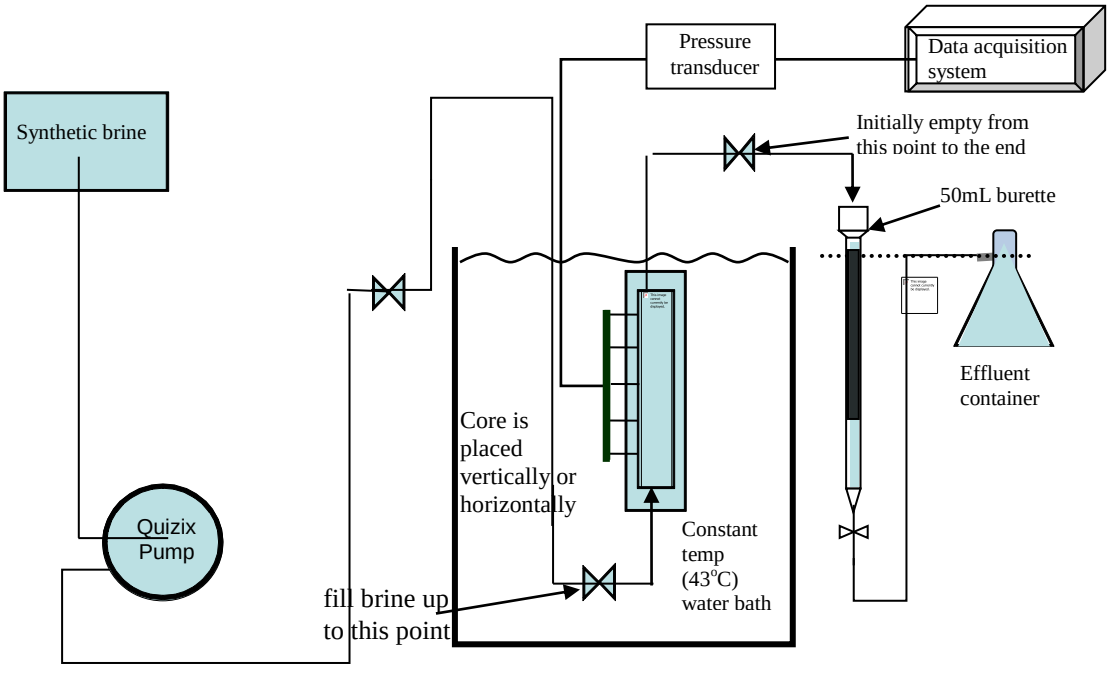

Figure 3.5 Waterflood apparatus setup

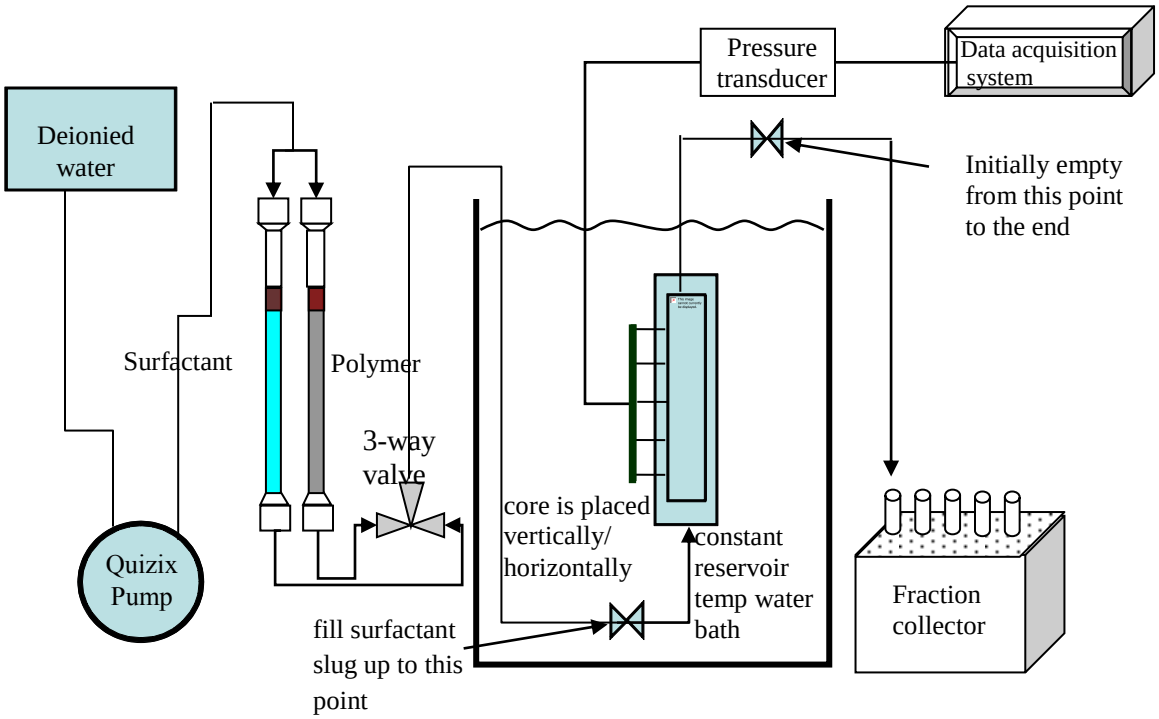

Figure 3.6 ASP Flood Apparatus Setup

Chapter 4 Phase Behavior Results

4.1 Introduction

The results of phase behavior experiments conducted in this research are presented in this chapter. The objective of experiments was to develop a surfactant formulation for core flooding of Wahrman crude oil. In Chapter 3, the criteria for a satisfactory surfactant system were introduced. These criteria are: 1) Aqueous Phase Stability Limit must be established at reservoir temperature; 2) Optimal salinity must be less than the Aqueous Phase Stability Limit; 3) Solubilization ratio must be greater than 10; 4) Equilibration time must be less than 7 days at reservoir temperature; 5) No viscous phases and 6) Criteria 1-5 must be maintained when polymer is added to increase the solution viscosity to the level required for mobility control during core floods. Normally, the salinity of the surfactant slug for injection will be the optimal salinity. In addition, Criteria 1-6, must be satisfied when alkali (Na_2CO_3) is added to increase pH which reduces retention in sandstone and carbonate cores.

First, the effects of parameters, e.g. surfactant type/ratio/concentration and cosolvent type/concentration on phase behavior are discussed to help understand how to adjust these parameters to develop and optimize a surfactant formulation satisfying all screening criteria. Then the processes involved with selecting surfactants and cosolvent are described. Problems occurred during the process and the methods to overcome the problems are described. The surfactant formulation finalized for core flooding is presented.

4.2 Initial Surfactant Formulation

Typical surfactant formulations in this research contain primary surfactant, cosurfactant, cosolvent, electrolyte and optional alkali and polymer. The selection of surfactant type and cosolvent type is critical to a successful formulation. In addition, the surfactant ratio, surfactant concentration, cosolvent concentration, alkali type and oil concentration influence the phase behavior results and need fine adjustment to optimize the surfactant formulation.

4.2.1 Primary Surfactant and Cosurfactant

The primary surfactant is discussed here because its structure can be varied to control solubilization and stability. Alcohol propoxy sulfates (APS) are excellent surfactants for crude oils in relatively low temperature reservoirs. Alcohol propoxy sulfates contain characteristic propoxy groups, which are more hydrophilic than the carbon chain tail. Varying the propoxy group number and/or carbon chain length alters the solubility of surfactant in aqueous phase and the optimal salinity from the phase behavior with crude oil.

Based on literature, the alcohol propoxy sulfate, C_{16-17}-7PO-SO_4^-, was an excellent primary surfactant for light crude oil. Therefore it was selected as the primary surfactant with cosurfactant C_{15-18} IOS and cosolvent (SBA) at various surfactant concentrations, surfactant ratios and cosolvent concentrations (Table 4.1). High surfactant concentration (1-2 %) resulted in solubilization ratios above 10 while low surfactant concentrations (0.5 %) had solubilization ratios below 10. Phase behavior experiments were usually conducted with 1% surfactant concentration. Formulations with surfactant ratios of 1.67-2.67 produced fluid microemulsion phases with high solubilization ratios (Figure 4. 1,

Figure 4. 2 and Figure 4. 3). Formulations with surfactant ratios higher than 3 produced liquid crystal phases even if more cosolvent (SBA) was added to the formulation (Table 4.1, 5-22, 5-27, 5-28, 5-29, 5-33-3, 5-34-3).

Because of the good performance of C_{16-17}-7PO-SO_4^- , similar surfactants with variable carbon chain length and propoxy groups were tested and compared with each other (Table 4.3). Among all these similar surfactants, C_{12-13}-8PO-SO_4^- was the most promising surfactant. Then this surfactant was tested with alkali (Table 4.2, Table 4.3) to take advantage of reducing anionic surfactant adsorption by increasing pH value. After some modification, a formulation containing 0.889% C_{12-13}-8PO-SO_4^- , 0.111% C_{15-18} IOS, 2% SBA, 0.3% NaOH produced fluid microemulsion phases with solubilization ratios above 10 (Table 3, 8-26; Figure 4. 4).

Other alcohol propoxy sulfates, Petrostep 8B, Petrostep 8C, Petrostep 13B and Petrostep 13C were tested with C_{15-18} IOS and SBA (Table 4.4). All of these surfactants showed viscous microemulsion phase therefore are not tested further. Another alcohol propoxy C_{13}-n PO-SO_4^- was tested with C_{15-18} IOS and SBA, and it showed good performance with fluid microemulsion phase and high solubilization ratio (Table 4.5, 11-74, 11-75, 11-78(2), 11-79(2), Figure 4. 5).

The primary surfactant selected for this research remained C_{16-17}-7PO-SO_4^- with combination of other components such as cosurfactant C_{15-18} IOS and cosolvent SBA in the formulation.

Internal olefin sulfonate, particularly C_{15-18} IOS, was used as the cosurfactant in the majority of the phase behavior experiments. Alcohol propoxy sulfates with a long carbon

chain tail are relatively more hydrophobic than the internal olefin sulfonate (C_{15-18} IOS). The IOS is more hydrophilic than the APS, balancing the solubilization. Increasing the surfactant ratio(S/COS) reduces the optimal salinity because the surfactant is more soluble in the oil phase and may increase the optimal solubilization ratio.

4.2.2 Cosolvent

Alcohol is necessary to meet phase behavior criteria. Alcohol helps to reduce or eliminate viscous phase, accelerate equilibration and increase aqueous solubility of surfactants. The main drawback of adding alcohol is that it lowers the solubilization ratio. Therefore effort was made to reduce alcohol concentration or replace it with other cosolvent/cosurfactant, e.g. alcohol ethoxylate, while maintaining other screening criteria met. Second butyl alcohol (SBA) was a proven cosolvent for light crude oil, and was tested in the preliminary phase behavior study for Wahrman crude oil.

4.2.3 Initial Phase Behavior Results

Various alcohol propoxy sulfates systems were formulated with 1 wt% C_{15-18}IOS and 2 wt% SBA at room temperature (~23 ℃) at S/COS ratios of 3 and 1.67. These solutions were also mixed with Wahrman crude oil (1:1 volume ratio) to determine the optimal salinity. Results are presented Figure 4. 6 in where salinity is plotted against surfactant composition for APS chain lengths of 12-13 and 14-15 with 8PO groups in each surfactant. The results in Figure 4. 6 show that increasing the length of the carbon chain reduces the aqueous phase stability limit (APSL) and optimal salinity (Figure 4. 6), but increases the optimal solubilization ratio. Results in Figure 4. 7 show that increasing the number of propoxy groups increases the APSL and reduces optimal salinity. However,

the surfactant systems in Figure 4. 7, did not meet the criterion that optimal salinity is less than APSL. Neither of the systems in Figure 4. 6, met this criterion.

Developing formulations where the APSL was greater than optimal salinity was the major challenge to develop a surfactant system for Wahrman crude oil.

Figure 4. 8 demonstrates that reducing the carbon chain length, increasing the number of propoxy groups and adding 0.5wt% Na2CO3 led to a surfactant system in which the optimal salinity was less than the APSL while retaining solubilization ratios over 14.

4.2.4 Passing Aqueous Phase Test

The objective of the aqueous phase test was to ensure the integrity of surfactant formulation when injecting it into the reservoir at reservoir temperature. The APSL was not evaluated until the late stage of experiment W5 when the aqueous phase separated into two phases at optimal salinity at room temperature (~23 ℃). The APSL was initially evaluated at room temperature (~23 ℃) because it was believed APSL would improve at elevated temperature. Subsequently it was found out that APSL at reservoir temperature was about 0.5%NaCl lower than APSL at room temperature (Figure 4. 9). Thus, it became apparent that APSL must be evaluated at Wahrman reservoir temperature (43 ℃);

Many combinations of surfactant, cosurfactant and cosolvent met all criteria except APSL. The major problem was that the optimal salinity was consistently higher than the APSL.

Tests were conducted to reduce the optimum salinity below the APSL by increasing surfactant ratio. Optimal salinities decreased but APSL also decreased to the same degree. The criterion was not met by this approach (Figure 4. 10 and Figure 4. 11). Another

primary surfactant (C_{12-13}-8PO-SO_4^-) was selected to meet the aqueous phase test criterion because of its slightly better hydrophilicity than C_{16-17}-7PO-SO_4^- and good microemulsion performance. Formulations with C_{12-13}-8PO-SO_4^- at low surfactant ratio (Table 4.2, 8-1, 8-6) and high surfactant ratio (to achieve low optimal salinity, high alcohol concentration and alkali (NaOH) were required to eliminate viscous phase, Table 4.2, 8-21, 8-22, 6-14, 6-15,) were tested but still failed the aqueous phase test evaluated at room temperature (Figure 4. 11).

A third primary surfactant C_{13}-n-PO-SO_4^- was introduced and tested with SBA. Formulations with this primary surfactant had much lower optimal salinity than formulations with C_{16-17}-7PO-SO_4^- but still barely passed aqueous phase with SBA (Table 4.5, 11-80, 11-89, Figure 4. 12).

The combination of SBA with surfactant C_{16-17}-7PO-SO_4^- and C_{12-13}-8PO-SO_4 failed the aqueous phase test (Figure 4. 9, Figure 4. 10 and Figure 4. 11). The combination of SBA with surfactant C_{13}-n-PO-SO_4^- just barely passed the aqueous phase test (Figure 4. 12) because of the improved hydrophilicity of surfactant with shorter carbon chain length and more PO groups. The gap was reduced or became negative (fail the aqueous phase test) when polymer was added to the formulation.

Glycol ether alcohols, including ethylene glycol butyl ether (EGBE), di-ethylene glycol butyl ether (DGBE) and tri-ethylene glycol butyl ether (TGBE), were introduced in later phase behavior studies to increase the APSL above the optimal salinity. Glycol ether alcohol, with the combination of hydrocarbon chain, ether and alcohol, provides versatile solvency with both polar and non-polar properties. The long hydrocarbon chain resists

solubilizing in water, while ether and alcohol groups promote hydrophilic solubility. This surfactant-like structure provides the compatibility between water and organic solvents, and the ability to couple unlike phases. Surfactant formulations using glycol ether alcohols for the cosolvent easily passed the aqueous phase test. The optimal salinity also increases with more ether groups in the alcohol. Among formulations with surfactant 0.75% C_{16-17}-7PO-SO_4^- , 0.25% C_{15-18} IOS, 1.75% glycol ether alcohols, formulation with TGBE has the highest APSL while formulation with DGBE has the widest gap between APSL and optimal salinity (Figure 4. 13). The ether group improves hydrophilicity and correspondingly reduces the HLB. Therefore more ether groups will decrease the optimal solubilization ratio (Figure 4.13). Among formulations with 0.75% C_{13}-n Ꝑ-SO_4^-, 0.25% C_{15-18} IOS, 1.75% alcohol, 0.5% Na_2CO_3, the gap between APSL and optimal salinity maintains positive all three alcohols (Figure 4. 14). The formulation with DGBE had the lowest solubilization ratio, lower than 10 but the largest gap between APSL and optimal salinity.

The effect of cosolvent was investigated by replacing SBA with glycol ether alcohol. It was much easier to increase APSL above the optimal salinity. Formulations with C_{16-17}-7PO-SO_4^- (Table 4.5, 11-44, 11-45, and 11-46), C_{12-13}-8PO-SO_4^- (Table 4.5, 11-31) and C_{13}-n Ꝑ-SO_4^- (Table 4.5, 11-64, 11-65 and 11-66) all passed the aqueous phase evaluated at reservoir temperature. Modifications like varying surfactant ratio, adding more than one alcohol (Table 4.5, 11-23-S, 11-32, 11-33-S, 11-39, etc.) and varying alcohol concentration (Table 4.5, 11-27, 11-29, 11-30, etc.) were made to increase the gap between APSL and optimal salinity. As noted earlier, DGBE had the widest

APSL/O.S. gap and became the main cosolvent in the later phase behavior studies. These changes are discussed in subsequent sections.

One formulation containing 0.73% C_{16-17}-7PO-SO_4^-, 0.27% % C_{15-18} IOS, 1.46% EGBE,0.29% DGBE, 0.5% Na_2CO_3 was found promising with solubilization ratio of 10 (Figure 4. 15), fast equilibration, about 3 days (Figure 4. 16), fluid microemulsion phase (Figure 4. 17) and APSL/O.S. gap of 0.35% NaCl; another similar formulation containing 0.75% C_{16-17}-7PO-SO_4^-, 0.25% % C_{15-18} IOS, 1.67% EGBE,0.33% DGBE, 0.5% Na_2CO_3 was also promising with solubilization ratio of 13 (Figure 4. 18), fast equilibration, about 3 days (Figure 4. 19), fluid microemulsion phase (Figure 4. 20) and APSL/O.S. gap of 0.35% NaCl. We also found that the value of the APSL may take several days to attain equilibrium as shown in Figure 4. 21.

4.3 Optimization of Surfactant Formulation

Optimization of surfactant formulation selects the best formulation among all the formulations that satisfy all screening criteria. It includes selection of primary surfactant, cosurfactant, cosolvent and the re-design of the formulation with the selected components.

4.3.1 Effect of Surfactant Ratio

Alcohol propoxy sulfates are relatively more hydrophobic therefore stronger oil solubilization ability than the internal olefin sulfonate (C_{15-18} IOS). Therefore increasing the surfactant ratio will reduce the optimal salinity and increase the optimal solubilization ratio (Figure 4. 22 and Figure 4. 23). The degree of reduction in optimal salinity is dependent on each individual surfactant structure, however, the optimal salinity reduces more when increasing surfactant ratio at the low range than at the high range (Figure 4. 11). Alcohol propoxy sulfate is less water soluble than internal olefin sulfonate, therefore

increasing the surfactant ratio will also reduce the APSL. However, formulations with too high surfactant ratio produce viscous or liquid crystal microemulsion phases. Cosurfactant is desirable in surfactant formulation because it has highly branched structure to disturb the orderly interfaces formed by surfactant and oil/water therefore avoid viscous/liquid crystal phases. The effects of increasing the surfactant ratio can be compensated by adding more cosolvent. Nevertheless, this requires much more cosolvent (e.g. SBA) and may still fail the aqueous phase test (Figure 4. 10) and comprise the solubilization ratio. When a surfactant formulation passes aqueous phase test, the gap between the APSL and optimal salinity does not increase much as increasing surfactant ratio, but higher surfactant ratio yielded higher optimal solubilization ratio (Figure 4. 22 and Figure 4. 23). The optimum surfactant ratio should be determined based on appearance of microemulsion and desired optimal salinity. Increasing the surfactant ratio is not an effective way to pass the aqueous phase test or increase the gap between APSL and optimal salinity.

4.3.2 Effect of Surfactant Concentration

Low surfactant concentration is desirable from an economic point of view. Reducing the surfactant concentration can increase the APSL as shown in Figure 4. 24, because more salt can be dissolved in the aqueous phase before causing the surfactant to precipitate. Reducing surfactant concentration also reduces optimal salinity (Figure 4. 24) because less surfactant requires less salt to drive surfactant to the oil phase and solubilize oil in the microemulsion to achieve equal oil and water solubilization ratio. For the surfactant system in Figure 4. 24, the APSL is greater than the optimal salinity for surfactant concentration less than 0.65 wt%. The solubilization ratio does not vary significantly with

surfactant concentration for this system. Lower surfactant concentration tends to produce a more fluid microemulsion phase and faster equilibration. Reducing surfactant concentration is an effective way to pass the aqueous phase test while still maintaining phase behavior performance. However, its capability to displace the oil in core flooding tests may be compromised because of extensive dispersion characteristics during displacement in porous rocks as discussed in Chapter 5.

4.3.3 Effects of Cosurfactant

C_{15-18}IOS was the initial cosurfactant studied and performed well in eliminating viscous phases and adjusting optimal salinity through changing the ratio of primary surfactant/cosurfactant. Other sulfonates were investigated to determine if phase behavior parameters could be improved. C_{20-24}IOS was examined but yielded extra low optimal salinity with low solubilization ratio. Viscous microemulsion phases formed when used as a cosurfactant alone. This surfactant was tested as a secondary cosurfactant with C_{15-18}IOS and DGBE in an attempt to utilize its low optimal salinity. Viscous microemulsion phases appeared after 50 days (Table 4.7, 13-25 to 13-39).

Two alpha olefin sulfonates, Petrostep C5 and Petrostep C1, were tested as cosurfactant but did not form distinct microemulsion phases with C_{16-17}-7PO-SO_4^- and SBA (Table 4.4, 9-1, 9-2, 9-5, 9-6). Therefore, they were not tested further.

Alcohol ethoxylates as cosurfactant had high optimal salinity due to their strong hydrophilicity even with small concentrations (e.g. 0.1%). Two alcohol ethoxylates C_{12-15}-12EO (Neodol 25-12) and C_{12-15}-9EO (Neodol 25-9) were added to surfactant formulation (0.36% C_{16-17}-7PO-SO_4^-, 0.14% C_{15-18}IOS, 1.75% DGBE, 1% Na_2CO_3) for core flood to determine whether the performance of the surfactant formulation could be

improved. The aqueous phase tests failed when either sulfonate was used as a cosurfactant because the optimal salinity increased and the APSL decreased (Table 4.7, 13-1, 13-2, 13-3).

In summary, C_{15-18}IOS was the only good cosurfactant found among the available surfactants and was tested in majority of the phase behavior study in this research.

4.3.4 Effect of Cosolvent Concentration

The disadvantage of adding cosolvent (alcohol) to a surfactant formulation is that the solubilization ratio is reduced. The amount of reduction depends on the surfactant formulation (Figure 4. 25 and Figure 4. 26). Formulations with less alcohol (e.g. 1.25% DGBE) equilibrate slower and have much higher solubilization ratio than formulations with more alcohol (e.g. 1.75% DGBE). However, after the microemulsion phase is equilibrated, the formulation containing 1.25% DGBE had only a slightly higher solubilization ratio than the formulation containing 1.75% DGBE.

Increasing cosolvent concentration affects optimal salinity depending of the hydrophobicity of the cosolvent. For example, increasing SBA reduces optimal salinity and increases APSL, which helps to pass the aqueous phase test (Figure 4. 12 and Figure 4. 25). Glycol ether alcohol because of its strong hydrophilicity increases optimal salinity and APSL at the same time (Figure 4. 26).

4.3.5 Effect of Alkali

The objective of adding alkali to the surfactant formulation is to reduce anionic surfactant adsorption through increasing the pH value therefore reversing the charge on the reservoir rock surface to negative. Sodium hydroxide and sodium carbonate were tested in this research. Na_2CO_3 acts like NaCl in terms of its effect on optimal salinity (Figure 4.

27). NaOH reduces optimal salinity more than Na_2CO_3 but does not help pass the aqueous phase test (Figure 4. 28). NaOH use was discontinued due to scaling problem in the field application.

A pH value higher than 9 is believed to be sufficient to the surface charge of carbonate rocks from positive to negative. A concentration of 0.5wt% Na2CO3 in the surfactant solution could raise the pH value higher than 9. Therefore in later phase behavior study, minimum concentration of 0.5% Na2CO3 was added to each formulation.

Alkali can accelerate microemulsion equilibration, particularly to the formulation with high surfactant ratio. Figure 4. 29 shows addition of 0.3% NaOH helps microemulsion phase equilibrate within 2 days while formulation without alkali takes much longer to equilibrate. Na_2CO_3 has similar effect on equilibration time, though not as dramatic as NaOH.

Another function of alkali (sodium carbonate) is to react with naphthenic acid in the crude oil and produce natural surfactants. Natural surfactants have lower optimal salinity than synthetic surfactant and therefore can reduce optimal salinity below APSL to pass aqueous phase test. The Wahrman crude oil has a, low acid number (0.014g KOH /g) and thus, contains little naphthenic acid. This is verified by phase behavior of Wahrman crude oil systems since sodium carbonate acts like sodium chloride in determining optimal salinity.,

4.3.6 Effect of Polymer

The surfactant formulation must contain polymer to increase its viscosity sufficient to obtain mobility control when displacing oil in the core or reservoir. Phase behavior was

determined for systems meeting Criteria 1-5 by adding polymer to the formulation. It is necessary to determine the APSL, optimal salinity and solubilization ratio after polymer is added to the formulation. The polymers used were partially hydrolyzed polyacrylamide with average molecular weight ranging from 8 MM Dalton to 20 MM Dalton. Figure 4. 30 shows that polymer (FP3530S) concentration changes both optimal salinity and solubilization ratio slightly. Polymers with different molecular weight (FP3330S, FP3430S and FP3530S) and different concentration caused a small change in phase behavior results (Figure 4. 31, Figure 4. 32 and Figure 4. 33). Adding polymer to surfactant formulation can reduce APSL below optimal salinity even though the formulation passes the aqueous phase test before addition of polymer. Reduction of surfactant concentration enabled these formulations to pass aqueous phase stability test.

4.3.7 Effect of Oil Concentration

Optimal salinity, solubilization ratio and the Type III phase boundary change with the ratio of oil to surfactant solution in phase behavior tubes. Oil concentration in the pores of laboratory core or reservoir decreases as oil is continually displaced by the injected surfactants In order to understand the oil displacement process and therefore design a more efficient surfactant formulation, phase behavior data were obtained at different oil concentrations. Oil concentration is the volume fraction of oil in a phase behavior tube before equilibration. The results shown in Figure 4.34, also known as crude oil activity diagram, give us a clear picture that how the phase behavior changes with oil concentration. For this surfactant system, optimal salinity increases while solubilization ratio decreases with decreasing oil concentration. The width of phase Type III window is

constant with varying oil concentration. The optimal salinity stays almost in the middle of the phase Type III window while slight inclines to the lower boundary of the window.

Design of a negative salinity gradient from the downstream (reservoir brine) to the upstream (following polymer drive) of surfactant slug in chemical flood is recommended for high performance of the surfactant slug in the reservoir. This design will increase the chance of surfactant slug passing through the phase Type III region. The negative slope of the phase Type III window is beneficial to the oil displacement because the phase type can transit from Type II to Type III to Type I as salinity/oil saturation decreases as shown by the arrow in Figure 4.34. Achieving phase type I at the end of surfactant slug helps reduce surfactant adsorption, while staying phase III will increase surfactant adsorption. Phase Type III window with positive slope increase the risk of phase type staying at Type III, which is not desirable to reduce surfactant adsorption.

4.3.8 Eliminating Viscous Phases

Even though glycol ether alcohols formulations passed the aqueous phase test, viscous microemulsion phases were formed in some formulations. In the previous section, the two surfactant formulations (Figure 4. 15, Figure 4. 16, Figure 4. 17, Figure 4. 18, Figure 4. 19 and Figure 4. 20) were identified that met all criteria for an efficient system. But after 21 days, both formulations produced viscous phases. The viscous phase appeared below the middle phase microemulsion at salinities below the optimal salinity and the viscous phase deteriorated with time. Photos of the salinity scan after 50 days for these two formulations are shown in Figure 4. 35 and Figure 4. 36. Viscous phases below the optimal salinity are not desirable in that these salinities would be encountered at the rear of the surfactant slug in the mixing zone with the polymer bank when the salinity

gradient concept is being employed. Viscous phases can cause surfactant entrapment in the porous rock and loss of chemical.

Formulation containing C_{13}-n-PO-SO_4^- and glycol ether alcohol produces even worse viscous/liquid crystal phases than C_{16-17}-7PO-SO_4^- (Table 4.5, 11-64, 11-65, 11-66). One modified formulation containing 0.67% C_{13}-n-PO-SO_4^-, 0.33% C_{15-18}IOS, 1.75% SBA and 0.5% Na_2CO_3 (Table 4.5, 11-89, 11-89-2) did not produce viscous phase after even 107 days (Figure 4. 37). The APSL and the optimal salinity both were 4.3% NaCl (Figure 4. 38). There is no gap between APSL and optimal salinity. Addition of polymer to chemical systems for this crude oil decreased the aqueous phase salinity limit (Table 4.5, 11-89-2P) below optimal salinity.

Several parameters were varied in order to find an effective chemical formulation free of viscous phase. For both the C_{16-17}-7PO-SO_4^- system, different cosolvents and different surfactant ratios were tested. It was found that reducing the ratio of the primary surfactant to the cosurfactant usually reduced or eliminated the appearance of viscous phases because the branched structure of cosurfactant disturbing the orderly layers causing viscous phases. Short carbon chain alcohol, e.g. SBA, does not produce viscous phase like glycol ether alcohols.

4.3.9 Optimized Surfactant Formulation

One formulation containing 0.73% C_{16-17}-7PO-SO_4^-, 0.27% wt% C_{15-18}IOS, 1.75wt% DGBE, 0.5wt% Na_2CO_3 met all the phase behavior screening criteria (Table 4.5, 11-71). The difference between the aqueous phase salinity limit and optimum salinity was more than 0.55%, a value that accommodated the addition of polymer. Determination of the optimal salinity and the optimum solubility parameters is shown in Figure 4. 39. Fast

equilibration of this system is shown in Figure 4. 40. No viscous phases were observed in the phase behavior tubes as shown in Figure 4. 41.

4.4 Finalized Surfactant Formulation for Core Flooding

The last step in the phase behavior studies was to determine if the addition of polymer addition to the surfactant slug altered compliance of the surfactant formulation with phase behavior criteria. Salinity scans show the addition of polymer to the promising formulation (0.73% C_{16-17}-7PO-SO_4^-, 0.27% C_{15-18}IOS, 1.75% DGBE, 0.5% Na_2CO_3) lowered the aqueous phase salinity limit to a value below the optimal salinity (Table 4.5, 11-71 and 11-71-3P). However, reduction of the total surfactant concentration to 0.5% was necessary to increase the aqueous phase salinity limit to an acceptable value above the optimal salinity (Table 4.6, 12-7).

Optimal salinity changes with oil concentration as was shown in Figure 4.34. Salinity of surfactant slug designed for chemical flooding should be the optimal salinity at corresponding oil concentration of the core or reservoir before chemical flooding. The typical residual oil saturation after water flood in the laboratory core is 30-40%, however, almost all the phase behavior study in experiment W5-W11, including formulation W11-71, is conducted at oil concentration of 50% (WOR=1). The phase behavior data at oil concentration of 33% (WOR=2) (Table 4.6, 12-33) indicated that the optimal salinity was 5.65%NaCl, slightly lower than the APSL (5.8% NaCl) when polymer was added to the formulation.

The chemical formulation selected for core flooding was W12-33. This formulation met the all phase behavior criteria (1) the aqueous surfactant mixture is one-phase, clear and homogeneous at reservoir temperature meeting the APSL limit, (2) optimal salinity less

than APSL, (3)values of the equilibrium solubilization parameters for both oil and brine are greater than ten (Figure 4. 42); (4) the microemulsion, type III, phase coalesce and equilibrate in less than seven days (Figure 4. 43); (5) absence of viscous phases in the microemulsion (Figure 4. 44); and (6) met Criteria 1-5 when polymer was added to the formulation.

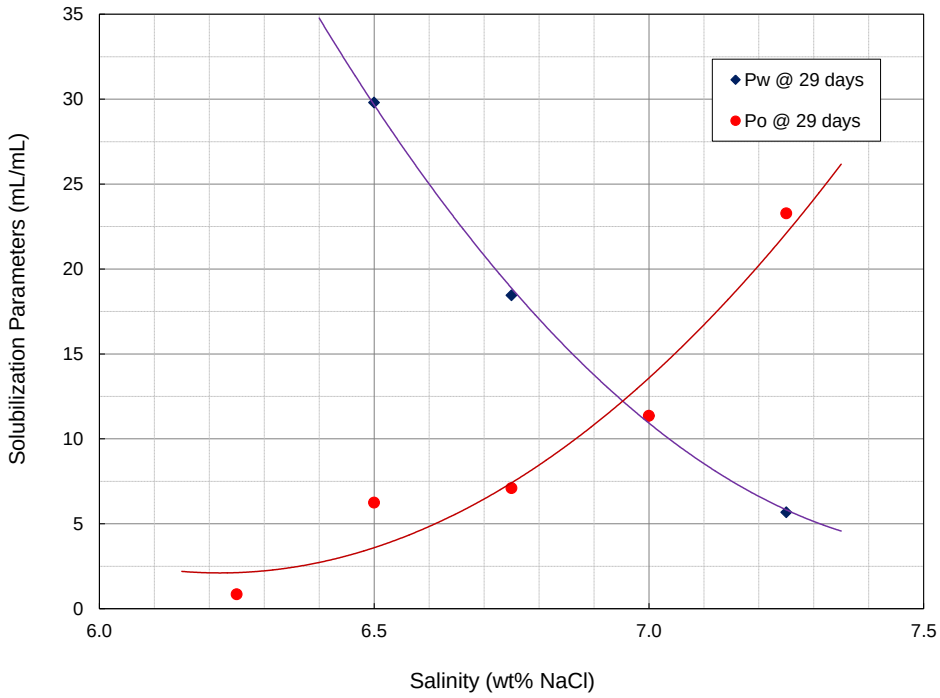

Figure 4. 1 Solubilization ratio plot of W5-17: 0.727% C_{16-17}-7PO-SO_4^-, 0.273% C_{15-18}IOS, 2% SBA at Res T (43 ℃)

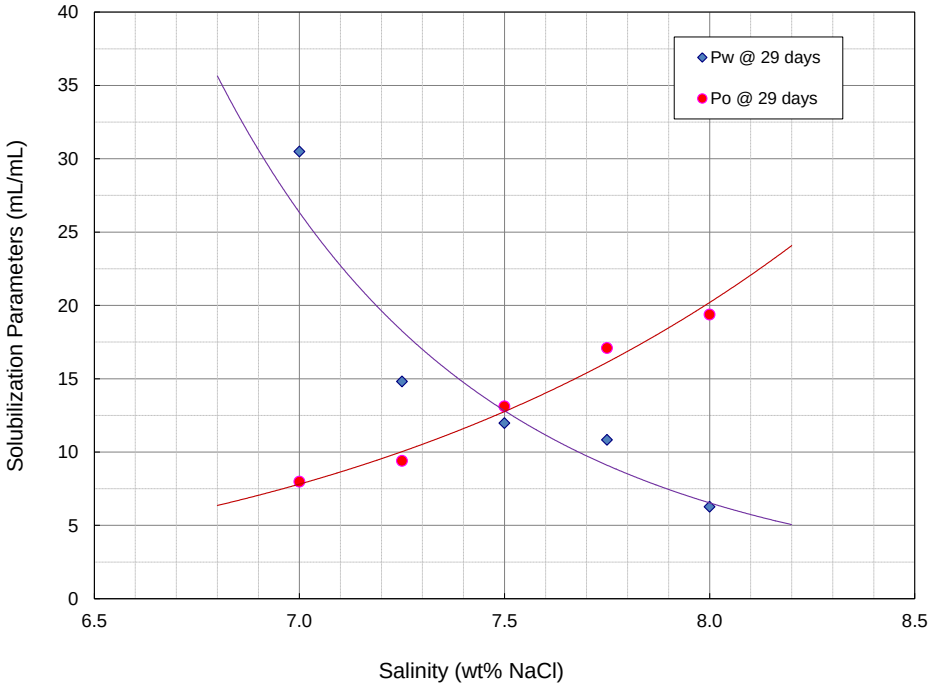

Figure 4. 2 Solubilization ratio plot of W5-18: 0.7 % C_{16-17}-7PO-SO_4^-, 0.3% C_{15-18}IOS, 2% SBA, oil conc.=50%, at Res T (43 ℃).

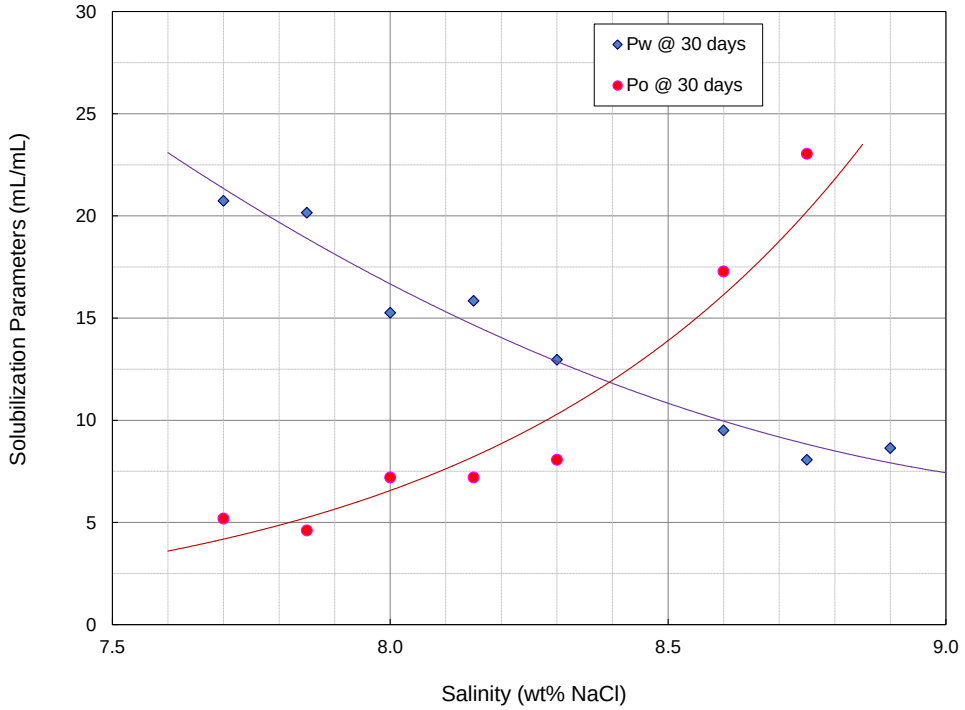

Figure 4. 3 Solubilization ratio plot of W5-19: 0.625 % C16-17-7PO-SO4-, 0.375% C15-18IOS, 2% SBA, oil conc.=50%, at Res T (43 ℃).

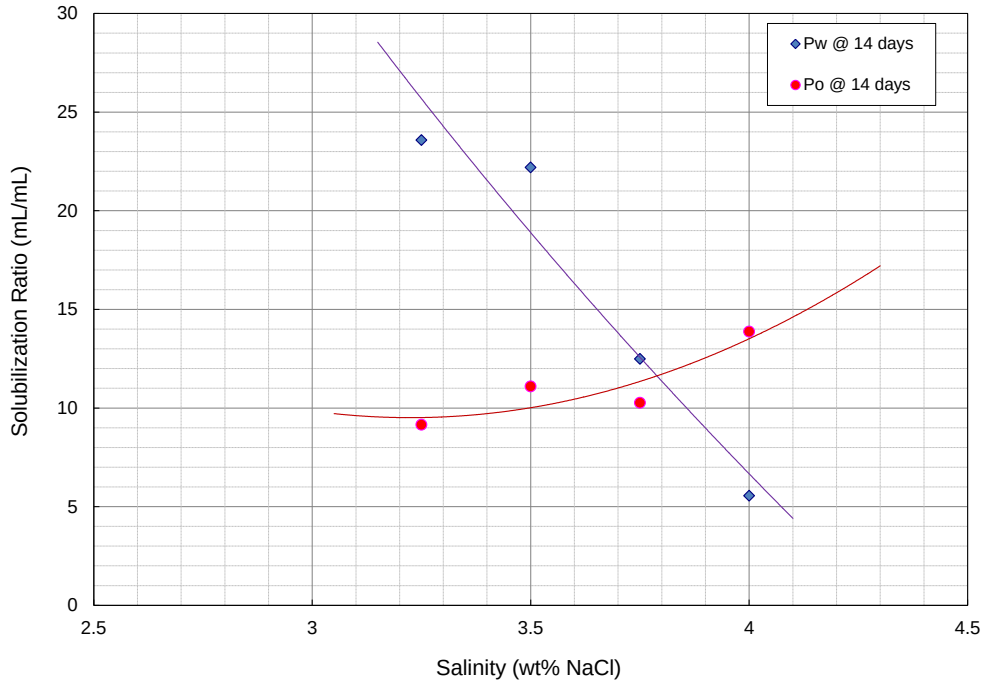

Figure 4. 4 Solubilization plot of W8-26: 0.889% C_{12-13}-8PO-SO_4^-, 0.111% C_{15-18} IOS, 2% SBA, 0.3% NaOH, oil conc.=50% at Res T (43 ℃).

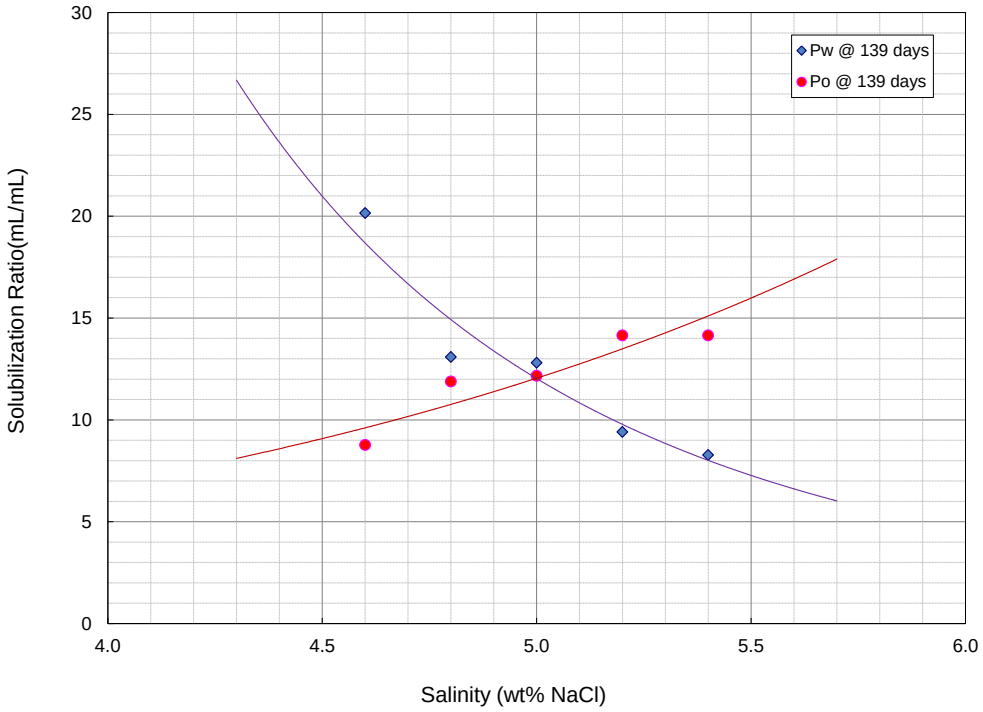

Figure 4. 5 Solubilization plot of W11-78-2: 0.75% C_{13}-n-PO-SO_4^-, 0.25% C_{15-18} IOS, 1.25% SBA, 0.5% Na_2CO_3, oil conc.=50% at Res T (43 ℃).

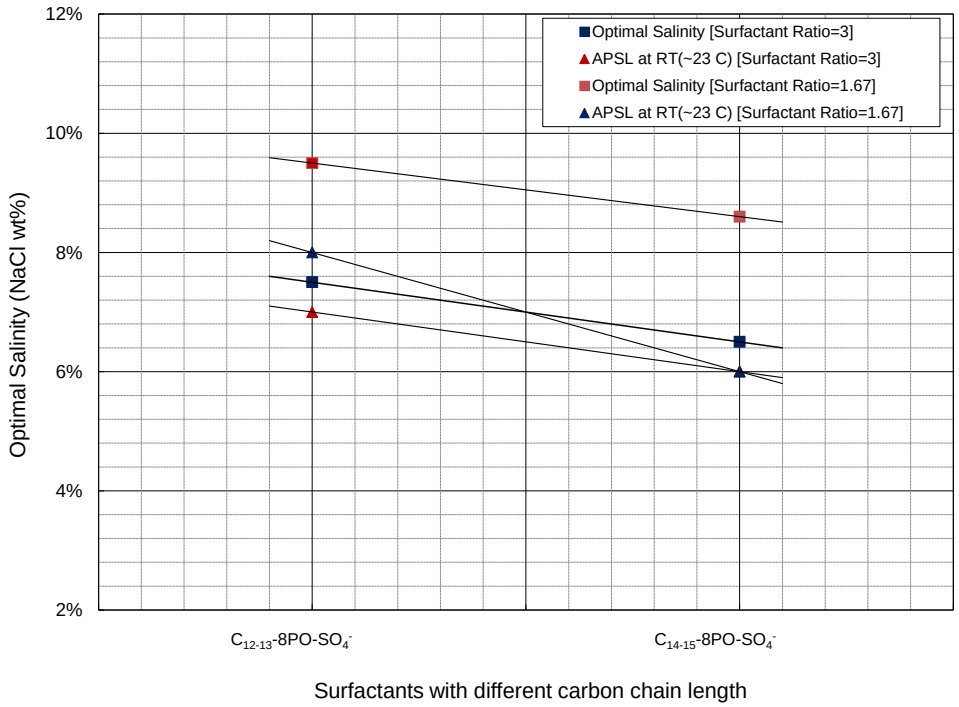

Figure 4. 6 Optimal salinity at 43 ℃ and APSL at RT (~23 ℃) change with carbon chain length of surfactants: primary surf. (indicated in the figure) + co-surf. (C_{15-18}IOS)=1%, 2% SBA, oil conc.=50%.

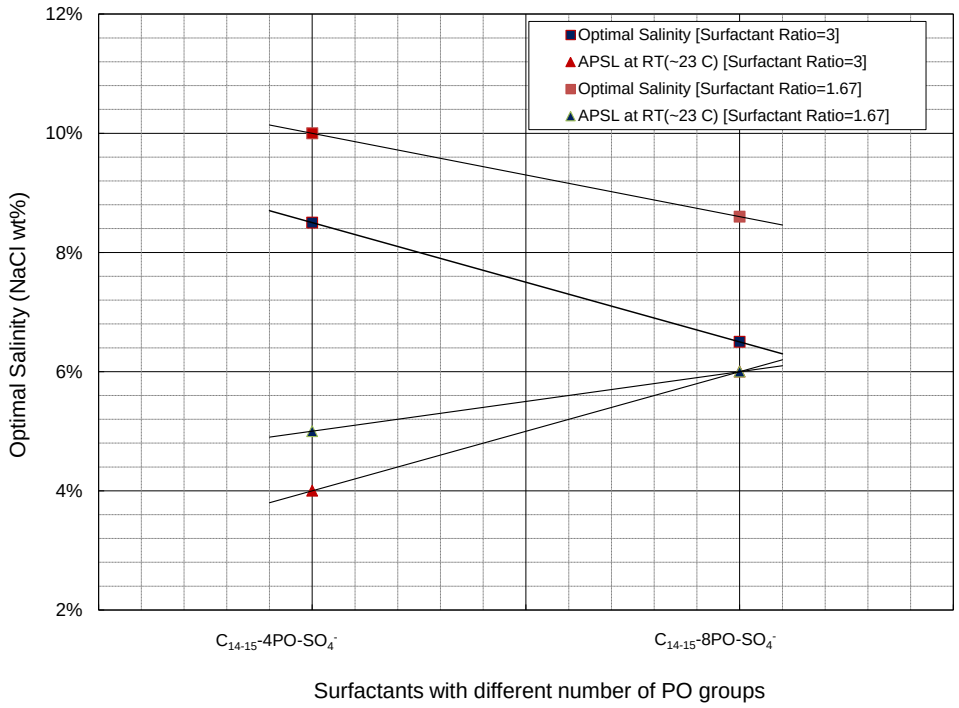

Figure 4. 7 Optimal salinity at Res T (43 ℃) and APSL at RT (~23 ℃) change with different number of PO groups in surfactants: primary surf. (indicated in the figure) + co-surf. (C_{15-18}IOS)=1%, 2% SBA.

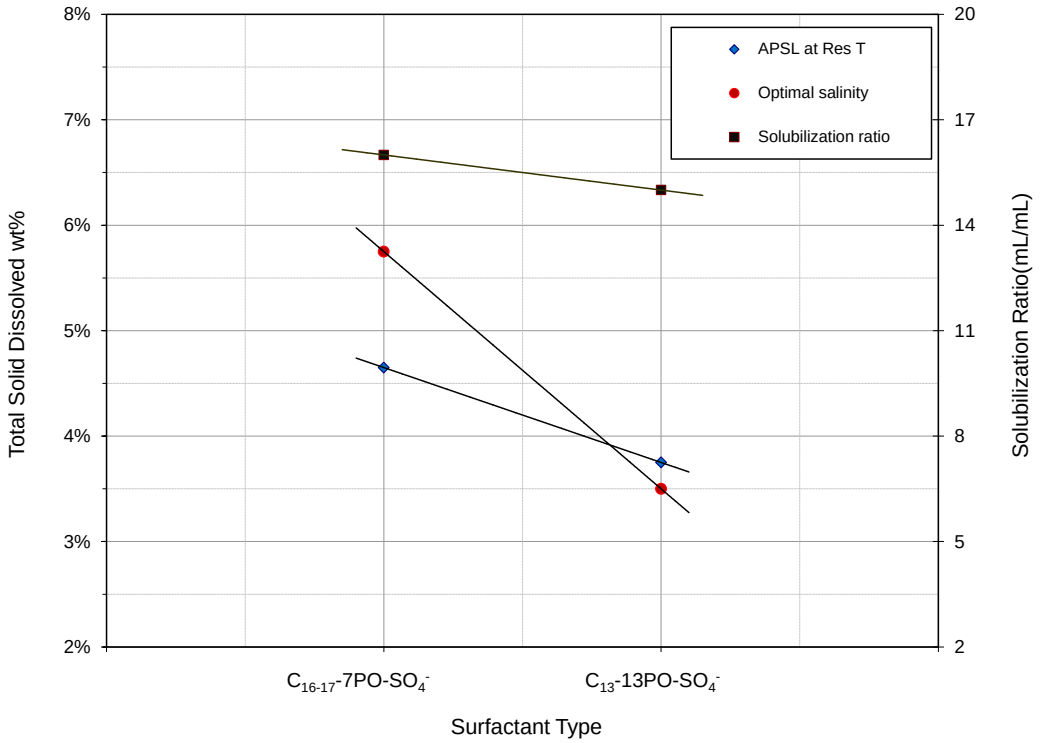

Figure 4. 8 Optimal salinity, solubilization ratio and APSL change with different surfactant type: 0.75% $C_{16\text{-}17}$-7PO-SO_4^-, 0.25% $C_{15\text{-}18}$ IOS, 2% SBA; 0.75% C_{13}-n PO-SO_4^-, 0.25% $C_{15\text{-}18}$ IOS, 2% SBA, 0.5% Na_2CO_3, oil conc.=50%, at Res T(43 ℃).

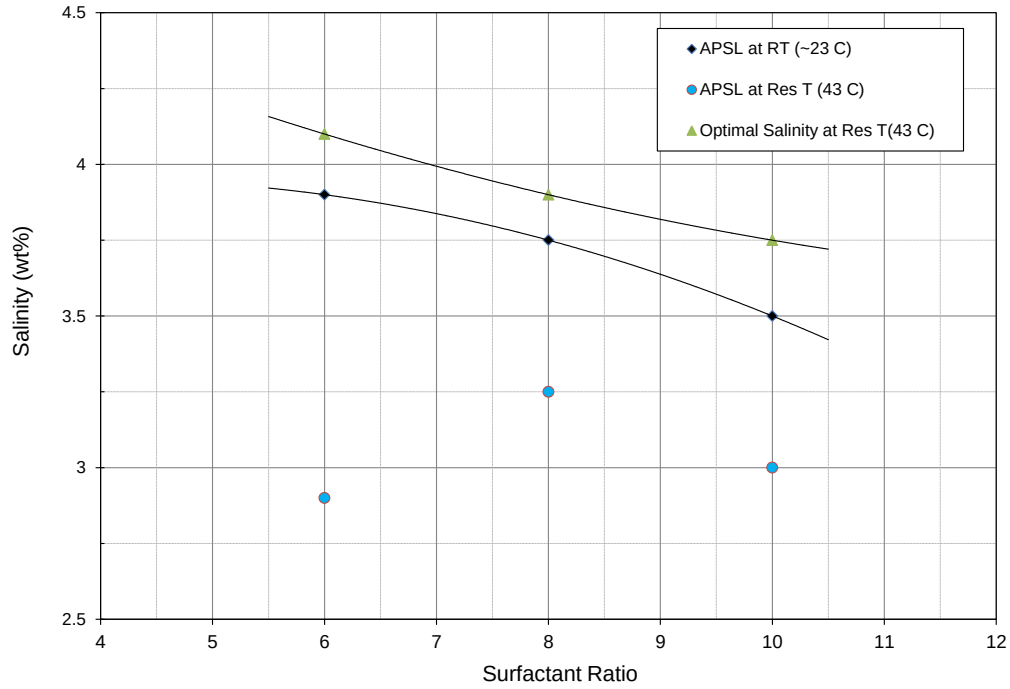

Figure 4. 9 Optimal salinity, APSL at RT (23 ℃) and at Res T (43 ℃) change with surfactant ratio: $C_{12\text{-}13}$-8PO-SO_4^- (primary surf.)+ $C_{15\text{-}18}$ IOS (co-surf.)=1%, 2.5% SBA.

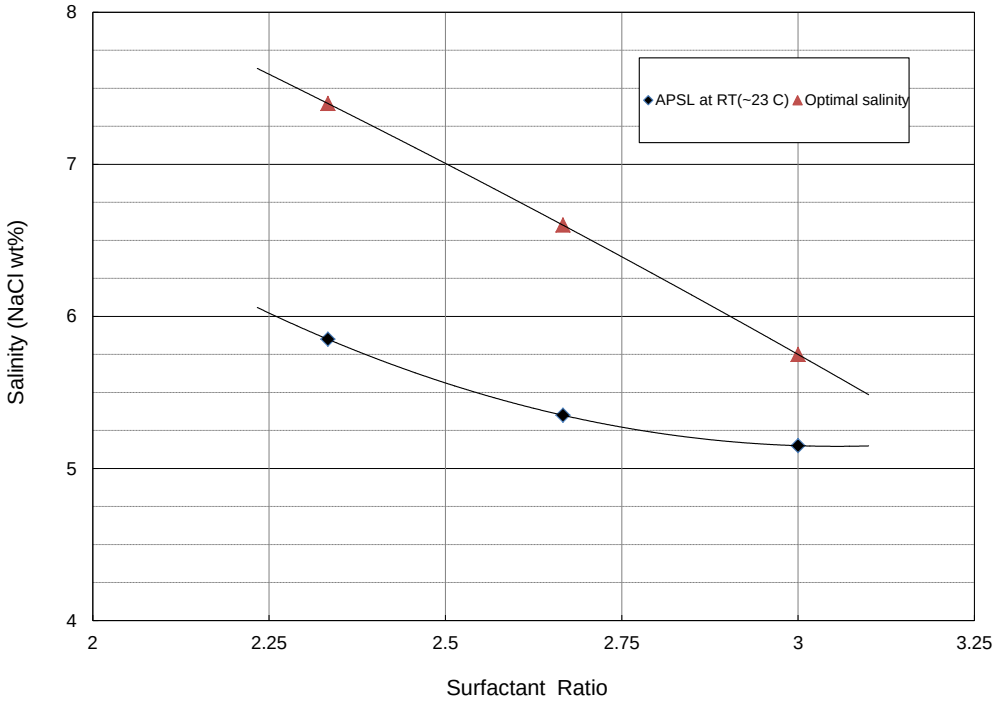

Figure 4. 10 Optimal salinity and APSL change with surfactant ratio: $C_{16\text{-}17}$-7PO-SO_4^- (primary surf.)+ $C_{15\text{-}18}$ IOS (co-surf.) =1%, 2% SBA, oil conc.=50%, at Res T(43 ℃).

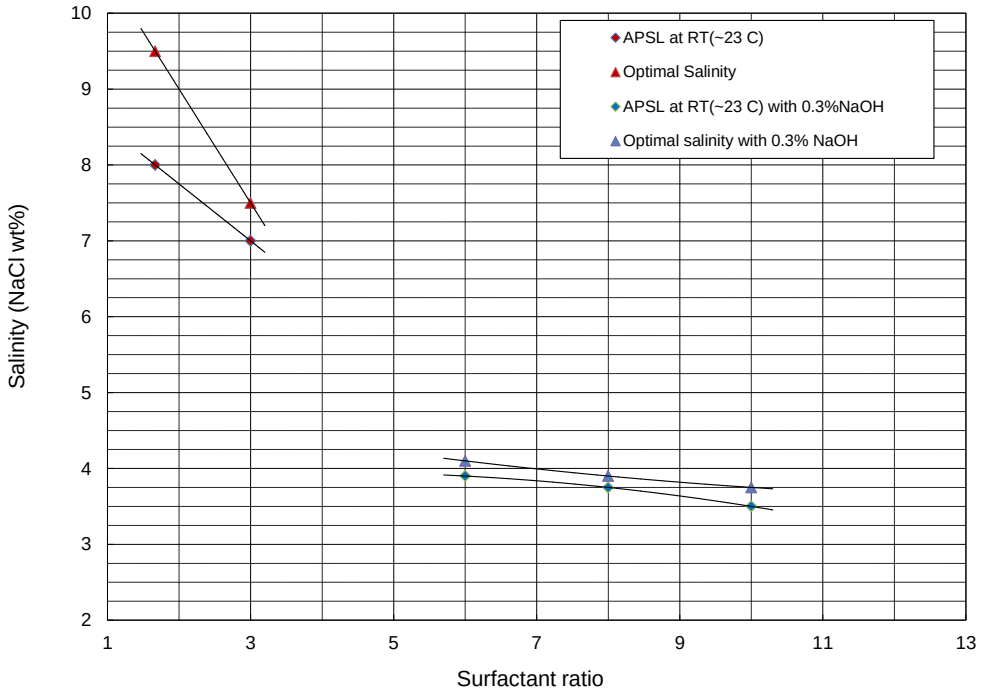

Figure 4. 11 Optimal salinity at Res T(43 ℃), APSL at RT (23 ℃) change with surfactant ratio: 0.889% $C_{12\text{-}13}$-8PO-SO_4^-, 0.111% $C_{15\text{-}18}$ IOS, 2.5% SBA, oil conc.=50%.

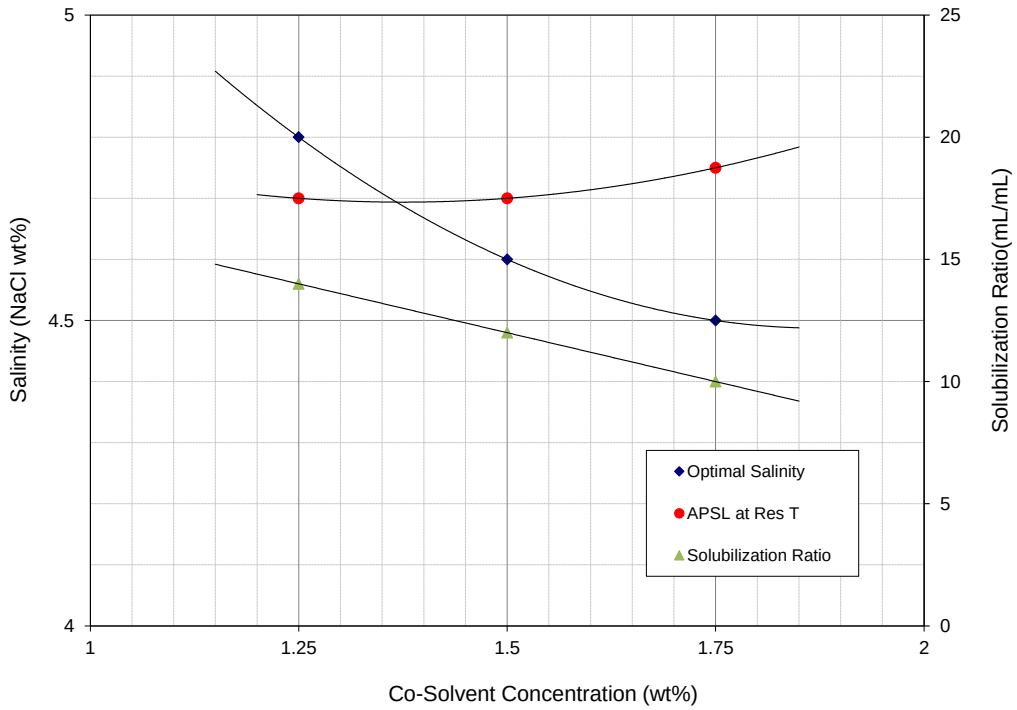

Figure 4. 12 Optimal salinity, solubilization ratio and APSL change with cosolvent (SBA) conc.: 0.625% C_{13}-n ÞPO-SO_4^-, 0.375% $C_{15\text{-}18}$IOS, 0.5% Na_2CO_3, oil conc.=50% at Res T(43 ℃).

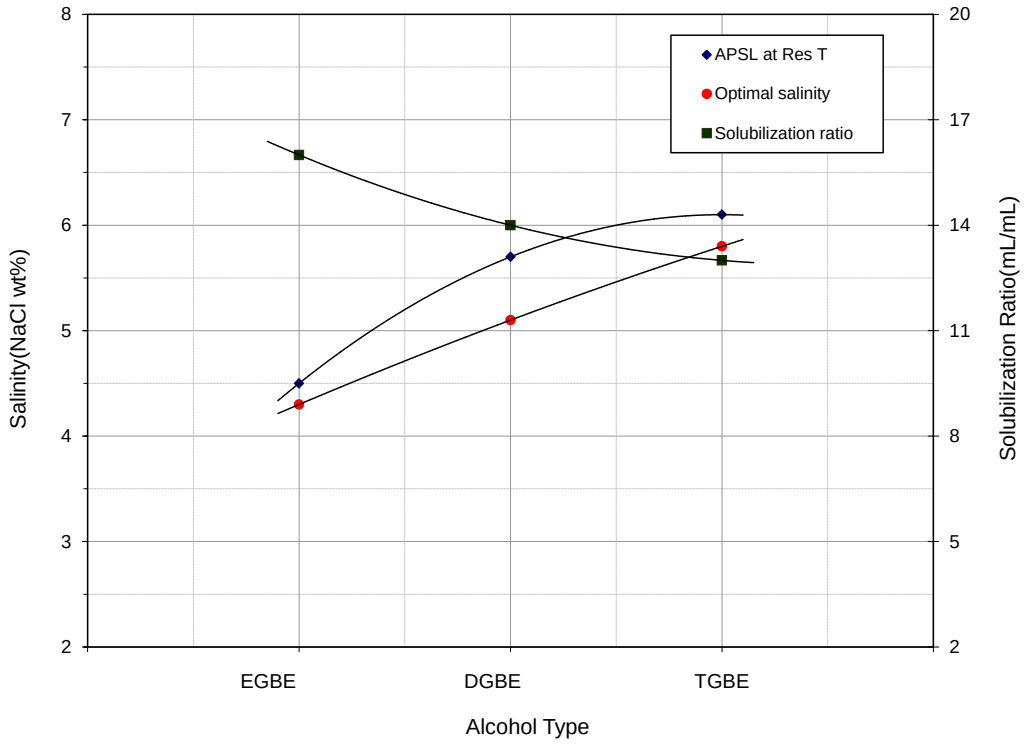

Figure 4. 13 Optimal salinity, solubilization ratio and APSL change with different glycol ether alcohol type: 0.75% $C_{16\text{-}17}$-7PO-SO_4^- , 0.25% $C_{15\text{-}18}$IOS, 1.75% alcohol, 0.5% Na_2CO_3, oil conc.=50% at Res T(43 ℃).

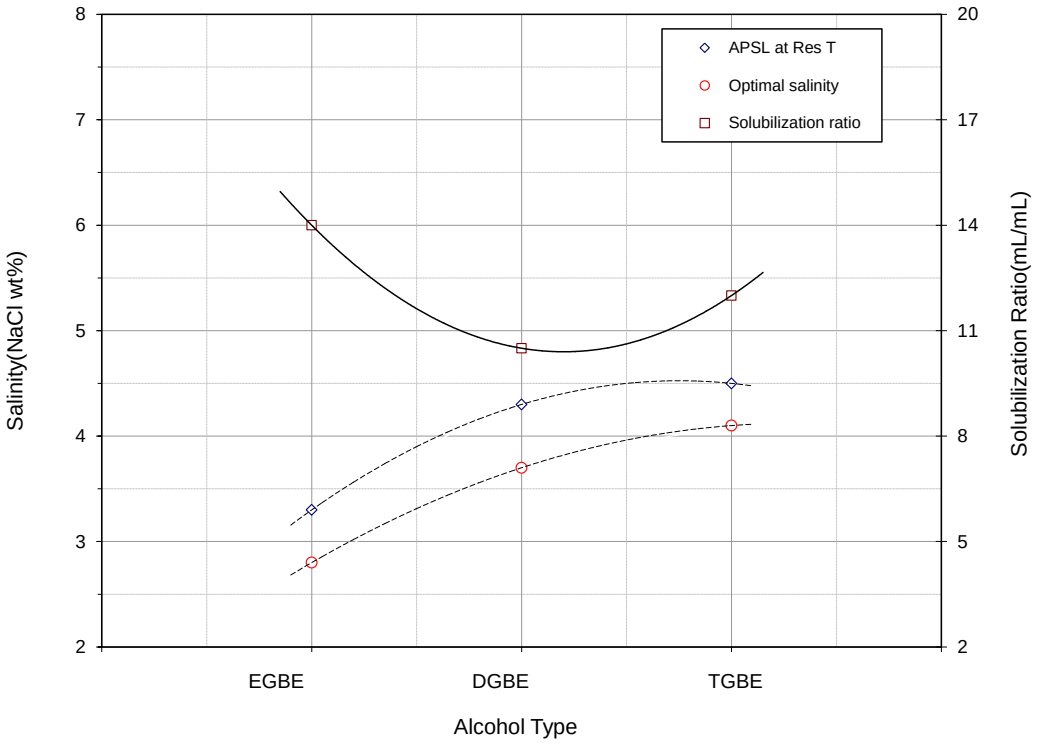

Figure 4. 14 Optimal salinity, solubilization ratio and APSL change with different alcohol type: 0.75% C_{13}-n PO-SO_4^-, 0.25% $C_{15\text{-}18}$ IOS, 1.75% alcohol, 0.5% Na_2CO_3, oil conc.=50% at Res T(43 ℃).

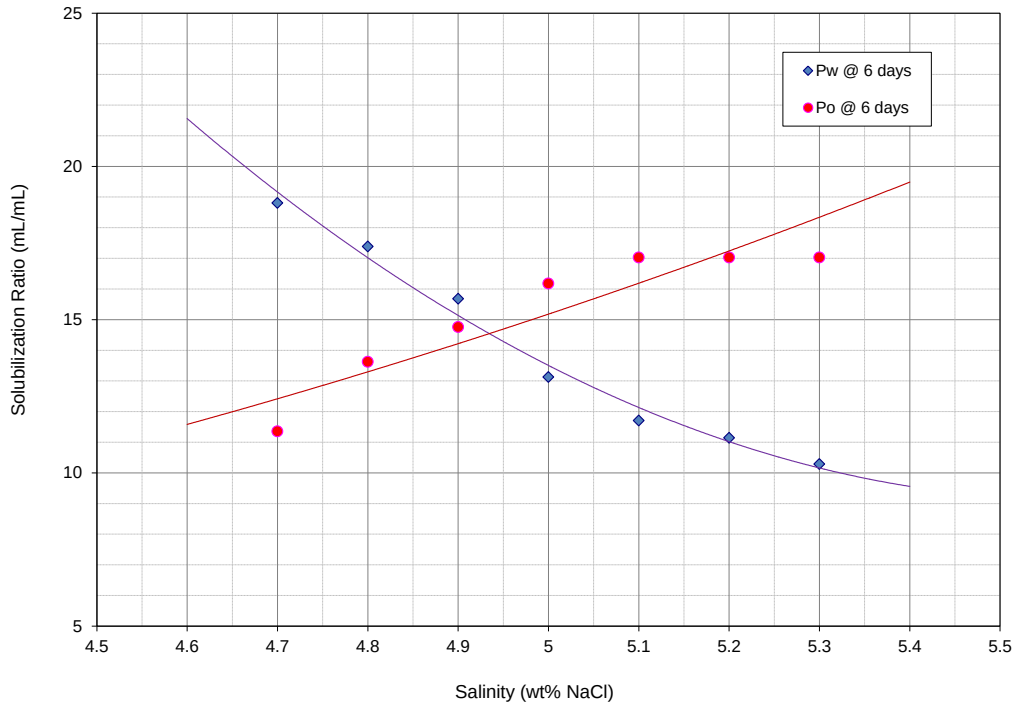

Figure 4. 15 Solubilization plot of W11-33-5: 0.73% C_{16-17}-7PO-SO_4^-, 0.27% % C_{15-18}IOS, 1.46% EGBE, 0.29% DGBE, 0.5% Na_2CO_3, after 6 days, oil conc.=50% at Res T (43 ℃).

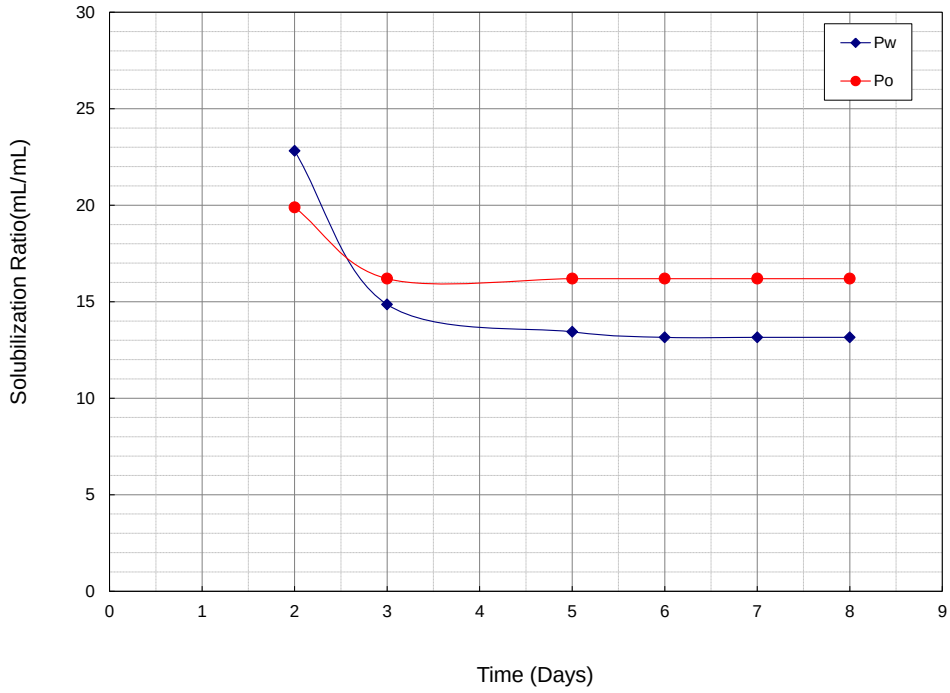

Figure 4. 16 Equilibration time of W11-33-5: 0.73% C_{16-17}-7PO-SO_4^-, 0.27% C_{15-18} IOS, 1.46% EGBE, 0.29% DGBE, 0.5% Na2CO3, after 6 days, oil conc.=50% at Res T (43 ℃).

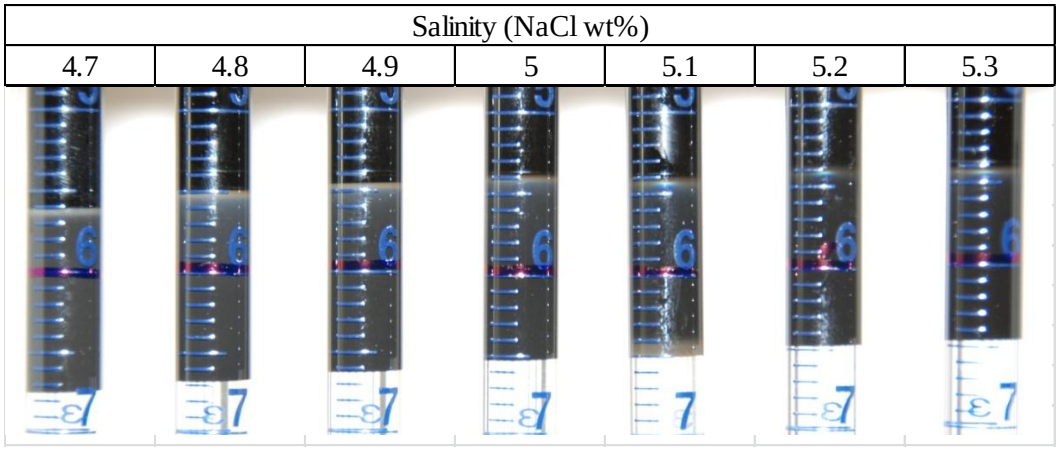

Figure 4. 17 Photo of W11-33-5: 0.73% C_{16-17}-7PO-SO_4^-, 0.27% C_{15-18} IOS, 1.46% EGBE, 0.29% DGBE, 0.5% Na_2CO_3, after 6 days, oil conc.=50% at Res T (43 ℃).

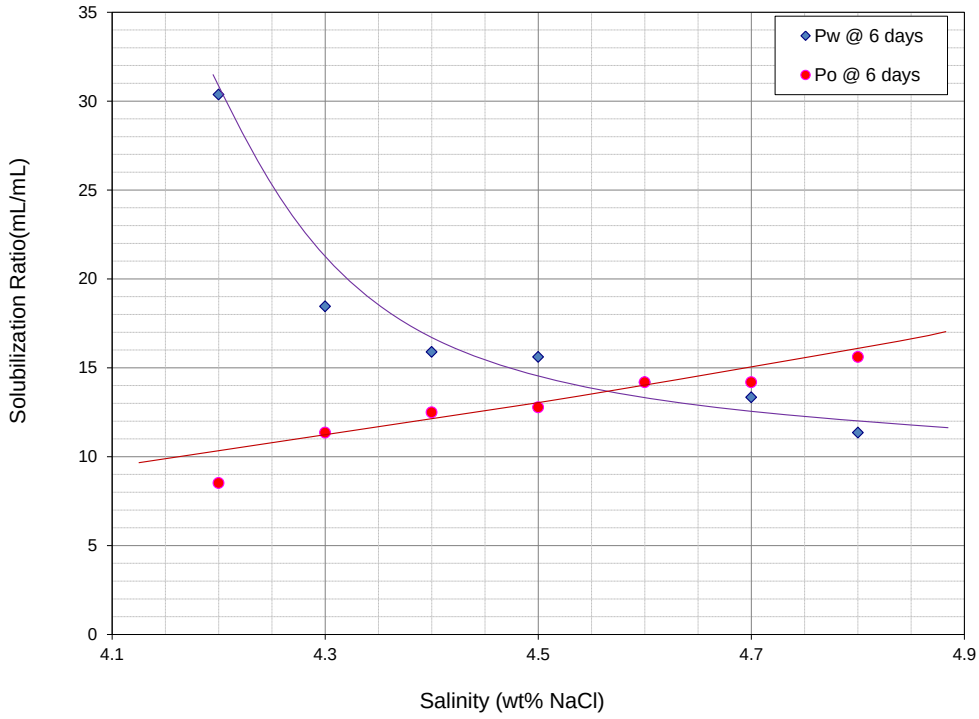

Figure 4. 18 Solubilization plot of W11-34-3: 0.75% $C_{16\text{-}17}$-7PO-SO_4^-, 0.25% $C_{15\text{-}18}$ IOS, 1.67% EGBE, 0.33% DGBE, 0.5% Na_2CO_3, after 6 days, oil conc.=50% at Res T (43 ℃).

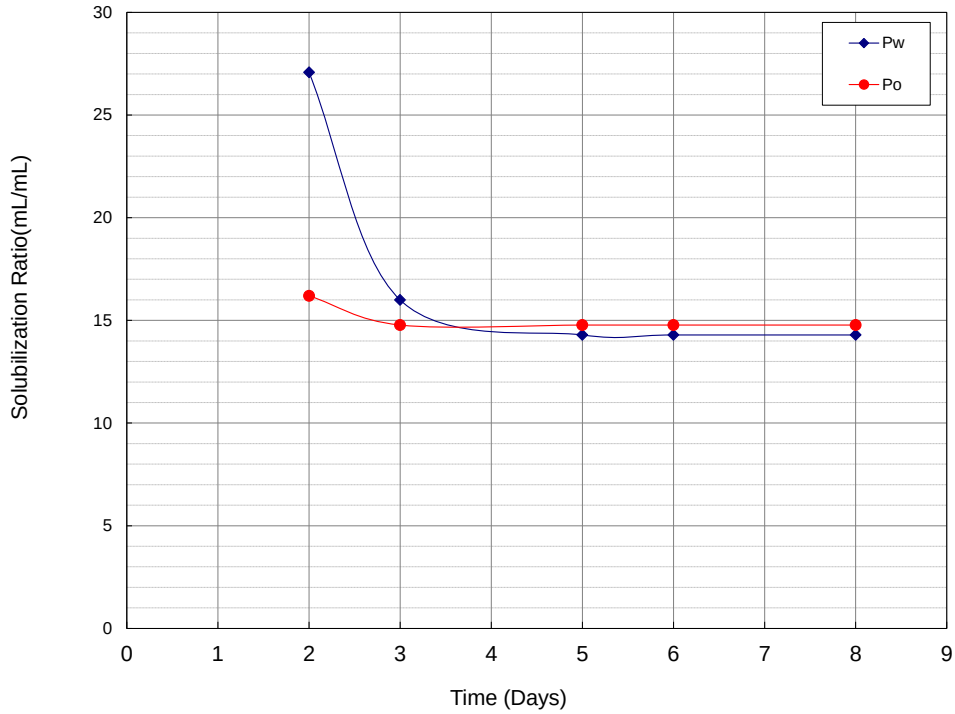

Figure 4. 19 Equilibration time of W11-34-3: 0.75% $C_{16\text{-}17}$-7PO-SO_4^-, 0.25% $C_{15\text{-}18}$ IOS, 1.67% EGBE, 0.33% DGBE, 0.5% Na_2CO_3, after 6 days, oil conc.=50% at Res T (43 ℃).

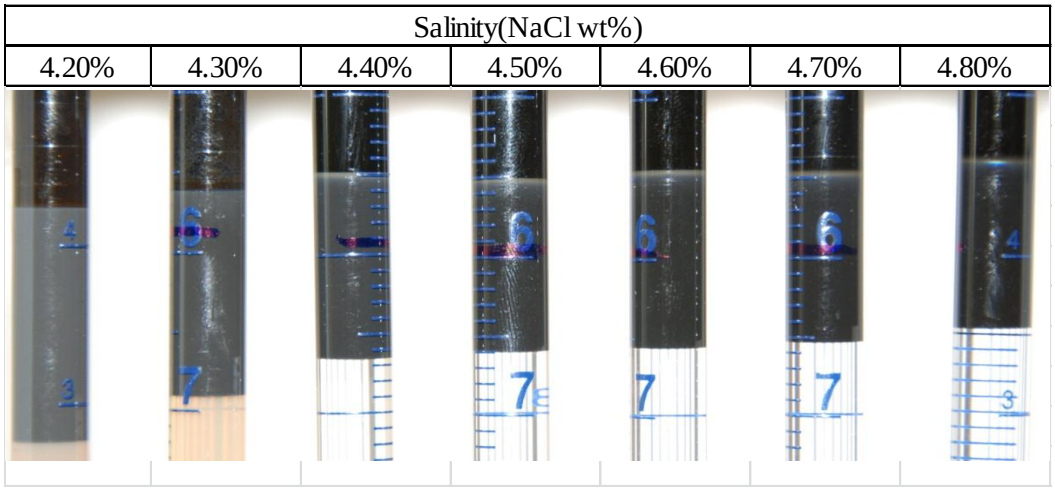

Figure 4. 20 Photo of W11-34-3: 0.75% C_{16-17}-7PO-SO_4^-, 0.25% C_{15-18} IOS, 1.67% EGBE, 0.33% DGBE, 0.5% Na_2CO_3, after 6 days, oil conc.=50% at Res T (43 ℃).

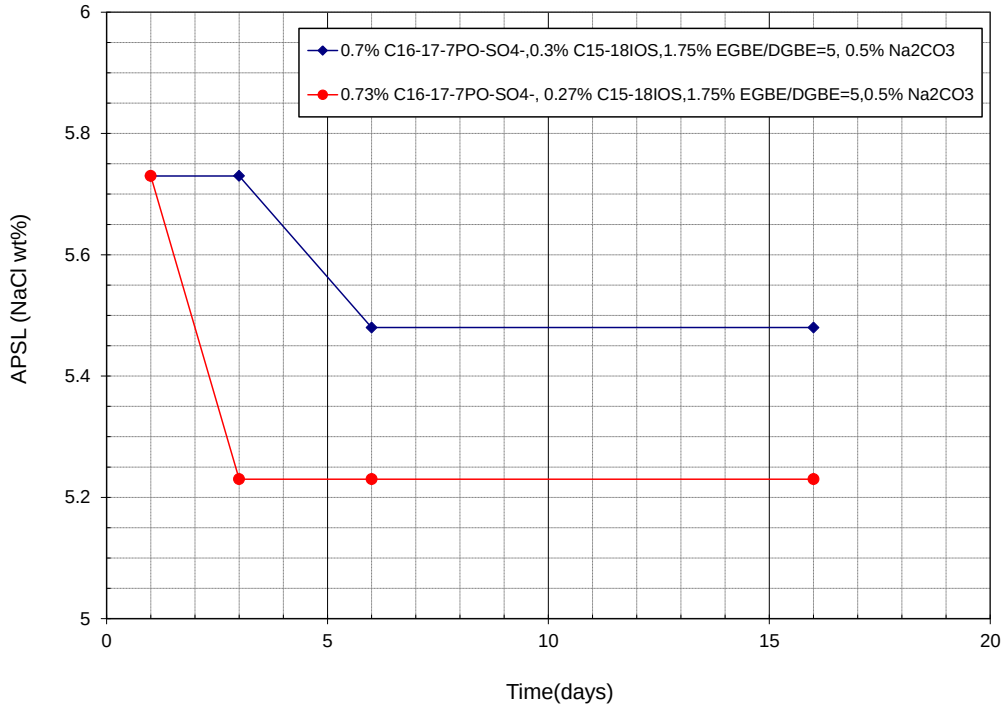

Figure 4. 21 APSL at Res T (43 ℃) changes with time for two typical surfactant formulations.

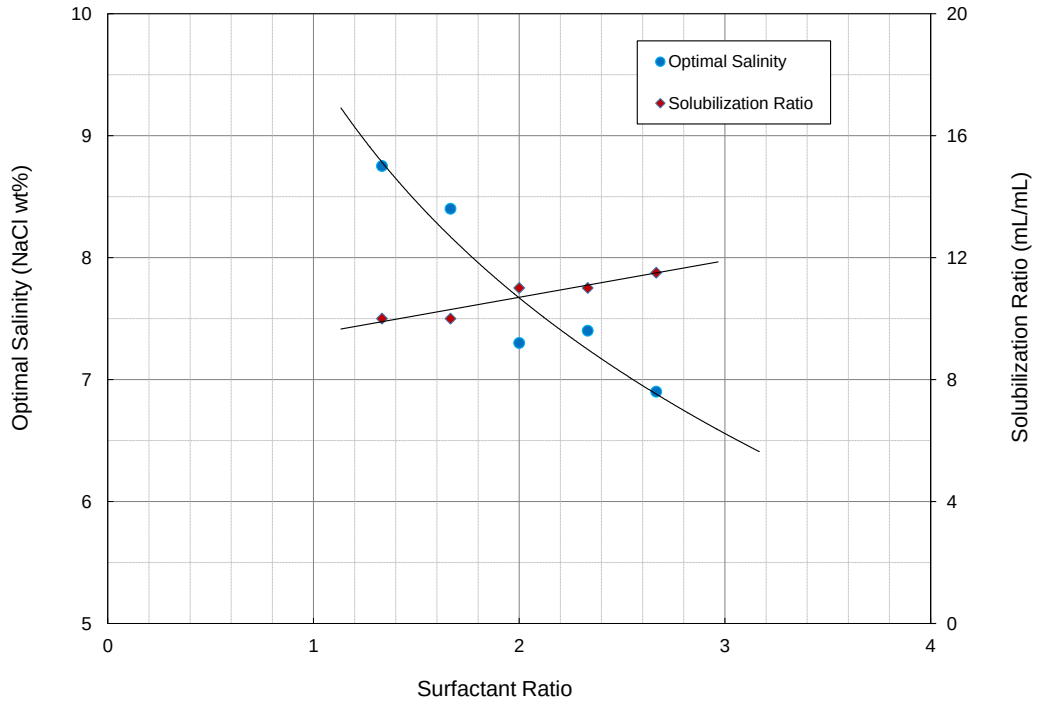

Figure 4. 22 Optimal salinity and solubilization ratio change with surfactant ratio: $C_{16\text{-}17}$-7PO-SO_4^- (primary surf.) + $C_{15\text{-}18}$ IOS (co-surf.) =1%, 2% SBA, oil conc.=50% at Res T (43 ℃).

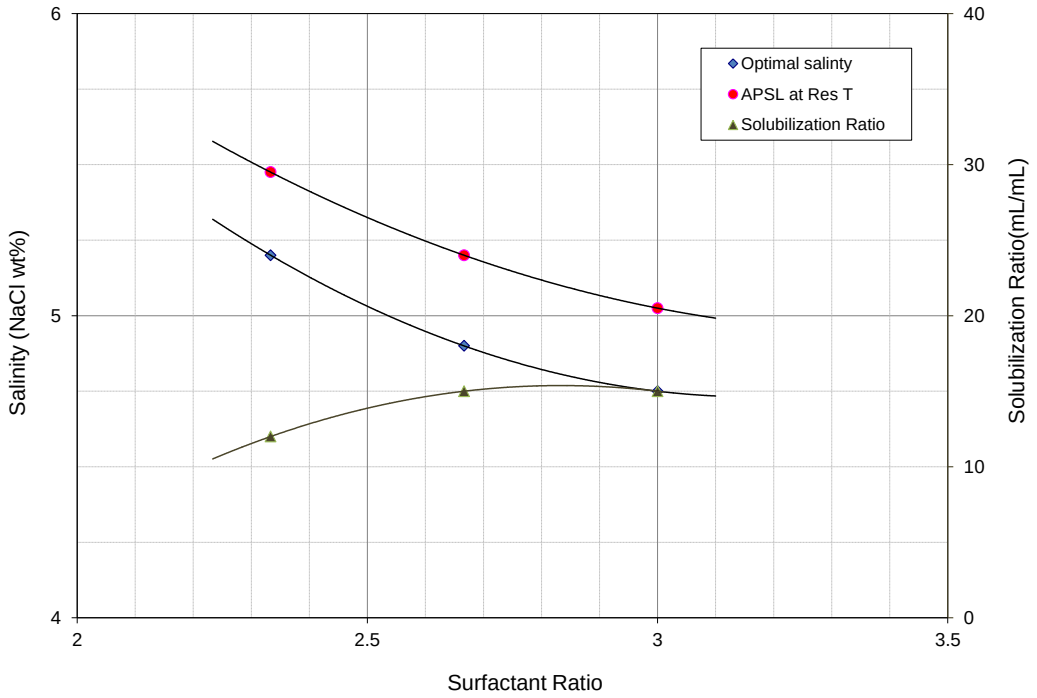

Figure 4. 23 Optimal salinity, solubilization ratio and APSL at Res T (43C) change with surfactant ratio: $C_{16\text{-}17}$-7PO-SO_4^- (primary surf.) + $C_{15\text{-}18}$ IOS (co-surf.) =1%, 1.46% EGBE, 0.29% DGBE, 0.5% Na_2CO_3, oil conc.=50% at Res T (43 ℃).

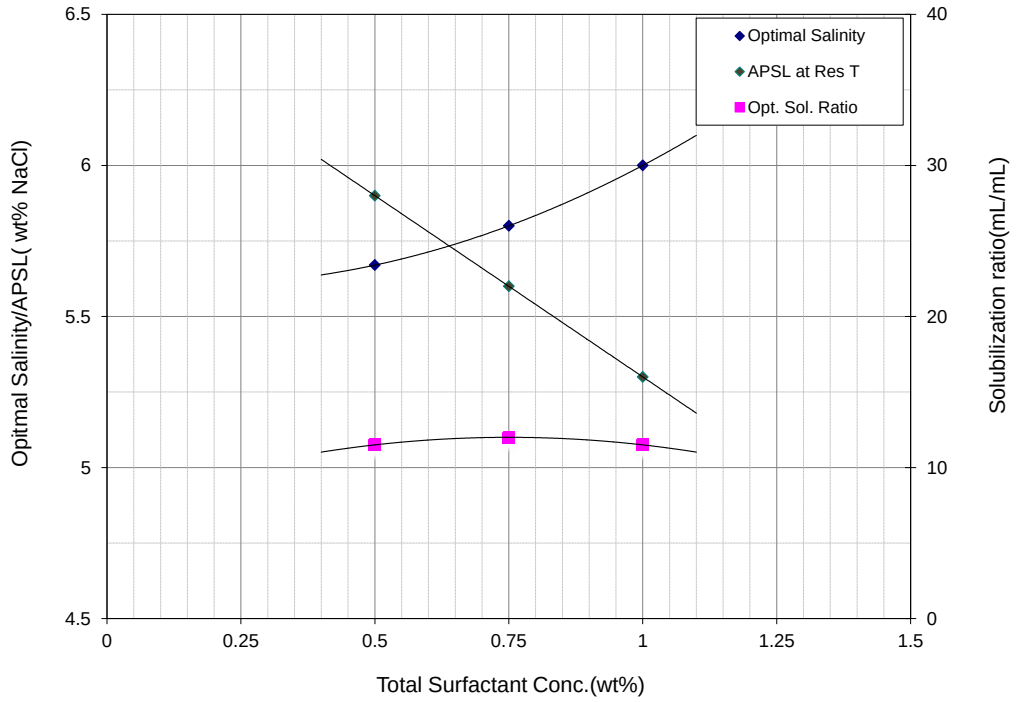

Figure 4. 24 Optimal salinity, solubilization ratio and APSL at change with total surfactant conc.: 0.36% $C_{16\text{-}17}$-7PO-SO_4^-, 0.14% $C_{15\text{-}18}$ IOS=2.67, 1.75% DGBE, 1% Na_2CO_3, 1800ppm FP3530S, oil conc.=33% at Res T (43 ℃).

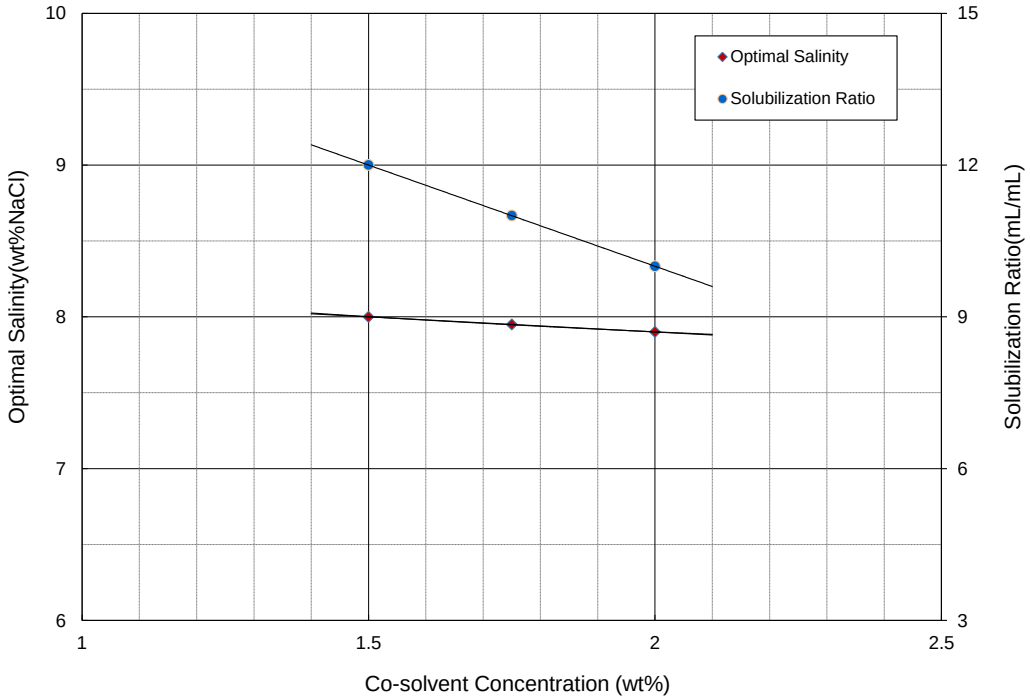

Figure 4. 25 Optimal salinity and solubilization ratio change with cosolvent (SBA) concentration: 0.625 % $C_{16\text{-}17}$-7PO-SO_4^-, 0.375% $C_{15\text{-}18}$IOS, oil conc.=50% at Res T (43 ℃).

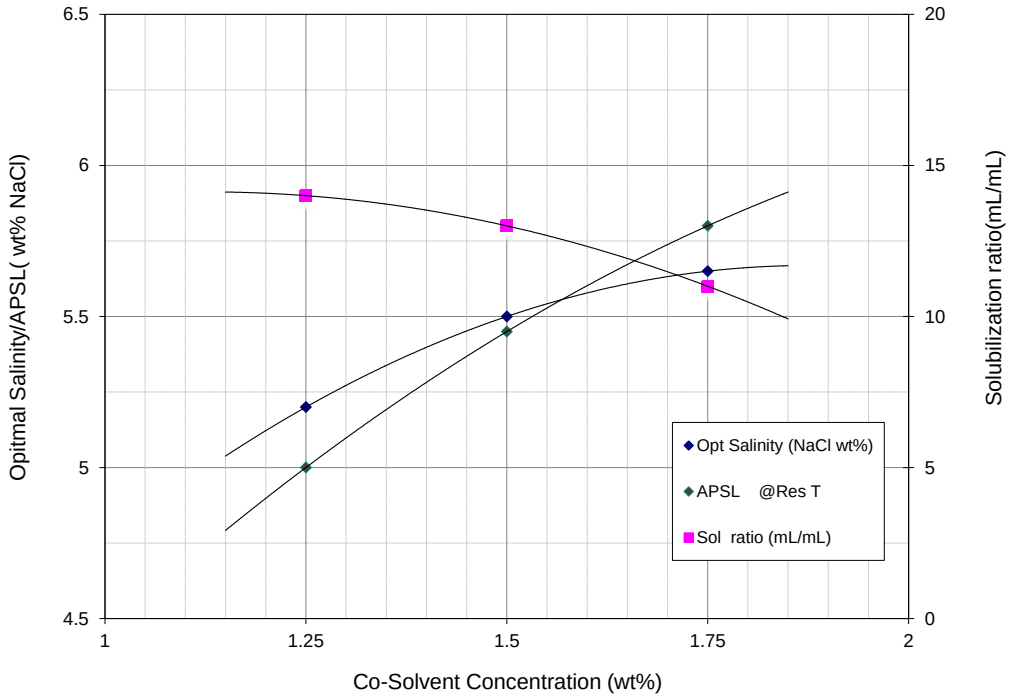

Figure 4. 26 Optimal salinity, solubilization ratio and APSL change with cosolvent (DGBE) conc.: 0.36% $C_{16\text{-}17}$-7PO-SO_4^- , 0.14% $C_{15\text{-}18}$ IOS , 1% Na_2CO_3, 2300ppm FP3530S, oil conc.=33% at Res T (43 ℃)

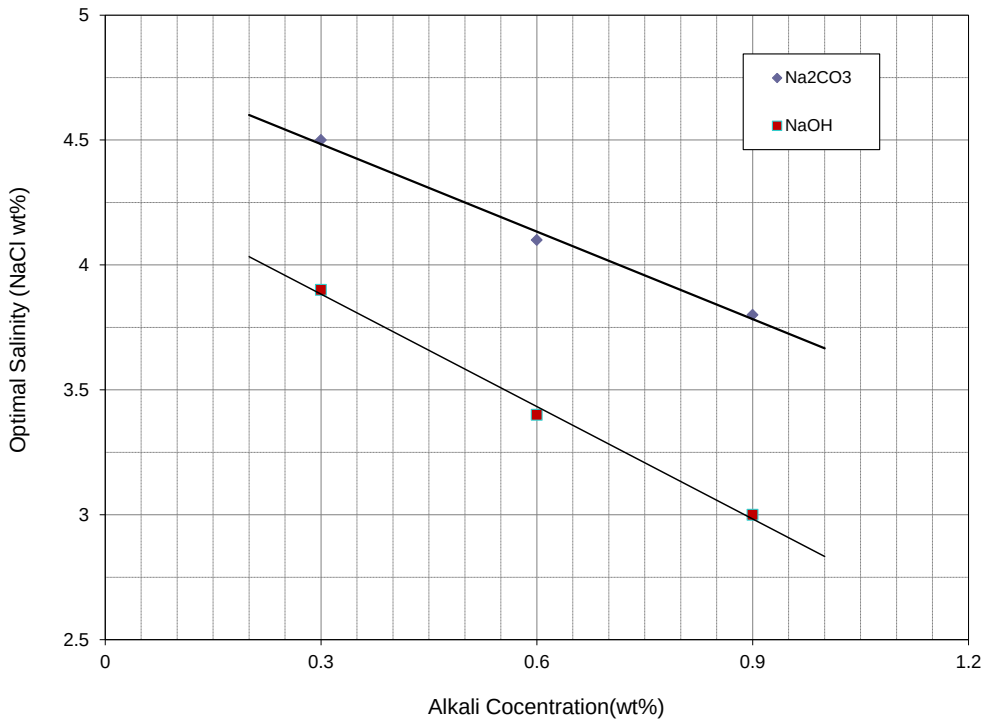

Figure 4. 27 Different alkali effect on optimal salinity: all series contains 0.889% C_{12-13}-8PO-SO_4^-, 0.111% C_{15-18}IOS, 2.5% SBA with variable alkali concentration, oil conc.=50% at Res T (43 ℃).

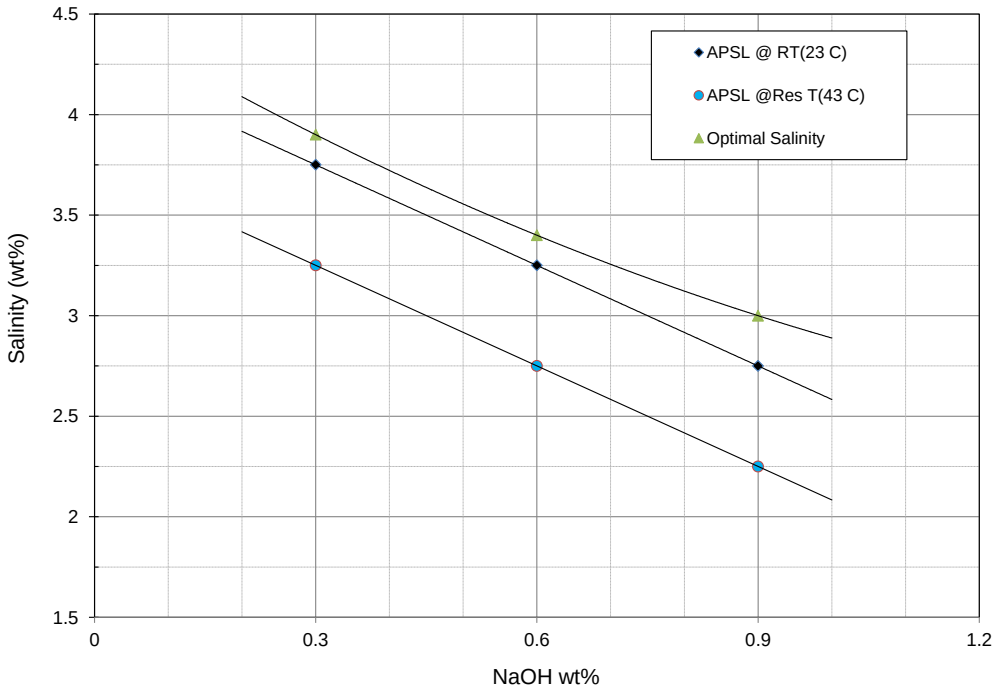

Figure 4. 28 Optimal salinity, APSL at RT (23 ℃) and at reservoir temperature (43 ℃) change with NaOH conc.: 0.889% $C_{12\text{-}13}$-8PO-SO_4^-, 0.111% $C_{15\text{-}18}$IOS, 2% SBA, oil conc.=50%.

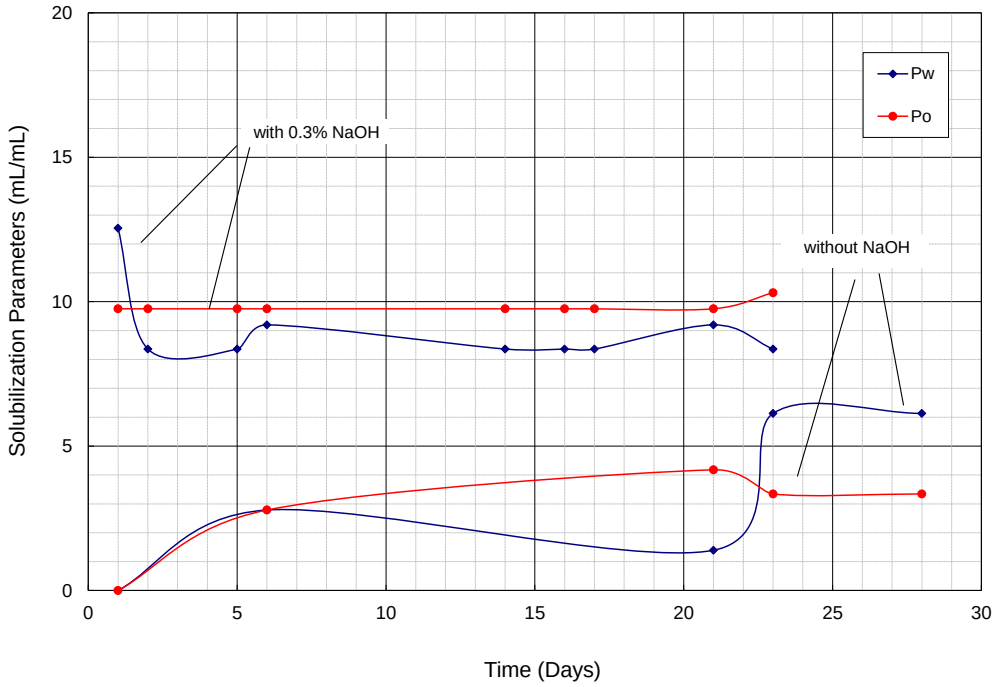

Figure 4. 29 Alkali (NaOH) effect on equilibration time: both series contains 0.857% $C_{12\text{-}13}$-8PO-SO_4^-, 0.143% $C_{15\text{-}18}$IOS, 2% SBA, oil conc.=50%, at Res T (43 ℃).

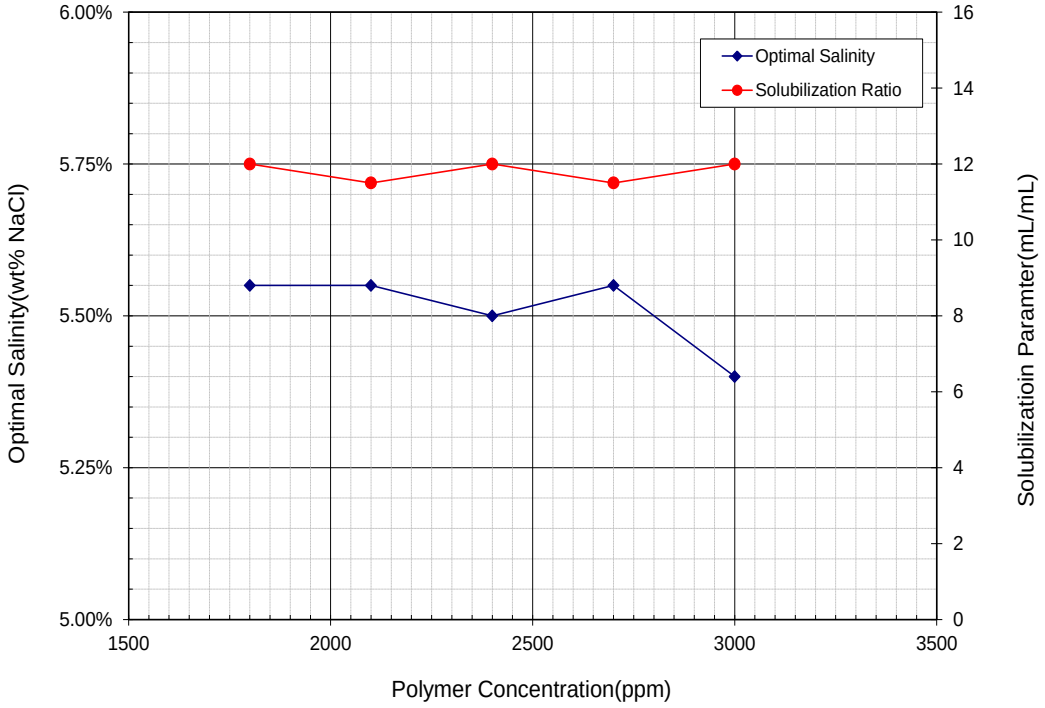

Figure 4. 30 Optimal salinity and optimal solubilization ratio of series with different polymer (FP3530S) conc.: 0.36% $C_{16\text{-}17}$-7PO-SO_4^-, 0.14% $C_{15\text{-}18}$IOS, 1.75% DGBE, 1% Na_2CO_3 after 16 days, oil conc.=33% at Res T (43 ℃).

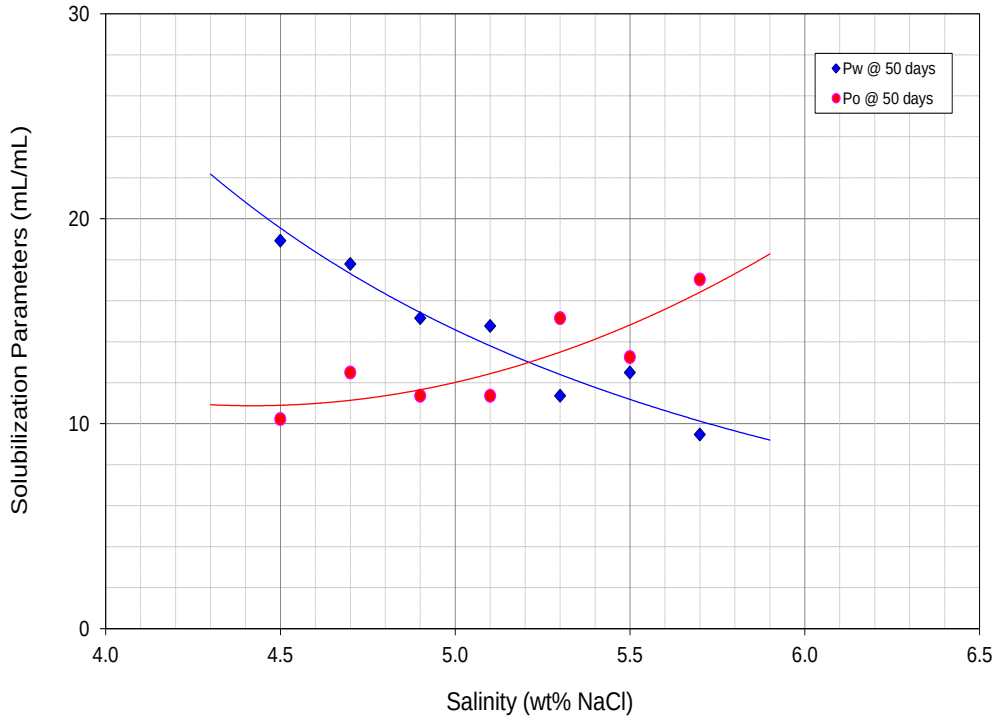

Figure 4. 31 Solubilization plot of W12-18: 0.36% $C_{16\text{-}17}$-7PO-SO_4^-, 0.14 % $C_{15\text{-}18}$ IOS, 1.75% DGBE, 1% Na_2CO_3, 2600ppm FP3330S after 50 days, oil conc.=33% at Res T (43 ℃).

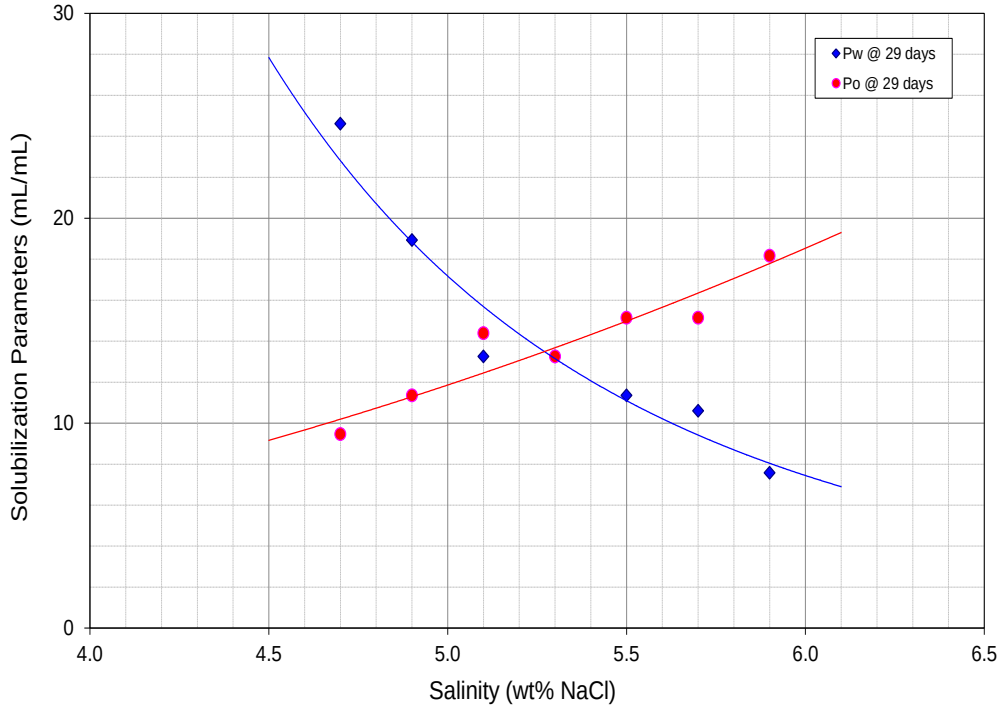

Figure 4. 32 Solubilization plot of W12-19: 0.36% $C_{16\text{-}17}$-7PO-SO_4^-, 0.14 % $C_{15\text{-}18}$ IOS, 1.75% DGBE, 1% Na_2CO_3, 2000ppm FP3530S after 29 days, oil conc.=33% at Res T (43 ℃).

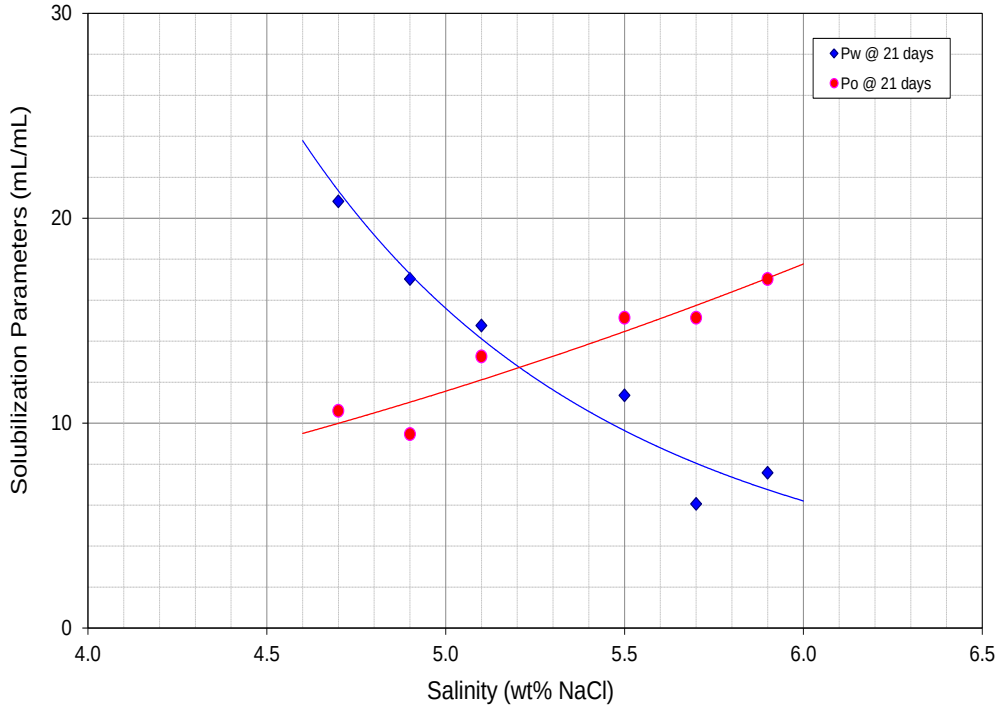

Figure 4. 33 Solubilization plot of W12-20: 0.36% C_{16-17}-7PO-SO_4^-, 0.14% C_{15-18} IOS, 1.75% DGBE, 1% Na_2CO_3, 2000ppm FP3430S after 21 days, oil conc.=33% at Res T (43 ℃).

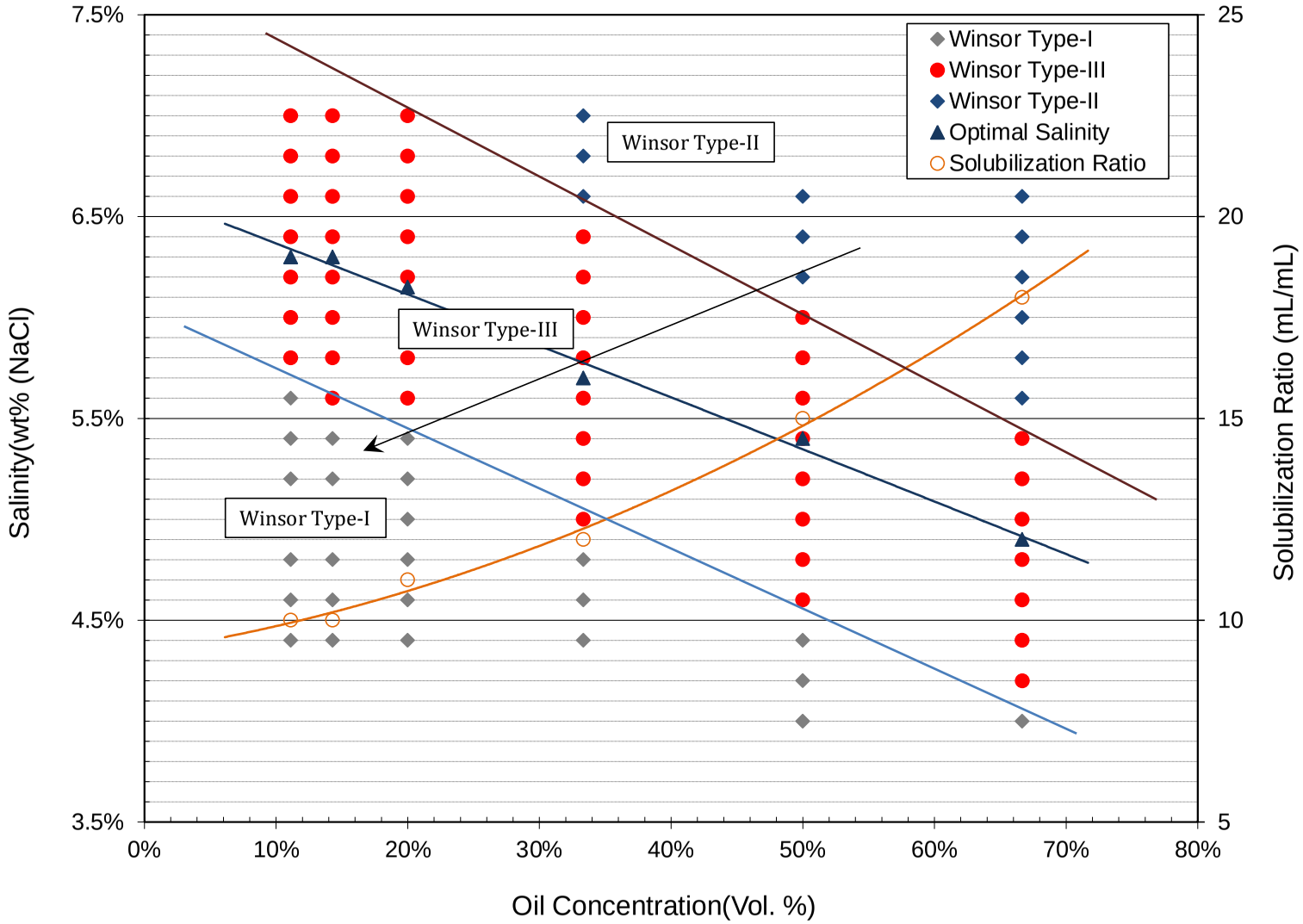

Figure 4. 34 Wahrman crude oil activity diagram: 0.36% $C_{16\text{-}17}$-7PO-SO_4^-, 0.14%, $C_{15\text{-}18}$IOS, 1% Na_2CO_3, oil conc.=33% at Res T (43 ℃).

Salinity (NaCl wt%)						
4.7	4.8	4.9	5	5.1	5.2	5.3

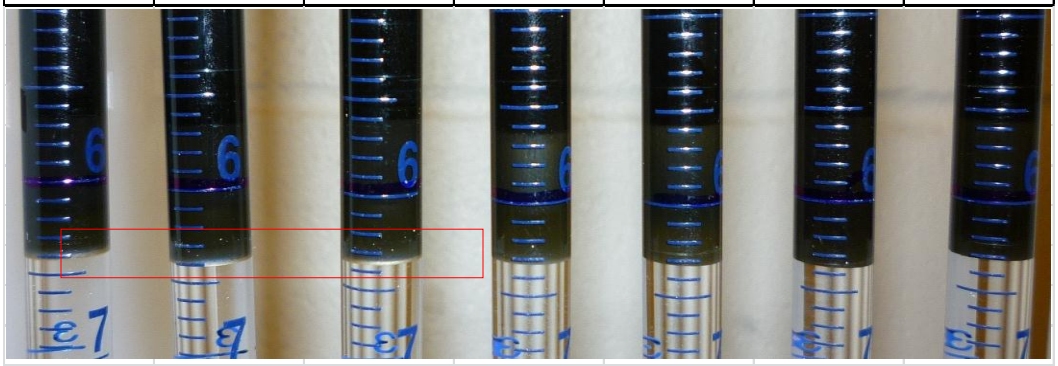

Figure 4. 35 Photo of W11-33-5: 0.73% C_{16-17}-7PO-SO_4^-, 0.27% C_{15-18} IOS, 1.46% EGBE, 0.29% DGBE, 0.5% Na_2CO_3, after 50 days, oil conc.=50% at Res T (43 ℃).

Salinity(NaCl wt%)						
4.20%	4.30%	4.40%	4.50%	4.60%	4.70%	4.80%

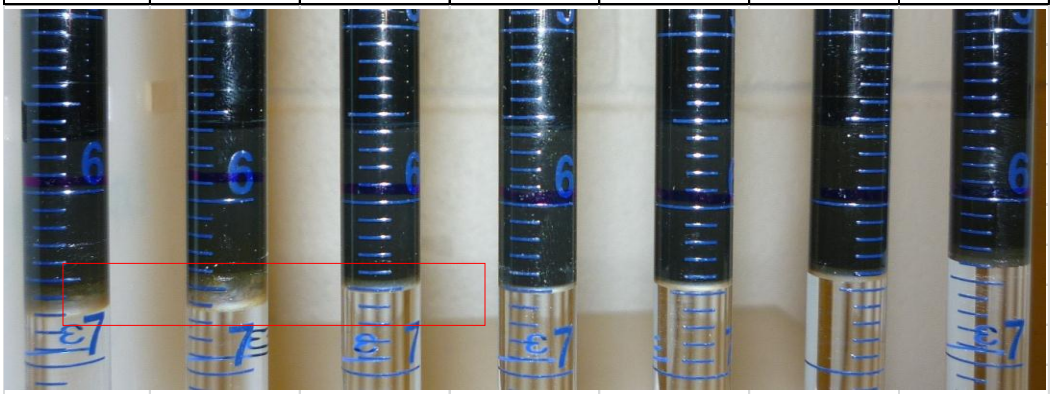

Figure 4. 36 Photo of W11-34-3: 0.75% C_{16-17}-7PO-SO_4^-, 0.25% C_{15-18} IOS, 1.67% EGBE, 0.33% DGBE, 0.5% Na_2CO_3, after 50 days, oil conc.=50% at Res T (43 ℃).

Salinity (NaCl wt%)						
3.60	3.80	4.00	4.20	4.40	4.60	4.80

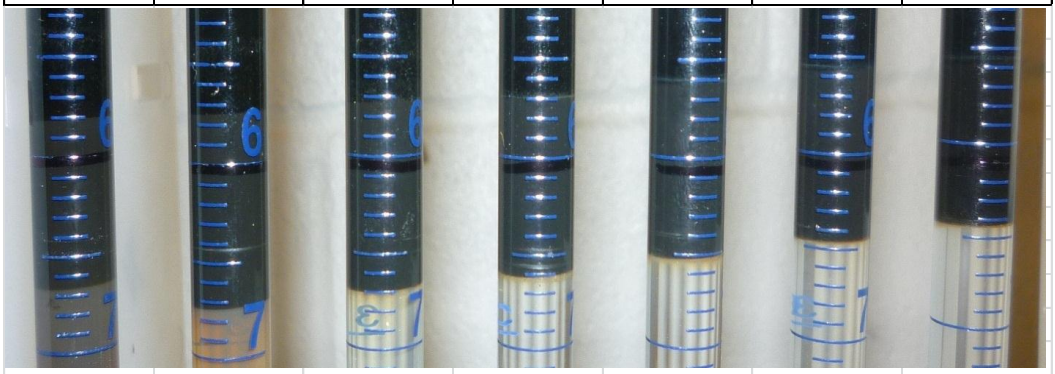

Figure 4. 37 Photo of W11-89-2: 0.67% C_{13}-13PO-SO_4^-, 0.33% C_{15-18}IOS, 1.75% SBA, 0.5% Na_2CO_3, after 107 day, oil conc.=50% at Res T (43 ℃).

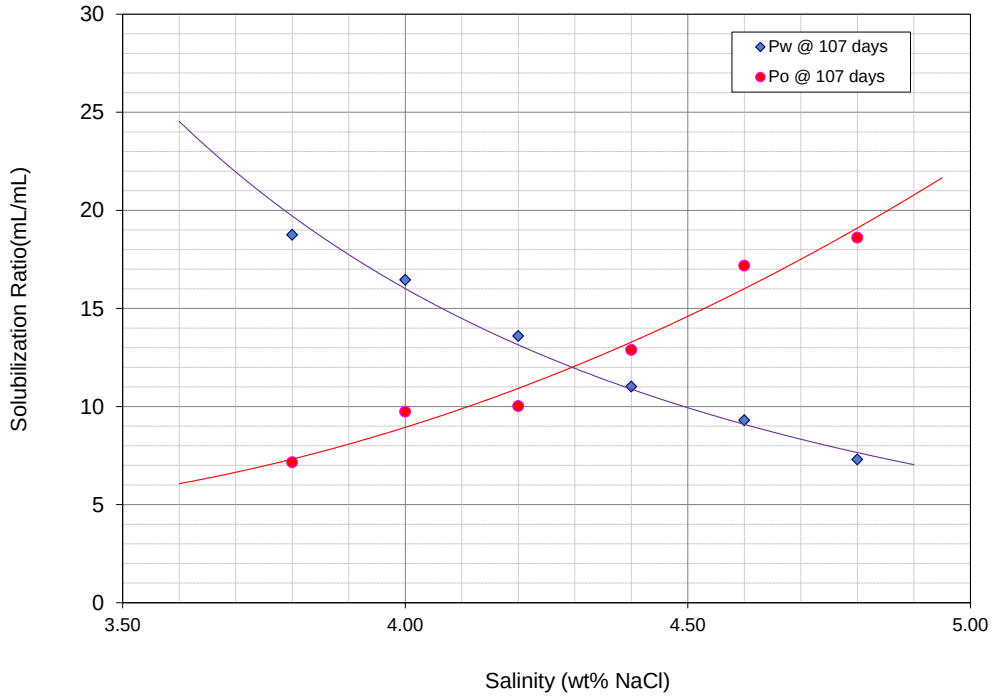

Figure 4. 38 Solubilization plot of W11-89-2: 0.67% C_{13}-13PO-SO_4^-, 0.33% C_{15-18}IOS, 1.75% SBA, 0.5% Na_2CO_3, after 107 day, oil conc.=50% at Res T (43 ℃).

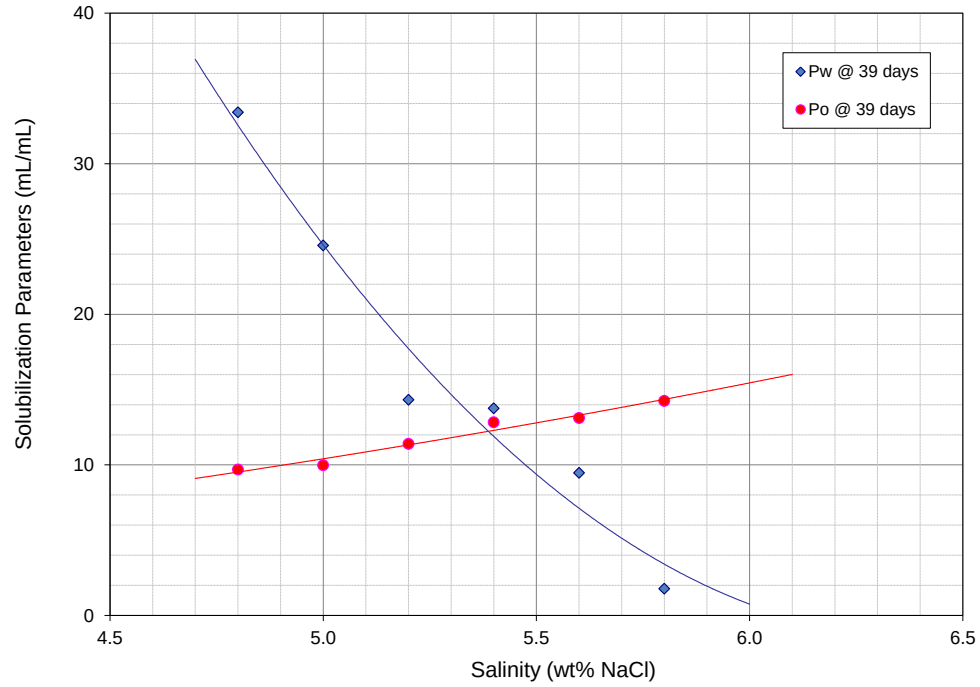

Figure 4. 39 Photo of W11-71: 0.73% C_{16-17}-7PO-SO_4^-, 0.27% C_{15-18} IOS, 1.75% DGBE, 0.5% Na_2CO_3, after 39 days, oil conc.=50% at Res T (43 ℃).

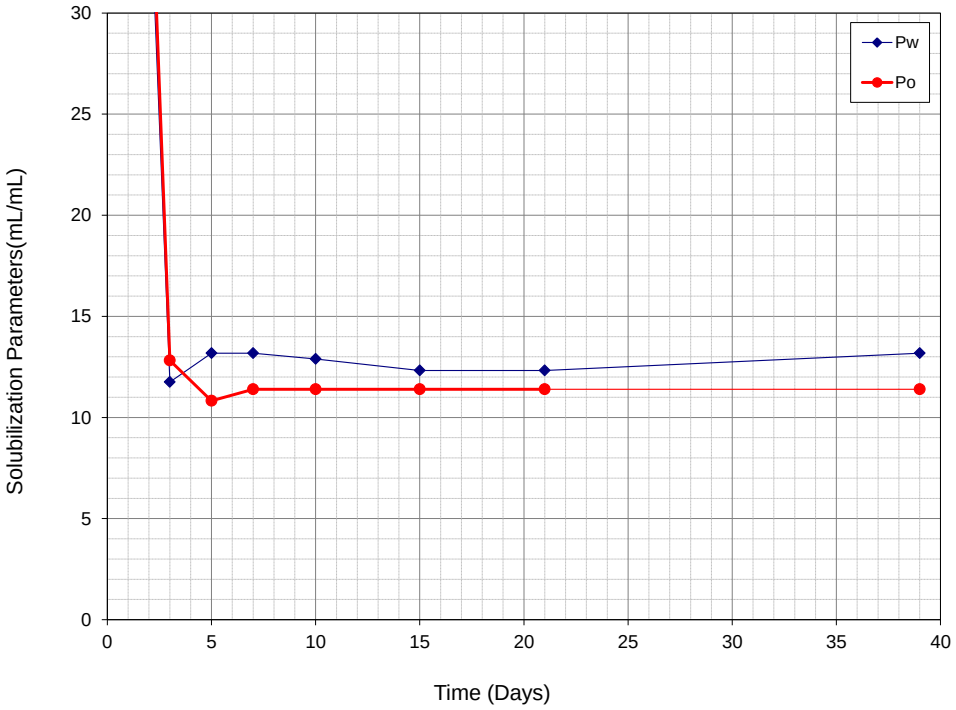

Figure 4. 40 Equilibration time of W11-71: 0.73% $C_{16\text{-}17}$-7PO-SO_4^-, 0.27% $C_{15\text{-}18}$ IOS, 1.75% DGBE, 0.5% Na_2CO_3, oil conc.=50% at Res T (43 ℃).

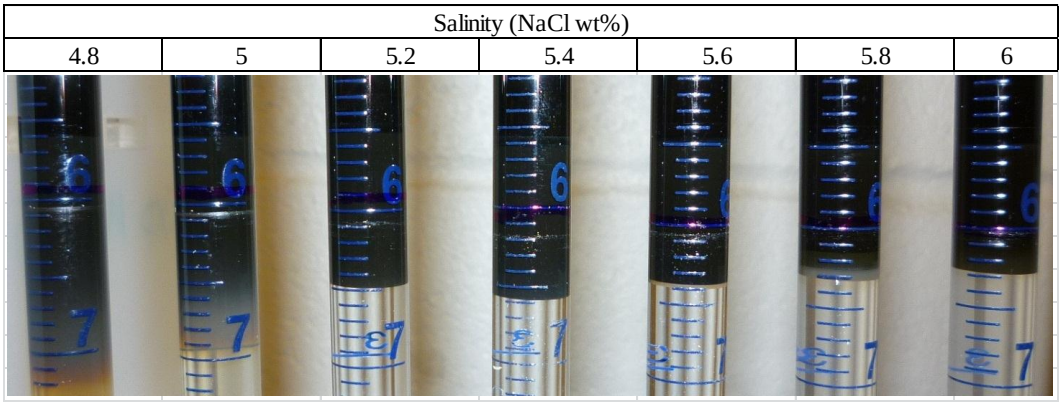

Figure 4. 41 Photo of W11-71: 0.73% $C_{16\text{-}17}$-7PO-SO_4^-, 0.27% $C_{15\text{-}18}$ IOS, 1.75% DGBE, 0.5% Na_2CO_3, after 39 days, oil conc.=50% at Res T (43 ℃).

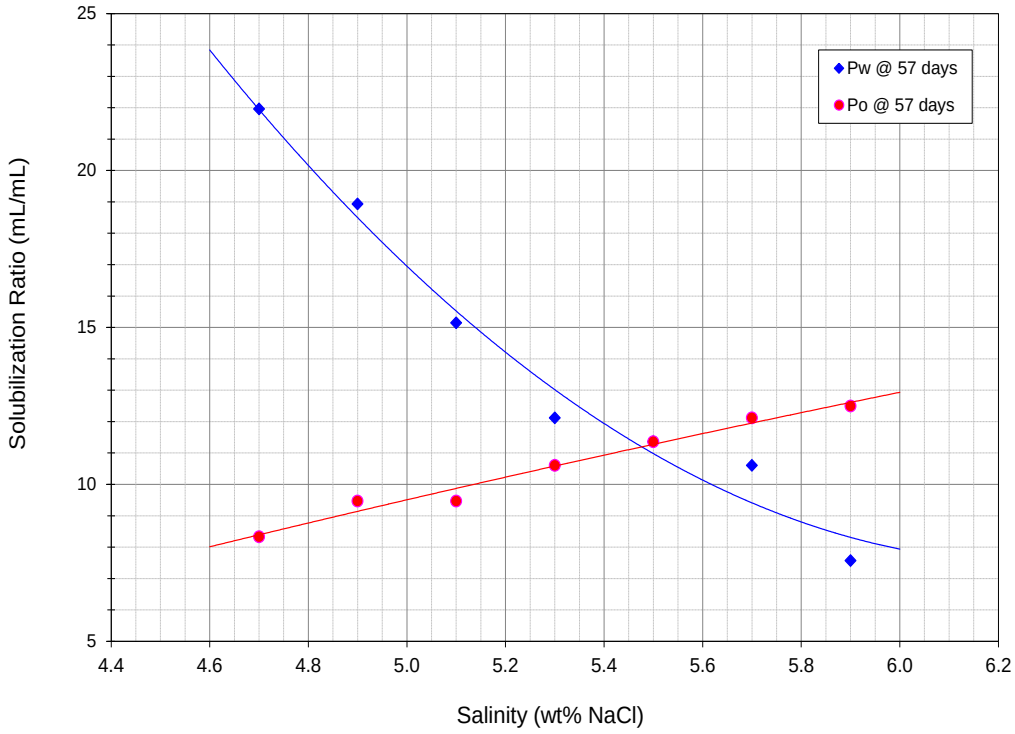

Figure 4. 42 Solubilization plot of W12-33: 0.36% $C_{16\text{-}17}$-7PO-SO_4^-, 0.14% $C_{15\text{-}18}$ IOS, 1.75% DGBE, 1% Na_2CO_3,2300ppm FP3530S, after 57 days, oil conc.=33% at Res T (43 ℃).

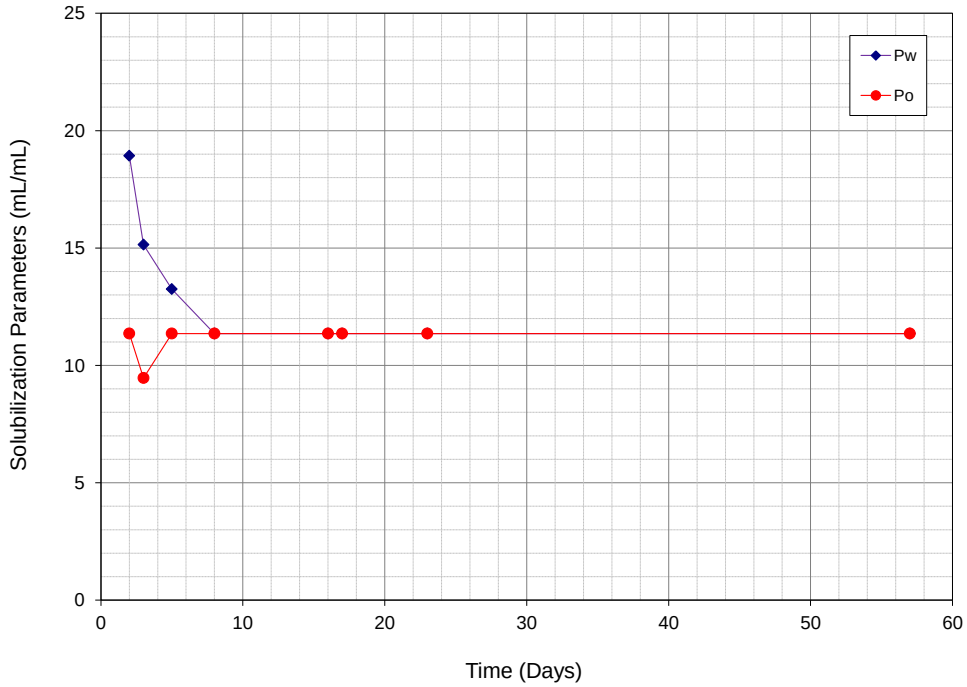

Figure 4. 43 Equilibration time of W12-33: 0.36% $C_{16\text{-}17}$-7PO-SO_4^-, 0.14% $C_{15\text{-}18}$ IOS, 1.75% DGBE, 1% Na_2CO_3, 2300ppm FP3530S, after 57 days, oil conc.=33% at Res T (43 ℃).

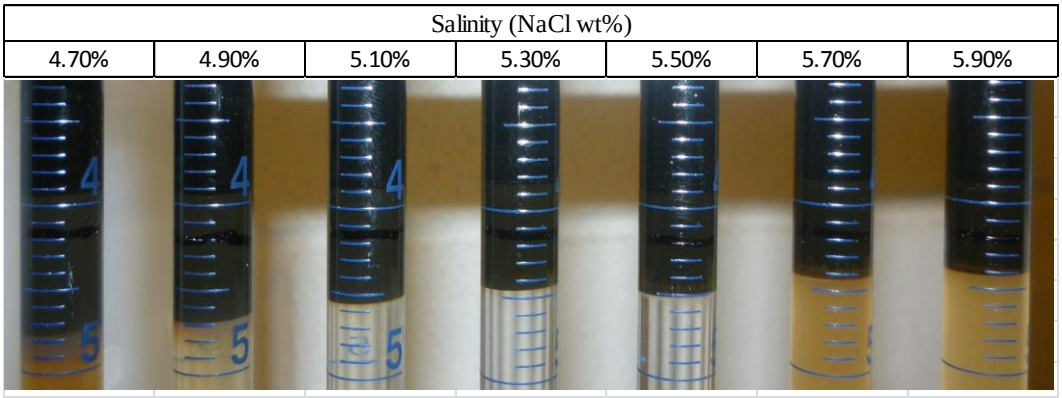

Figure 4. 44 Photo of W12-33: 0.36% $C_{16\text{-}17}$-7PO-SO_4^-, 0.14% $C_{15\text{-}18}$ IOS, 1.75% DGBE, 1% Na_2CO_3, 2300ppm FP3530S, after 57 days, oil conc.=33% at Res T (43 ℃).

Table 4.1 Summary of phase behavior results of Wahrman crude oil with C_{16-17}-7PO-SO_4^- as primary surfactant.

Series # W-	Primary Surf. (wt%)	Co-Surf. (wt%)	Co-Sol. (wt%)	APSL at RT(~23C) (wt%)	O.S. (wt%)	Opt. Sol.Ratio (mL/mL)	Eq.Time (Days)	Comments
	C_{16-17}-7PO-SO_4^-	C_{15-18} IOS	SBA	NaCl	NaCl			
5-1	0.750	0.250	1.00	N/A	6	16	N/A	
5-2	0.625	0.375	1.00	N/A	7.5	30	N/A	
5-3	0.500	0.500	1.00	N/A	9.8	26	N/A	
5-4	0.375	0.125	0.50	N/A	5.8	26	N/A	
5-5	1.500	0.500	2.00	N/A	5.9	30	N/A	
5-6	0.750	0.250	2.50	N/A	6.1	8	11	
5-7	0.625	0.375	2.50	N/A	7.9	9	12	
5-8	0.500	0.500	2.50	N/A	9.75	8.5	8	ME formed after 4 days
5-9	0.375	0.125	1.25	N/A	6.5	5	4	small ME phase
5-10	0.313	0.188	1.25	N/A	9.2	6	N/A	small ME phase
5-11	0.250	0.250	1.25	N/A	N/A	N/A	N/A	no ME phase
5-12	0.625	0.375	2.00	N/A	7.9	10	8	
5-13	0.625	0.375	1.75	N/A	7.95	11	8	
5-14	0.625	0.375	1.50	N/A	8	12	3	
5-15	0.667	0.333	2.00	N/A	7.3	11	8	
5-16	0.571	0.429	2.00	N/A	8.75	10	6	
5-17	0.727	0.273	2.00	5.60%	6.9	12.5	N/A	
5-18	0.700	0.300	2.00	5.85%	7.4	12.5	N/A	
5-19	0.625	0.375	2.00	<7.1%	8.4	12	N/A	
5-20	1.500	0.500	4.00	5.30%	6.2	12	N/A	
5-17-2	0.727	0.273	2.00	5.60%	7.1	11	N/A	Repeat 5-17
5-18-2	0.700	0.300	2.00	5.85%	7.5	12	N/A	Repeat 5-18
5-19-2	0.625	0.375	2.00	<7.1%	8.7	9	<15	Repeat 5-19
5-20-2	1.500	0.500	4.00	5.30%	6.25	10	<15	Repeat 5-20

Table 4.1 Summary of phase behavior results of Wahrman crude oil with C_{16-17}-7PO-SO_4^- as primary surfactant.

Series # W-	Primary Surf. (wt%)	Co-Surf. (wt%)	Co-Sol. (wt%)	APSL at RT(~23C) (wt%)	O.S. (wt%)	Opt. Sol.Ratio (mL/mL)	Eq.Time (Days)	Comments
	C_{16-17}-7PO-SO_4^-	C_{15-18} IOS	SBA	NaCl	NaCl			
5-1	0.750	0.250	1.00	N/A	6	16	N/A	
5-2	0.625	0.375	1.00	N/A	7.5	30	N/A	
5-3	0.500	0.500	1.00	N/A	9.8	26	N/A	
5-4	0.375	0.125	0.50	N/A	5.8	26	N/A	
5-5	1.500	0.500	2.00	N/A	5.9	30	N/A	
5-6	0.750	0.250	2.50	N/A	6.1	8	11	
5-7	0.625	0.375	2.50	N/A	7.9	9	12	
5-8	0.500	0.500	2.50	N/A	9.75	8.5	8	ME formed after 4 days
5-9	0.375	0.125	1.25	N/A	6.5	5	4	small ME phase
5-10	0.313	0.188	1.25	N/A	9.2	6	N/A	small ME phase
5-11	0.250	0.250	1.25	N/A	N/A	N/A	N/A	no ME phase
5-12	0.625	0.375	2.00	N/A	7.9	10	8	
5-13	0.625	0.375	1.75	N/A	7.95	11	8	
5-14	0.625	0.375	1.50	N/A	8	12	3	
5-15	0.667	0.333	2.00	N/A	7.3	11	8	
5-16	0.571	0.429	2.00	N/A	8.75	10	6	
5-17	0.727	0.273	2.00	5.60%	6.9	12.5	N/A	
5-18	0.700	0.300	2.00	5.85%	7.4	12.5	N/A	
5-19	0.625	0.375	2.00	<7.1%	8.4	12	N/A	
5-20	1.500	0.500	4.00	5.30%	6.2	12	N/A	
5-17-2	0.727	0.273	2.00	5.60%	7.1	11	N/A	Repeat 5-17
5-18-2	0.700	0.300	2.00	5.85%	7.5	12	N/A	Repeat 5-18
5-19-2	0.625	0.375	2.00	<7.1%	8.7	9	<15	Repeat 5-19
5-20-2	1.500	0.500	4.00	5.30%	6.25	10	<15	Repeat 5-20

Table 4.1 Summary of phase behavior results of Wahrman crude oil with C_{16-17}-7PO-SO_4^- as primary surfactant(cont.)

Series # W-	Primary Surf. (wt%)	Co-Surf. (wt%)	Co-Sol. (wt%)	APSL at RT(~23C) (wt%)	O.S. (wt%)	Opt. Sol.Ratio (mL/mL)	Eq.Time (Days)	Comments
	C_{16-17}-7PO-SO_4^-	C_{15-18} IOS	SBA	NaCl	NaCl			
5-21	1.250	0.750	4.00	6.15%	7.1	11	<27	
5-22	0.750	0.250	2.00	5.15%	5.75	14	<15	Crystal ME phase
5-23	0.727	0.273	2.00	5.35%	6.2	13	<15	Oil conc.=25%
5-25	0.727	0.273	2.00	5.35%	6.6	10	7	
5-27	0.800	0.200	3.00	4.85%	5	15	N/A	liquid cyrstal ME phase
5-28	0.857	0.143	3.00	4.35%	4.25	16	N/A	liquid cyrstal ME phase
5-29	1.000	0.000	3.00	3.00%	N/A	N/A	N/A	gel/viscous phase
5-30	0.400	0.100	1.50	4.65%	N/A	N/A	N/A	no ME phase
5-31	0.429	0.071	1.50	4.35%	N/A	N/A	N/A	no ME phase
5-32	0.500	0.000	1.50	2.60%	N/A	N/A	N/A	viscous ME phase
5-33	0.800	0.200	3.00	*5.55%*	N/A	N/A	N/A	no ME phase, probematic SBA
5-34	0.857	0.143	3.00	4.80%	N/A	N/A	N/A	no ME phase, probematic SBA
5-33-2	0.800	0.200	3.00	*5.55%*	5.6	<5	N/A	very small MP
5-34-2	0.857	0.143	3.00	4.80%	5.05	<5	N/A	very small MP
5-33-3	0.800	0.200	3.00	*5.55%*	5.8	4.5	N/A	liquid crystal ME phase
5-34-3	0.857	0.143	3.00	4.80%	5.05	1.5	N/A	liquid crystal ME phase

Table 4.2 Phase behavior results of Wahrman crude oil with surfactant of Alfoterra series from Sasol as primary surfactant

Series # W	Primary Surf.		Co-Surf. (wt%)	Surf ratio	Co-Solvent (wt%)	Opt. Salinity (OS) (wt%)	Opt. Sol. Ratio (mL/mL)	APSL at RT(~23°C)	Comments
	Type	(wt%)	C_{15-18} IOS	main surf./co-	SBA	NaCl			
8-1	C_{12-13}-8PO-SO_4^-	0.625	0.375	1.67	2.5	9.5	9.5	8.0%	
8-2	C_{14-15}-4PO-SO_4^-	0.625	0.375	1.67	2.5	10	N/A	5.0%	Opt S*>9.5%
8-3	C_{14-15}-8PO-SO_4^-	0.625	0.375	1.67	2.5	8.6	10~15	6.0%	
8-4	C_{16-17}-4PO-SO_4^-	0.625	0.375	1.67	2.5	10	9~20	6.0%	Opt S*>9.5%
8-5	C_{16-17}-7PO-SO_4^-	0.625	0.375	1.67	2.5	8.4	10~17.5	6.5%	
8-6	C_{12-13}-8PO-SO_4^-	0.750	0.250	3.00	2.5	7.5	10	7.0%	
8-7	C_{14-15}-4PO-SO_4^-	0.750	0.250	3.00	2.5	8.5	5~12	4.0%	
8-8	C_{14-15}-8PO-SO_4^-	0.750	0.250	3.00	2.5	6.5	15~27	6.0%	
8-9	C_{16-17}-4PO-SO_4^-	0.750	0.250	3.00	2.5	0	N/A	5.0%	no ME phase
8-10	C_{16-17}-7PO-SO_4^-	0.750	0.250	3.00	2.5	6.5	19~36	6.0%	
8-11	C_{16-17}-7PO-SO_4^-	0.750	0.250	3.00	2.5	N/A	N/A	8.0%	primary surf from Stepan
8-12	C_{16-17}-7PO-SO_4^-	0.750	0.250	3.00	2.5	6.5	15~27	8.0%	primary surf from Stepan
8-13	C_{12-13}-8PO-SO_4^-	0.750	0.250	3.00	2	7.5	~20	6.5%	

Table 4.2 Phase behavior results of Wahrman crude oil with surfactant of Alfoterra series from Sasol as primary surfactant (cont.)

Series # W	Primary Surf.		Co-Surf. (wt%)	Surf ratio	Co-Solvent (wt%)	Opt. Salinity (OS) (wt%)	Opt. Sol. Ratio (mL/mL)	APSL at RT(~23°C)	Comments
	Type	(wt%)	C_{15-18} IOS	main surf./co-	SBA	NaCl			
8-14	C_{14-15}-8PO-SO_4^-	0.750	0.250	3.00	2	6.5	~19	5.85%	
8-15	C_{16-17}-7PO-SO_4^-	0.750	0.250	3.00	2	N/A	N/A	8.0%	
8-16	C_{16-17}-7PO-SO_4^-	0.750	0.250	3.00	2	7.75	10.00%	7.4%	primary surf from Stepan
8-17	C_{12-13}-8PO-SO_4^-	0.750	0.250	3.00	2.5	6.5	~20	9.5%	
8-18	C_{14-15}-8PO-SO_4^-	0.750	0.250	3.00	2.5	5	~19	5.85%	
8-19	C_{16-17}-7PO-SO_4^-	0.750	0.250	3.00	2.5	5.25	~20	<5%	
8-20	C_{16-17}-7PO-SO_4^-	0.750	0.250	3.00	2.5	5.5	N/A	<5%	primary surf from Stepan
8-21	C_{12-13}-8PO-SO_4^-	0.857	0.143	6.00	2	4.25	5	4.25%	viscous ME phase
8-22	C_{12-13}-8PO-SO_4^-	1.000	0.000	+oo	2	3.6	5.5	>7.5%	viscous ME phase
8-23	C_{12-13}-8PO-SO_4^-	0.857	0.143	6.00	2	3.9	10	4.25%	with 0.3% NaOH
8-24	C_{12-13}-8PO-SO_4^-	0.923	0.077	12.00	2	3.6	11	3.75%	with 0.3% NaOH
8-25	C_{12-13}-8PO-SO_4^-	0.857	0.143	6.00	2	4.2	10	4.35%	with 0.3% NaOH
8-26	C_{12-13}-8PO-SO_4^-	0.889	0.111	8.00	2	3.8	11	4.10%	with 0.3% NaOH

Table 4.2 Phase behavior results of Wahrman crude oil with surfactant of Alfoterra series from Sasol as primary surfactant (cont.)

Series # W	Primary Surf.		Co-Surf. (wt%)	Surf ratio	Co-Solvent (wt%)	Opt. Salinity (OS) (wt%)	Opt. Sol. Ratio (mL/mL)	APSL at RT(~23°C)	Comments
	Type	(wt%)	C_{15-18} IOS	main surf /co-surf	SBA	NaCl			
8-27	C_{12-13}-8PO-SO_4^-	0.909	0.091	10.00	2	3.75	13	3.85%	with 0.3% NaOH
8-28	C_{12-13}-8PO-SO_4^-	0.923	0.077	12.00	2	3.3	12	3.60%	with 0.3% NaOH
8-29	C_{12-13}-8PO-SO_4^-	0.857	0.143	6.00	1.5	4	12	4.35%	with 0.3% NaOH
8-30	C_{12-13}-8PO-SO_4^-	0.889	0.111	8.00	1.5	N/A	N/A	3.85%	with 0.3% NaOH
8-31	C_{12-13}-8PO-SO_4^-	0.909	0.091	10.00	1.5	N/A	N/A	3.65%	with 0.3% NaOH
8-32	C_{12-13}-8PO-SO_4^-	0.857	0.143	6.00	2.5	4.15	10	4.15%	with 0.3% NaOH
8-33	C_{12-13}-8PO-SO_4^-	0.889	0.111	8.00	2.5	4	10	4.15%	with 0.3% NaOH
8-34	C_{12-13}-8PO-SO_4^-	0.909	0.091	10.00	2.5	3.75	12	3.60%	with 0.3% NaOH

Table 4.3 Phase behavior result of Wahrman crude oil with alkali

Series #	Primary Surf (wt%)	Co-Surf (wt%)	Co-Solvent (wt%)	Akali (wt%)		Opt. Salinity (OS) (wt%)	APSL at RT(~23°C)	Opt. Sol. Ratio (mL/mL)	Comments
	C_{12-13}-8PO-SO_4^-	C_{15-18}	SBA	NaOH	Na_2CO_3	NaCl			
6-12	0.857	0.143	2.5		0.15	4.75	4.25	17.6	fluid ME phase at OS
6-13	0.857	0.143	2.5		0.3	4.6	3.85	16	fluid ME phase at OS
6-14	0.889	0.111	2.5	0.3		3.9	3.75	10	fluid ME phase at OS
6-15	0.889	0.111	2.5	0.6		3.4	3.35	13	fluid ME phase, LP clear at OS
6-16	0.889	0.111	2.5	0.9		3.5	>4.75	N/A	no ME phase
6-20	0.889	0.111	2.5	0.9		3	N/A	13	fluid ME phase, LP clear at OS
6-22	0.889	0.111	2.5	0.9		3	3.4	12	fluid ME phase, LP clear at OS
6-17	0.889	0.111	2.5		0.3	4.5	3.6	11	fluid ME phase, LP hazy at OS
6-18	0.889	0.111	2.5		0.6	4.1	3.6	12	fluid ME phase, LP hazy at OS
6-19	0.889	0.111	2.5		0.9	3.9	3.25	11	fluid ME phase, LP clear at OS
6-21	0.889	0.111	2.5		0.9	3.8	3.5	14	fluid ME phase, LP clear at OS
6-23	0.889	0.111	2.5		0.2	N/A	N/A	N/A	No ME phase
6-24	0.889	0.111	2.5		0.1	4.4	N/A	18	
6-25	0.750	0.250	2		0.2	N/A	N/A	N/A	No ME phase
6-26	0.750	0.250	2		0.1	N/A	N/A	N/A	No ME phase
6-27	0.750	0.250	2		0.3	N/A	N/A	N/A	No ME phase
6-28	0.857	0.143	2.5		0.2	4.6	N/A	13	
6-29	0.857	0.143	2.5		0.1	N/A	N/A	N/A	No ME phase

Table 4.3 Phase behavior result of Wahrman crude oil with alkali (cont.)

Series #	Primary Surf.(wt%)	Co-Surf. (wt%)	Co-Sol. (wt%)	Akali (wt%)		O.S. (wt%)	APSL at RT(~23°C)	Opt. Sol. Ratio (mL/mL)	Comments
	C_{12-13}-8PO-SO_4^-	C_{15-18} IOS	SBA	NaOH	Na_2CO_3	NaCl			
6-30	0.857	0.143	2.5		0.3	4.6	N/A	12	
6-31	0.909	0.091	2.5		0.2	4.3	N/A	12	
6-32	0.909	0.091	2.5		0.1	4.3	N/A	16	
6-33	0.909	0.091	2.5		0.3	4.1	N/A	15	
6-34	0.857	0.143	2		0.1	N/A	N/A	N/A	No ME phase,primary surf:C_{16-17}-7PO-SO_4^-
6-35	0.800	0.200	2		0.1	5	N/A	N/A	crystal ME phase,primary surf:C_{16-17}-7PO-SO_4^-
6-36	0.750	0.250	2		0.1	>5	N/A	N/A	primary surf:C_{16-17}-7PO-SO_4^-

Figure 4.4 Phase behavior results of Wahrman crude oil with other alcohol propoxy sulfates as primary surfactant

Series # W	Primary Surf.		Co-Surf.		Co-Sol. (wt%)	O.S. (wt%)	Opt. Sol. Ratio (mL/mL)	Comments
	Type	(wt%)	Type	(wt%)	SBA	NaCl		
9-1	C_{16-17}-7PO-SO_4^-	0.750	Petrostep C5	0.250	2	N/A	N/A	Petrostep C5 is alpha olefin sulfonate, structure not available, no ME phase
9-2	C_{16-17}-7PO-SO_4^-	0.750	Petrostep C1	0.250	2	N/A	N/A	Petrostep C1 is alpha olefin sulfonate, structure not available, no ME phase
9-3	C_{16-17}-7PO-SO_4^-	0.750	C_{13}-12PO-SO_4^-	0.250	2	N/A	N/A	no ME phase
9-4	C_{16-17}-7PO-SO_4^-	0.750	C_{13}-9PO-SO_4^-	0.250	2	N/A	N/A	no ME phase
9-5	C_{12-13}-8PO-SO_4^-	0.900	Petrostep C5	0.100	2	N/A	N/A	Petrostep C5 is alpha olefin sulfonate, structure not available, no ME phase
9-6	C_{12-13}-8PO-SO_4^-	0.750	Petrostep C5	0.250	2	N/A	N/A	Petrostep C5 is alpha olefin sulfonate, structure not available, no ME phase
9-7	C_{13}-7PO-SO_4^-	0.625	C_{15-18} IOS	0.375	2	7.5	N/A	primary surfactant: Petrostep S-8B, ME phase below initial level
9-8	C_{13}-7PO-SO_4^-	0.625	C_{15-18} IOS	0.375	2	7	N/A	primary surfactant: Petrostep S-8C, ME phase viscous
9-9	C_{13}-9PO-SO_4^-	0.625	C_{15-18} IOS	0.375	2	8.5	N/A	primary surfactant: Petrostep S-13B, ME phase viscous
9-10	C_{13}-9PO-SO_4^-	0.625	C_{15-18} IOS	0.375	2	N/A	N/A	primary surfactant: Petrostep S-13C,ME phase viscous and difficult to determine OS

Table 4.5 Phase behavior results of Wahrman crude oil with different cosolvent, oil conc.=50%

Series #W	Primary Surf		Co-Surf. (wt%)	Co-Sol.		Alkali (wt%)	APSL @ Res T (wt%)	O.S.(wt%)	Opt. Sol. Ratio (mL/mL)	Eq time to update (Days)	Comments
	Structure	(wt%)	C_{15-18} IOS	Type	(wt%)	Na_2CO_3		NaCl			
11-1	C_{16-17}-7PO-SO_4^- [1]	0.625	0.375	EGBE	2	0	N/A	~7%	13	N/A	
11-2	C_{16-17}-7PO-SO_4^- [1]	0.625	0.375	2-Methyl-1-Butonal	2	0	N/A	N/A	N/A	N/A	No ME phase, viscous phase at over OS
11-3	C_{16-17}-7PO-SO_4^- [1]	0.625	0.375	3-Methyl-1-Butonal	2	0	N/A	N/A	N/A	N/A	No ME phase, viscous phase at over OS
11-4	C_{16-17}-7PO-SO_4^- [1]	0.625	0.375	SBA	2	0	N/A	~7.2%	24	N/A	
11-4-2	C_{16-17}-7PO-SO_4^- [1]	0.625	0.375	SBA	2	0	N/A	~7%	20	N/A	
11-5	C_{16-17}-7PO-SO_4^- [1]	0.625	0.375	EGBE	2	0.5	5.75	5.5-6.5	N/A	N/A	Viscous/liquid crystal ME phase
11-5-6	C_{16-17}-7PO-SO_4^- [2]	0.625	0.375	EGBE	2	0.5	<5.25	6.55	7.5	6	
11-5-2	C_{16-17}-7PO-SO_4^- [2]	0.625	0.375	EGBE	2	1	N/A	6.25	8	6	
11-5-3	C_{16-17}-7PO-SO_4^- [2]	0.625	0.375	EGBE	2	1.5	N/A	5.75	7.5	6	
11-5-7	C_{16-17}-7PO-SO_4^- [2]	0.625	0.375	EGBE	2	2	N/A	5.35	8	6	
11-6	C_{16-17}-7PO-SO_4^- [1]	0.625	0.375	SBA	2	0.5	N/A	6.75	9.2	N/A	Viscous/liquid crystal ME phase

Table 4.5 Phase behavior results of Wahrman crude oil with different cosolvent, oil conc.=50% (cont.)

Series #W	Primary Surf		Co-Surf. (wt%)	Co-Sol.		Alkali (wt%)	APSL @ Res T (wt%)	O.S.(wt%)	Opt. Sol. Ratio (mL/mL)	Eq time to update (Days)	Comments
	Structure	(wt%)	C_{15-18} IOS	Type	(wt%)	NaOH		NaCl			
11-7	C_{16-17}-7PO-SO_4^- [1]	0.625	0.375	EGBE	2	0.5	N/A	5.6	9	N/A	
11-8	C_{16-17}-7PO-SO_4^- [1]	0.625	0.375	SBA	2	0.5	N/A	5.6	[7-22]	N/A	Viscous/liquid crystal ME phase
11-9	C_{12-13}-8PO-SO_4^-	0.889	0.111	EGBE	2.5	0.3	N/A	3.6	10	N/A	
11-10	C_{12-13}-8PO-SO_4^-	0.889	0.111	2-Methyl-1-Butonal	2.5	0.3	N/A	N/A	N/A	N/A	salinity range is too low,no ME phase
11-11	C_{12-13}-8PO-SO_4^-	0.889	0.111	3-Methyl-1-Butonal	2.5	0.3	N/A	N/A	N/A	N/A	salinity range is too low,no ME phase
11-12	C_{12-13}-8PO-SO_4^-	0.889	0.111	SBA	2.5	0.3	N/A	3.9	[7-15]	N/A	
11-7-2	C_{16-17}-7PO-SO_4^- [1]	0.625	0.375	EGBE	2	0.5	N/A	5.5	N/A	N/A	
11-7-3	C_{16-17}-7PO-SO_4^- [1]	0.625	0.375	EGBE	2	0.5	N/A	5.5	N/A	N/A	
11-9-2	C_{12-13}-8PO-SO_4^-	0.889	0.111	EGBE	2.5	0.3	N/A	3.6	N/A	N/A	

Table 4.5 Phase behavior results of Wahrman crude oil with different cosolvent, oil conc.=50% (cont.)

Series #W	Primary Surf		Co-Surf. (wt%)	Co-Sol.		Alkali (wt%)	APSL @ Res T (wt%)	O.S.(wt%)	Opt. Sol. Ratio (mL/mL)	Eq time to update (Days)	Comments
	Structure	(wt%)	C_{15-18} IOS	Type	(wt%)	Na_2CO_3		NaCl			
11-13	C_{16-17}-7PO-SO_4^- [1]	0.625	0.375	EGBE	2	2	N/A	N/A	N/A	N/A	salinity range is too low,no ME phase;
11-14	C_{16-17}-7PO-SO_4^- [1]	0.625	0.375	EGBE	1.5	1.5	N/A	N/A	N/A	N/A	
11-15	C_{16-17}-7PO-SO_4^- [1]	0.625	0.375	EGBE	1	1.5	N/A	N/A	N/A	N/A	
11-16	C_{16-17}-7PO-SO_4^- [1]	0.625	0.375	EGBE	0.5	1.5	N/A	N/A	N/A	N/A	
11-17	C_{16-17}-7PO-SO_4^- [2]	0.625	0.375	DGBE	2	0.5	N/A	N/A	N/A	N/A	
11-18	C_{16-17}-7PO-SO_4^- [2]	0.625	0.375	DGBE	2	1.5	N/A	N/A	N/A	N/A	
11-19	C_{16-17}-7PO-SO_4^- [2]	0.625	0.375	TGBE	2	0.5	N/A	N/A	N/A	N/A	
11-20	C_{16-17}-7PO-SO_4^- [2]	0.625	0.375	TGBE	2	1.5	N/A	N/A	N/A	N/A	
11-17-2	C_{16-17}-7PO-SO_4^- [2]	0.625	0.375	DGBE	2	0.5	N/A	7.85	N/A	N/A	low sol. ratio
11-18-2	C_{16-17}-7PO-SO_4^- [2]	0.625	0.375	DGBE	2	1.5	N/A	7.1	[6-9]	N/A	fluid ME phase
11-19-2	C_{16-17}-7PO-SO_4^- [2]	0.625	0.375	TGBE	2	0.5	N/A	>8.5	N/A	N/A	salinity range is too low,no ME phase salinity
11-20-2	C_{16-17}-7PO-SO_4^- [2]	0.625	0.375	TGBE	2	1.5	N/A	>7.5	N/A	N/A	

Table 4.5 Phase behavior results of Wahrman crude oil with different cosolvent, oil conc.=50% (cont.)

Series #W	Primary Surf		Co-Surf. (wt%)	Co-Sol.		Alkali (wt%)	APSL @ Res T (wt%)	O.S.(wt%)	Opt. Sol. Ratio (mL/mL)	Eq time to update (Days)	Comments
	Structure	(wt%)	C_{15-18} IOS	Type	(wt%)	Na_2CO_3		NaCl			
11-21	C_{16-17}-7PO-SO_4^- [1]	0.625	0.375	EGBE	1.5	0.5	<6	6.15	N/A	N/A	only 2 reading
11-22	C_{16-17}-7PO-SO_4^- [1]	0.625	0.375	EGBE	0.5	0.5	N/A	N/A	N/A	N/A	no ME phase
11-23	C_{16-17}-7PO-SO_4^- [1]	0.625	0.375	EGBE/ DGBE=5	2	0.5	6.125	6	N/A	10	
11-23-2	C_{16-17}-7PO-SO_4^- [1]	0.625	0.375	EGBE/ DGBE=5	2	0.5	6.075	6.1	9	9	
11-23-2R1	C_{16-17}-7PO-SO_4^- [1]	0.625	0.375	EGBE/ DGBE=5	2	0.5	6.075	5.95	7.5	7	
11-23-2R2	C_{16-17}-7PO-SO_4^- [1]	0.625	0.375	EGBE/ DGBE=5	2	0.5	6.075	5.9	8	20	
11-23-2R3	C_{16-17}-7PO-SO_4^- [1]	0.625	0.375	EGBE/ DGBE=5	2	0.5	6.075	6.05	8	7	
11-23-3	C_{16-17}-7PO-SO_4^- [1]	0.625	0.375	EGBE/ DGBE=5	2	0.5	>6.4	N/A	N/A	N/A	no ME phase
11-23-S	C_{16-17}-7PO-SO_4^- [1]	0.625	0.375	EGBE/ DGBE=5	2	0.5	6.1	5.95	8.5	N/A	
11-24	C_{12-13}-8PO-SO_4^-	0.889	0.111	EGBE	1.5	0.5	N/A	4.2	N/A	N/A	
11-25	C_{16-17}-7PO-SO_4^- [1]	0.750	0.250	EGBE	2	0.5	4.625	4.6	12	10	
11-25-2	C_{16-17}-7PO-SO_4^- [1]	0.750	0.250	EGBE/ DGBE=5	2	0.5	>4.75	4.6	12	7	

Table 4.5 Phase behavior results of Wahrman crude oil with different cosolvent, oil conc.=50% (cont.)

Series #W	Primary Surf		Co-Surf. (wt%)	Co-Sol.		Alkali (wt%)	APSL @ Res T (wt%)	O.S.(wt%)	Opt. Sol. Ratio (mL/mL)	Eq time to update (Days)	Comments
	Structure	(wt%)	C_{15-18} IOS	Type	(wt%)	Na_2CO_3		NaCl			
11-25-S	C_{16-17}-7PO-SO_4^- [1]	0.750	0.250	EGBE/ DGBE=5	2	0.5	4.63	4.6	12	7	
11-26	C_{16-17}-7PO-SO_4^- [1]	0.625	0.375	EGBE/ DGBE=5	1	0.5	5.825	6.45	11	3	
11-26-2	C_{16-17}-7PO-SO_4^- [1]	0.625	0.375	EGBE/ DGBE=5	1	0.5	<5.6	6.3	15	7	
11-26-S	C_{16-17}-7PO-SO_4^- [1]	0.625	0.375	EGBE/ DGBE=5	1	0.5	5.83	6.4	15	7	
11-27	C_{16-17}-7PO-SO_4^- [1]	0.700	0.300	EGBE	2	0.5	4.975	4.8	11	12	
11-27-2	C_{16-17}-7PO-SO_4^- [1]	0.700	0.300	EGBE	2	0.5	5.25	5.1	11	10	
11-28	C_{16-17}-7PO-SO_4^- [1]	0.700	0.300	EGBE/ DGBE=5	2	0.5	5.475	4.85	11	8	
11-28-2	C_{16-17}-7PO-SO_4^- [1]	0.700	0.300	EGBE/ DGBE=5	2	0.5	5.475	4.95	11	11	Viscous ME phase
11-28-3	C_{16-17}-7PO-SO_4^- [1]	0.700	0.300	EGBE/ DGBE=5	2	0.5	5.45	5.15	15	5	made with error,discard
11-28-4	C_{16-17}-7PO-SO_4^- [1]	0.700	0.300	EGBE/ DGBE=5	2	0.5	5.725	5	11	7	
11-28-S	C_{16-17}-7PO-SO_4^- [1]	0.700	0.300	EGBE/ DGBE=5	2	0.5	5.48	5	11	N/A	
11-29	C_{16-17}-7PO-SO_4^- [1]	0.700	0.300	EGBE	1.5	0.5	4.975	5.2	17	6	
11-30	C_{16-17}-7PO-SO_4^- [1]	0.700	0.300	EGBE	1	0.5	4.98	5.4	22	6	
11-31	C_{12-13}-8PO-SO_4^-	0.750	0.250	EGBE	1	0.5	5.75	5.4	20	15	

Table 4.5 Phase behavior results of Wahrman crude oil with different cosolvent, oil conc.=50% (cont.)

Series #W	Primary Surf		Co-Surf. (wt%)	Co-Sol.		Alkali (wt%)	APSL @ Res T (wt%)	O.S.(wt%)	Opt. Sol. Ratio (mL/mL)	Eq time to update (Days)	Comments
	Structure	(wt%)	C_{15-18} IOS	Type	(wt%)	Na_2CO_3		NaCl			
11-32	C_{16-17}-7PO-SO_4^- [1]	0.700	0.300	EGBE/ DGBE=5	1.75	0.5	5.475	5.2	12	5	viscous ME phase appeared
11-33	C_{16-17}-7PO-SO_4^- [1]	0.727	0.273	EGBE/ DGBE=5	1.75	0.5	5.225	5	13.5	5	
11-33-2	C_{16-17}-7PO-SO_4^- [1]	0.727	0.273	EGBE/ DGBE=5	1.75	0.5	5.35	5.1	12.5	3	
11-33-3	C_{16-17}-7PO-SO_4^- [1]	0.727	0.273	EGBE/ DGBE=5	1.75	0.5	5.25	5.05	13	5	
11-33-4	C_{16-17}-7PO-SO_4^- [1]	0.727	0.273	EGBE/ DGBE=5	1.75	0.5	5.325	5.05	14	2	
11-33-5	C_{16-17}-7PO-SO_4^- [1]	0.727	0.273	EGBE/ DGBE=5	1.75	0.5	5.15	4.9	15	3	
11-33-6	C_{16-17}-7PO-SO_4^- [1]	0.727	0.273	EGBE/ DGBE=5	1.75	0.5	5.2	4.8	14.5	N/A	
11-33-7	C_{16-17}-7PO-SO_4^- [1]	0.727	0.273	EGBE/ DGBE=5	1.75	0.5	5.2	4.85	16	N/A	
11-33-S	C_{16-17}-7PO-SO_4^- [1]	0.727	0.273	EGBE/ DGBE=5	1.75	0.5	5.2	4.9	15	4	
11-34	C_{16-17}-7PO-SO_4^- [1]	0.750	0.250	EGBE/ DGBE=5	2	0.5	5	4.85	13	10	Viscous ME phase
11-34-2	C_{16-17}-7PO-SO_4^- [1]	0.750	0.250	EGBE/ DGBE=5	2	0.5	5.025	4.65	13.5	3	Viscous ME phase
11-34-3	C_{16-17}-7PO-SO_4^- [1]	0.750	0.250	EGBE/ DGBE=5	2	0.5	>4.8	4.6	14	3	Viscous ME phase
11-34-S	C_{16-17}-7PO-SO_4^- [1]	0.750	0.250	EGBE/ DGBE=5	2	0.5	5	4.6	14	3	

Table 4.5 Phase behavior results of Wahrman crude oil with different cosolvent, oil conc.=50% (cont.)

Series #W	Primary Surf		Co-Surf. (wt%)	Co-Sol.		Alkali (wt%)	APSL @ Res T (wt%)	O.S.(wt%)	Opt. Sol. Ratio (mL/mL)	Eq time to update (Days)	Comments
	Structure	(wt%)	C_{15-18} IOS	Type	(wt%)	Na_2CO_3		NaCl			
11-39	C_{16-17}-7PO-SO_4^- [1]	0.750	0.250	EGBE/ DGBE=5	1.75	0.5	5.025	4.75	15	7	viscousME phase
11-41	C_{16-17}-7PO-SO_4^- [1]	0.727	0.273	EGBE/ DGBE=5	1.75	0.5	5.2	4.9	12.5	4	
11-40	C_{16-17}-7PO-SO_4^- [1]	0.727	0.273	EGBE	1.75	0.5	4.7	4.4	12.5	4	
11-42	C_{16-17}-7PO-SO_4^- [1]	0.727	0.273	DGBE	1.75	0.5	5.9	5.2	13	4	
11-43	C_{16-17}-7PO-SO_4^- [1]	0.727	0.273	T/TGBE	1.75	0.5	6.5	6.2	13	4	
11-44	C_{16-17}-7PO-SO_4^- [1]	0.750	0.250	EGBE	1.75	0.5	4.5	4.3	16	3	viscousME phase
11-45	C_{16-17}-7PO-SO_4^- [1]	0.750	0.250	DGBE	1.75	0.5	5.7	5	9	51	
11-45-2	C_{16-17}-7PO-SO_4^- [1]	0.750	0.250	DGBE	1.75	0.5	5.7	5.2	13	7	
11-46	C_{16-17}-7PO-SO_4^- [1]	0.750	0.250	T/TGBE	1.75	0.5	6.1	5.8	13	21	
11-47	C_{16-17}-7PO-SO_4^- [1]	0.769	0.231	EGBE	1.75	0.5	4.5	4.35	16	5	

Table 4.5 Phase behavior results of Wahrman crude oil with different cosolvent, oil conc.=50% (cont.)

Series #W	Primary Surf		Co-Surf. (wt%)	Co-Sol.		Alkali (wt%)	APSL @ Res T (wt%)	O.S.(wt%)	Opt. Sol. Ratio (mL/mL)	Eq time to update (Days)	Comments
	Structure	(wt%)	C_{15-18} IOS	Type	(wt%)	Na_2CO_3		NaCl			
11-48	C_{16-17}-7PO-$SO_4^{-[1]}$	0.769	0.231	DGBE	1.75	0.5	5.6	5.05	16	5	viscous/liquid crystal ME phase
11-49	C_{16-17}-7PO-$SO_4^{-[1]}$	0.769	0.231	T/TGBE	1.75	0.5	5.9	5.5	<10	5	
11-50	C_{16-17}-7PO-$SO_4^{-[1]}$	0.769	0.231	EGBE	1.5	0.5	4.5	4.4	21	4	
11-51	C_{16-17}-7PO-$SO_4^{-[1]}$	0.769	0.231	DGBE	1.5	0.5	5.3	5.2	17	4	
11-52	C_{16-17}-7PO-$SO_4^{-[1]}$	0.769	0.231	T/TGBE	1.5	0.5	N/A	N/A	N/A	4	
11-52-2	C_{16-17}-7PO-$SO_4^{-[1]}$	0.769	0.231	T/TGBE	1.5	0.5	5.7	5.75	20	4	
11-53	C_{16-17}-7PO-$SO_4^{-[1]}$	0.750	0.250	DGBE	1.5	0.5	5.5	5.35	16	7	
11-53-2	C_{16-17}-7PO-$SO_4^{-[1]}$	0.750	0.250	DGBE	1.5	0.5	5.5	5.25	14	7	
11-54	C_{16-17}-7PO-$SO_4^{-[1]}$	0.750	0.250	DGBE	1.25	0.5	5.3	<5.2	~17	2	

Table 4.5 Phase behavior results of Wahrman crude oil with different cosolvent, oil conc.=50% (cont.)

Series #W	Primary Surf		Co-Surf. (wt%)	Co-Sol.		Alkali (wt%)	APSL @ Res T (wt%)	O.S.(wt%)	Opt. Sol. Ratio (mL/mL)	Eq time to update (Days)	Comments
	Structure	(wt%)	C_{15-18} IOS	Type	(wt%)	Na_2CO_3		NaCl			
11-55	C_{16-17}-7PO-SO_4^- [1]	0.750	0.250	DGBE	1	0.5	<5.6	N/A	N/A	2	Viscous ME phase
11-56	C_{13}-13PO-SO_4^-	0.750	0.250	EGBE	1.75	0.5	3.6	3.5	13	5	
11-57	C_{13}-13PO-SO_4^-	0.750	0.250	DGBE	1.75	0.5	4.4	4.4	12	5	salinity range is over OS
11-58	C_{13}-13PO-SO_4^-	0.750	0.250	T/TGBE	1.75	0.5	<5.2	5.75	15	43	salinity range is over OS
11-59	C_{16-17}-7PO-SO_4^- [1]	0.750	0.250	EGBE	2	0.5	N/A	N/A	N/A	N/A	Viscous ME phase
11-59-2	C_{16-17}-7PO-SO_4^- [1]	0.750	0.250	EGBE	2	0.5	4.7	4.6	13.5	3	Viscous ME phase
11-59-3	C_{16-17}-7PO-SO_4^- [1]	0.750	0.250	EGBE	2	0.5					
11-60	C_{16-17}-7PO-SO_4^- [1]	0.750	0.250	DGBE	2	0.5	N/A	5.3	12	153	
11-60-2	C_{16-17}-7PO-SO_4^- [1]	0.750	0.250	DGBE	2	0.5	4.8	5.7	12	3	
11-61	C_{16-17}-7PO-SO_4^- [1]	0.727	0.273	EGBE	1.75	0.5	5	4.8	14	3	Viscous ME phase
11-62	C_{16-17}-7PO-SO_4^- [1]	0.727	0.273	DGBE	1.75	0.5	6	5.6	12	46	
11-63	C_{16-17}-7PO-SO_4^- [1]	0.727	0.273	T/TGBE	1.75	0.5	6.6	6.2	11	21	

Table 4.5 Phase behavior results of Wahrman crude oil with different cosolvent, oil conc.=50% (cont.)

Series #W	Primary Surf		Co-Surf. (wt%)	Co-Sol.		Alkali (wt%)	APSL @ Res T (wt%)	O.S.(wt%)	Opt. Sol. Ratio (mL/mL)	Eq time to update (Days)	Comments
	Structure	(wt%)	C_{15-18} IOS	Type	(wt%)	Na_2CO_3		NaCl			
11-64	C_{13}-13PO-SO_4^- [1]	0.750	0.250	EGBE	1.75	0.5	3.5	2.85	9	7	viscous/liquid crystal ME phase
11-64-2	C_{13}-13PO-SO_4^-	0.750	0.250	EGBE	1.75	0.5	N/A	2.8	15	7	
11-64-3	C_{13}-13PO-SO_4^-	0.750	0.250	EGBE	1.75	0.5	3.3	2.8	14	7	
11-65	C_{13}-13PO-SO_4^-	0.750	0.250	DGBE	1.75	0.5	4.3	3.7	10.5	7	
11-66	C_{13}-13PO-SO_4^-	0.750	0.250	T/TGBE	1.75	0.5	4.5	4.1	12	7	
11-67	C_{16-17}-7PO-SO_4^- [1]	0.750	0.250	EGBE/ SBA=7	1.75	0.5	4.7	4.25	13	7	viscous/liquid crystal ME phase
11-67-2	C_{16-17}-7PO-SO_4^- [1]	0.750	0.250	EGBE/ SBA=7	1.75	0.5	4.5	4.3	11	5	
11-68	C_{16-17}-7PO-SO_4^- [1]	0.750	0.250	DGBE/ SBA=7	1.75	0.5	5.7	4.8	11	7	
11-69	C_{16-17}-7PO-SO_4^- [1]	0.750	0.250	T/TGBE/ SBA=7	1.75	0.5	6.1	5.6	<10	7	
11-70	C_{16-17}-7PO-SO_4^- [1]	0.727	0.273	EGBE	1.75	0.5	4.7	4.45	13	21	

Table 4.5 Phase behavior results of Wahrman crude oil with different cosolvent, oil conc.=50% (cont.)

Series #W	Primary Surf		Co-Surf. (wt%)	Co-Sol.		Alkali (wt%)	APSL @ Res T (wt%)	O.S.(wt%)	Opt. Sol. Ratio (mL/mL)	Eq time to update (Days)	Comments
	Structure	(wt%)	C_{15-18} IOS	Type	(wt%)	Na_2CO_3		NaCl			
11-71	C_{16-17}-7PO-SO_4^- [1]	0.727	0.273	DGBE	1.75	0.5	>6	5.45	13	39	
11-71-2	C_{16-17}-7PO-SO_4^- [1]	0.727	0.273	DGBE	1.75	0.5	>6	5.75	14	3	oil conc.=33%
11-71-3	C_{16-17}-7PO-SO_4^- [1]	0.727	0.273	DGBE	1.75	0.5	6.3	5.8	15	1	oil conc.=33%
11-71-3P	C_{16-17}-7PO-SO_4^- [1]	0.727	0.273	DGBE	1.75	0.5	5.7	5.9	11	10	oil conc.=33%
11-71-4	C_{16-17}-7PO-SO_4^- [1]	0.727	0.273	DGBE	1.75	0.5	6.3	5.6	20	3	
11-72	C_{16-17}-7PO-SO_4^- [1]	0.727	0.273	T/TGBE	1.75	0.5	6.3	6.2	12	21	
11-73	C_{13}-13PO-SO_4^- [1]	0.750	0.250	SBA	1.75	0.5	3.25	3	15	3	
11-74	C_{13}-13PO-SO_4^-	0.625	0.375	SBA	1.75	0.5	4.75	4.5	10	15	
11-75	C_{13}-13PO-SO_4^-	0.750	0.250	SBA	1.75	0.5	3.3	3	16	3	Viscous ME phase
11-76	C_{16-17}-7PO-SO_4^- [1]	0.750	0.250	EGBE/ SBA=3	1.75	0.5	4.7	4.2	14	7	
11-76-2	C_{16-17}-7PO-SO_4^- [1]	0.750	0.250	EGBE/ SBA=3	1.75	0.5	4.3	4.55	18	3	
11-76-3	C_{16-17}-7PO-SO_4^- [1]	0.750	0.250	EGBE/ SBA=3	1.75	0.5	N/A	4.2	N/A	1	
11-77	C_{16-17}-7PO-SO_4^- [1]	0.750	0.250	EGBE/ SBA=3	1.75	0.5	5.5	4.8	13	7	
11-77-2	C_{16-17}-7PO-SO_4^- [1]	0.750	0.250	EGBE/ SBA=3	1.75	0.5	5.1	5.2	13	3	

Table 4.5 Phase behavior results of Wahrman crude oil with different cosolvent, oil conc.=50% (cont.)

Series #W	Primary Surf		Co-Surf. (wt%)	Co-Sol.		Alkali (wt%)	APSL @ Res T (wt%)	O.S.(wt%)	Opt. Sol. Ratio (mL/mL)	Eq time to update (Days)	Comments
	Structure	(wt%)	C_{15-18} IOS	Type	(wt%)	Na_2CO_3		NaCl			
11-77-3	C_{16-17}-7PO-SO_4^- [1]	0.750	0.250	EGBE/ SBA=3	1.75	0.5	N/A	5	12	10	
11-78	C_{13}-13PO-SO_4^-	0.625	0.375	SBA	1.25	0.5	4.7	4.8	14	5	
11-78-2	C_{13}-13PO-SO_4^-	0.625	0.375	SBA	1.25	0.5	4.7	4.8	12	10	
11-79	C_{13}-13PO-SO_4^-	0.625	0.375	IBA	1.25	0.5	N/A	4.5	13	139	
11-79-2	C_{13}-13PO-SO_4^-	0.625	0.375	IBA	1.25	0.5	4.1	4.25	15	3	
11-80	C_{13}-13PO-SO_4^-	0.625	0.375	SBA	1.5	0.5	4.7	4.6	12	10	
11-80-2	C_{13}-13PO-SO_4^-	0.625	0.375	SBA	1.5	0.5	5	5	15	50	
11-81	C_{16-17}-7PO-SO_4^- [1]	0.300	0.100	EGBE/ SBA=3	0.7	0.5	N/A	4.5	N/A	N/A	
11-82	C_{16-17}-7PO-SO_4^- [1]	0.750	0.250	SBA	1.75	0.5	<4.6	4.6	23	50	
11-83	C_{16-17}-7PO-SO_4^- [1]	0.750	0.250	EGBE/ SBA=1	1.75	0.5	4.5	4.4	16	5	
11-84	C_{16-17}-7PO-SO_4^- [1]	0.750	0.250	DGBE/ SBA=1	1.75	0.5	<4.8	4.95	14	23	
11-85	C_{16-17}-7PO-SO_4^- [1]	0.750	0.250	3-Methyl-1-Butonal	1.75	0.5	<1	1.75	N/A	N/A	
11-86-2	C_{16-17}-7PO-SO_4^- [1]	0.667	0.333	EGBE/ SBA=3	1.75	0.5	5.5	5.5	12	3	
11-87-2	C_{16-17}-7PO-SO_4^- [1]	0.667	0.333	DGBE/ SBA=3	1.75	0.5	6.5	6.2	12	3	

Table 4.5 Phase behavior results of Wahrman crude oil with different cosolvent, oil conc.=50% (cont.)

Series #W	Primary Surf.		Co-Surf. (wt%)	Co-Sol.		Alkali (wt%)	APSL @ Res T (wt%)	O.S.(wt%)	Opt. Sol. Ratio (mL/mL)	Eq time to update (Days)	Comments
	Structure	(wt%)	C_{15-18} IOS	Type	(wt%)	Na_2CO_3		NaCl			
11-88	C_{16-17}-7PO-SO_4^- [1]	0.375	0.125	SBA	1.75	0.5	N/A	4.4	8	22	
11-89	C_{13}-13PO-SO_4^-	0.667	0.333	SBA	1.5	0.5	4.3	4.3	13	22	
11-89-2	C_{13}-13PO-SO_4^-	0.667	0.333	SBA	1.5	0.5	4.3	4.3	13	21	
11-89-2P	C_{13}-13PO-SO_4^-	0.667	0.333	SBA	1.5	0.5	4.1	4.35	12.5	21	with polymer
11-89-2R	C_{13}-13PO-SO_4^-	0.667	0.333	SBA	1.5	0.5	4.3	4.5	13	21	oil conc=33%
11-90	C_{13}-13PO-SO_4^-	0.667	0.333	SBA	1.5	0	N/A	4.7	14	5	
11-91	C_{13}-13PO-SO_4^-	0.333	0.167	SBA	1.5	0.5	4.3	3.65	12.5	10	
11-92	C_{13}-13PO-SO_4^-	0.333	0.167	SBA	1.5	0	N/A	4	13	5	
11-93	C_{13}-13PO-SO_4^-	0.333	0.167	SBA	1	0.5	4.1	4	15	50	
11-93-2	C_{13}-13PO-SO_4^-	0.333	0.167	SBA	1	0.5	4.3	4	15	15	
11-93-3	C_{13}-13PO-SO_4^-	0.333	0.167	SBA	1	0.5	4.3	4.2	16	8	
11-93-3R	C_{13}-13PO-SO_4^-	0.333	0.167	SBA	1	0.5	4.3	4.5	23	1	oil conc.=33%

* C_{16-17}-8PO-SO_4^-[1] is from Stepan/TIORCO and C_{16-17}-8PO-SO_4^-[2] is from Sasol.

Table 4.6 Phase behavior results of Wahrman crude oil with polymer, oil conc.=33% unless otherwise specified

Series #W	Primary Surf (wt%)	Co-Surf (wt%)	Co-Sol. (wt%)	Alkali (wt%)	Polymer		APSL at Res. T (wt%)	O.S. (wt%)	Opt. Sol. Ratio	Eq. time to update (Days)	Comments
	C_{16-17}-7PO-SO_4^-	C_{15-18} IOS	DGBE	Na_2CO_3	Type	wt%	NaCl	NaCl	(mL/mL)		
12-1	0.75	0.25	2.5	0.5	N/A	N/A	N/A	>3.0	N/A	272	oil conc.=50%
12-2	0.75	0.25	2.5	0.5	N/A	N/A	N/A	5.15	11	272	oil conc.=50%
12-3	0.67	0.33	2.5	0.5	N/A	N/A	N/A	>6.2	~10	272	oil conc.=50%
12-4	0.33	0.17	1.5	0.5	N/A	N/A	4.1	4	15	15	oil conc.=50%
12-5	0.50	0.25	1.5	0.5	N/A	N/A	4.1	4.3	13	15	oil conc.=50%
12-4R	0.33	0.17	1.5	0.5	N/A	N/A	4.1?	4.1	13	10	
12-6	C_{13}-13PO-SO_4^-:0.56% C_{16-17}-8PO-SO_4^-:0.19%	0.25	1.75	0.5	N/A	N/A	N/A	N/A	N/A	N/A	oil conc.=50%, viscous ME phase
12-7	0.36	0.14	1.75	0.5	FP 3330S	0.23	6.1	5.6	11	10	Eq. time=4 days
12-7-3	0.36	0.14	1.75	0.5	FP 3330S	0.23	6.1	5.3	12	3	
12-8	0.33	0.17	1.75	0.5	FP 3330S	0.25	N/A	4.15	9.5/10	10	
12-10	0.36	0.14	1.5	0.5	FP 3330S	0.23	~5.7	5.5	13	8	

Table 4.6 Phase behavior results of Wahrman crude oil with polymer, oil conc.=33% unless otherwise specified (cont.)

Series #W	Primary Surf (wt%)	Co-Surf (wt%)	Co-Sol. (wt%)	Alkali (wt%)	Polymer		APSL at Res. T (wt%)	O.S. (wt%)	Opt. Sol. Ratio	Eq. time to update (Days)	Comments
	C_{16-17}-7PO-SO_4^-	C_{15-18} IOS	DGBE	Na_2CO_3	Type	wt%	NaCl	NaCl	(mL/mL)		
12-11	0.73	0.27	1.75	0.5	N/A	N/A	6.3	5.7	9.5	6	To repeat 11-71
12-12	0.55	0.20	1.75	0.5	N/A	N/A	N/A	5.32	10	7	repeat 12-9, without polymer
12-13	0.36	0.14	1.5	0.5	N/A	N/A	5.9	5.4	11	6	To repeat 12-10 without polymer
12-13-2	0.36	0.14	1.5	0.5	N/A	N/A	N/A	5.3	13	140	
12-14	0.36	0.14	1.5	1	FP 3330S	0.23	5.4	4.9	**9**	12	
12-15	0.36	0.14	1.5	0.5	FP 3330S	0.3	5.5	5.4	12	22	increase polymer conc.
12-16	0.55	0.20	1.75	0.5	FP 3330S	0.3	N/A	5.6	12	51	increase polymer conc.
12-17	0.36	0.14	1.75	1	FP 3330S	0.23	5.6	5.1	10	13	increase DGBE .
12-17-2	0.36	0.14	1.75	1	FP 3330S	0.23	N/A	5.6	12	51	with more aqueous volume
12-18	0.36	0.14	1.5	1	FP 3330S	0.26	5.4	5.2	13	50	with more aqueous volume
12-19	0.36	0.14	1.5	1	FP 3530S	0.2	5.4	5.3	13	29	with more aqueous volume

Table 4.6 Phase behavior results of Wahrman crude oil with polymer, oil conc.=33% unless otherwise specified (cont.)

Series #W	Primary Surf. (wt%)	Co-Surf. (wt%)	Co-Sol. (wt%)	Alkali (wt%)	Polymer		APSL at Res. T (wt%)	O.S. (wt%)	Opt. Sol. Ratio	Eq. time to update (Days)	Comments
	C_{16-17}-7PO-SO_4^-	C_{15-18} IOS	DGBE	Na_2CO_3	Type	wt%	NaCl	NaCl	(mL/mL)		
12-20	0.36	0.14	1.5	1	FP 3430S	0.2	5.4	5.2	13	21	with more aqueous volume
12-21	0.36	0.14	1.75	1	FP 3530S	0.23	5.8	5.35	12	11	
12-22	0.36	0.14	1.75	1	FP 3430S	0.23	5.8	5.41	12.5	3	
12-23	0.36	0.14	1.5	1	FP 3530S	0.23	5.4	5.1	13.5	8	test alcohol conc. effect
12-25	0.36	0.14	1.75	1	FP 3530S	0.23	5.8	4.95	15	6	
12-26	0.36	0.14	1.75	1	FP 3530S	0.23	5.8	5.27	13	6	repeat formulation for core flood
12-27	0.36	0.14	1.75	1	FP 3530S	0.23	5.8	5.45	10	6	
12-28	0.36	0.14	1.75	1	FP 3530S	0.23	5.8	5.5	10	6	
12-29	0.36	0.14	1.75	1	FP 3530S	0.23	5.8	5.6	9.5	6	
12-30	0.36	0.14	1.5	1	FP 3530S	0.23	5.4	5.27	14	5	test alcohol conc. effect
12-31	0.36	0.14	1.25	1	FP 3530S	0.23	5	5.2	14	23	
12-32	0.36	0.14	1.5	1	FP 3530S	0.23	5.45	5.5	13	23	

Table 4.6 Phase behavior results of Wahrman crude oil with polymer, oil conc.=33% unless otherwise specified (cont.)

Series #W	Primary Surf (wt%)	Co-Surf (wt%)	Co-Sol. (wt%)	Alkali (wt%)	Polymer (wt%)	APSL at Res. T (wt%)	O.S. (wt%)	Opt. Sol. Ratio	Eq. time to update (Days)	Comments
	C_{16-17}-7PO-SO_4^-	C_{15-18} IOS	DGBE	Na_2CO_3	FP 3530S	NaCl	NaCl	(mL/mL)		
12-33	0.36	0.14	1.75	1	0.23	5.8	5.65	11	23	test alcohol conc. effect
12-34	0.36	0.14	1.75	1	0.23	[5.8]	5.4	12	11	34-2nd time received oil, 35-3rd time received oil
12-35	0.36	0.14	1.75	1	0.23	[5.8]	5.6	11.5	21	
12-36	0.36	0.14	1.5	1	0.23	N/A	5.6	12	21	with lower alcohol conc.
12-37	0.36	0.14	1.75	1	0.23	N/A	5.55	13	13	prepare core flood surfactant slug
12-38	0.36	0.14	1.25	1	0	N/A	5.7	15	26	test alcohol conc. effect
12-39	0.36	0.14	1.5	1	0	N/A	5.75	13	26	
12-40	0.36	0.14	1.75	1	0	N/A	5.7	12	26	
12-41	0.36	0.14	1.75	1	0.23	N/A	5.65	12	13	to compare phase behavior results with/without polymer
12-42	0.36	0.14	1.75	1	0	N/A	5.65	11	8	
12-43	0.36	0.14	1.75	1	0	N/A	5.9	11	60	filtered crude oil
12-44	0.36	0.14	1.75	1	0	N/A	5	11	61	unfiltered crude oil
12-45	0.36	0.14	1.75	1	0.23	N/A	5.6	10	57	filtered crude oil

Table 4.7 Phase behavior results of Wahrman crude oil to optimize surfactant slug after Core Flooding W#1

Series #W	Primary Surf (wt%)	Co-Surf (wt%)	Co-Sol. (wt%)	Alkali (wt%)	Polymer/Surf-3		APSL at Res. T (wt%)	O.S. (wt%)	Sol. Ratio	Eq. time to update (Days)	Comments
	C_{16-17}-7PO-SO_4^-	C_{15-18} IOS	DGBE	Na_2CO_3	Type	wt%	NaCl	NaCl	(mL/mL)		
13-1	0.36	0.14	1.75	1	Neodol 25-12	0.1	5.4	>6.4%	N/A	16	
13-2	0.36	0.14	1.75	1	Neodol 25-9	0.1	5	>6.5	>10	17	
13-3	0.36	0.14	1.75	1	Neodol 25-12	0.1	5.8	>6.4	>13	13	
13-4	0.75	0.25	1.75	1	N/A	N/A	3.5?	>4.4	N/A	13	
13-5	0.36	0.14	1.75	1	N/A	N/A	N/A	5.55	10	7	
13-6	0.36	0.14	1.75	1	FP3530S	0.3	5.85	5.5	10	55	
13-7	0.36	0.14	1.75	1	FP3530S	0.3	5.85	5.6	9	157	
13-8	0.75	0.25	1.75	1	N/A	N/A	N/A	~3.7	7	8	Primary Surf: C_{13}-13PO-SO_4^-
13-9	0.75	0.25	1.75	1	N/A	N/A	N/A	N/A	N/A	N/A	Primary Surf: C13-13PO-SO4- No ME phase
13-10	0.36	0.14	1.75	1	FP3530S	0.3	N/A	5.7	11	48	
13-11	0.36	0.14	1.75	1	Neodol 25-12	0.1	N/A	N/A	N/A	N/A	No ME phase
13-12	0.36	0.14	1.75	1	Neodol 25-12	0.1	>7.2	6.9	11	51	
13-13	0.36	0.14	1.75	1	Neodol 25-12	0.1	N/A	7.1	10	156	
13-14	0.36	0.14	1.25	1	Neodol 25-12	0.1	~6.4	6.95	15	8	

Table 4.7 Phase behavior results of Wahrman crude oil to optimize surfactant slug after Core Flooding W#1(cont.)

Series #W	Primary Surf. (wt%)	Co-Surf. (wt%)	Co-Sol. wt%)	Alkali (wt%)	Polymer/Surf-3		APSL at Res. T (wt%)	O.S. (wt%)	Sol. Ratio	Eq. time to update (Days)	Comments
	C_{16-17}-7PO-SO_4^-	C_{15-18} IOS	DGBE	Na_2CO_3	Type	wt%	NaCl	NaCl	(mL/mL)		
13-15	0.55	0.20	1.75	1	N/A	N/A	N/A	6	9	154	viscous phase exist
13-16	0.73	0.27	1.25	1	N/A	N/A	N/A	6	7	152	viscous phase exist
13-17	0.36	0.14	1.25	1	Neodol 25-12	0.2	~7.4	8	14	50	
13-18	0.36	0.14	1.25	1	Neodol 25-12	0.3	N/A	9.5	12	50	
13-19	0.36	0.14	1.75	1	FP3530S	0.3	N/A	5.9	11	60	
13-20	0.36	0.14	1.75	1	FP3530S	0.3	5.85	5.6	9	49	viscous phase after 50 days,with oil from CFW#2 oil flood effluent
13-21	0.36	0.14	1.75	1	FP3630S	0.3	N/A	5.6	12	16	viscous ME phase after 50 days,
13-22	0.36	0.14	1.75	1	FP3530S	0.3	5.85	5.6	10	83	with oil from CFW#1 oil flood effluent
13-23	0.36	0.14	1.75	1	FP3530S	0.3	5.85	5.6	11	25	viscous ME phase after 50 days,
13-24	0.73	0.27	1.75	1	FP3530S	0.3	6	6	10	22	viscous ME phase after 50 days,

Table 4.7 Phase behavior results of Wahrman crude oil to optimize surfactant slug after Core Flooding W#1(cont.)

Series #W	Primary Surf (wt%)	Co-Surf (wt%)	Cosolvent (wt%)	Alkali (wt%)	Polymer/Surf-3		APSL at Res. T (wt%)	O.S. (wt%)	Sol. Ratio	Eq. time to update (Days)	Comments
	C_{16-17}-7PO-SO_4^-	C_{15-18} IOS	DGBE	Na_2CO_3	Type	wt%	NaCl	NaCl	(mL/mL)		
13-25	0.36	0.14	1.75	1	Neodol 25-12	0.1	6.4	7	9	22	viscous ME phase after 50 days,
13-26	0.36	0.14	1.75	1	Petrostep S3	0.1	5.75	5.2	12	21	viscous ME phase after 50 days,
13-27	0.36	0.14	1.75	1	Petrostep S3	0.1	5.3	5.2	12	21	viscous ME phase after 50 days,
13-28	0.36	0.14	1.5	1	Petrostep S3	0.1	5.25	5.15	13	11	viscous ME phase after 50 days,
13-29	0.36	0.14	1.75	1	Petrostep S3	0.1	>5.5	5.2	11	11	viscous ME phase after 50 days,
13-30	0.36	0.14	1.75	1	Petrostep S3	0.1	5.6	5.1	11	15	viscous ME phase after 50 days,
13-31	0.36	0.14	1.5	1	Petrostep S3	0.1	5.2	5.3	11	15	viscous ME phase after 50 days,
13-32	0.36	0.14	1.75	1	Petrostep S3:0.1; FP3530S:0.3		N/A	N/A	N/A	N/A	not made
13-33	0.36	0.14	1.5	1	Petrostep S3	0.1	4.25	4.2	10	15	as13-31,Primary Surf:C_{13}-13PO-SO_4^-
13-34	0.36	0.14	1.75	1	Petrostep S3	0.15	5.1	5.25	9	21	
13-35	0.35	0.15	1.5	1	Petrostep S3	0.15	4.35	4.2	9	11	as 13-31, Primary Surf: C_{13}-13PO-SO_4^-

Table 4.7 Phase behavior results of Wahrman crude oil to optimize surfactant slug after Core Flooding W#1(cont.)

Series #W	Primary Surf	Co-Surf (wt%)	Co-Sol. (wt%)	Alkali (wt%)	Polymer/Surf-3		APSL at Res. T (wt%)	O.S. (wt%)	Sol. Ratio	Eq. time to update (Days)	Comments
	(wt%)	C_{15-18} IOS	DGBE	Na_2CO_3	Type	wt%	NaCl	NaCl	(mL/mL)		
13-36	0.38	0.13	1.75	1	Petrostep S3	0.15	5.35	5.3	9	67	as 13-31,
13-37	0.38	0.13	1.5	1	Petrostep S3	0.15	4.05	3.8	13	23	as 13-31, Primary Surf: C_{13}-13PO-SO_4^-
13-38	0.33	0.17	1.75	1	Petrostep S3	0.15	5.6	5.7	11	64	as 13-31,
13-39	0.38	0.13	1.25	1	Petrostep S3	0.15	<5(5.15)	5.6	16	22	as 13-31,
13-42	0.10	0.10	0	1	Neodol 25-12	0.1	>7.0	N/A	N/A	N/A	No ME phase
13-41	0.15	0.15	0	1	Neodol 25-12	0.1	>6.0	N/A	N/A	N/A	No ME phase,below OS range
13-43	0.15	0.15	0.3	1	Neodol 25-12	0.1	>6.0	N/A	N/A	N/A	No ME phase,below OS range
13-44	0.15	0.15	0.9	1	Neodol 25-12	0.1	4.75	N/A	N/A	N/A	No ME phase
13-41-2	0.15	0.15	0	1	Neodol 25-12	0.1	N/A	>9.0	N/A	N/A	No ME phase
13-45	0.20	0.10	0	1	Neodol 25-12	0.1	N/A	~6.8	>10	15	
13-46	0.23	0.08	0	1	Neodol 25-12	0.1	N/A	N/A	N/A	N/A	No ME phase
13-40	0.15	0.15	0	1	Neodol 25-12	0.1	3.75	>6.0	N/A	N/A	No ME phaes,below OS range

Table 4.7 Phase behavior results of Wahrman crude oil to optimize surfactant slug after Core Flooding W#1(cont.)

Series #W	Primary Surf.	Co-Surf. (wt%)	Cosolvent		Alkali (wt%)	Polymer/Surf-3		APSL at Res. T (wt%)	O.S. (wt%)	Sol. Ratio	Eq. time to update (Days)	Comments
	(wt%)	C_{15-18} IOS	Type	(wt%)	Na_2CO_3	Type	wt%	NaCl	NaCl	(mL/mL)		
13-47	0.20	0.10	DGBE	0	1	Neodol 25-12	0.1	N/A	8	18	6	
13-48	0.23	0.08	DGBE	0	1	Neodol 25-12	0.1	N/A	>8	N/A	N/A	No ME phase, below OS range
13-49	0.20	0.10	DGBE	0	1	Neodol 25-12	0.1	<6.5	~7	N/A	N/A	Primary Surf: C13-13PO-SO4-, viscous ME phase
13-49-2	0.20	0.10	DGBE	0	1	Neodol 25-12	0.1	N/A	N/A	N/A	N/A	Primary Surf: C13-13PO-SO4-, no ME phase
13-50	0.36	0.14	Surfonic L6-6	1.75	1	N/A	N/A	>7	N/A	N/A	N/A	no ME phase
13-51	0.36	0.14	Surfonic X200	1.75	1	N/A	N/A	N/A	N/A	N/A	N/A	no ME phase
13-52	0.36	0.14	SurfonicL4-1	1.75	1	FP3530S	0.3	N/A	3.7	17	3	
13-53	0.36	0.14	SurfonicL4-2	1.75	1	FP3530S	0.3	N/A	6~7	N/A	7	
13-53-2	0.36	0.14	SurfonicL4-2	1.75	1	FP3530S	0.3	<5.5	5.5	14	2	
13-54	0.36	0.14	SurfonicL4-3	1.75	1	FP3530S	0.3	N/A	N/A	N/A	N/A	no ME phase
13-55	0.36	0.14	DGBE	1.75	1	FP3530S	0.3	5.675	6	9	18	

Table 4.7 Phase behavior results of Wahrman crude oil to optimize surfactant slug after Core Flooding W#1 (cont.)

Series #W	Primary Surf.	Co-Surf. (wt%)	Co-Sol.		Alkali (wt%)	Polymer (wt%)	APSL at Res. T (wt%)	O.S. (wt%)	Sol. Ratio	Eq. time to update (Days)	Comments
	(wt%)	C_{15-18} IOS	Type	(wt%)	Na_2CO_3	FP3530S	NaCl	NaCl	(mL/mL)		
13-56	0.36	0.14	DGBE	1.75	1	0.3	N/A	N/A	N/A	N/A	No ME phase, below OS range
13-57	0.36	0.14	DGBE	1.75	1	0.3	5.675	5.5	10	16	
13-58	0.36	0.14	DGBE	1.75	1	0	5.9	N/A	N/A	N/A	No initial aquoeus phase level
13-59	0.36	0.14	DGBE	1.75	1	0.3	5.55	5.6	9.5	101	
13-59-1	0.36	0.14	DGBE	1.75	1	0.3	5.525	5.5	10	97	
13-59-2	0.36	0.14	DGBE	1.75	1	0.3	5.75	5.7	11	10	
13-60	0.36	0.14	DGBE	1.75	1	0	N/A	6	12	2	
13-60-1	0.36	0.14	DGBE	1.75	1	0	5.9	5.2	11	97	
13-60-2	0.36	0.14	DGBE	1.75	1	0	<5.2	6.2	9	11	oil from CFW#2 oil flood
13-63	0.36	0.14	DGBE	1.75	1	0	N/A	>6.4	N/A	11	
13-63-2	0.36	0.14	DGBE	1.75	1	0	5.6	6.1	10	9	
13-63-3	0.36	0.14	DGBE	1.75	1	0	6.2	5.5	12	10	
13-64	0.22	0.08	Surfonic L4-2	1.75	1	0	6.2	6.2	12	34	

Table 4.7 Phase behavior results of Wahrman crude oil to optimize surfactant slug after Core Flooding W#1 (cont.)

Series #W	Primary Surf.	Co-Surf. (wt%)	Co-Sol. (wt%)	Alkali (wt%)	Polymer (wt%)	APSL at Res. T (wt%)	O.S. (wt%)	Sol. Ratio	Eq. time to update (Days)	Comments
	(wt%)	C_{15-18} IOS	DGBE	Na_2CO_3	FP3530S	NaCl	NaCl	(mL/mL)		
13-69	0.36	0.14	1.75	1	0	N/A	6	10	6	determineType III boundary
13-70	0.36	0.14	1.75	1	0	N/A	4.9-6.3	N/A	6	oil conc.=20%
13-71	0.36	0.14	1.75	1	0	N/A	5.9	9	6	oil conc.=14%
13-72	0.36	0.14	1.75	1	0	N/A	6.3	7.5	6	oil conc.=11%
13-73	0.36	0.14	1.75	1	0	N/A	5.7	9	50	
13-73-2	0.36	0.14	1.75	1	0	N/A	>5.3	N/A	5	
13-73-3	0.36	0.14	1.75	1	0	N/A	6.1	13	5	
13-74	0.36	0.14	1.75	1	0	N/A	4.9~6.7	N/A	50	oil conc.=20%
13-74-2	0.36	0.14	1.75	1	0	N/A	4.9~6.7	N/A	50	oil conc.=20%
13-74-3	0.36	0.14	1.75	1	0	N/A	6.3	10	49	oil conc.=20%
13-75	0.36	0.14	1.75	1	0	N/A	4.6-6.7	N/A	50	oil conc.=14%
13-75-2	0.36	0.14	1.75	1	0	N/A	>5.6	N/A	48	oil conc.=14%
13-75-3	0.36	0.14	1.75	1	0	N/A	6.5	8	48	oil conc.=14%

Table 4.7 Phase behavior results of Wahrman crude oil to optimize surfactant slug after Core Flooding W#1(cont.)

Series #W	Primary Surf	Co-Surf (wt%)	Co-Sol. (wt%)	Alkali (wt%)	Polymer (wt%)	APSL at Res. T (wt%)	O.S. (wt%)	Sol. Ratio	Eq. time to update (Days)	Comments
	(wt%)	C_{15-18} IOS	DGBE	Na_2CO_3	FP3530S	NaCl	NaCl	(mL/mL)		
13-76	0.36	0.14	1.75	1	0	N/A	4.6-6.7	N/A	50	oil conc.=11%
13-76-2	0.36	0.14	1.75	1	0	N/A	4.6-6.7	N/A	50	oil conc.=11%
13-76-3	0.36	0.14	1.75	1	0	N/A	6.5	10	46	oil conc.=11%
13-77	0.36	0.14	1.75	1	0	N/A	5.1-6.5	N/A	50	
13-77-2	0.36	0.14	1.75	1	0	N/A	5.2	13	50	
13-77-3	0.36	0.14	1.75	1	0	N/A	5.4	13	46	
13-78	0.36	0.14	1.75	1	0	N/A	5.1	15	50	oil conc.=67%
13-78-2	0.36	0.14	1.75	1	0	N/A	4.6	19	46	oil conc.=67%
13-78-3	0.36	0.14	1.75	1	0	N/A	<5.4	N/A	46	oil conc.=67%

Table 4.8 Phase behavior results of Wahrman crude oil to examine polymer and alkali effect

Series #W	Primary Surf. (wt%)	Co-Surf. (wt%)	Co-Sol. (wt%)	Base Salinity/Alkalinity		Polymer (ppm)	Salinity/Alkalinty Evaluated	O.S.	Opt.Sol. Ratio	Eq time to update (Days)	Comments
	C_{16-17}-7PO-SO_4^-	C_{15-18} IOS	DGBE	Type	(wt%)	FP 3530S	Type	(wt%)	(mL/mL)		
14-1	0.36	0.14	1.75	Na_2CO_3	1	1800	NaCl	5.7	12	25	test polymer effect
14-2	0.36	0.14	1.75	Na_2CO_3	1	2100	NaCl	5.75	11	25	test polymer effect
14-3	0.36	0.14	1.75	Na_2CO_3	1	2400	NaCl	5.55	11	25	test polymer effect
14-4	0.36	0.14	1.75	Na_2CO_3	1	2700	NaCl	5.65	12	25	test polymer effect
14-5	0.36	0.14	1.75	Na_2CO_3	1	3000	NaCl	5.5	12	25	test polymer effect
14-11	0.36	0.14	1.75	NaCl	3	0	Na_2CO_3	>2.1	N/A	2	oil conc.=50%, Na2CO3 scan
14-11-2	0.36	0.14	1.75	NaCl	3	0	Na_2CO_3	4.5	11.5	19	oil conc.=50%, Na2CO3 scan
14-11-3	0.36	0.14	1.75	NaCl	3	0	Na_2CO_3	4.25	12	16	oil conc.=50%, Na2CO3 scan
14-11-4	0.36	0.14	1.75	NaCl	3	0	Na_2CO_3	N/A ~3.75	~10	11	oil conc.=50%, Na2CO3 scan
14-11-5	0.36	0.14	1.75	NaCl	3	0	Na_2CO_3	<4.75	N/A	16	oil conc.=50%, Na2CO3 scan
14-12	0.36	0.14	1.75	NaCl	3	0	Na_2CO_3	>2.8	N/A	2	oil conc.=50%, Na2CO3 scan
14-12-2	0.36	0.14	1.75	NaCl	3	0	Na_2CO_3	4.5	9	4	oil conc.=33%, Na2CO3 scan
14-12-3	0.36	0.14	1.75	NaCl	3	0	Na_2CO_3	5	9	16	oil conc.=33%, Na2CO3 scan
14-12-4	0.36	0.14	1.75	NaCl	3	0	Na_2CO_3	4.25	11	11	oil conc.=33%, Na2CO3 scan

Table 4.8 Phase behavior results of Wahrman crude oil to examine polymer and alkali effect (cont.)

Series #W	Primary Surf. (wt%)	Co-Surf. (wt%)	Co-Sol. (wt%)	Base Salinity/Alkalinity		Polymer (ppm)	Salinity/Alkalinty Evaluated	O.S.	Opt. Sol. Ratio	Eq time to update (Days)	Comments
	C_{16-17}-7PO-SO_4^-	C_{15-18} IOS	DGBE	Type	(wt%)	Flopaam 3530S	Type	(wt%)	(mL/mL)		
14-14-6	0.36	0.14	1.75	NaCl	3	0	Na_2CO_3	<7.25	N/A	6	oil conc.=14%, Na2CO3 scan
14-15	0.36	0.14	1.75	NaCl	3	0	Na_2CO_3	4.9	8	19	oil conc.=11%, Na2CO3 scan
14-15-2	0.36	0.14	1.75	NaCl	3	0	Na_2CO_3	5.1	10	4	oil conc.=11%, Na2CO3 scan
14-15-3	0.36	0.14	1.75	NaCl	3	0	Na_2CO_3	5.3	6	11	oil conc.=11%, Na2CO3 scan
14-15-4	0.36	0.14	1.75	NaCl	3	0	Na_2CO_3	<6.25	N/A	11	oil conc.=11%, Na2CO3 scan
14-15-5	0.36	0.14	1.75	NaCl	3	0	Na_2CO_3	>4.5	N/A	6	oil conc.=11%, Na2CO3 scan
14-15-6	0.36	0.14	1.75	NaCl	3	0	Na_2CO_3	7.75	N/A	6	oil conc.=11%, Na2CO3 scan

Table 4.9 Phase behavior results of Wahrman crude oil for core flood with SFB and limestone

Series #W	Primary Surf. (wt%)	Co-Surf. (wt%)	Co-Sol. (wt%)	Alkali (wt%)	Polymer (ppm)	APSL at Res. T (wt%)	O.S. (wt%)	Opt. Sol. Ratio	Eq.Time to Update	Comments
	C_{16-17}-7PO-SO_4^-	C_{15-18} IOS	DGBE	Na_2CO_3	FP 3530S	NaCl	NaCl	(mL/mL)	(Days)	
15-1	0.36	0.14	1.25	1	1800	5.15	5.8	15	3	
15-2	0.36	0.14	1.75	1	0	<5.9	6.2	11	3	
15-3	0.36	0.14	1.75	1	2500	N/A	5.8	20	4	with polymer FP3330S
15-3-2	0.36	0.14	1.75	1	2500	N/A	5.9	12	4	with polymer FP3330S
15-3-3	0.36	0.14	1.75	1	2500	N/A	5.9	14	1	with polymer FP3330S
15-4	0.36	0.14	1.75	1	2500	5.75	>5.6	>10	89	with polymer FP3330S
15-5	0.36	0.14	1.5	1	2500	5.45	5.6	13	89	with polymer FP3330S
15-6	0.36	0.14	1.75	1	0	N/A	5.7	12.5	19	
15-6-2	0.36	0.14	1.75	1	0	N/A	5.8	11.5	12	
15-7	0.36	0.14	1.75	0	0	N/A	6.7	15	19	
15-7-2	0.36	0.14	1.75	0	0	N/A	6.9	17	13	
15-8	0.36	0.14	1.75	0	0	N/A	6.5	16	19	without Na2CO3 with SFB
15-8-2	0.36	0.14	1.75	0	0	N/A	N/A	N/A	N/A	without Na2CO3 with SFB,over OS range

Table 4.9 Phase behavior results of Wahrman crude oil for core flood with SFB and limestone (cont.)

Series #W	Primary Surf. (wt%)	Co-Surf. (wt%)	Co-Sol. (wt%)	Alkali (wt%)	Polymer (ppm)	APSL at Res. T (wt%)	O.S. (wt%)	Opt. Sol. Ratio	Eq.Time to Update	Comments
	C_{16-17}-7PO-SO_4^-	C_{15-18} IOS	DGBE	Na_2CO_3	FP 3530S	NaCl	NaCl	(mL/mL)	(Days)	
15-8-3	0.36	0.14	1.75	0	0	N/A	6.4	18	13	without Na2CO3 with SFB
15-8-4	0.36	0.14	1.75	0	0	N/A	6.5	20	8	without Na2CO3 with SFB
15-9	0.36	0.14	1.75	0	0	<5.2	6	N/A	1	oil conc.=50%
15-9-2	0.36	0.14	1.75	0	0	N/A	6	20	1	oil conc.=50%
15-10	0.36	0.14	1.75	0	0	<5.4	~5.75	N/A	1	oil conc.=25%, no distinct ME phase
15-10-2	0.36	0.14	1.75	0	0	N/A	~6.5	N/A	1	oil conc.=25%, no distinct ME phase
15-11	0.36	0.14	1.75	0	0	N/A	7.2	9	16	oil conc.=16%
15-11-2	0.36	0.14	1.75	0	0	N/A	6.8	18	1	oil conc.=16%, no distinct ME phase
15-11-3	0.36	0.14	1.75	1	1800	5.9	5.75	10	1	
15-12	0.55	0.20	1.75	1	1800	5.6	5.8	12	3	
15-17	0.55	0.20	2	1	1800	5.75	5.65	11	1	
15-19	0.58	0.17	2	1	0	4.95	5.4	11	1	

Table 4.9 Phase behavior results of Wahrman crude oil for core flood with SFB and limestone (cont.)

Series #W	Primary Surf. (wt%)	Co-Surf. (wt%)	Co-Sol. (wt%)	Alkali (wt%)	Polymer (ppm)	APSL at Res. T (wt%)	O.S. (wt%)	Opt. Sol. Ratio	Eq.Time to Update	Comments
	C_{16-17}-7PO-SO_4^-	C_{15-18} IOS	DGBE	Na_2CO_3	FP 3530S	NaCl	NaCl	(mL/mL)	(Days)	
15-15	0.55	0.20	2.625	1	0	N/A	6.5	6	2	
15-13	0.73	0.27	1.75	1	1800	<5.4	6	11.5	3	
15-18	0.77	0.23	2.2	1	0	5.45	5.6	8.5	1	
15-16	0.73	0.27	2.35	1	0	6.25	6.2	8	1	
15-14	0.73	0.27	3.5	1	0	N/A	7.5	5	2	
15-20	0.36	0.14	2	1	2300	4.95	5.4	11	2	
15-22	0.22	0.08	1.05	0.6	0	4.75	>5.2	N/A	1	
15-23	0.07	0.03	0.35	0.2	0	4.05	3.6	30	1	
15-24	0.36	0.14	1.75	2	2100	<4.7	4.9	11	4	
15-24-2	0.36	0.14	1.75	2	2100	4.8	5.5	11	23	
15-25	0.36	0.14	1.75	2	0	N/A	>5.3	N/A	27	
15-26	0.36	0.14	1.75	3	0	N/A	4.5	9	27	
15-27	0.36	0.14	1.75	4	0	N/A	3.6	9	27	

Table 4.9 Phase behavior results of Wahrman crude oil for core flood with SFB and limestone (cont.)

Series #W	Primary Surf. (wt%)	Co-Surf. (wt%)	Co-Sol. (wt%)	Alkali (wt%)	Polymer (ppm)	APSL at Res. T (wt%)	O.S. (wt%)	Opt. Sol. Ratio	Eq.Time to Update	Comments
	C_{16-17}-7PO-SO_4^-	C_{15-18} IOS	DGBE	Na_2CO_3	FP 3530S	NaCl	NaCl	(mL/mL)	(Days)	
15-28	0.36	0.14	1.75	2	1800	<4.5	4.9	8	22	
15-29-2	0.07	0.03	0.35	0.2	0	N/A	N/A	N/A	7	no ME phase
15-29-3	0.07	0.03	0.35	0.2	0	N/A	N/A	N/A	7	no ME phase, lower phase cloudy around 3.1%
15-29-4	0.07	0.03	0.35	0.2	0	N/A	N/A	N/A	1	no ME phase
15-30	0.18	0.07	0.875	0.5	0	N/A	~3.2	>100	7	full tube ME phase at 3.2%
15-30-2	0.18	0.07	0.875	0.5	0	N/A	<4.1	N/A	7	salinity range over OS
15-30-3	0.18	0.07	0.875	0.5	0	N/A	3.9	40	2	
15-30-3	0.36	0.14	1.75	1	0	N/A	N/A	N/A	2	test new Petrostep S2
15-32	0.27	0.10	1.75	1	0	N/A	3.7	27	2	
15-32-2	0.27	0.10	1.313	0.75	0	N/A	N/A	N/A	2	no ME phase

Chapter 5 Core Flooding Results

5.1 Introduction

Chemical floods were conducted in Berea and Indiana limestone cores using the surfactant formulation identified in Chapter 4 that passed all screening criteria. The purpose of these core tests was to demonstrate the capability of the surfactant system to recover waterflood residual oil saturation. Results and analysis of the results are presented in Chapter 5.

Six corefloods (Cores 5, 8, 12, 14, 17 and 22) were conducted in Berea sandstone cores. Two corefloods (Cores 28 and 29) were conducted in Indiana limestone cores. Each core was prepared by determining the pore volume by saturation and tracer analysis. The initial saturating fluid for most experiments was soft brine with equivalent salinity to surfactant slug but there are some differences between runs. Core properties and saturating fluids are summarized in Table 5.1. Wahrman oil was injected into each core until negligible amount of water was produced. Oil and water saturations were determined by material balance. Permeability to oil at initial water saturation was determined. Residual oil saturations were obtained by injecting water at a constant rate until the oil rate was considered negligible. These saturations were determined by material balance. Brine permeability at residual oil saturation was determined from pressure measurements.

Chemical flooding was done by injecting either 0.3 or 0.6 PV of the surfactant solution at a constant rate of 0.15 mL/min followed by polymer injection at the same rate. Surfactant compositions used in the corefloods are described in Table 5.2. Effluent samples were collected in 4.5 mL increments and analyzed to determine oil cut, surfactant breakthrough and properties

such as pH, viscosity and salinity. Surfactant and polymer concentration were not determined in the effluents.

Oil recovery was determined by material balance. There were some differences between corefloods as adjustments were made to various parts of the procedure to improve oil recovery. Table 5.1 summarizes the results of the eight corefloods. Mobilities of the various regions moving through the core were determined from the analysis of pressure data. Recovery of residual oil from Berea cores varied from 70.2 to 99.6% Recovery from Indiana limestone cores were 27.6 and 40.7 % of the residual oil. Results from individual core floods are presented in the remainder of this chapter.

Mobility control between the surfactant slug and oil bank and between the polymer and surfactant slug is essential to maintain a stable displacement in each coreflood. Mobilities of oil bank, surfactant slug and polymer drive calculated from pressure data are summarized in Tables 5.3-Table 5.6 for Cores 5, 8, 12 and 14. The data indicate satisfactory mobility control during the chemical floods.

5.2 Berea Sandstones Core Flood Results

5.2.1 Core Flood CFW#1(Core #5)

The first core flood for Wahrman crude oil CFW#1 was done in Berea sandstone Core #5. All floods in CFW#1 were conducted vertically to limit gravity effects in the oil displacement processes. Core#5 was saturated with 2% NaCl to determine porosity and to measure brine permeability at room temperature (~23 ℃). The tracer test (Figure 5.1) shows Core#5 was homogeneous and had relative small dispersion feature. The integration of tracer test curve gave pore volume of 99 mL. Pore volume determined by material balance was 100mL, which was lower than tracer test because of present gas, indicated by compressibility test. Therefore the

pore volume determined from the tracer test was used in later calculation. The porosity was 0.175. Overall brine permeability was 223 mD. Table 5.7 presents properties of each section in the core.

5.2.1.1 Brine/Oil/Water Flood

Core#5 was flooded by a brine solution containing 5.65% NaCl and 1% Na_2CO_3 before the oil flood. After the brine flood, the core was placed in a water bath at reservoir temperature (43 ℃) for overnight to achieve temperature equilibration. About 3 PV Wahrman crude oil were injected into the core. The injection rate was 10 mL/min (~140 ft/day) initially, then was gradually reduced to 3 mL/min to contain overall and section pressures within pressure transducer limit (Figure 5.2). Oil relative permeability at residual water saturation (S_{wr}) determined from the pressure data (Figure 5.2) at the end of oil flood was 0.969. The initial oil saturation (S_{oi}) was 0.686 (Table 5.1). Core#5 was water flooded after the oil flood with 0.86 PV brine solution containing 5.65%NaCl and 1% Na_2CO_3 at injection rate of 0.3 mL/min (~4.2 ft/day). The residual oil saturation was 0.302. Relative permeability to water at residual oil saturation (S_{or}) determined from the pressure data (Figure 5.3) at the end of water flood was 0.093 (Table 5.1).

5.2.1.2 Chemical Flood

The surfactant formulation F-4A was used for Core 5. The salinity of the surfactant slug corresponds to the optimum salinity of the formulation at 33% oil concentration, which was close to the residual oil concentration after water flood. The salinity of the polymer drive was 60% of surfactant slug salinity to ensure a phase change in the microemulsion from Winsor type III to Type I as the flood proceeds. The surfactant viscosity was designed to be approximately three times of the apparent viscosity (5 cP) calculated for the oil/water bank. Polymer concentration was increased by 30% in the polymer drive to increase the viscosity to have good mobility control between the surfactant slug and polymer drive. Viscosity of the surfactant slug and the

polymer drive were measured with a Brookfield DV-II+ Pro viscometer and viscosities as a function of shear rate are shown in Figure 5.4. The surfactant slug size was 0.3 PV followed by 1.7 PV of polymer drive.

5.2.1.2.1 Oil Recovery

The chemical flood recovered 70% of the residual oil leaving an oil residual saturation following chemical flood of 9% (Figure 5.5). The initial oil cut in the oil bank was 40% and 55% of the oil was recovered in the oil bank, which was accompanied by surfactant free brine. Figure 5.6 is a photograph of effluent vials after 5 days of equilibration at reservoir temperature. The oil bank arrived at 0.41 PVI and surfactant breakthrough occurred at approximately 1.05 PVI (Table 5.1). Surfactant breakthrough was followed by Winsor Type I micro-emulsion phases to the end (Vials #23 to #40 in Figure 5.6). No Winsor Type II/III phase appeared to exist in the effluent vials, which maybe the reason of low oil recovery. Another reason for low recovery was insufficient surfactant to push oil out of the core due to small surfactant slug size.

5.2.1.2.2 Pressure Analysis

Pressure drops across the core and across six 2-inch sections for the chemical flooding of Core#5 for Wahrman oil are shown in Figure 5.7. The overall pressure drop increased linearly until oil breakthrough at 0.41 PVI and thereafter generally remained constant or increased. Good or favorable mobility control is indicated by pressure gradients that slightly increase from the front of the flood to the rear of the flood throughout the process. Pressure drops across the six sections of the core provide a more enhanced assessment of the pressure gradient along the length of the flood. Pressure drops in each of the sections were about 0.2 psi as water flowed past at the residual oil saturation. A sharp increase in the pressure drops occurred at each section with the arrival of the oil bank. Thereafter, the pressure drops increased with the arrival of surfactant bank, decreased and then increased again with the arrival of the polymer bank. The mobility of

oil/surfactant/polymer bank at each section during the chemical flood is tabulated in Table 5.3. The decreasing mobility from oil bank to surfactant bank to polymer bank indicates good mobility control between oil bank and surfactant slug, surfactant slug and polymer drive.

5.2.1.2.3 Effluent Analysis

The viscosity, pH and equivalent salinity of aqueous effluents from the chemical flood after equilibrating at reservoir temperature (43 ℃) for 5 days were measured and plotted in Figure 5.8, 5.9, 5.10. Effluent viscosities were measured by Brookfield LVDVI+CP viscometer, at a shear rate of 30 s^{-1} due to the small size of samples. Effluent viscosity started to increase at 0.6 PVI and continued to increase after surfactant breakthrough (1.05 PVI) to polymer drive viscosity. pH of the effluent started and maintained at 10.4 (due to 1%Na_2CO_3 in the core saturation and water flood brine) until 1.05 PVI, then it decreased slightly until the end of core flood. The salinity of the effluent started and maintained the same salinity as surfactant slug salinity (same as core saturation brine salinity) until 1.05 PVI, after then it gradually decreased to polymer drive salinity.

The increase in viscosity of the aqueous effluent indicates that the polymer in the surfactant slug arrived at the end of the core. In this coreflood, there was no visible evidence of surfactant in the effluent samples until about 1.05 PVI. Surfactant breakthrough was estimated to be about 1.05 PVI from the appearance of the effluent aqueous phase and the pH and salinity profile. The late breakthrough of surfactant may be caused by retention of surfactant in the core.

5.2.2 Core Flood CFW#2(Core #8)

The second core flood for Wahrman crude oil CFW#2 was done on a Berea sandstone Core#8. All the floods were conducted horizontally instead of vertically for the convenience of operation. Gravity effects in the displacement process seemed did not affect oil recovery from other core

floods conducted by my colleagues. The tracer test (Figure 5.11) shows Core#8 has relative good dispersion feature. The integration of tracer test curve gave pore volume of 100. Pore volume determined by material balance was 98mL, which was lower than tracer test because of present gas indicated by compressibility test. Therefore the pore volume determined from the tracer test was used in later calculation. The porosity was 0.175. Its brine permeability was measured to be 131 mD overall. Table 5.7 summarizes properties of each section in the core.

5.2.2.1 Brine/Oil/Water Flood

Core#8 was saturated with 2% NaCl to measure its brine permeability and then was flooded with 6.55% NaCl, equivalent salinity to 5.65%NaCl and 1% Na_2CO_3 in surfactant slug. Then the core was placed in a water bath at reservoir temperature to achieve temperature equilibration.

About 3.1PV Wahrman crude oil was injected into the core at the injection rate of 1.5 mL/min (~21 ft/day). The initial oil saturation (S_{oi}) after oil flood was 0.66 (Figure 5.12) and oil relative permeability at residual water saturation (S_{wr}) determined from the pressure data (Figure 5.13) at the end of oil flood was 1.

After oil flood, Core#8 was flooded with 0.52 PV brine solution containing 6.55% NaCl at injection rate of 0.3 mL/min (~4.2 ft/day). The residual oil saturation after water flood was 0.395 (Figure 5.14). Permeability to water at residual oil saturation (S_{or}) determined from the pressure data (Figure 5.15) at the end of water flood was 0.053 (Table 5.1).

5.2.2.2 Chemical Flood

In Core#8 surfactant formulation F-4B was developed in which ; (1) polymer concentration was increased to 3000ppm to improve mobility control between oil bank and surfactant slug and (2) phase behavior studies were conducted with containing higher polymer concentration to find the optimum salinities at oil concentration at 33% (WOR=2), which was close to residual oil saturation after water flood. This salinity (6.65%-including 1 % Na_2CO_3) was selected as the salinity of the surfactant slug. In addition, the polymer concentration in the polymer drive was increased to 3000 ppm, and polymer drive salinity was increased from 3.9% NaCl to 4.6% to establish a slow phase transition from Winsor Type-III-> Type-I to keep phase behavior between oil bank and surfactant slug in Winsor Type-III (low interfacial tension) as long as possible; Surfactant slug and polymer drive composition for CFW#2(Core#8) and CFW#1(Core#5) compared in Table 5.1. The phase behavior results of modified surfactant formulation F-4B are presented in Table 5.2.

Viscosities of surfactant slug F-4B and polymer drive were measured by Brookfield LVDVI+CP viscometer and are shown in Figure 5.16.

5.2.2.2.1 Oil Recovery

The chemical flood consisted of injecting 0.6 PV of surfactant slug followed by a polymer drive of 1.2 PV (Table 5.1) at the flow rate of 0.15mL/min (2.1 ft/day) at the reservoir temperature (43℃). A cumulative oil recovery of 97% (Figure 5.17) of the residual oil and a highest oil cut of 55% were achieved at 0.41PV. 65% of the oil was recovered in the oil bank, which is accompanied by surfactant free brine and about 85% oil was recovered after 1PV of slug was injected. Earlier oil breakthrough, higher oil cut, longer oil bank and higher cumulative oil recovery were achieved in core flood of core#8 than core#5. Earlier oil breakthrough and higher

oil cut might due to more viscous displacing fluid; while longer oil bank might mainly because of bigger surfactant slug size. The photo of effluent from chemical flood is shown in Figure 5.18.

5.2.2.2.2 Pressure Analysis

The differential pressure during the chemical flooding is presented in Figure 5.19. In order to examine whether there is mobility control during chemical flood, the mobility of the oil bank/surfactant bank at each section was calculated from the pressure data when they arrived at the end of that section. The mobility results are compared in Table 5.4. The mobility of surfactant bank was lower than mobility of oil bank in each section indicating there was good mobility control between oil bank and surfactant slug. The mobility of polymer drive was slightly higher than surfactant slug due to its slightly lower viscosity than surfactant slug but still there was good mobility control between surfactant slug and polymer drive.

5.2.2.2.3 Effluent Properties

Properties of the aqueous effluent samples from chemical flood after equilibrating at reservoir temperature (43℃) for 9 days ((viscosity, pH and equivalent salinity) were measured and presented in Figure 5.20, 5.21 and 5.22. The viscosity started to increase at the time of surfactant breakthrough (0.71PV). Because the polymer drive viscosity was slightly lower than surfactant slug (Figure 5.16**)**, the viscosity of effluent continued to increase until polymer breakthrough (1.55PV). The pH of the effluent started at a point higher than water flood brine, which indicated the core was more inclined to be alkaline. It decreased slightly and maintained the same before surfactant slug breakthrough. Because the surfactant slug contained sodium carbonate while polymer drive did not, the pH started to increase when surfactant breakthrough and decreased when polymer breakthrough. The effluent salinity started and maintained at water flood brine salinity and reduced to surfactant slug salinity, which was slightly lower salinity than water flood

brine due to the presence of sodium carbonate. The effluent salinity continued to decrease after the breakthrough of polymer drive.

5.2.2.2.4 Oil Cut Dispersion Model

The oil displacement process after the breakthrough of surfactant slug was believed to be a dispersion process due to the low interfacial tension and good mobility control between surfactant slug and oil bank. A dispersion model based on oil cut behavior after surfactant breakthrough was developed and fitted the oil cut curve (Figure 5.23), which verifies the oil displacement after surfactant breakthrough as a dispersion process.

5.2.3 Core Flood CFW#3 (Core #12)

Core Flood CWF#3(Core#12) was conducted with the same formulation as Core #8 except the surfactant slug size was reduced to 0.3PV. All the floods were conducted horizontally. The tracer test (Figure 5.24) showed Core#12 was homogeneous and had relative small dispersion feature. The integration of tracer test curve gave pore volume of 98 mL. The pore volume determined from material balance was 98mL. The porosity was 0.166. Brine permeability was 190 mD overall. Table 5.7 summarizes properties of each section in the core.

5.2.3.1 Brine/Oil/Water Flood

Core#12 was saturated with 2% NaCl first to measure its brine permeability but was not flooded with 6.55% NaCl as it was supposed to be. The effect is discussed in Water Flood and Effluent Properties sections. The core was placed in a water bath at reservoir temperature to achieve temperature equilibration as usual.

Two oil floods were done on Core#12 because of a problem which occurred during first oil flood. About 2.5PV Wahrman crude oil was injected into the core at the injection rate of 2 mL/min (~28 ft/day) before the some of the low salinity brine (~0.1%NaCl), which was used to displace

the crude oil from the transfer cylinder was injected into the core. The invasion of low salinity brine into the core can be observed in the pressure profile (Figure 5.26). Because the amount of the brine injected to the core could be calculated from analyzing the pressure response and the oil saturation could be calculated correctly, therefore the core was continually oil flooded (second oil flood) but in the opposite direction to displace the low salinity brine and 2% NaCl brine. About another 4.5 PV Wahrman crude oil was injected to the core until no significant pressure change. Low salinity brine was believed to be displaced completely and 2% NaCl was assumed to remain in the residual brine after the second oil flood. The pressures during second oil flood were not presented here. The final oil saturation (S_{oi}) after oil flood was 0.663 (Figure 5.25) and oil relative permeability at residual water saturation (S_{wr}) determined from the oil permeability test at the end of oil flood was 1.

After the second oil flood, Core#12 was flooded with 0.42 PV brine solution containing 6.55% NaCl at injection rate of 0.3 mL/min (~4.2 ft/day). The injected rate was reduced to 0.15 mL/min, which was the same as chemical flood rate to determine the pressure drop to examine the pressure consistency of residual brine at the end of water flood and the beginning of chemical flood. The residual oil saturation after water flood was 0.414 (Figure 5.27). Because only 0.42 PV of 6.55%NaCl solution was injected, the 2% NaCl solution in the core was not completely displaced from the core. The fluid distribution in the core after water flood was: 41% oil, 42% 6.55% NaCl and 17% 2%NaCl. Permeability to water at residual oil saturation (S_{or}) determined from the pressure data (Figure 5.28) at the end of water flood was 0.032 (Table 5.1). After the water flood, the pressures at zero flow rate were not consistent with the pressure before water flood at zero flow rate. This was because of the capillary pressure caused by invasion of oil drops

to the pressure tubings, which were filled with brine. Pressure tubings were rinsed with water flood brine from inside the core after water flood to eliminate the capillary pressures.

5.2.3.2 Chemical Flood

Viscosities of the surfactant slug (Formulation F4B) and polymer drive for CFW#3 were measured with Brookfield LVDV+CP viscometer and are shown in Figure 5.29**.** The viscosities of surfactant slug and polymer drive of CFW#3 are similar to those of CFW#2.

5.2.3.2.1 Oil Recovery

The chemical flood consisted of injecting 0.3 PV of surfactant slug followed by a polymer drive of 1.6 PV (Table 5.1). A cumulative oil recovery of 87.3% (Figure 5.30 and 5.31) of the residual oil and a highest oil cut of 57% were achieved at 0.28PV. 70% of the oil was recovered in the oil bank, which was accompanied by surfactant free brine and about 83% oil was recovered after 1PV of slug was injected. Oil breakthrough occurred slightly earlier (0.16 PVI rather than 0.21 in CFW#2) and surfactant breakthrough slightly later (0.8 PVI rather than 0.71 PVI in CFW#2); the oil cut immediately after surfactant breakthrough was close both in CFW#2 and CFW#3, but the oil cut at the end of oil bank and after surfactant breakthrough in CFW#3 was lower than that in CFW#2. This was believed due to a smaller surfactant slug size. The oil cut curve was fitted by dispersion model curve (Figure 5.32).

5.2.3.2.2 Pressure Analysis

Pressure drops across the core and across six 2-inch sections for the chemical flooding of Core#12 are shown in Figure 5.33. The mobilities of oil/surfactant/polymer banks at each section during the chemical flood were calculated and are tabulated in Table 5.5. Surfactant bank had much lower mobility than oil bank, indicating good mobility control between surfactant slug and oil bank. However, surfactant slug mobility had lower mobility than polymer drive even though surfactant slug had lower viscosity than polymer drive (Figure 5.29), which may be attributed to

a viscous phase produced by mixing of the surfactant slug and crude oil. CFW#3 overall and section pressures were much higher than that of CFW#2 even though their viscosities of surfactant slug and polymer drive were the same (Figure 5.16 and 5.29). This possibility was investigated in CWF#4.

When the oil/surfactant/polymer enters or leaves each section, there is always a differential pressure change. Figure 5.34 is an example of how pressure change correlating with oil/surfactant/polymer bank enters/leaves section 2 of Core#12 during chemical flood. The time when pressure started to increase was when oil bank front entered that section; when pressure started to decease was when oil bank front left that section; when pressure reduced to first local minimum was when surfactant bank front entered that section; when pressure increased to maximum was when surfactant bank front left that section; when pressure reduced to second local minimum was when polymer bank entered that section; when pressure started to stabilize was when polymer bank left that section.

In order to help visualize how the oil/surfactant/polymer bank travelled in the core, the dimensionless distance of oil/surfactant/polymer bank traveled along the core at the time of pore volumes injected was plotted in Figure 5.35. The dimensionless distance of 0, which was the beginning of section 1, correlates to forming of oil bank and start of injection of surfactant slug/polymer drive. The dimensionless distance of 1, which was the end of section 6, correlated to the breakthrough of oil/surfactant/polymer bank. Since the time (PVI) when oil/surfactant/polymer bank started (start of the injection) and ended (breakthrough of the core) was known, straight lines representing the front movement of oil/surfactant/polymer were drawn assuming the oil/surfactant/polymer banks traveled linearly. The characteristic points of pressure behavior of each section, described in Figure 5.34, were also plotted in Figure 5.35. The good

correlation of the pressure behavior characteristic points with straight line of oil/surfactant/polymer banks showed that oil/surfactant/polymers bank traveled linearly along the core.

5.2.3.2.3 Effluent Properties

The properties of aqueous effluents from CFW#3 equilibrating at reservoir temperature (43 ℃) for 2 days, like viscosity, pH and equivalent salinity were measured and presented in Figure 5.36, 5.37 and 5.38

The effluent viscosity started to increase sharply at the time of surfactant breakthrough (0.77PV), after it increased to maximum viscosity at 1.1PV, then it maintained at a viscosity slightly below surfactant slug/polymer until the end of core flood (Figure 5.36). The effluent viscosity was close to surfactant slug and polymer drive viscosity and this indicated that either high differential pressure were caused by viscous phase formed in situ during chemical flooding and "de-viscous" after breakthrough out of the core, or high differential pressures were caused by other factors, like ineffective oil displacement by surfactant.

The effluent pH started around 8 and then increased to around pH of surfactant slug (Figure 5.37), which shared similar behavior as in CFW#2.

Because about 0.17PV 2% NaCl resided in the core after water flood, the equivalent salinity started to increase from 2% to surfactant slug salinity at surfactant breakthrough (Figure 5.38). The salinity gradually decreased to polymer drive salinity after polymer breakthrough (1PV). The 2%NaCl in the core seemed did not affect the oil recovery because 0.17PV 2% NaCl was displaced out of the core already before surfactant breakthrough (0.77PV), which means surfactant slug did not contact with 2% NaCl brine.

The mobility of oil/surfactant/polymer bank is compared in Table 5.5. The mobility of surfactant was much lower than mobility of oil bank in each section indicating there was good mobility control between oil bank and surfactant slug. The mobility of polymer drive was slightly lower than mobility of surfactant slug indicating there was good mobility control between surfactant slug and polymer drive.

5.2.4 Core Flood CFW#4(Core #14)

Since the mobilities of the surfactant slug and polymer drive in CFW#2 and CFW#3 were much lower than oil bank mobility (Table 5.4 and 5.5), it was estimated that polymer concentration in surfactant slug and polymer drive could be reduced by 40% to have same mobility as the oil bank. Polymer concentration was reduced to 1800ppm and 2100ppm in surfactant slug and polymer drive of CFW#4. The phase behavior of surfactant formulation F-4C (Table 5.2) containing 1800ppm FP3530S was examined before chemical flood (Table 5.2). CFW#4(Core #14) was conducted with the polymer drive and same slug size (0.6PV) as CFW#2.

All the floods in CFW#4 were conducted horizontally. The tracer test (Figure 5.39) shows Core#14 was homogeneous and had relative good dispersion feature. The integration of tracer test curve gave pore volume of 96.4 mL. The pore volume determined from material balance was 97.3 mL. The porosity was 0.163. Its brine permeability was measured to be 178 mD overall. Table 5.7 includes properties of each section in the core.

5.2.4.1 Brine/Oil/Water Flood

Core#14 was saturated with 2% NaCl to measure its brine permeability and was flooded with 6.55% NaCl. The core was placed in a water bath at reservoir temperature to achieve temperature equilibration..

About 3.1 PV Wahrman crude oil was injected to the core until no significant brine produced. The oil saturation (S_{oi}) after oil flood is 0.582 (Figure 5.40) and oil relative permeability at residual water saturation (S_{wr}) determined from the pressure data (Figure 5.41) at the end of oil flood was 0.99.

After oil flood, Core#14 was flooded with 0.4 PV brine solution containing 6.55% NaCl at injection rate of 0.3 mL/min (~4.2 ft/day). The injected rate was reduced to 0.15 mL/min (same as chemical flood rate) to examine the pressure consistency of residual brine at the end of water flood and the beginning of chemical flood. The residual oil saturation after water flood was 0.418 (Figure 5.42). The pressure profile during water flood is presented in Figure 5.43. Pressure tubings were rinsed with water flood brine from inside the core after water flood to minimize capillary pressure effects.

5.2.4.2 Chemical Flood

The design of viscosity of surfactant slug and polymer drive was based on the viscosity measured at a shear rate of 30 s^{-1}. However, the viscosity of surfactant slug and polymer in situ during chemical flood was thought to be at a shear rate, about 1 s^{-1}. A Bohlin rheometer was used to measure the viscosity surfactant slug and polymer drive at low shear rate (1 s^{-1}) (the points in Figure 5.44). The Carreau model was used to fit the viscosity-shear rate relationship for polymer Figure 5.44). Low shear rate viscosities of polymer solutions containing different concentration of FP3530S and 4.6% NaCl (typical polymer drive salinity in this research) were measured by Bohlin rheometer (Figure 5.45). These were used for calculating polymer concentration given desired viscosity in later experiments.

5.2.4.2.1 Oil Recovery

The chemical flood consisted of injecting 0.6 PV of surfactant slug followed by a polymer drive of 1.2 PV (Table 5.1) at injection rate was 0.15mL/min (2.1 ft/day). Cumulative oil recovery was 99.6% (Figure 5.46 and 5.47) of the residual oil and a highest oil cut of 59% were achieved at 0.28PV. 72% of the oil was recovered in the oil bank, which was accompanied by surfactant free brine and about 85% oil was recovered after 1PV of slug is injected. Again, the oil cut curve after surfactant breakthrough was fitted by a dispersion model curve (Figure 5.48).

5.2.4.2.2 Pressure Analysis

Pressure drops across the core and across six 2-inch sections for the chemical flooding of Core#14 for Wahrman oil are shown in Figure 5.49. The dimensionless distance that the oil/surfactant/polymer bank traveled along the core was plotted versus the pore volumes injected in Figure 5.50; the characteristic points of differential pressures during chemical flood were plotted in Figure 5.50 and correlated with travelling path of oil/surfactant/polymer bank, indicating the oil/surfactant/polymer bank traveled linearly in the core.

Mobilities of oil/surfactant/polymer banks are presented in in Table 5.6. The mobility of surfactant was lower than mobility of oil bank in each section indicating there was good mobility control between oil bank and surfactant slug. The mobility of polymer drive was slightly lower than mobility of surfactant slug indicating there was good mobility control between surfactant slug and polymer drive.

5.2.4.2.3 Effluent Properties

Effluent viscosities of CFW#4 started to increase at surfactant breakthrough, but not as sharp as in CFW#3/CFW#2 because more mixing existed between surfactant and oil bank caused by lower surfactant concentration in the surfactant slug of CW#4. The, effluent viscosity exceeded the polymer viscosity and then decreased to polymer drive viscosity (Figure 5.51). This

unexpected viscosity increase suggested that a viscous phase might be produced by the mixing of surfactant and in situ oil. The effluent pH behavior followed the typical pH behavior: started at pH around 8 then increased to the pH of surfactant slug and started to decrease at 1.7PV, after polymer breakthrough (Figure 5.52). Effluent salinity started at water flood brine salinity, which was equivalent to surfactant slug salinity, and maintained at surfactant slug salinity until 1.4PV. Then it gradually decreased to polymer slug salinity till the end of chemical flood (Figure 5.53). In summary, the surfactant bank breakthrough at 0.77PV could be derived at viscosity/pH/equivalent salinity profile. The viscosity and equivalent salinity indicates polymer bank breakthrough at 1.4PV. pH is not a good indication of polymer breakthrough because 0.5%-1% Na2CO3 gave very close pH value.

5.2.4.2.4 Microemulsion Phase Viscosity

A pressure peak occurred when surfactant left each section. The cause of this pressure spike was suspected to be due to a viscous phase produced by mixing of surfactant slug and crude oil in situ during chemical flooding. In order to examine this hypothesis, CFW#4 surfactant slug and Wahrman crude oil were mixed at different ratio and equilibrated at 43.3 ℃ for 4 days. Three phases formed after equilibration and the middle phase (microemulsion phase) was extracted with syringe to measure their viscosities. The results are presented in Figure 5.54. The microemulsion phase viscosity at different oil concentration was similar to surfactant slug (viscosity with 0% oil) and varies slightly from each other. . Viscosities measured by the Brookfield LVDV+CP viscometer are presented in Figure 5.54 and 5.55.

Another experiment was conducted to examine this hypothesis. CFW#4 surfactant slug and Wahrman crude oil were mixed at different ratio and equilibrated at 43.3 ℃ for only 2 hours. Only a homogeneous mixture formed instead three phases because of short time equilibration.

The mixture viscosity was measured because usually it only took several hours for surfactant slug to mix with crude oil and produce pressure peak during laboratory core flood. The results of mixture viscosities at different oil concentration are presented in Figure 5.55. The mixture viscosities at different oil concentration were even closer to surfactant slug than microemulsion phase viscosities.

In summary, the viscosities of microemulsion phase or mixture were close to surfactant slug viscosity, which was not able to cause such pressure peak seen in the pressure data. The pressure peak when surfactant entered each section may be due to the natural mechanism how it displaced oil since similar pressure peak occurred in every core flood.

5.2.5 Core Flood CFW#5(Core #17)

Reproducibility of core flood is important to examine the accuracy and reliability of core flood results. Core flood CFW#5 was done on Berea sandstone Core#17 to reproduce CFW#4(Core#14). Core#14 and Core#17 shared similar core dimensions, porosity and permeabilities (Table 5.1). Their diffusion characteristics showing from tracer tests were very similar (Figure 5.56). The similar core conditions between these two cores made them to be perfect to repeat chemical flood on each other. The pore volume determined from tracer test was 98.6mL. The pore volume determined from material balance was 98.4 mL. The porosity was 0.167. The permeability to brine is 186mD overall. Table 5.7 includes properties of each section in the core.

5.2.5.1 Brine/Oil/Water Flood

Core#17 was flooded with 6.55% NaCl before oil flood as Core#14. After about 3.4 PV Wahrman crude oil was injected into the core, the oil saturation (S_{oi}) was 0.664 (Figure 5.57) and oil relative permeability at residual water saturation (S_{wr}) determined from the pressure data

(Figure 5.58) at the end of oil flood was 1. After oil flood, Core#17 was flooded with 0.5 PV brine solution containing 6.55% NaCl at injection rate of 0.3 mL/min (~4.2 ft/day). The residual oil saturation after water flood was 0.423 (Figure 5.59). The water relative permeability at interstitial water saturation was 0.036. Pressure tubings were rinsed with water flood brine from inside the core after water flood to eliminate the capillary pressures (Figure 5.60). Core#14 and Core#17 were treated very similarly during water and oil floods and both cores had similar residual oil saturation as a target for chemical flood.

5.2.5.2 Chemical Flood

CFW#5 had same design on surfactant formulation, slug salinity, slug size, polymer concentration in slug and drive as CFW#4 (Table 5.1). The viscosities of CFW#5 surfactant slug and polymer drive were measured and were about 3-4 cP larger than CFW#4 surfactant slug and polymer drive (Figure 5.44 and Figure 5.61).

5.2.5.2.1 Oil Recovery

The oil recovery results for both core floods are compared in Figure 5.62. The cumulative oil recovery for CFW#3 and CFW#4 was close, 99% and 95% respectively. Oil cut at oil bank for CFW#5 dropped slightly faster than CFW#4 after surfactant slug breakthrough causing slightly lower cumulative oil recovery. Overall CFW#5 was a good reproduction of CFW#4 based on the oil recovery results. The photos of the effluents of CFW#5 are shown in Figure 5.63. The oil cut curve could be fitted with oil dispersion model (Figure 5.64).

5.2.5.2.2 Pressure Analysis

Mobility analysis on CFW#5 was difficult due to severe capillary pressure disturbance on pressure behavior (Figure 5.65). However, high oil recovery results suggested there was probably good mobility control in chemical flood of CFW#5. The overall pressures for both cores are compared in Figure 5.66, the pressures difference agreed well with the viscosity

difference of surfactant slug and polymer drive of CFW#4 and CFW#5 (Figure 5.44 and 5.61). The dimensionless distance versus pore volumes injected plot for CFW#5 (Figure 5.67) was similar to that of CFW#4 (Figure 5.50).

5.2.5.2.3 Effluent Properties

CFW#5 effluent samples properties, for example, the viscosity, salinity and pH were measured and compared with that of CFW#4 in Figure 5.68, 5.69 and 5.70. All the properties for CFW#5 and CFW#4 were similar to those measured in CFW#4. CFW#5 reproduced chemical flood results of CFW#4 relatively well in terms of oil recovery, differential pressure and effluent properties.

5.2.5.2.4 Polymer Flow Analysis

Following the chemical flood, polymer was injected into Core 17 to estimate the shear rate the polymer experienced in situ during chemical flood and to determine the effect of flow rate on the polymer mobility. The polymer drive solution was injected into the core at different flow rates and pressures were recorded. Apparent viscosities of the polymer drive at each section were calculated assuming permeability reduction factor, R_k, of 1. The viscosity of polymer drive versus shear rate was cross plotted with apparent viscosity of polymer drive calculated from the polymer flow test. After some adjustment of the shear rate in X-axis and the flow rate in secondary X-axis, the solution viscosity curve overlapped with apparent viscosity curve as shown in Figure 5.71 for Sections 2-6. The flow rate of 0.15mL/min for the chemical flood appears to be consistent with a shear rate of 1 s^{-1}. Therefore viscosity at shear rate of 1 1/s was recommended to be measured and used in design of mobility control.

5.2.6 Core Flood CFW#6(Core #22)

CFW#6(Core #22) was designed to repeat CFW#4/CFW#5 in Berea sandstone Core#22 with synthetic formation brine used to saturate and water flood the core. The formation brine had relatively high salinity (121669 ppm) and relatively low divalent ions (2484 ppm) (Table 5.8). The high salinity and divalent ions may affect the phase behavior of surfactant slug and precipitate surfactants. The tracer test (Figure 5.72) shows Core#22 was homogeneous and had relative small dispersion feature. The integration of tracer test curve gave pore volume of 98.4 mLThe porosity was 0.178. Its brine permeability was measured to be 186 mD overall. Table 5.7 includes properties of each section in the core.

5.2.6.1 Brine/Oil/Water Flood

Core#22 was flooded with Wahrman oil formation synthetic brine before oil flood. The synthetic formation brine components are listed in Table 5.7. After about 3.1 PV Wahrman crude oil were injected to the core. The oil saturation (S_{oi}) was 0.651 (Figure 5.73) and oil relative permeability at residual water saturation (S_{wr}) determined from the pressure data (Figure 5.74) at the end of oil flood was 0.956. After oil flood, Core#17 was flooded with 0.44 PV Wahrman oil synthetic formation brine at injection rate of 0.3 mL/min (~4.2 ft/day). The residual oil saturation after water flood was 0.44 (Figure 5.75). The water relative permeability was 0.033. Pressure tubings were rinsed with water flood brine from the core after water flood to eliminate the capillary pressures (Figure 5.76).

5.2.6.2 Chemical Flood

. Surfactant formulation F-4C was used in CFW#6. The viscosities of surfactant slug and polymer drive were similar to those of Core#14 (Figure 5.77).

5.2.6.2.1 Oil Recovery

Oil recovery results of CFW#6 are presented and compared with CFW#4 in Figure 5.78. Even though synthetic formation brine was used in CFW#6, it had very similar oil cut and cumulative oil recovery as CFW#4, 98% and 99% respectively. The differential pressure and photos of effluent vials of CFW#6 chemical flood are shown in Figures 5.79 and 5.80. The oil cut curve was fitted by oil dispersion model as shown in Figure 5.81.

5.2.6.2.2 Effluent Properties

Effluent properties (viscosity, pH and total dissolved solids (TDS)) were measured and are plotted in Figures 5.82, 5.83 and 5.84. The viscosity and pH of CFW#6 effluents had similar values to CFW#5 (Figures 5.68, 5.69, 5.82 and 5.83) except the TDS profiles (Figure 5.70 and Figure 5.84). In CFW#6, TDS started at the TDS of the synthetic formation brine, decreased to surfactant slug salinity after surfactant breakthrough and then gradually declined to polymer drive salinity. The surfactant breakthrough at 0.8PVI, was consistent with CFW#4 and CFW#5, which contributed to a big oil bank and high oil recovery.

5.2.6.2.3 Mobility Design

Water/oil relative end permeabilities were determined at the end of water/oil floods and water/oil relative permeability curves were estimated from analysis of oil bank breakthrough in the chemical flood. Total mobility was calculated based on the water/oil relative permeability curves (Figure 5.85). Surfactant slug should have mobility lower than minimum total mobility of the water/oil bank. For example, for CFW#6, minimum total mobility was about 10 mD/cP, the overall core permeability was about 190mD, therefore the lowest slug viscosity was 190/10 [mD/(mD/cP)]=19cP, the design viscosity of the surfactant slug. This design was relatively conservative since the actual total mobility during chemical flood was expected to be higher than total mobility at residual oil saturation after water flood.

Even though the resident brine in CFW#6 had high TDS and low concentration of divalent ions, the cumulative oil recovery was expected to be high as long as surfactant breakthrough occurred relatively late (0.7-0.8PVI), oil cut maintained high before surfactant breakthrough and TDS of slug passed by optimal salinity soon after surfactant breakthrough,.

5.3 Indiana Limestone Core Flood Results

5.3.1 Core Flood CFW#7(Core #28)

The Wahrman reservoir rock is limestone. Indiana limestone cores were obtained to determine if the formulation developed in Berea cores recovered the same amount of residual oil in a limestone core. Core#28 was an Indiana limestone core which had similar dimensions and porosity as Core#22. Tracer tests (Figure 5.86) showed Core#28 had about 5-6 times more dispersion than Core#22. This indicated more heterogeneity of Core#28 than Core#22 and may contribute to oil recovery of chemical flood reversely. The pore volume determined from tracer test was 106mL. The pore volume determined from material balance was 108mL. The porosity was 0.173 The permeability to brine is 190mD overall. Table 5.7 includes properties of each section in the core.

5.3.1.1 Brine/Oil/Water Flood

Core#28 was flooded with Wahrman oil synthetic formation brine before oil flood. About 3.1 PV Wahrman crude oil was injected to the core to reduce the brine saturation to residual. The initial oil saturation (S_{oi}) was 0.526, much lower than observed in Berea core Core#22(S_{oi}= 0.651 Figure 5.87). Oil relative permeability at residual water saturation (S_{wr}) determined from the pressure data (Figure 5.88) at the end of oil flood was 1. Core#28 was flooded with 0.5 PV Wahrman oil synthetic formation brine at injection rate of 0.3 mL/min (~4.2 ft/day). Water breakthrough occurred at 0.12 PV, much earlier than water breakthrough on Core#22,(0.27PVI). About 0.1PV oil was produced after water breakthrough in limestone Core# 28 while almost no

oil was produced from sandstone Core#22 after water breakthrough. The residual oil saturation after water flood was 0.336, much lower than residual oil saturation of Core#22, 0.44 (Figure 5.89). This is due to the difference in pore structure and rock material between limestone and sandstone. The water relative permeability determined from pressure data during water flood (Figure 5.90) was 0.062.

5.3.1.2 Chemical Flood

Anhydrite (CaSO4) was found in some carbonate rocks may severely affect oil recovery in alkaline surfactant floods when the calcium dissolves and reacts with the carbonate, precipitating calcium carbonate and reducing the pH[Levitt, *et al*. 2006]. Brine from displacement experiments in Core #28 was analyzed using plasma (ICP) (Table 5.9) to determine if CaSO4 was present. Table 5.9 shows that small concentrations of calcium and magnesium were dissolved from the core along with a small amount of sulfur. Therefore it was not necessary to modify the current surfactant slug used in previous successful core floods on sandstone. The injection plan for CFW#7 is presented in Table 5.1. The viscosity of surfactant slug and polymer drive were measured at reservoir temperature and presented in Figure 5.91.

5.3.1.2.1 Oil Recovery

The oil recovery for Core#28 is presented and compared with Core#22 in Figure 5.92. The oil bank average oil cut was about 19%, far less than the average oil cut at oil bank, 48%, for Core#22(Figure 5.91). Oil breakthrough occurred very early, at 0.08PVI, and surfactant breakthrough occurred also early, at 0.3PVI. The low oil cut at oil bank suggested that surfactant slug integrity may be compromised therefore was not able to displace oil efficiently. The compromise may be due to the excessive mixing between surfactant slug and residual brine/oil due to the large dispersion observed in Core#28 compared toCore#22 (Figure 5.86). The data indicate that the surfactant slug was not able to create a large oil bank as observed in Berea cores.

The photos of the effluent vials from CFW#7 are presented in Figure 5.93. There was no microemulsion phase in the effluent and the aqueous phase of CFW#7 had much lighter color than CFW#6, which indicated that much less surfactant were recovered and collected in the effluent and therefore more surfactant was absorbed in the core. The differential pressures measured during chemical flood are presented in Figure 5.94.

5.3.1.2.2 Effluent Properties

Core#28 chemical flood effluent properties (viscosity, pH and TDS) were measured and presented in Figures 5.95, 5.96 and 5.97. The viscosity profile in Figure 5.95 showed slight viscosity increased after 0.3PV and sudden increase at 0.7PV, indicating surfactant breakthrough at 0.3PV an. The majority of the surfactant breakthrough occurred at 0.7PV. Precipitation of sodium carbonate in surfactant slug with divalent ions in formation brine delayed pH breakthrough, at around 0.8PV (Figure 5.96). TDS of effluents comparison between Core#28 and Core#22 in Figure 5.97 showed much early surfactant breakthrough occurred on Core#28 than Core#22. It is hypothesized that early surfactant breakthrough of Core#28 could cause the surfactant slug to mix with high salinity residue brine and to enter phase Type II, which trapped the surfactant. Extensive dispersion could dilute the surfactant slug causing low surfactant concentration with lower optimal salinity, while the residual brine had much higher salinity, the phase type was forced to enter phase Type II, which again traps the surfactant from recovering oil.

5.3.1.2.3 Tracer test

A tracer test was conducted after chemical flood was done to find out if there was a channel which caused early surfactant breakthrough in water flood and chemical flood (Figure 5.98, S_{or}=0.2). Tracer breakthrough took place at about 0.1PV, similar to water breakthrough during water flood. Another tracer test (Figure 5.98, S_{or}=0~0.2) was done after the core was toluene

flooded (2.5PV) and methanol flooded (2.5PV). The tracer test showed some residual oil still remained in the core. Both tracer tests showed excessive dispersion behavior but no channel in limestone Core#28. Therefore early surfactant breakthrough appeared to be due to extensive dispersion.

5.3.1.2.4 Core Cross-Section

Core#28 was sliced into seven sections. Photos of six cross sections are shown in Figure 5.99. Even though the toluene and methanol flood probably changed the appearance of oil distribution on the cross sections, it was still clear that less residual oil existed in the beginning sections and more in the ending sections. It was possible that the surfactant slug deteriorated as it proceeded in the core and mixed with residual oil/brine so extensively that the oil it moved in the beginning sections was trapped in the ending sections. The residual oil appeared to be at the bottom corner of the core, which eliminated the possibility that chemical flood was affected by gravity effect. Gravity effect was not found to cause adverse effect to high oil recovery on Berea sandstone; however, next core flood on limestone was suggested to be conducted vertically to eliminate gravity effect. The core photos demonstrate that the vertical cross section was not uniformly swept by the injected surfactant. The dispersion curve following the chemical flood indicates that the dispersion in the limestone core is as least an order of magnitude larger than in Berea. There is also the possibility that heterogeneity in this core following trapping of residual oil prevents generation of a uniform displacement front in the vertical cross section.

The low oil recovery in Core#28 was the result of early surfactant breakthrough and the failure to generate an oil bank with an oil cut of ~0.5 for larger. It is possible that extensive dispersions in this Indiana limestone core compromised surfactant slug integrity and prevented it from reducing water/oil interfacial tension and displacing oil effectively.

5.3.2 Core Flood CFW#8(Core#29)

The objective of CFW#8 was to conduct a chemical flood on a limestone core Core#29 with 6.55% NaCl as residual brine before oil flood. The residual brine of 6.55% NaCl ensured surfactant slug to be at constant designed optimal salinity; and therefore to reduce water/oil interfacial tension maximally. Core#29 had similar dimensions and porosity as Core#28. The pore volume determined from material balance was 104.7mL. The porosity was 0.171. The permeability to brine is 163mD overall. Table 5.7 includes properties of each section in the core.

A tracer tests in Core#29 at 100% brine saturation was very similar to Core#28 and dispersion was much larger than Core#22 (Figure 5.100). All core floods were done vertically to eliminate gravity effects.

5.3.2.1 Brine/Oil/Water Flood

Core#29 was flooded with 6.55% NaCl at reservoir temperature and then flooded with oil. About 3.1 PV Wahrman crude oil was injected into the core (Figure 5.101) but brine continued to be produced from the core. A second oil flood (Figure 5.102) with 2.2PV oil was done until no pressure change and almost no water produced. The oil saturation (S_{oi}) after second oil flood was 0.533, very close to Core#28 and much lower than Core#22 (Figure 5.103). Oil relative permeability at residual water saturation (S_{wr}) at the end of oil flood was 0.95. After oil flood, Core#29 was flooded with 0.65 PV 6.55% NaCl at an injection rate of 0.3 mL/min (~4.2 ft/day). Water breakthrough occurred at 0.26 PVI, similar to Core#22, 0.27PVI. The residual oil saturation after water flood was 0.276, lower than residual oil saturation of Core#28 (Figure 5.104). Water relative permeability from pressure data at the end of the water flood (Figure 5.105) was 0.063.

5.3.2.2 Chemical Flood

Core#29 was brine and water flooded with 6.55% NaCl, which was the equivalent salinity of the surfactant slug. One reason attributed to the low oil recovery on Core#28 was high salinity residual brine that deviated surfactant slug from its optimal salinity to reduce interfacial tension sufficiently to displace oil. Another reason was the extensive mixing between surfactant slug and residual oil/brine. The same surfactant formulation F-4C (Table 5.2) was still used in CFW#8. The injection design of CFW#8 was presented and compared with CFW#7 in Table 5.1.

The surfactant slug and polymer drive of CFW#8 had higher viscosities than CFW#7 (Figure 5.91 and 5.106). The slightly higher viscosity of CFW#8 should not cause problem of obtaining high oil recovery.

5.3.2.2.1 Oil Recovery

The cumulative oil recovery was about 27%, even lower than CFW#7. Highest oil cut was about 15% at 0.6PV. Oil/surfactant breakthrough both later than CFW#7(Core#28) (Figure 5.107), are 0.3 PVI and 0.5 PVI respectively. The delayed oil breakthrough and low peak oil cut led to low oil recovery of CFW#8. The photos of the effluents are presented in Figure 5.108. No microemulsion phase was observed in any effluent samples. This indicated surfactant slug was not at its optimal salinity in the core. The light color of the aqueous phase suggested surfactant was either absorbed severely in the core or dispersed extensively. It was suggested to measure surfactant concentration in the effluent to determine whether severe surfactant absorption led to low oil recovery.

5.3.2.2.2 Pressure Analysis

Section pressures during chemical flood (Figure 5.109**)** increased continually which was probably was due to the fact that surfactant did not to displace much oil. The photos of sliced cross sections (Figure 5.110) showed similar oil distribution as CFW#8 (Figure 5.99) on the

cross section and along the core from section 1 to section 6. Core#29 cross sections showed higher residual oil saturation than Core#28 because it had lower oil recovery and not flooded by toluene and methanol after chemical flood. But again it seemed that the surfactant slug deteriorated as it proceeded in the core and low oil displacement efficiency caused pressure continuous increase during chemical flood of CFW#8.

5.3.2.2.3 Effluent Properties

CFW#8 chemical flood effluent properties (viscosity, pH and TDS) were measured and compared with CFW#7 effluent properties in Figures 5.111, 5.112 and 5.113. The viscosity of CFW#8 showed similar behavior as CFW#7. CFW#8(Core#29) had much earlier pH breakthrough than CFW#7(Core#28) (Figure 5.112). Precipitation of sodium carbonate in CFW#7 surfactant slug with divalent ions in formation brine delayed pH breakthrough. The salinity profile of CFW#8 aqueous effluent showed the salinity in the core was at or near optimal salinity of the injected surfactant slug (Figure 5.113). CFW#8 had lower oil recovery than CFW#7 suggested that 6.55% NaCl in the residual brine was not the optimal salinity of surfactant slug in situ, which was compromised due to the mixing of surfactant with residual brine and oil. Instead residual brine with salinity higher than 6.55% NaCl led to higher oil recovery was more close to optimal salinity of surfactant slug in situ.

5.3.2.2.4 Tracer test

Dispersion of limestone and sandstone was studied and compared to investigate the reasons of low oil recovery in limestone. Figure 5.114 show tracer tests results of Core#29 (limestone) before and after water flood, comparing to the tracer test results before and after water flood of Core#31 (used by a colleague) (Figure 5.115), a typical Berea sandstone with similar tracer test results before water flood like cores used in CFW#1-6. Tracer test after water flood of Core#29 (limestone) showed much earlier tracer breakthrough comparing to tracer test before oil flood;

while tracer test after water flood of Core#31 (sandstone) had slightly earlier tracer breakthrough comparing to tracer test before oil flood. This comparison showed larger dispersion of limestone than sandstone after water flood may contribute to the lower oil recovery of chemical flood in limestone than sandstone. Tracer tests with different tracer slug size on limestone and sandstone (Figure 5.116 and 5.117) showed that in order to obtain the 100% injected tracer concentration at the core outlet, limestone needed a tracer slug with 0.23PV bigger than sandstone. Even though the oil cut at oil bank is irrelevant to the surfactant slug size, it is recommended that surfactant slug bigger than 0.6PV, e.g. 1PV, should be used on limestone core flood to improve surfactant slug performance throughout the core and therefore increase oil recovery.

In sum, the oil recovery in two limestone core floods may be improved by increasing surfactant slug size and surfactant concentration (if possible) to compensate the large dispersion of limestone.

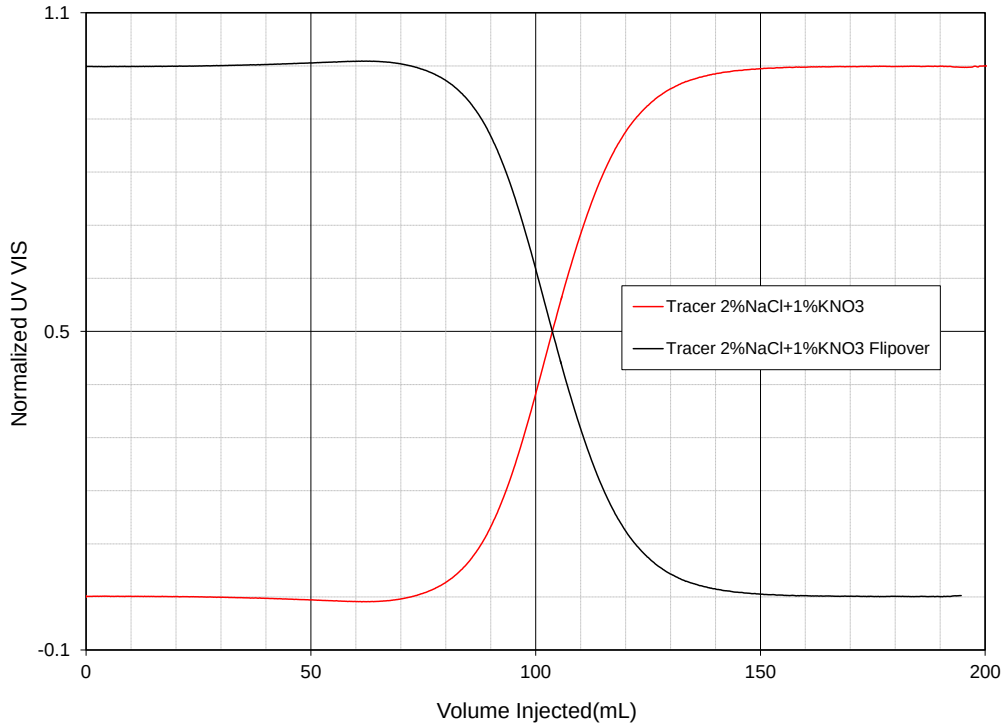

Figure 5.1 CFW#1(Core#5) tracer test results

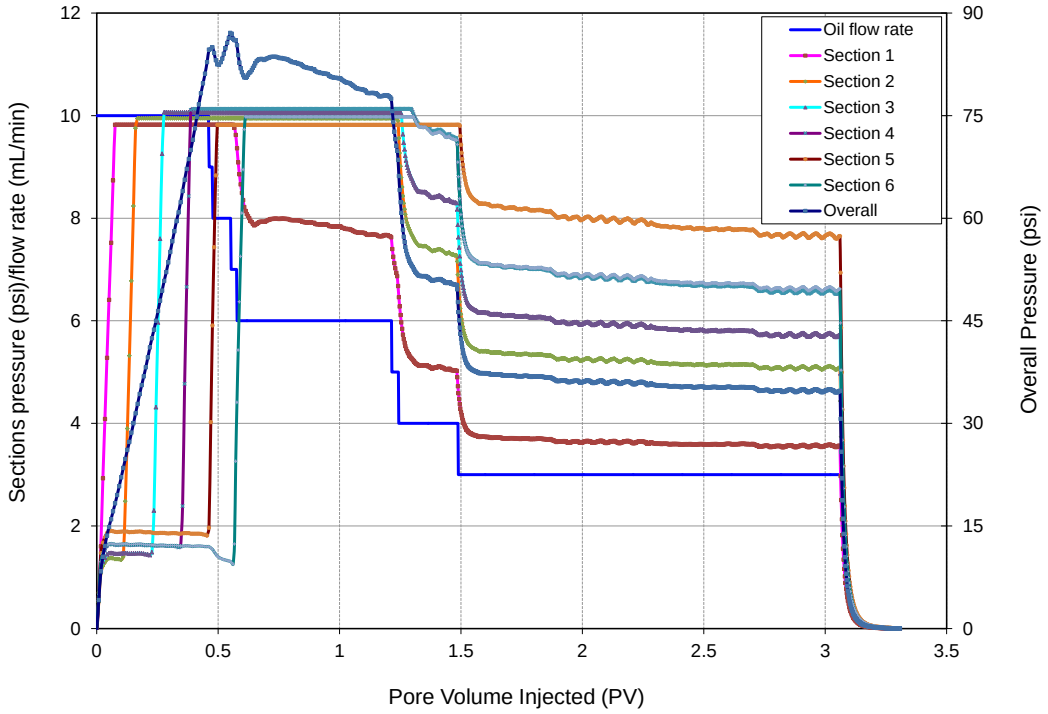

Figure 5.2 Injection rate and differential pressure profile during CFW#1(Core#5) oil flood at 43 ℃

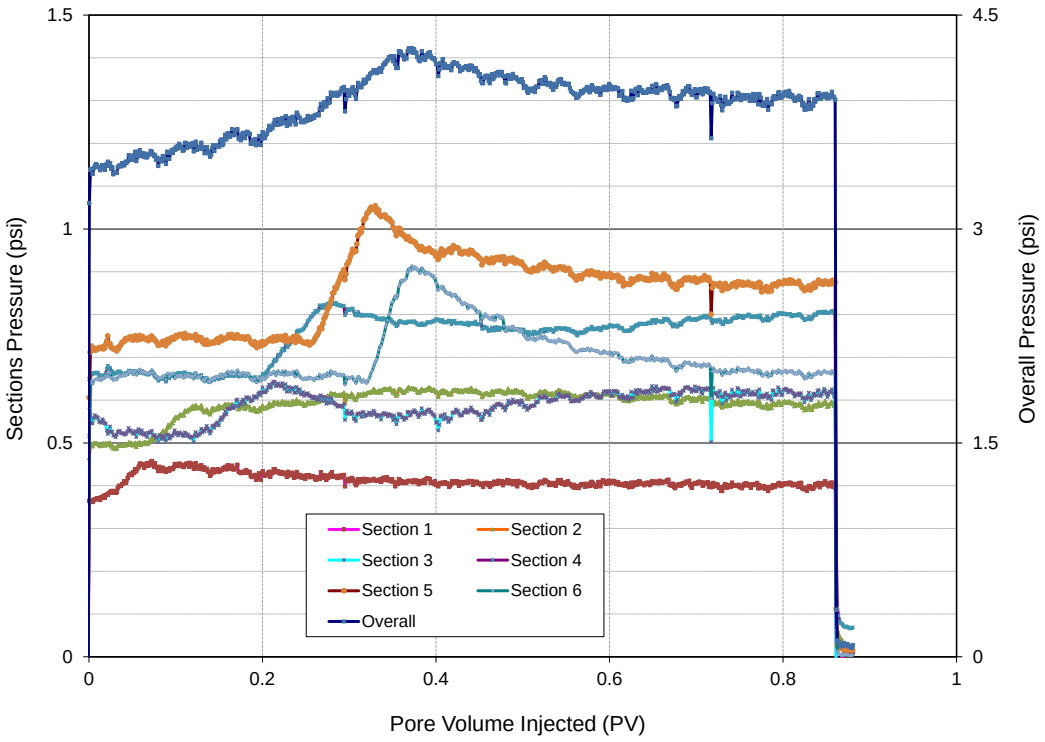

Figure 5.3 Differential pressure profile during CFW#1(Core#5) water flood at 43 ℃

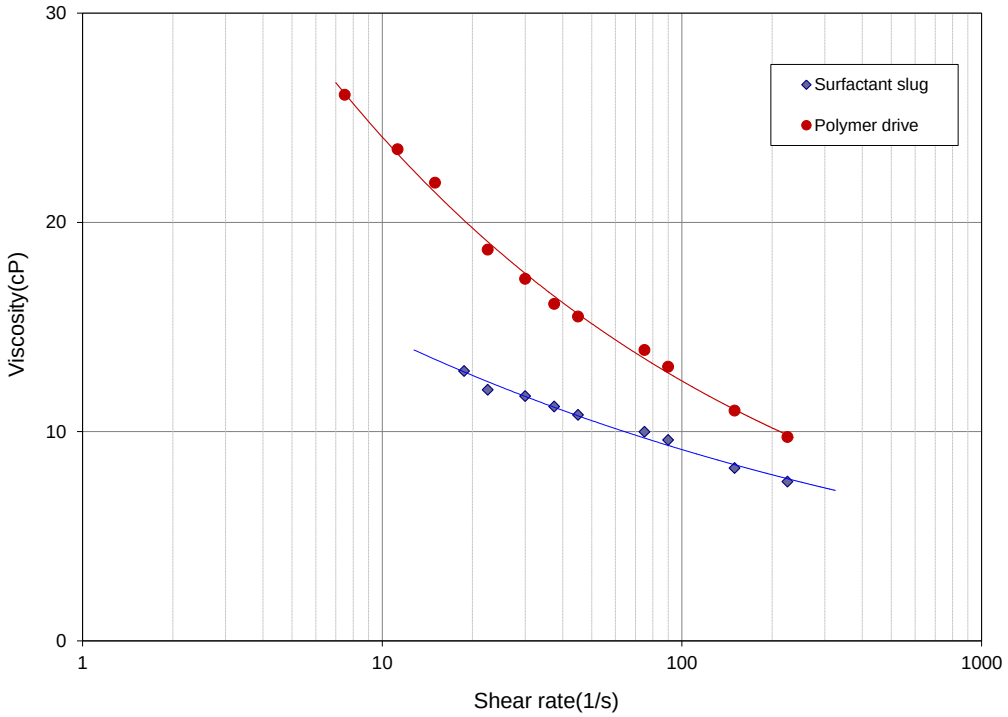

Figure 5.4 Viscosity of CFW#1(Core#5) surfactant slug and polymer drive measured by Brookfield DV-II+Pro viscometer at at 43 ℃

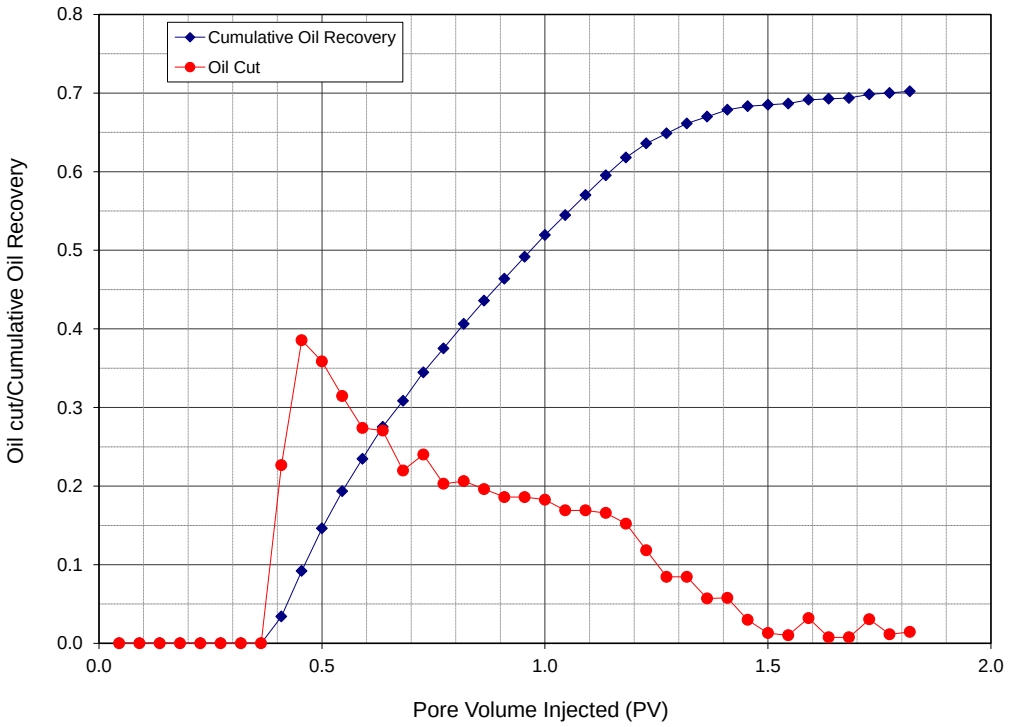

Figure 5.5 CFW#1(Core#5) chemical flood oil cut and cumulative oil recovery profile

Vial#	1	2	3	4	5	6	7	8	9	10
PV	0.045	0.091	0.136	0.182	0.227	0.273	0.318	0.364	0.409	0.455

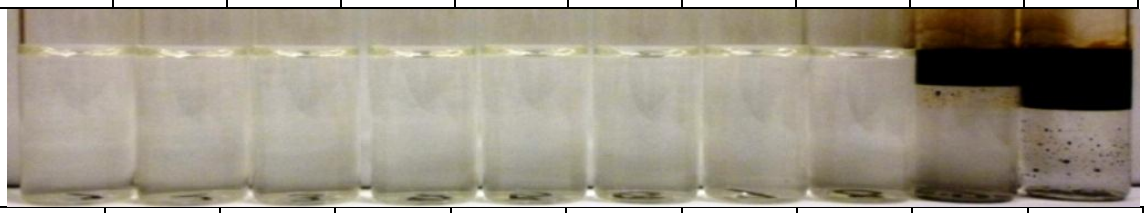

Vial#	11	12	13	14	15	16	17	18	19	20
PV	0.500	0.545	0.591	0.636	0.682	0.727	0.773	0.818	0.864	0.909

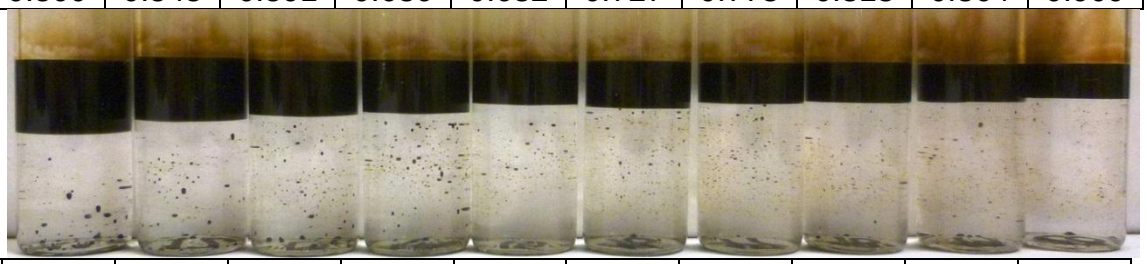

Vial#	21	22	23	24	25	26	27	28	29	30
PV	0.955	1.000	1.045	1.091	1.136	1.182	1.227	1.273	1.318	1.364

Vial#	31	32	33	34	35	36	37	38	39	40
PV	1.409	1.455	1.500	1.545	1.591	1.636	1.682	1.727	1.773	1.818

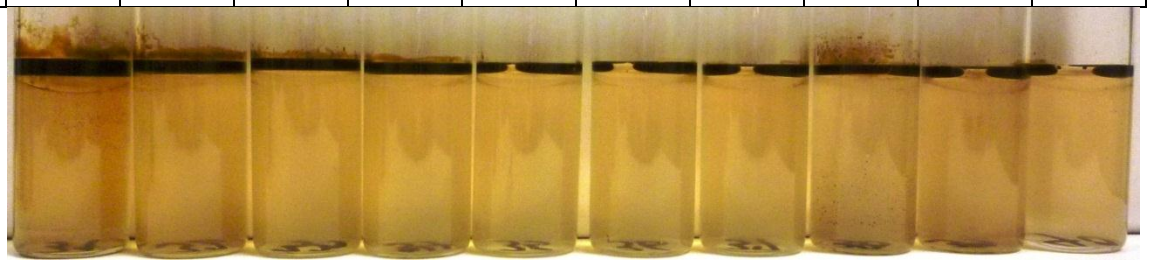

Figure 5.6 Photo of effluent vials from chemical flood of CFW#1(Core#5) after equilibrating at 43 ℃ for 5 days

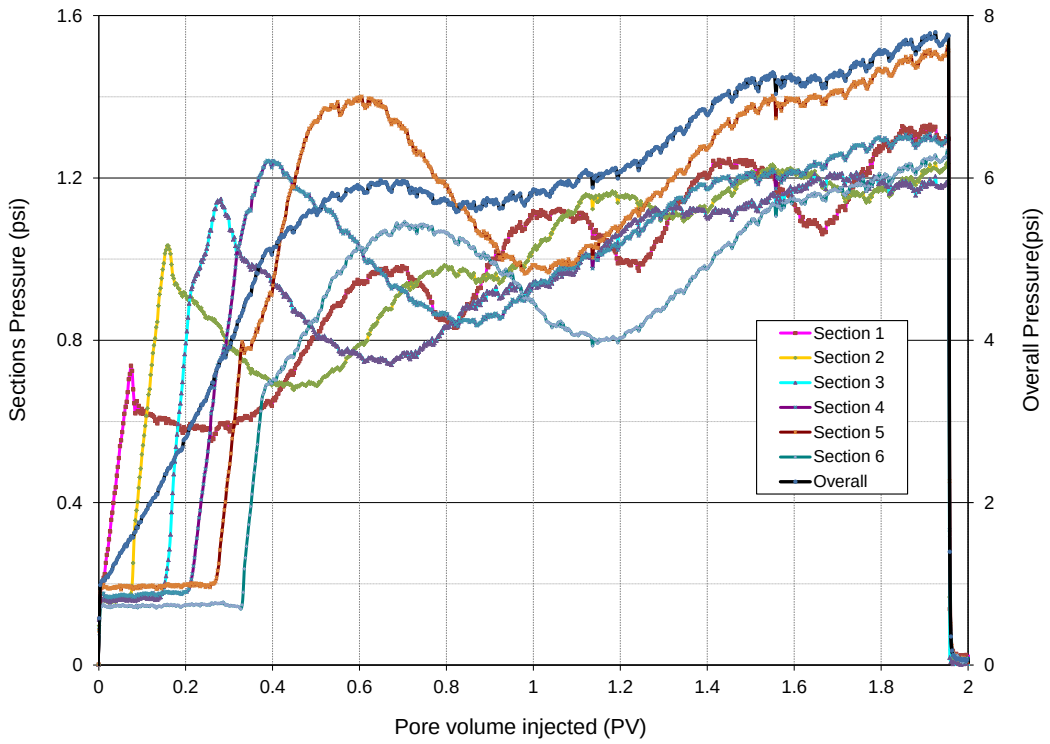

Figure 5.7 CFW#1(Core#5) differential pressures profile during chemical flood

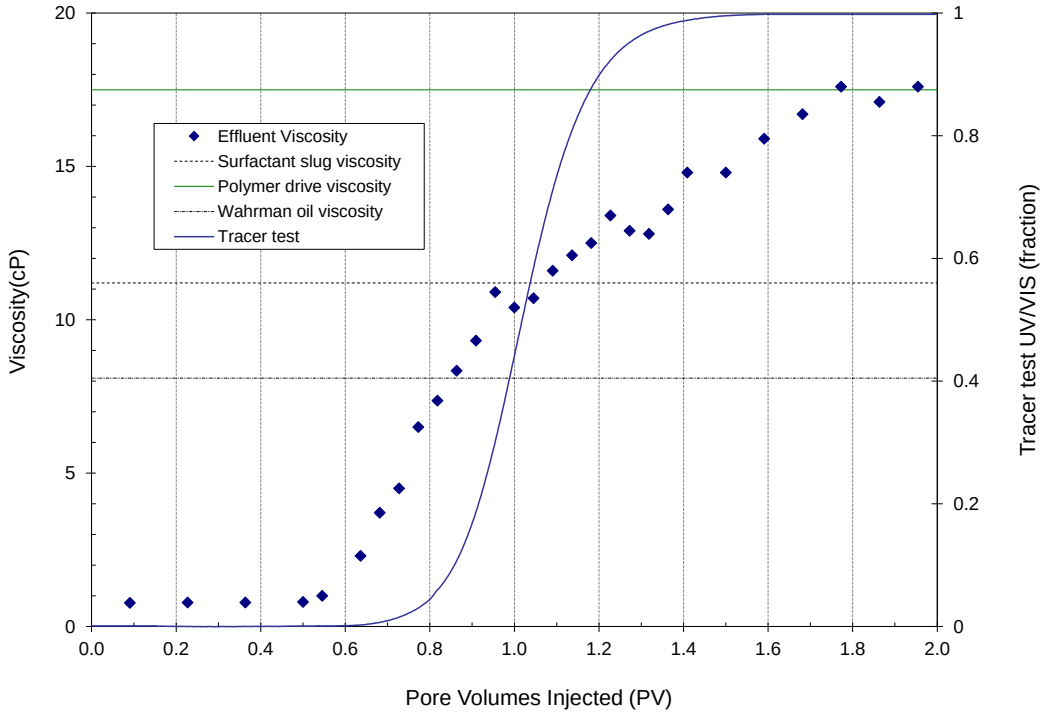

Figure 5.8 CFW#1(Core#5) chemical flood effluent viscosity (at 30 s^{-1}) profile at 43 ℃

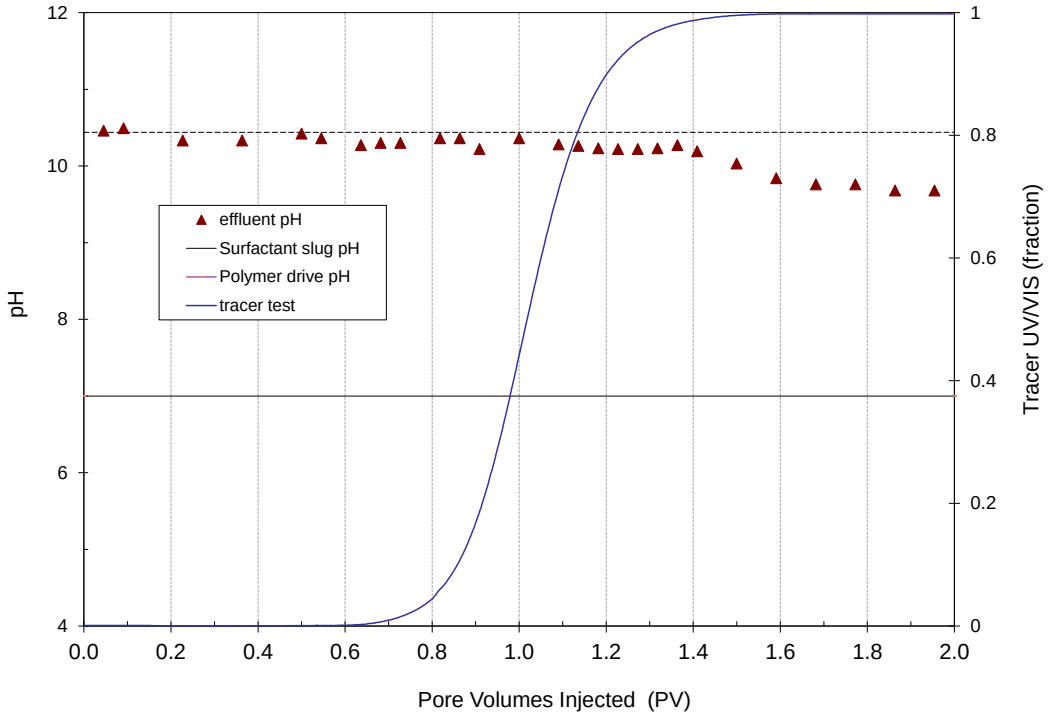

Figure 5.9 CFW#1(Core#5) chemical flood effluent pH profile

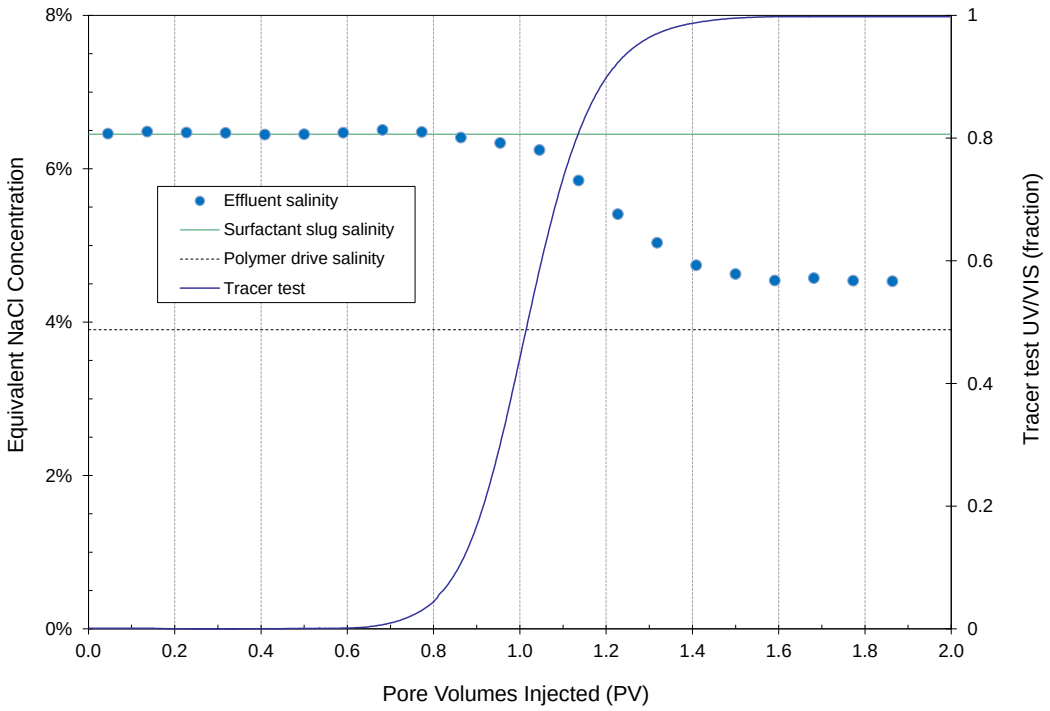

Figure 5.10 CFW#1(Core#5) chemical flood effluent equivalent salinity profile

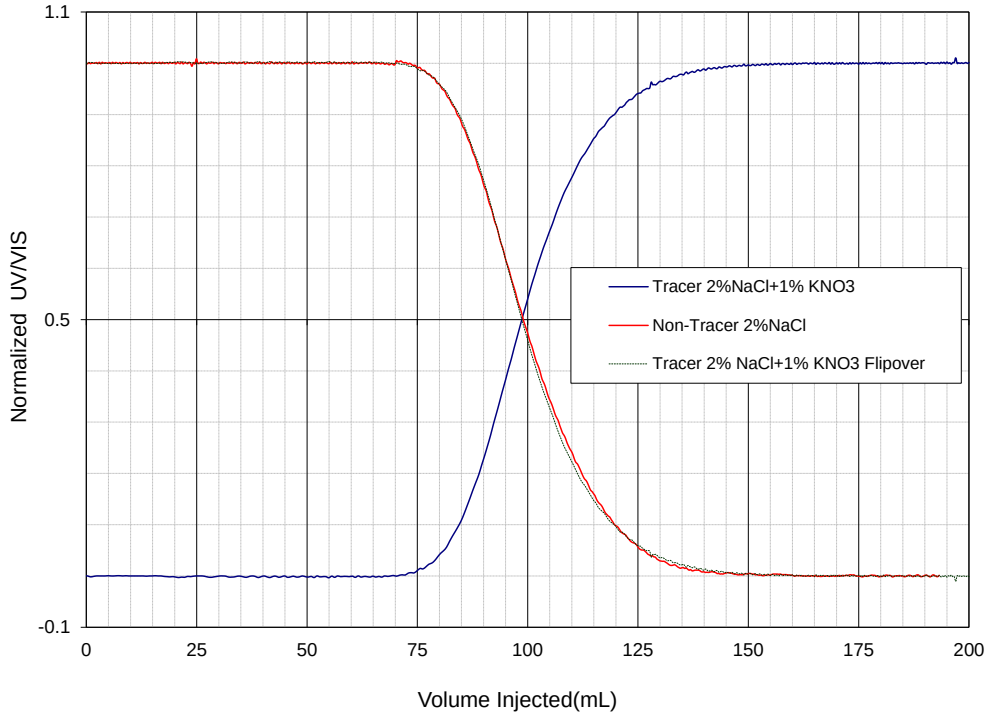

Figure 5.11 CFW#2(Core#8) tracer test results

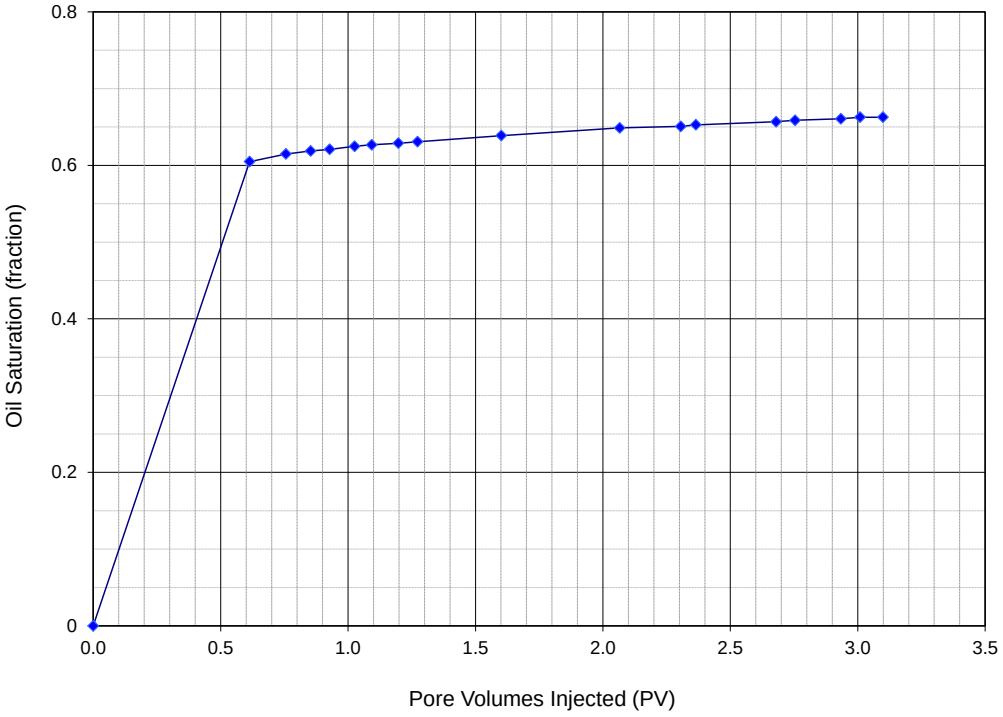

Figure 5.12 CFW#2(Core#8) oil saturation profile during oil flood at 43 ℃

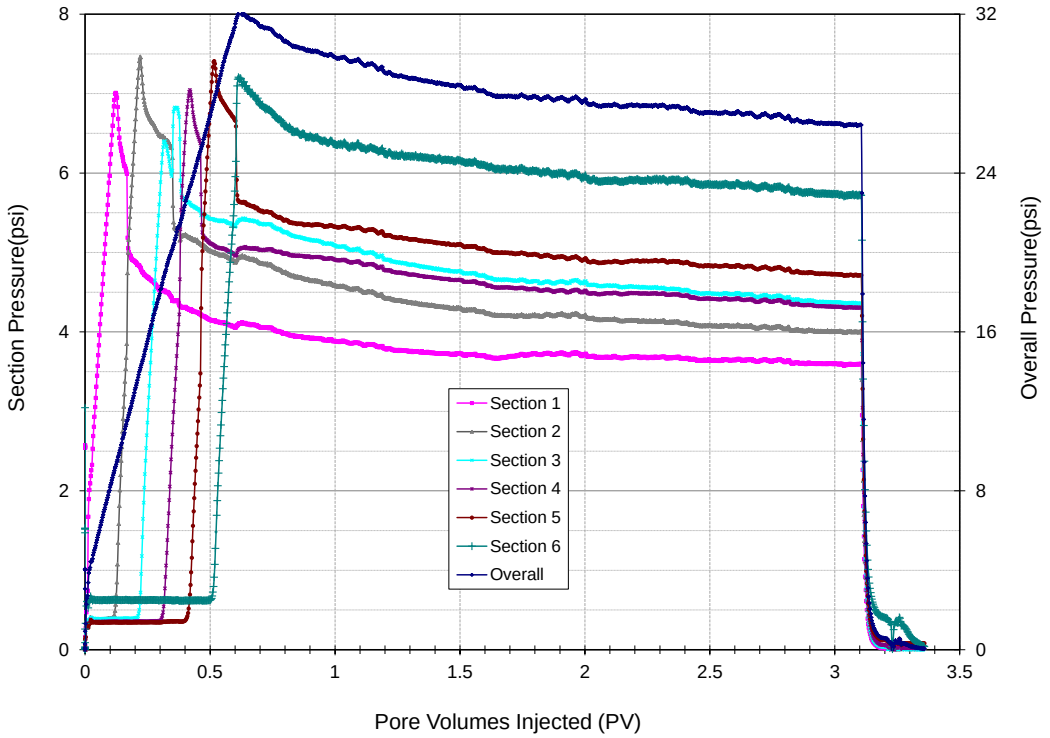

Figure 5.13 CFW#2 (Core#8) oil flood at 43 ℃ pressure profile

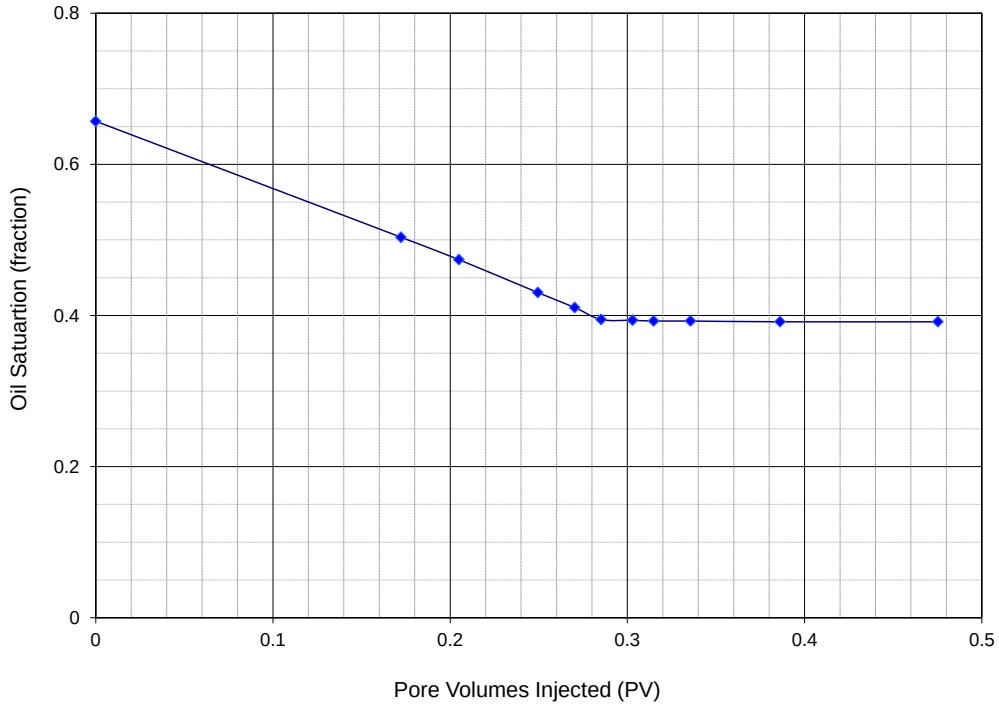

Figure 5.14 CFW#2(Core#8) oil saturation profile during water flood at 43 ℃

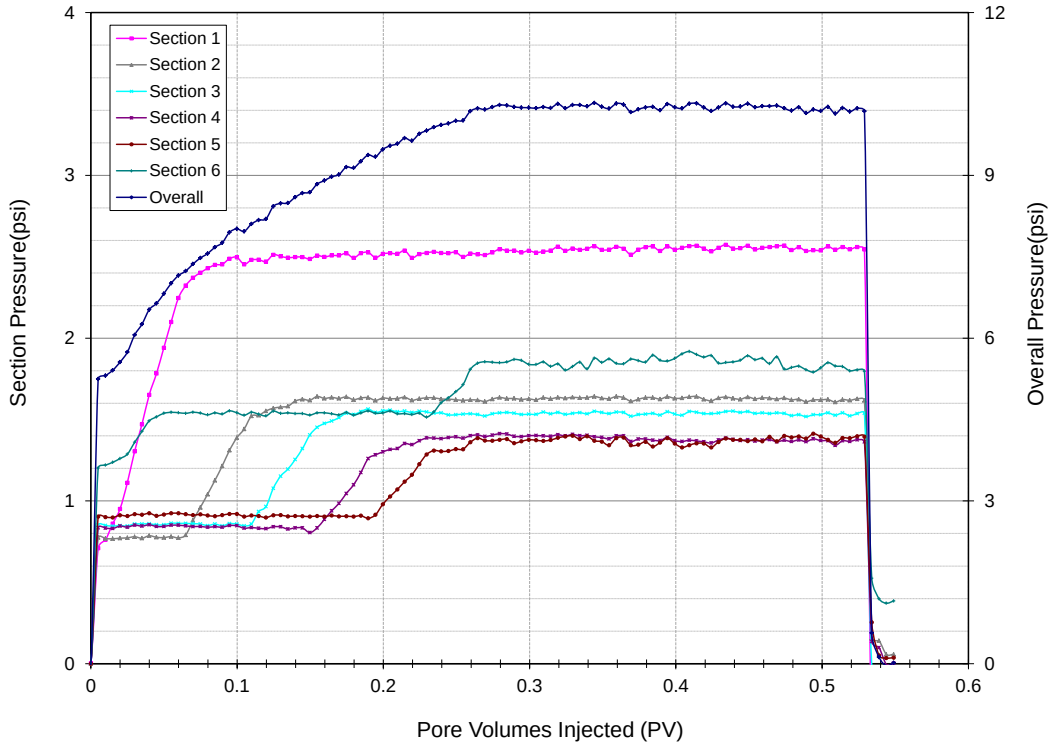

Figure 5.15 CFW#2(Core#8) pressure profile during water flood at 43 ℃

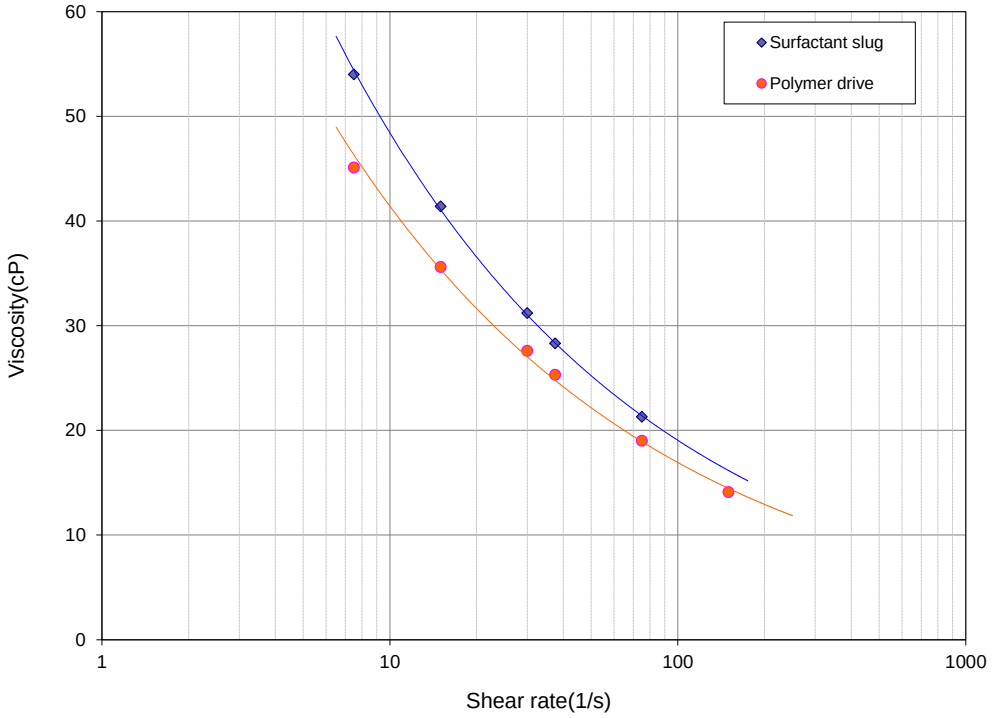

Figure 5.16 CFW#2(Core#8) viscosity of surfactant slug and polymer drive at 43 ℃

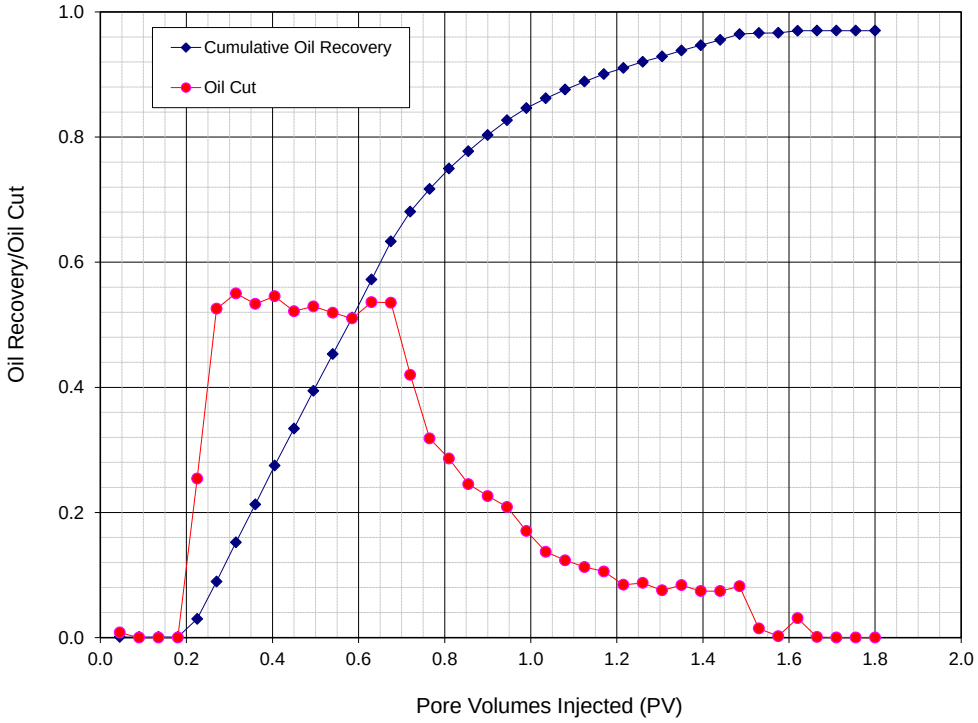

Figure 5.17 CFW#2 (Core#8) chemical flood oil cut and cumulative oil recovery

Vial #	1	2	3	4	5	6	7	8	9	10
PV	0.045	0.090	0.135	0.180	0.225	0.269	0.314	0.359	0.404	0.449

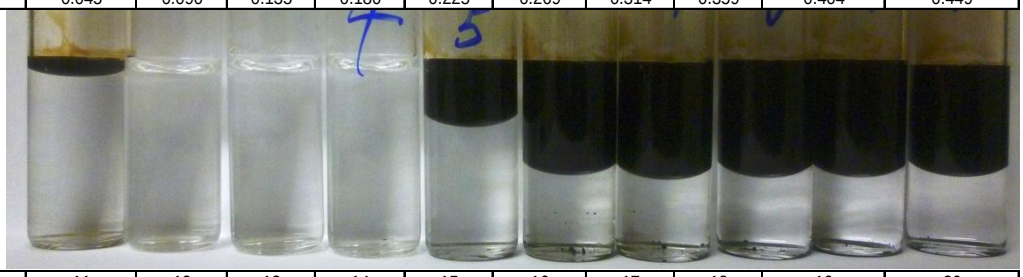

Vial #	11	12	13	14	15	16	17	18	19	20
PV	0.494	0.539	0.584	0.629	0.674	0.719	0.763	0.808	0.853	0.898

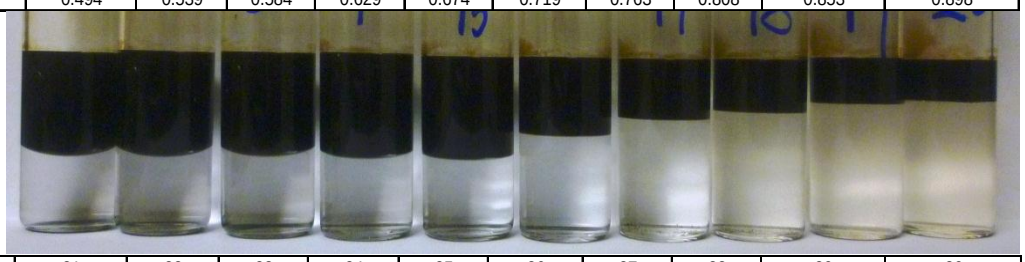

Vial #	21	22	23	24	25	26	27	28	29	30
PV	0.943	0.988	1.033	1.078	1.123	1.168	1.213	1.257	1.302	1.347

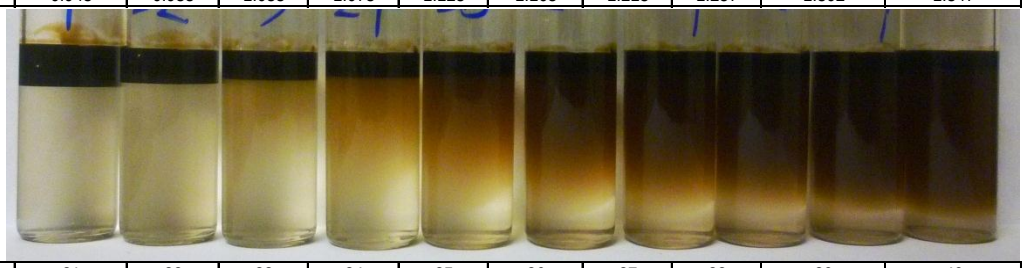

Vial #	31	32	33	34	35	36	37	38	39	40
PV	1.392	1.437	1.482	1.527	1.572	1.617	1.662	1.707	1.751	1.796

Figure 5.18 Photos of effluent vials from chemical flood of CFW#2 (Core#8) after equilibrating at reservoir temperature, 43 ℃ for 9 days.

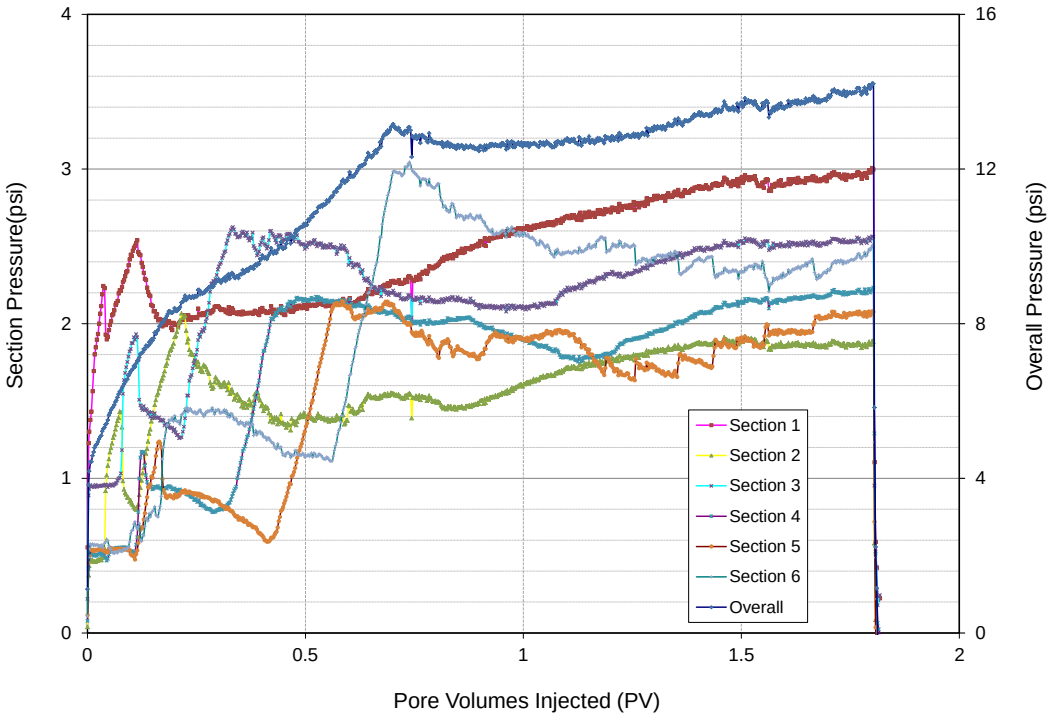

Figure 5.19 CFW#2(Core#8) differential pressure profile during chemical flood at 43 ℃

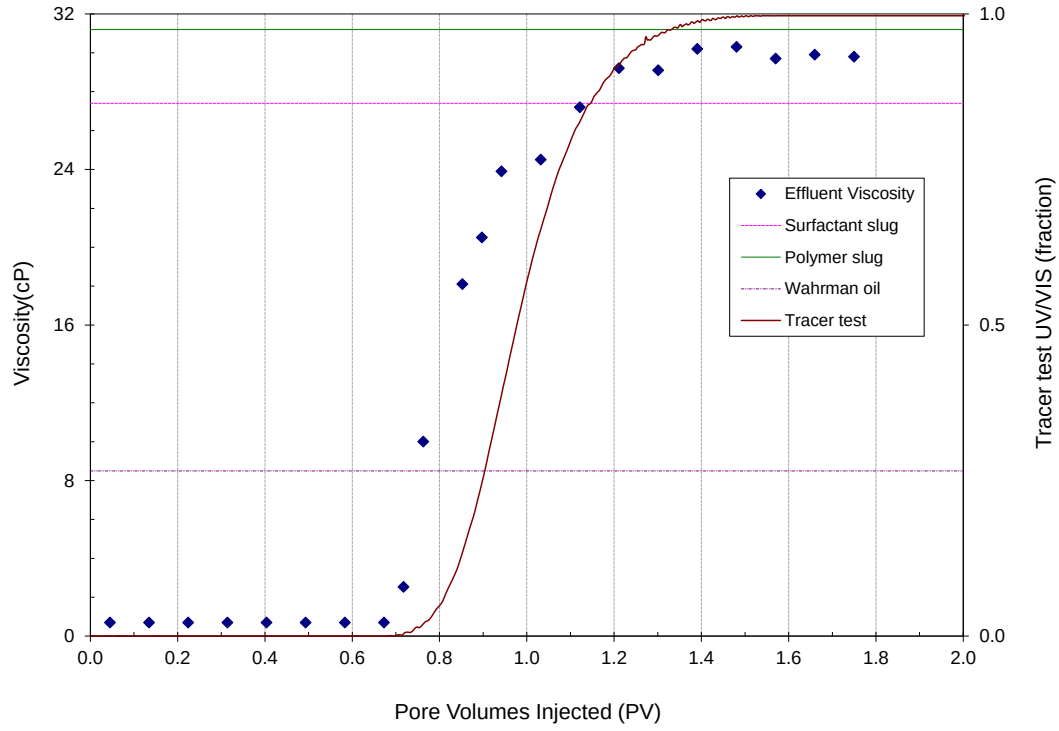

Figure 5.20 CFW#2(Core#8) chemical flood effluent viscosity (at 30 s^{-1}) profile at 43 ℃

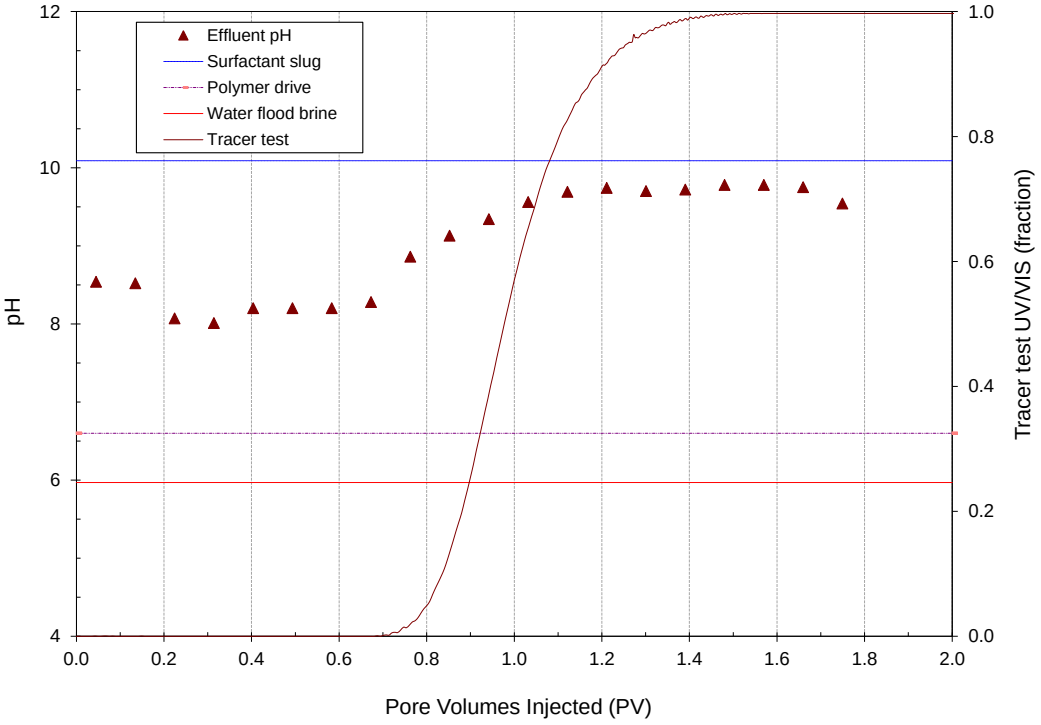

Figure 5.21 CFW#2 (Core#8) chemical flood effluent pH profile

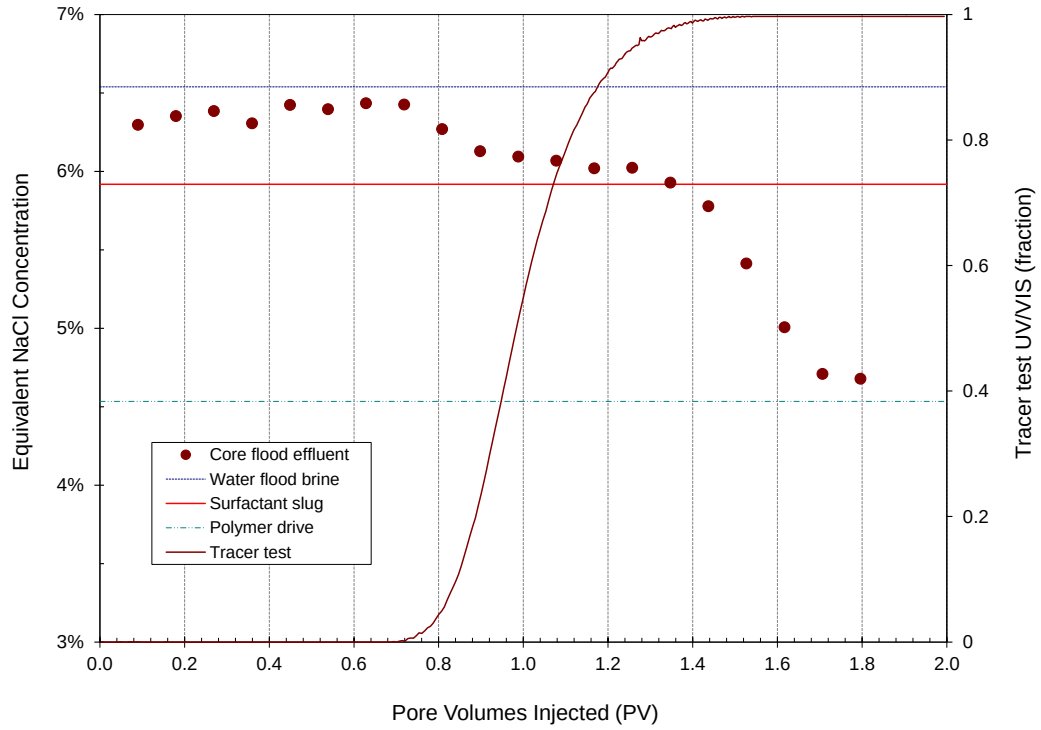

Figure 5.22 CFW#2(Core#8) chemical flood effluent equivalent salinity profile

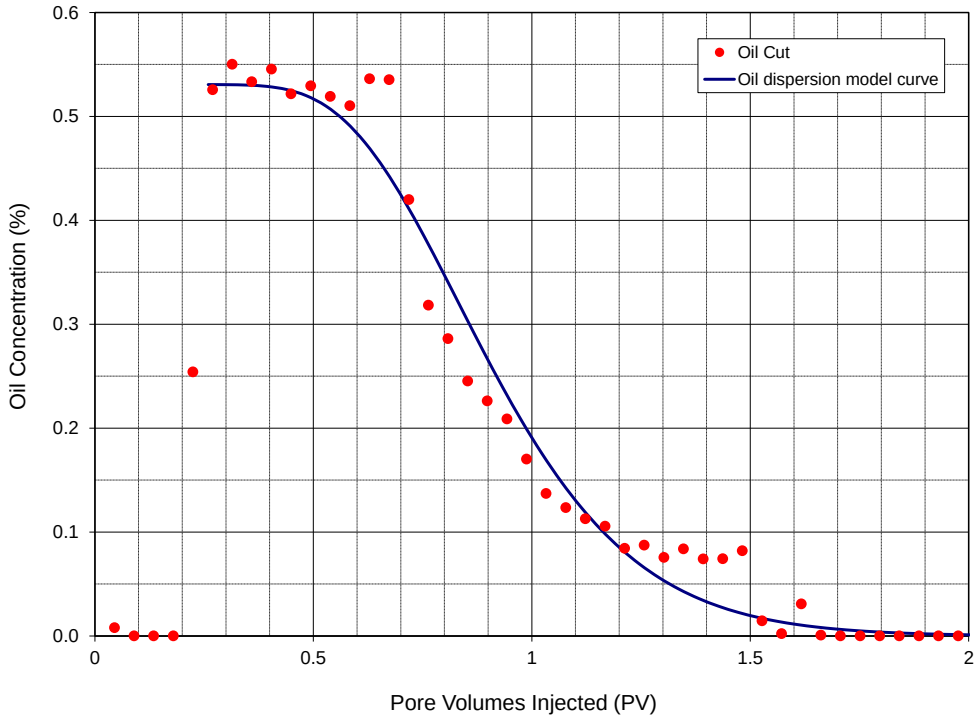

Figure 5.23 CFW#2(Core#8) chemical flood oil cut dispersion model

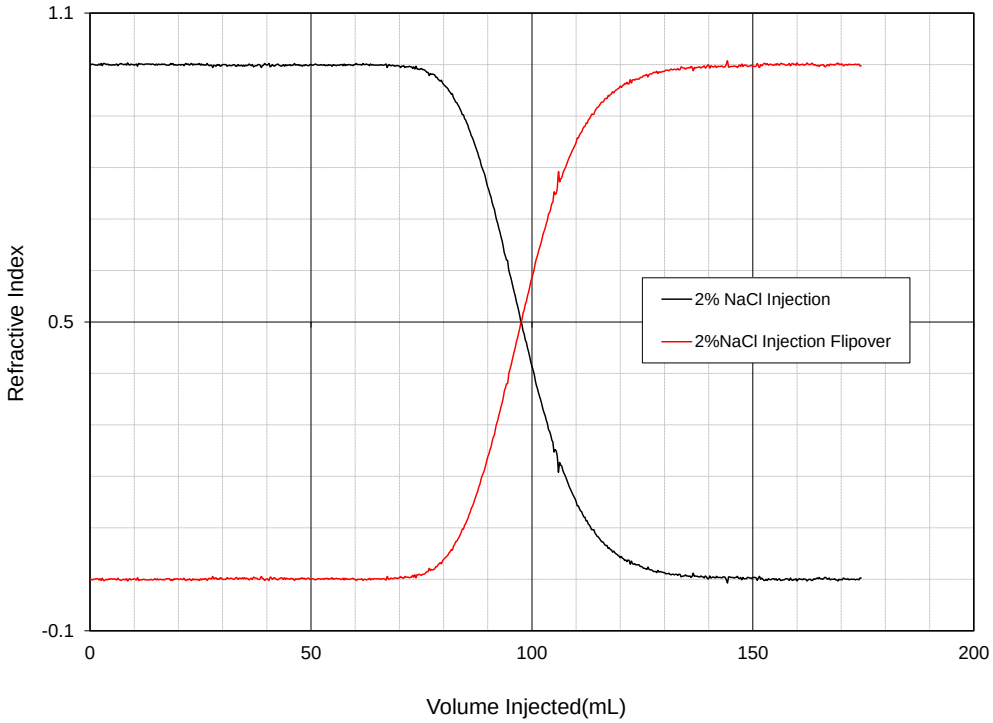

Figure 5.24 CFW#3 (Core#12) tracer test results

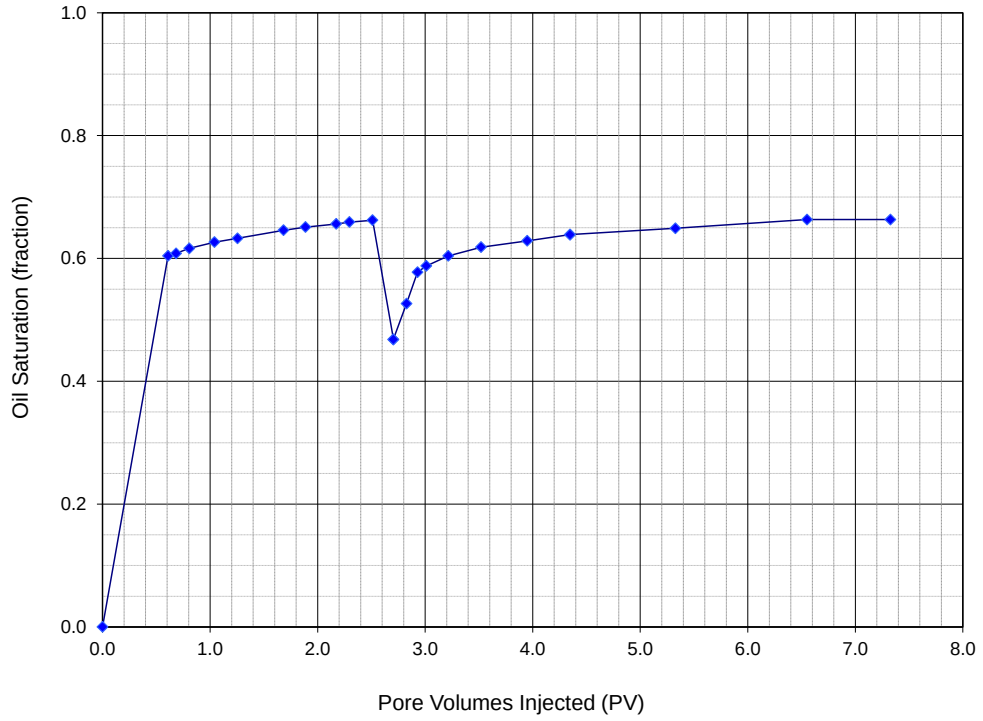

Figure 5.25 CFW#3(Core#12) oil saturation profile during oil flood at 43 ℃

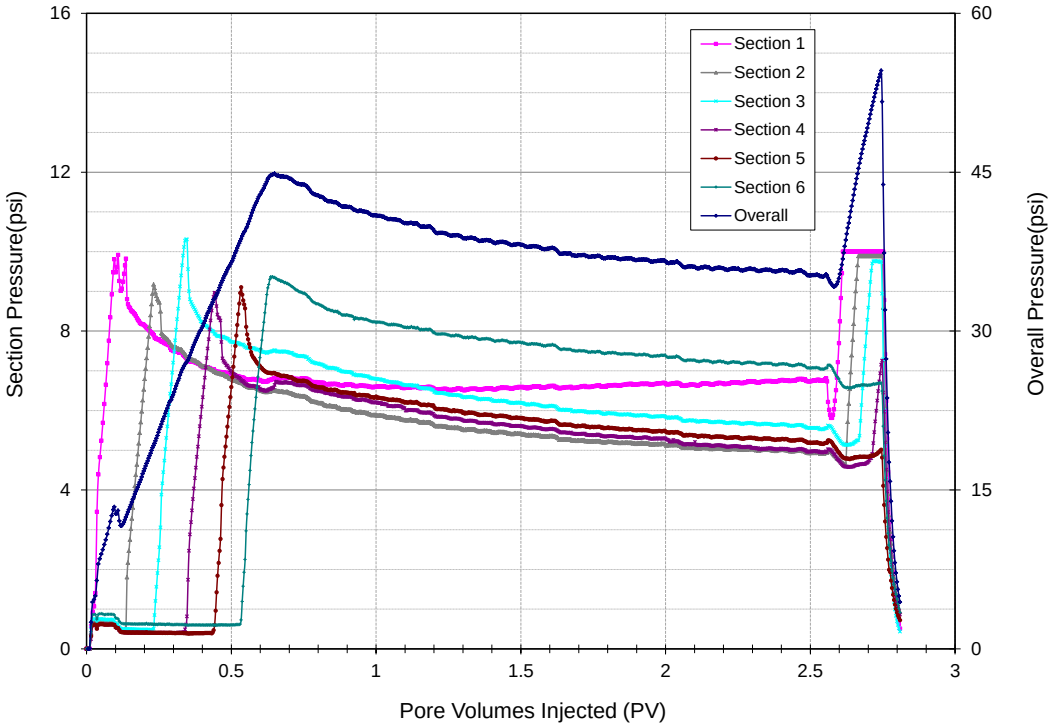

Figure 5.26 CFW#3 (Core#12) pressure profile during first oil flood at 43 ℃

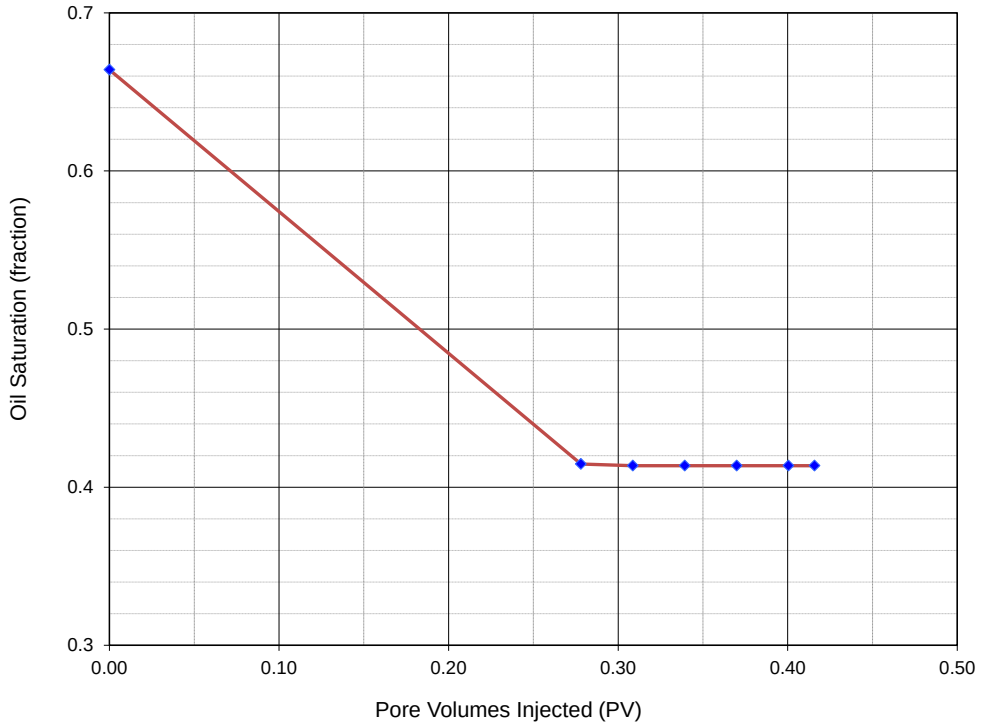

Figure 5.27 CFW#3 (Core#12) oil saturation profile during water flood at 43 ℃

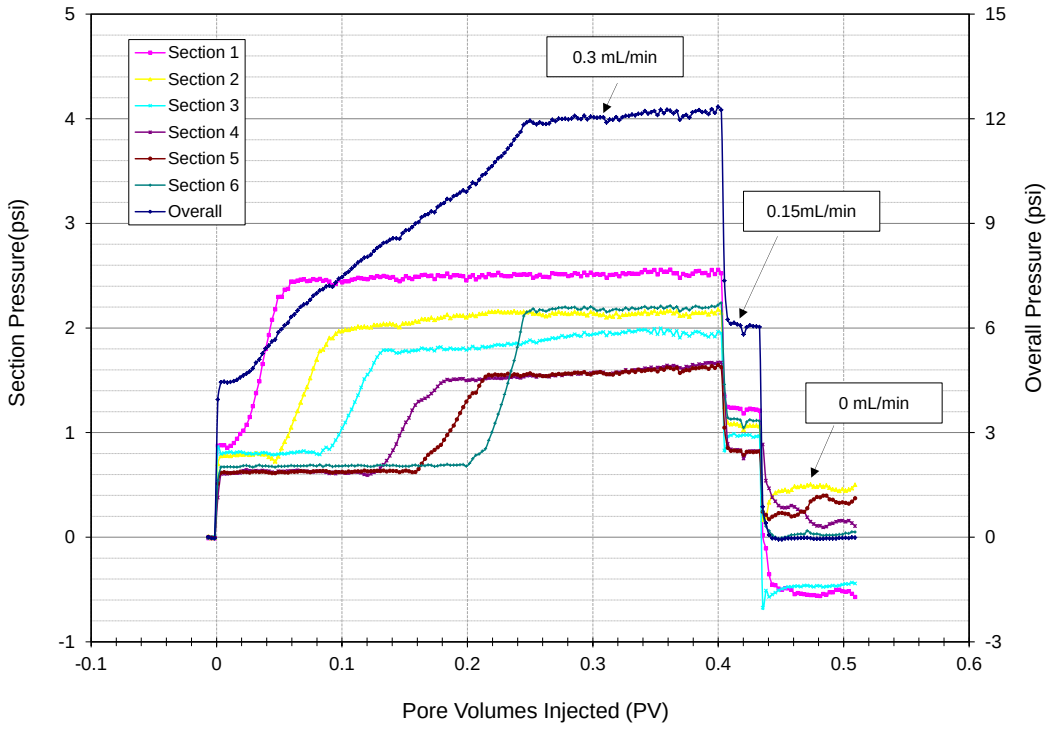

Figure 5.28 CFW#3(Core#12) pressure profile during water flood at 43 ℃

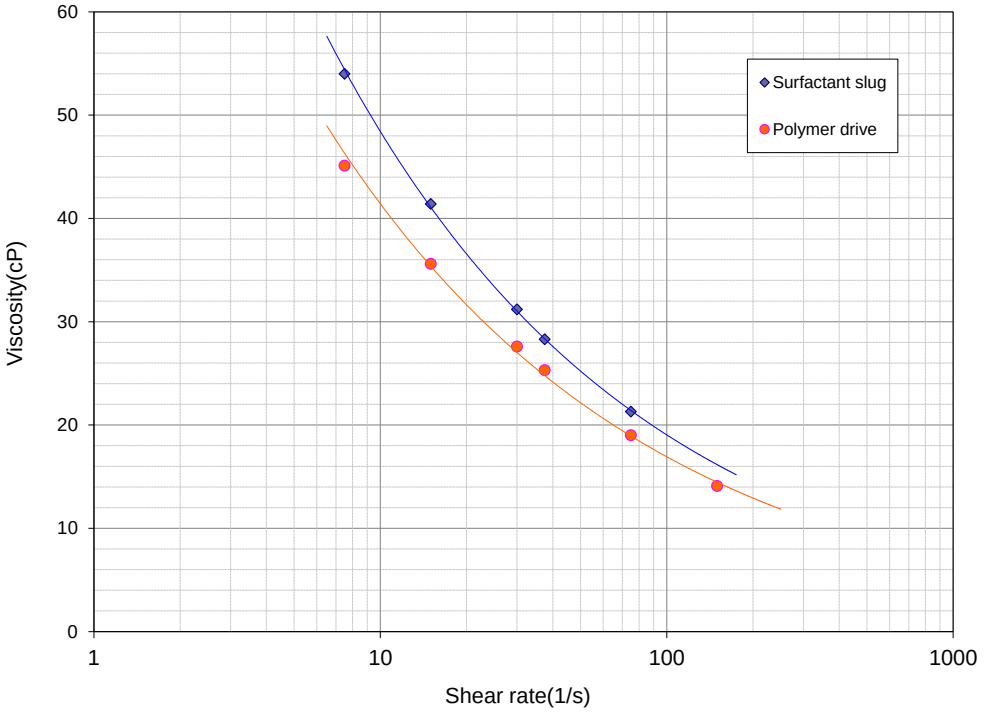

Figure 5.29 CFW#3(Core#12) viscosity of surfactant slug and polymer drive at 43 ℃

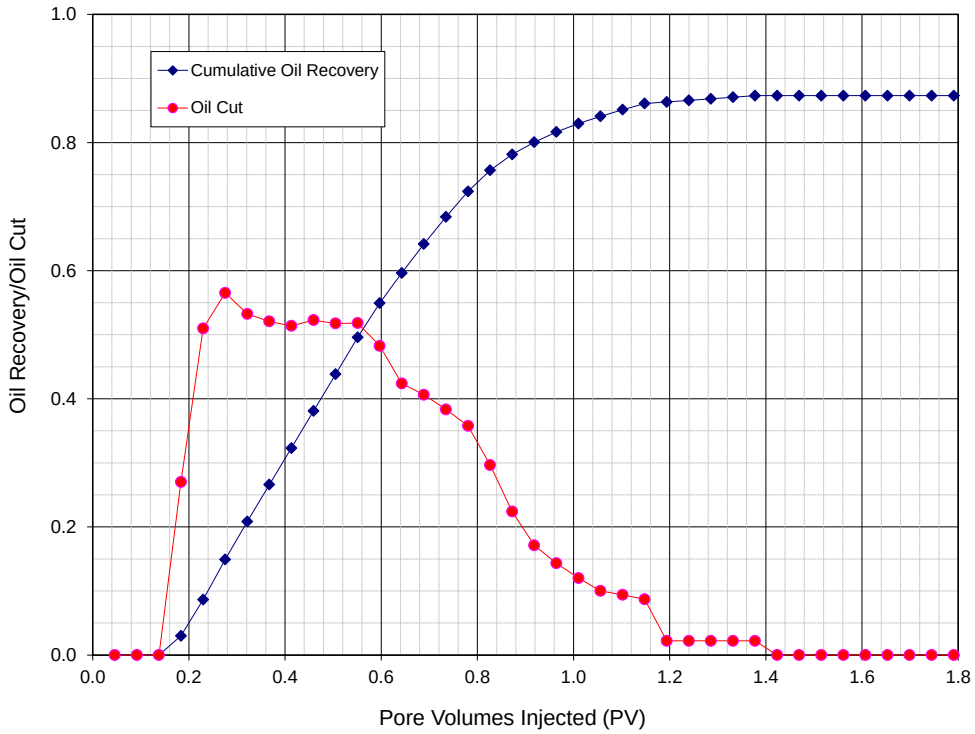

Figure 5.30 CFW#3(Core#12) chemical flood oil recovery and oil cut

Vial #	1	2	3	4	5	6	7	8	9	10
PV	0.046	0.092	0.138	0.184	0.230	0.276	0.321	0.367	0.413	0.459

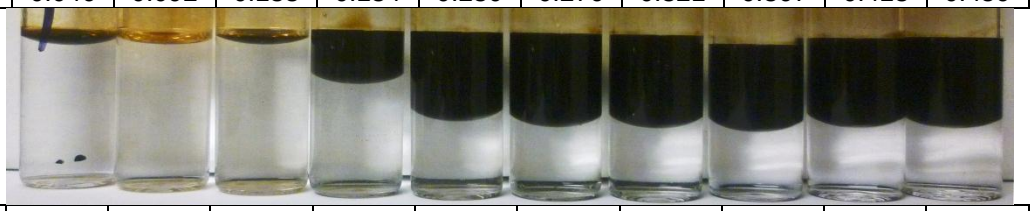

Vial #	11	12	13	14	15	16	17	18	19	20
PV	0.505	0.551	0.597	0.643	0.689	0.735	0.781	0.827	0.872	0.918

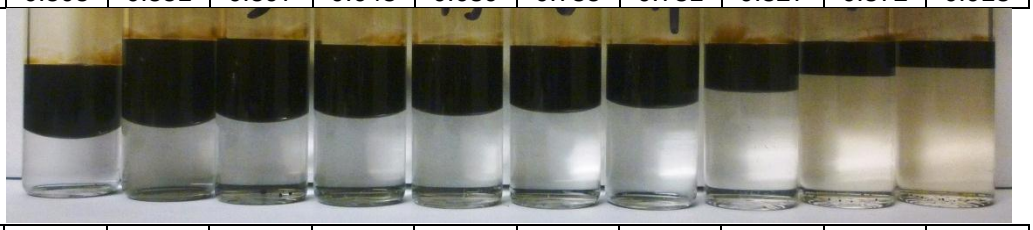

Vial #	21	22	23	24	25	26	27	28	29	30
PV	0.964	1.010	1.056	1.102	1.148	1.194	1.240	1.286	1.332	1.378

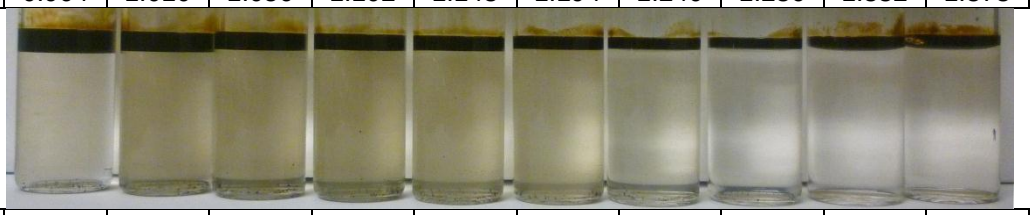

Vial #	31	32	33	34	35	36	37	38	39	40
PV	1.423	1.469	1.515	1.561	1.607	1.653	1.699	1.745	1.791	1.837

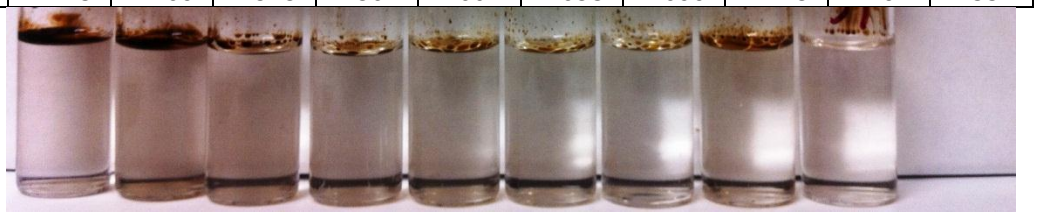

Figure 5.31 CFW#3 (Core#12) chemical flood effluent vial photos at equilibrating at 43 ℃ for 2 days

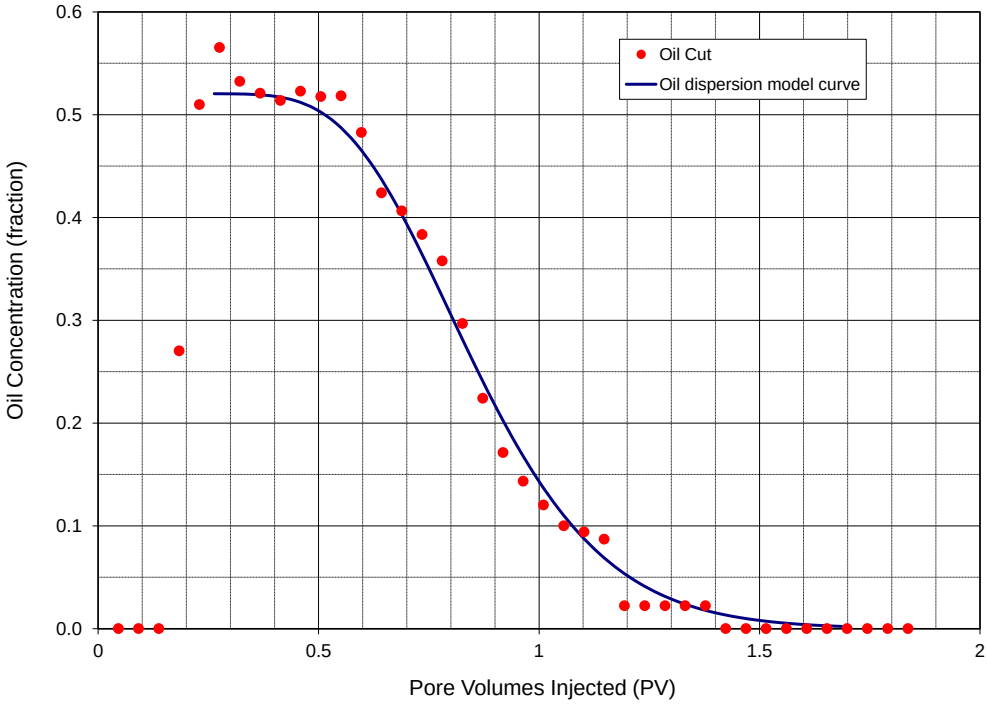

Figure 5.32 CFW#3 (Core#12) chemical flood oil cut fitted by dispersion model

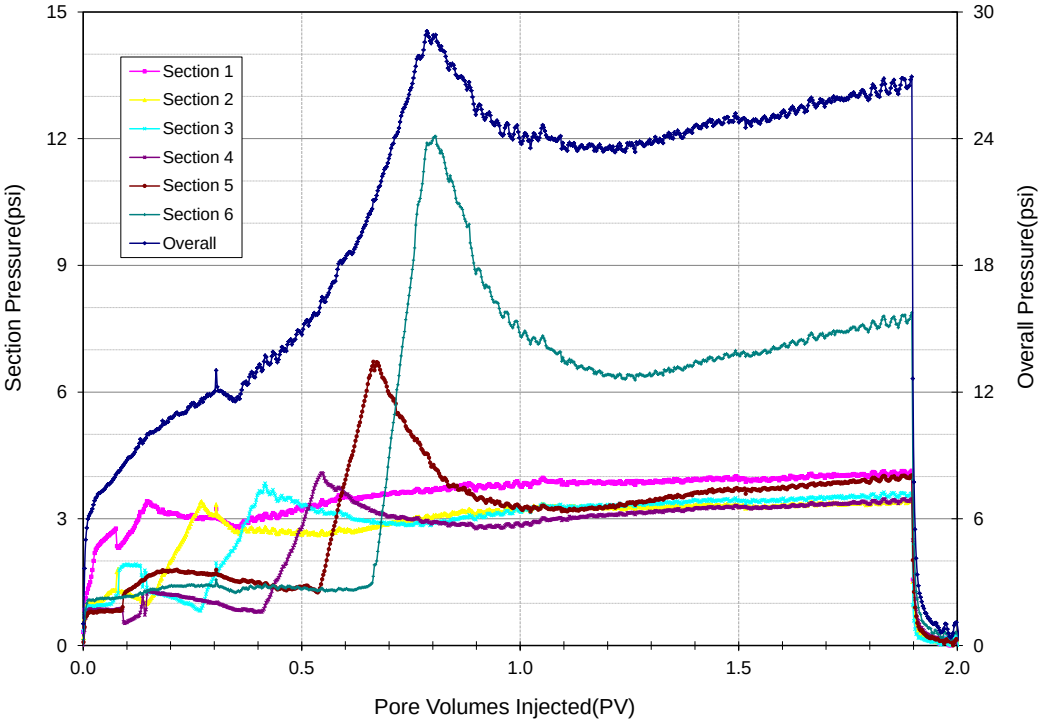

Figure 5.33 CFW#3(Core#12) differential pressure profile during chemical flood at 43 ℃

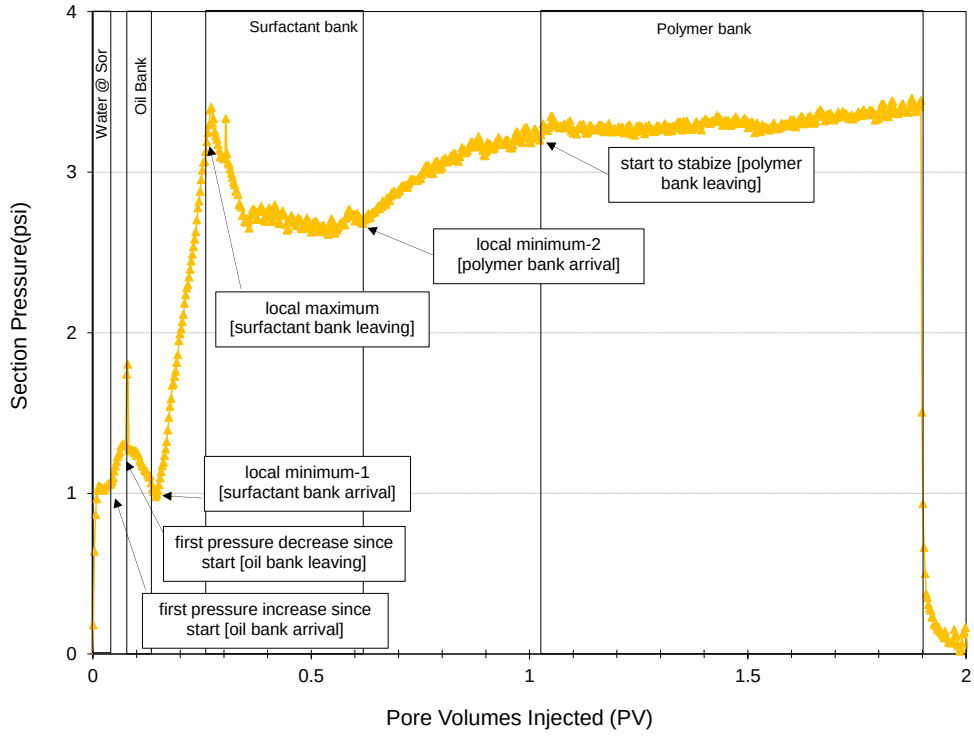

Figure 5.34 CFW#3 (Core#12) section 2 differential pressure during chemical flood at 43 ℃.

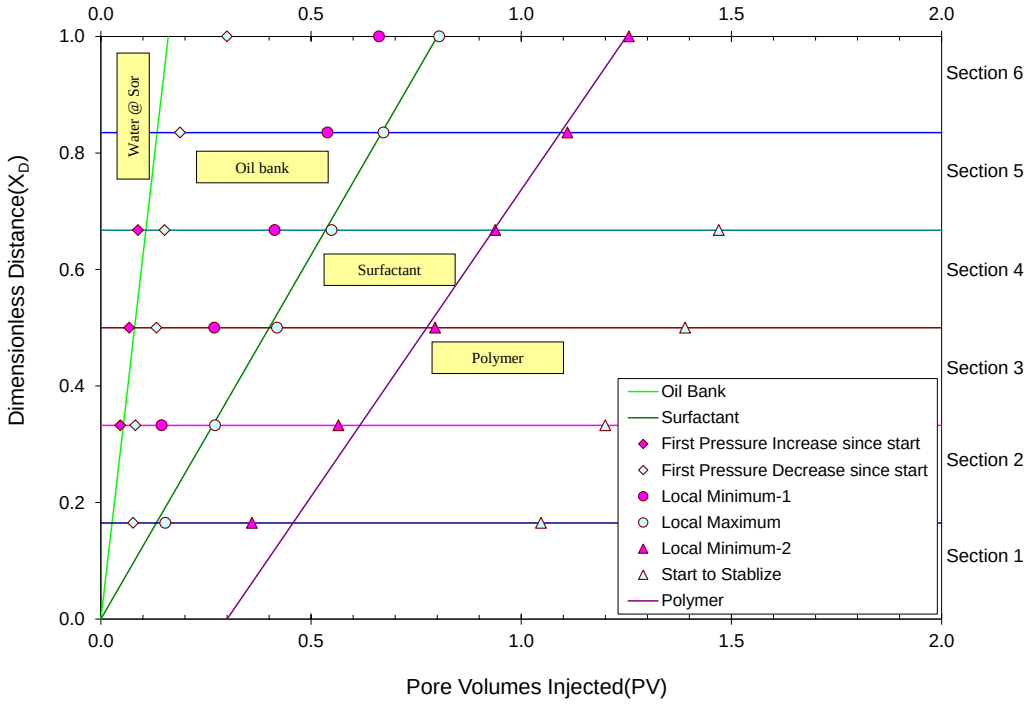

Figure 5.35 CFW#3 (Core#12) oil/surfactant/polymer bank front velocity profile during chemical flood at 43 ℃

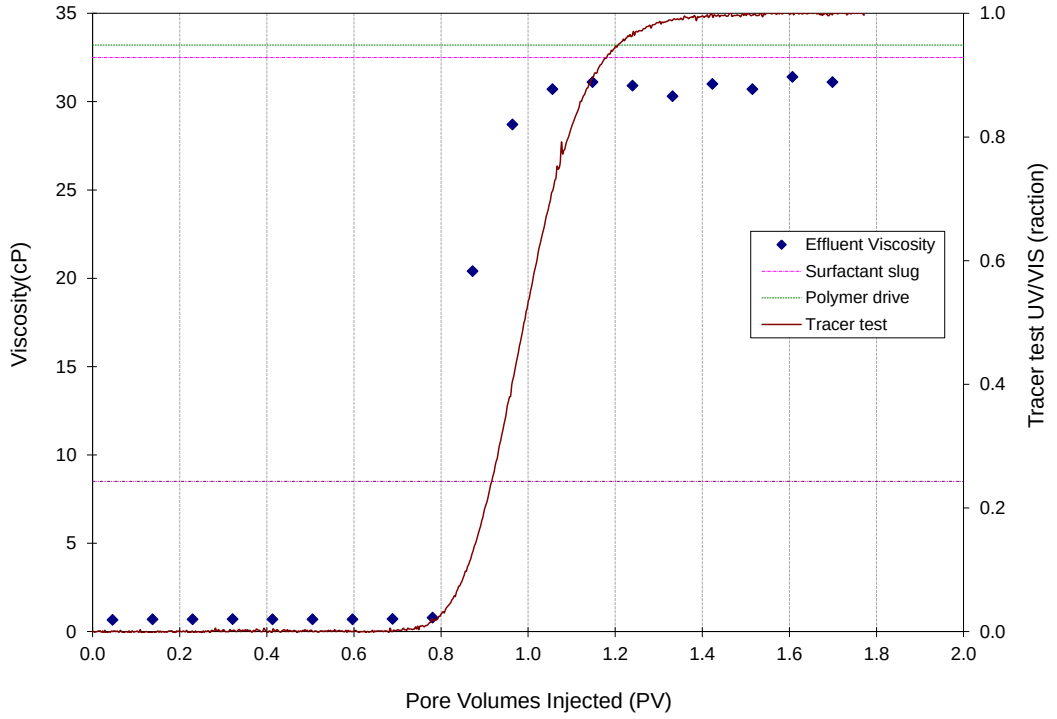

Figure 5.36 CFW#3(Core#12) chemical flood effluent viscosity (at 30 s^{-1}) profile at 43 ℃

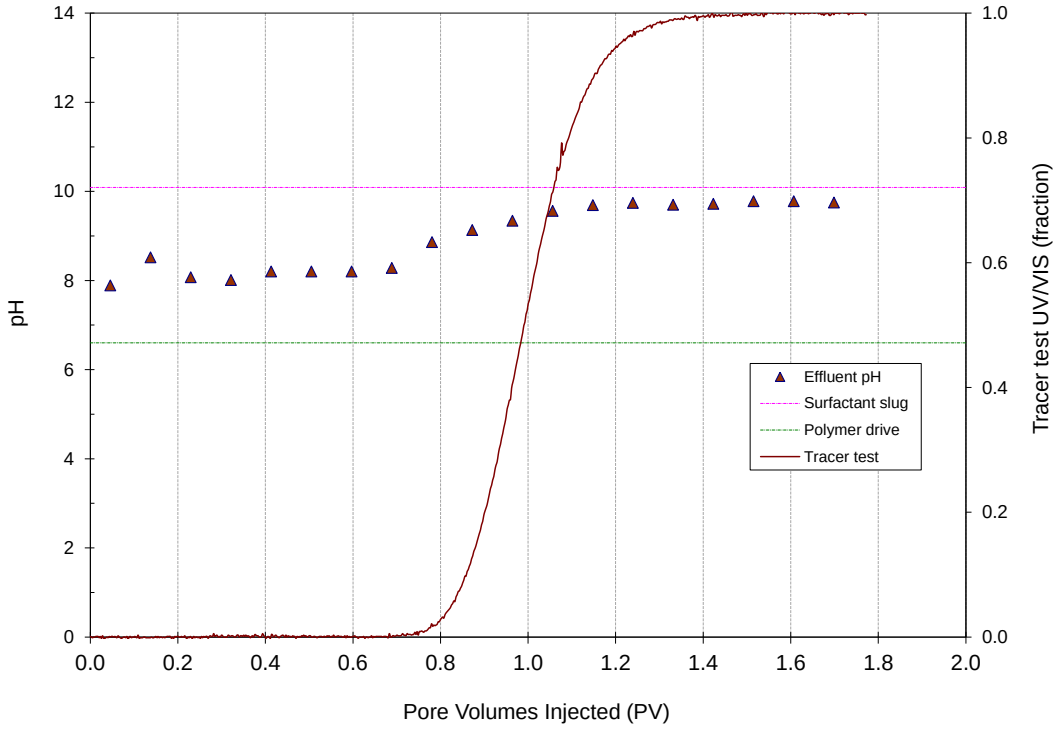

Figure 5.37 CFW#3(Core#12) chemical flood effluent pH profile

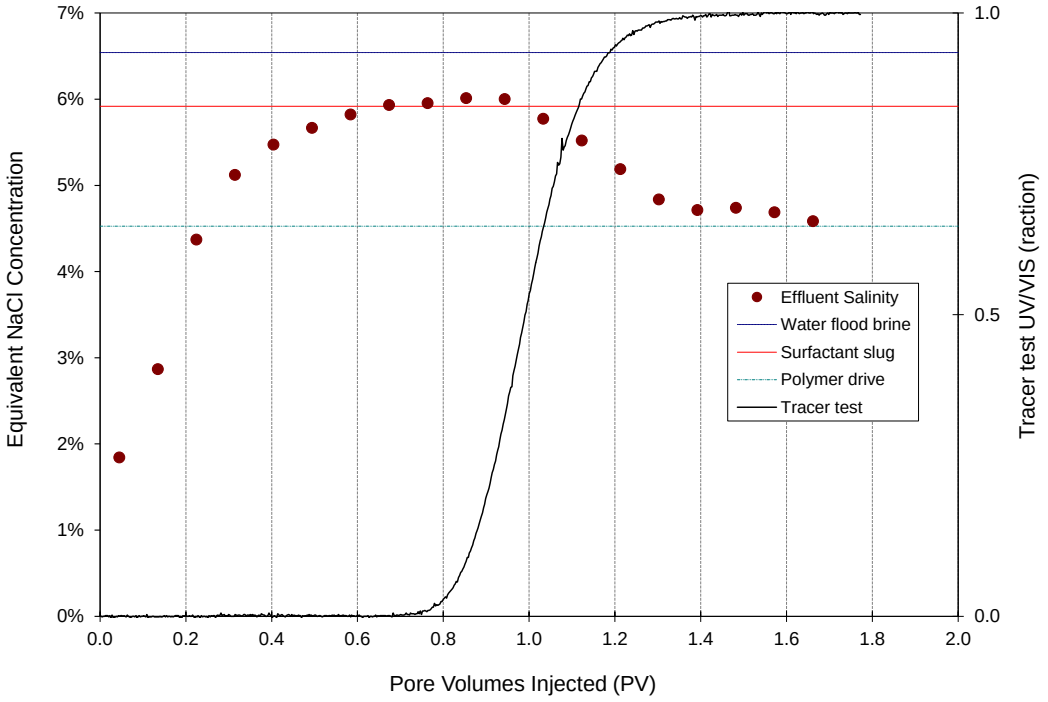

Figure 5.38 CFW#3(Core#12) chemical flood effluent equivalent salinity

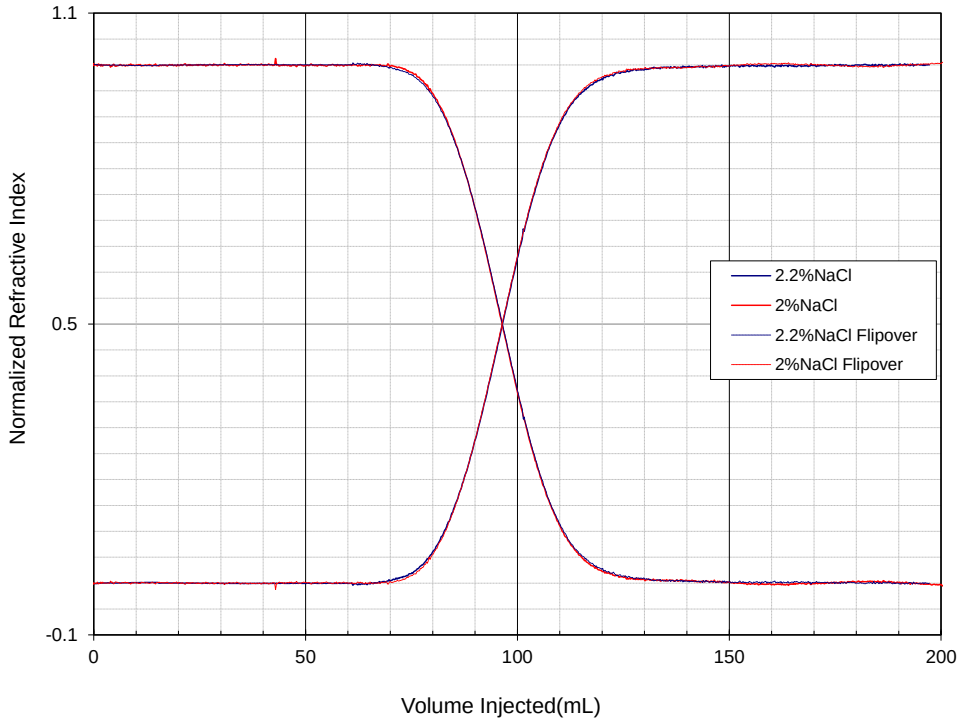

Figure 5.39 CFW#4 (Core#14) tracer test results

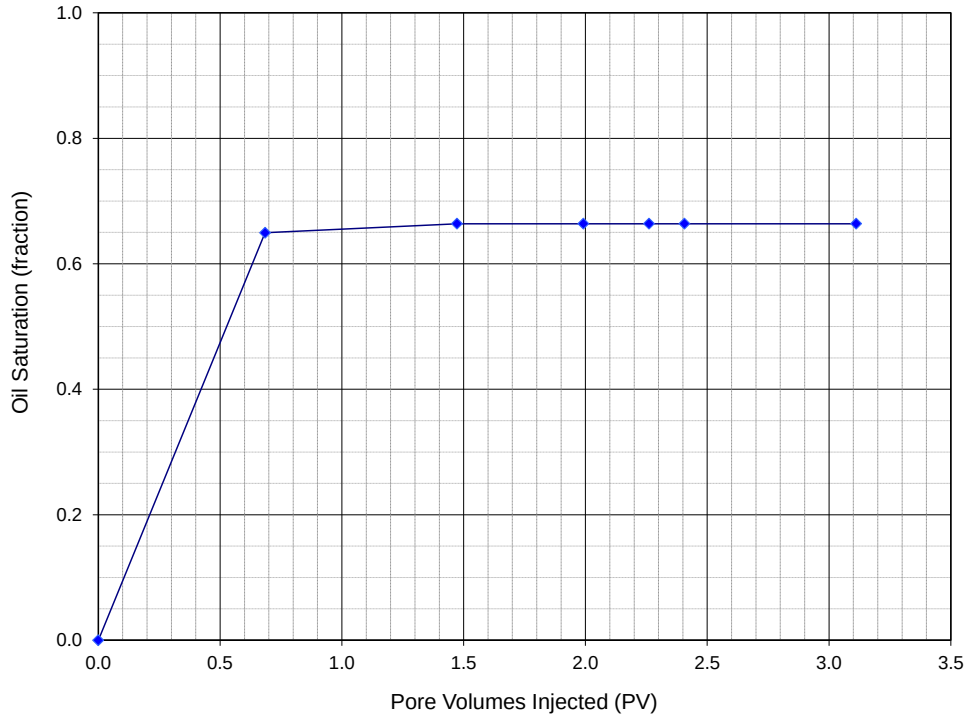

Figure 5.40 CFW#4(Core#14) oil saturation profile during oil flood at 43 ℃

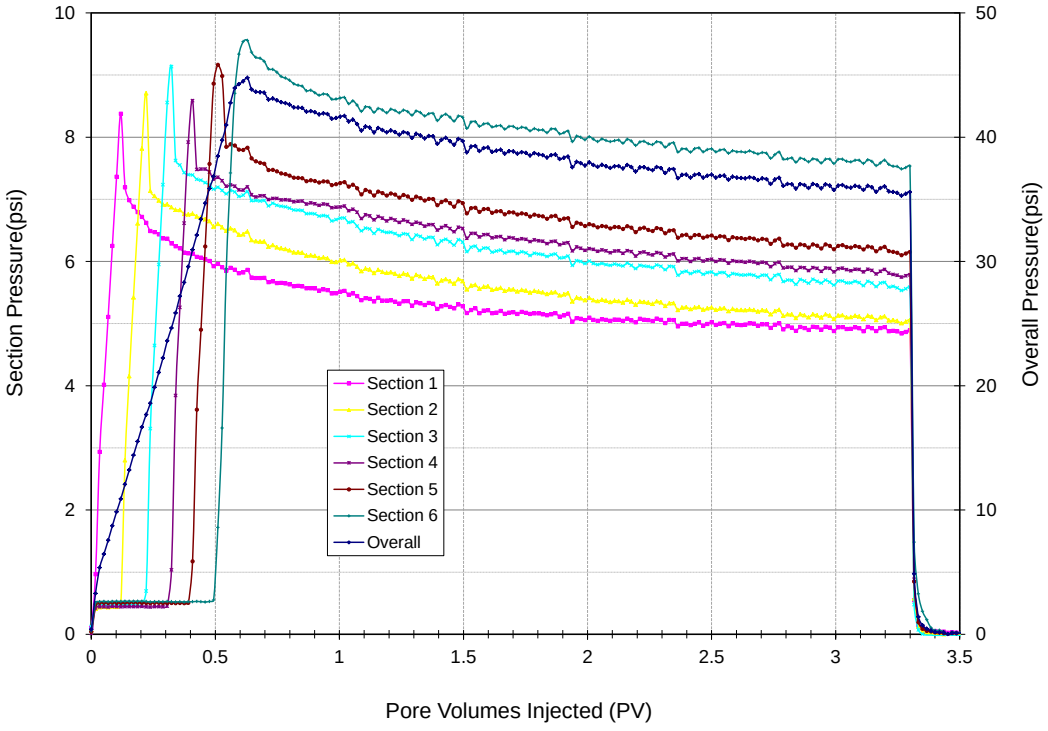

Figure 5.41 CFW#4(Core#14) pressure profile during oil flood at 43 ℃

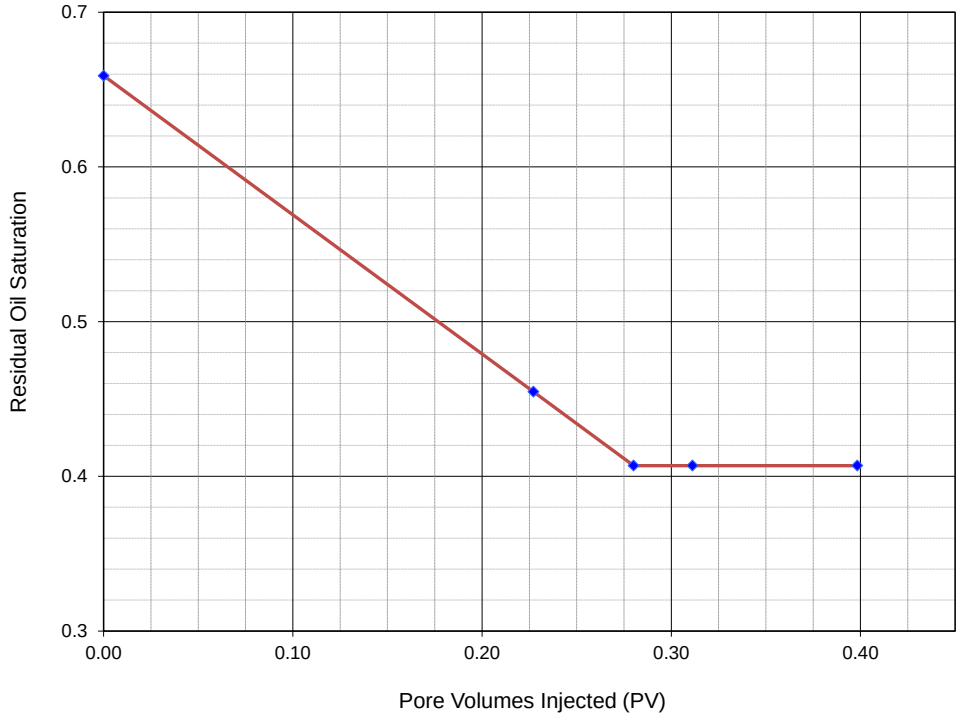

Figure 5.42 CFW#4(Core#14) oil saturation profile during water flood at 43 ℃

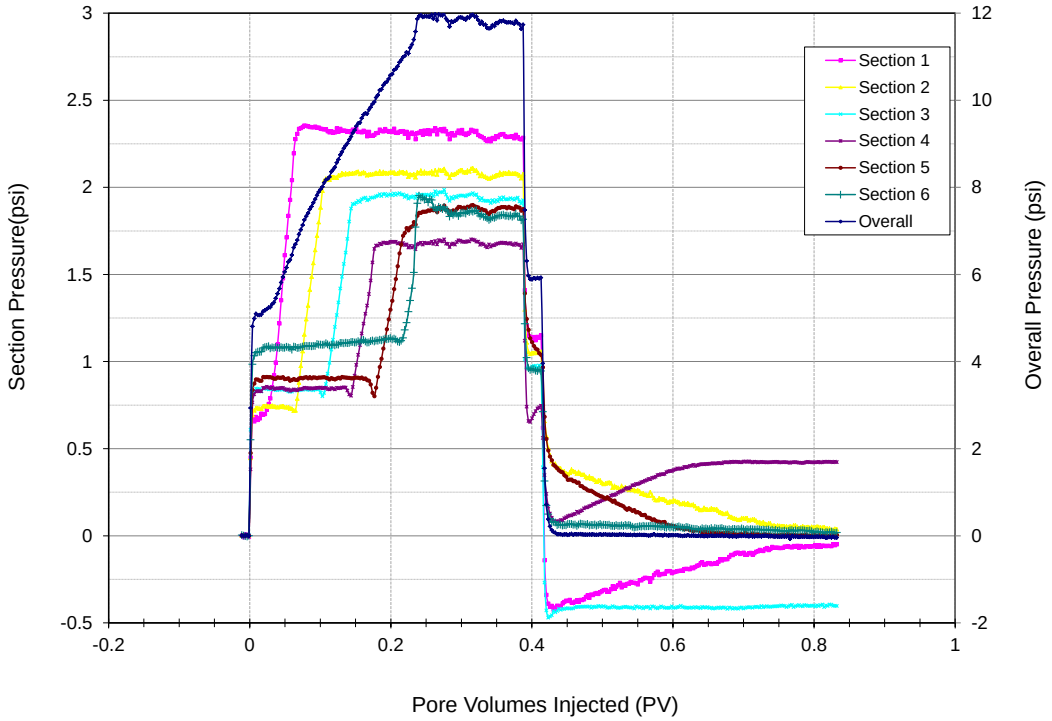

Figure 5.43 CFW#4(Core#14) pressure profile during water flood at 43 ℃

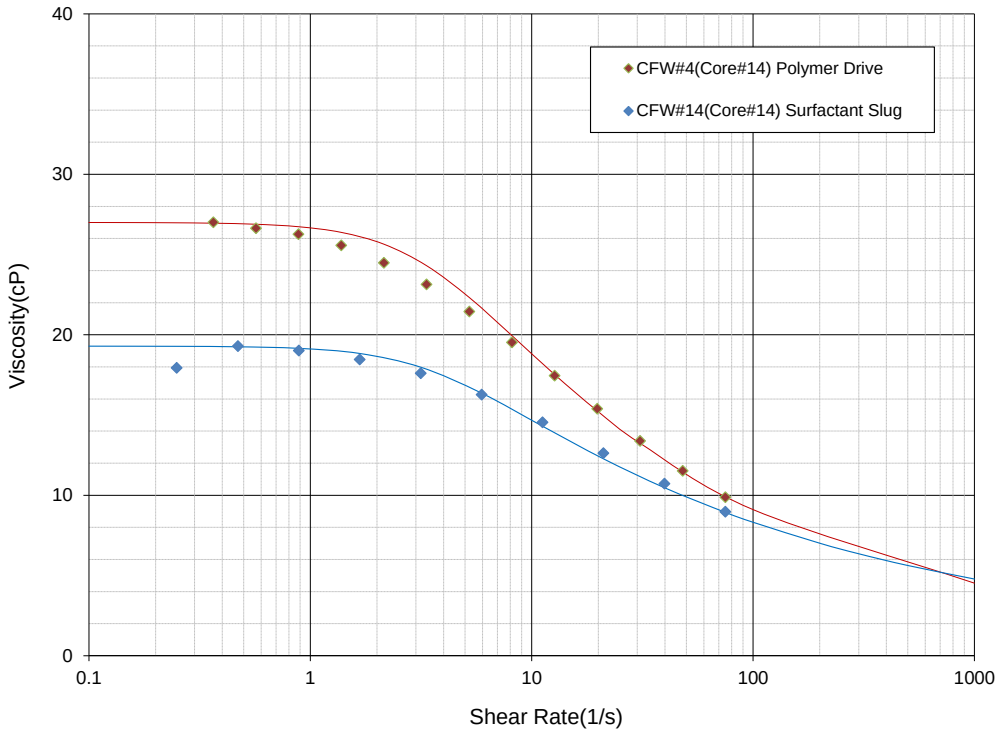

Figure 5.44 CFW#4 (Core#14) rheology diagram of surfactant slug and polymer drive at 43 ℃

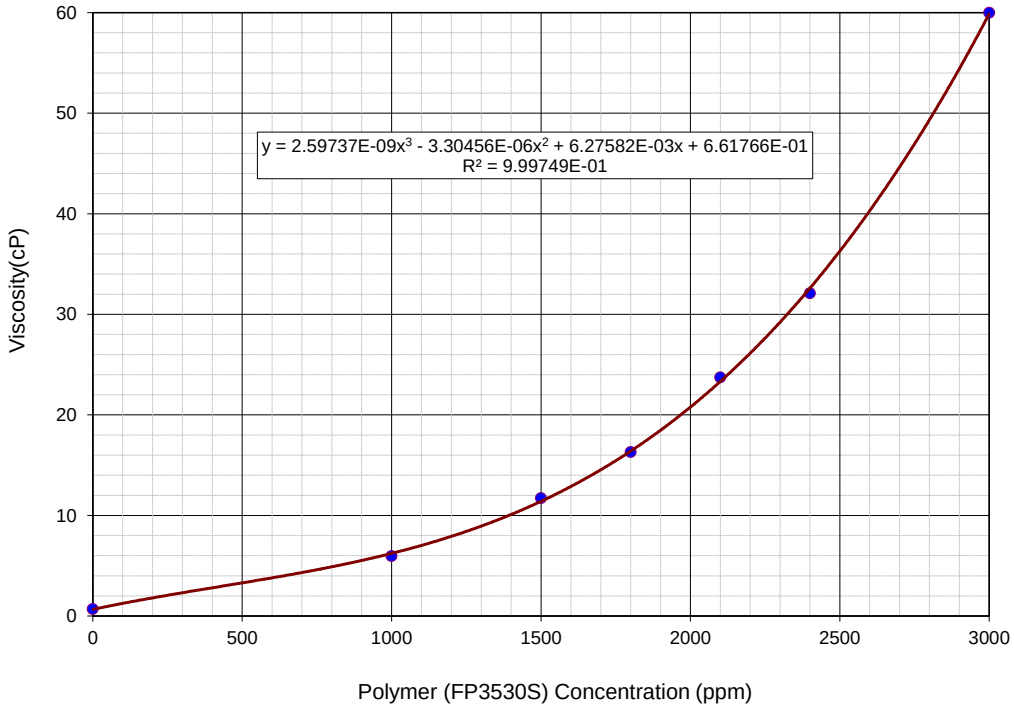

Figure 5.45 Low shear rate (~1 s^{-1}) viscosity of polymer solution containing different concentration of FP3530S and 4.6%NaCl at 43 ℃

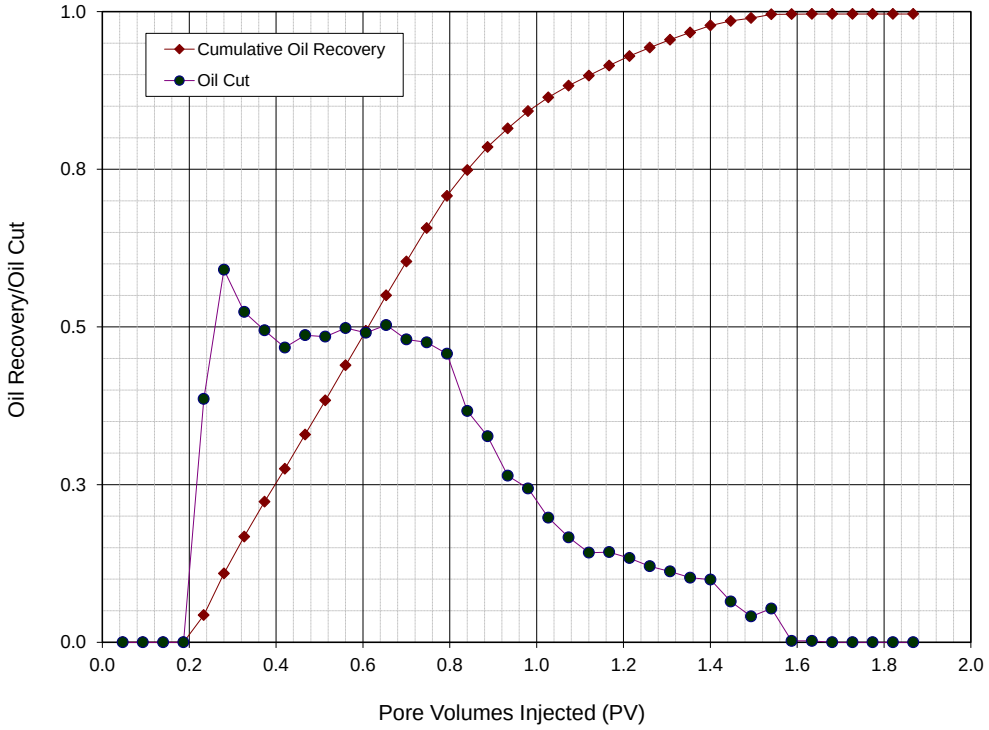

Figure 5.46 CFW#4(Core#14) chemical flood oil recovery and oil cut

Vial #	1	2	3	4	5	6	7	8	9	10
PV	0.047	0.093	0.140	0.187	0.233	0.280	0.327	0.373	0.420	0.467

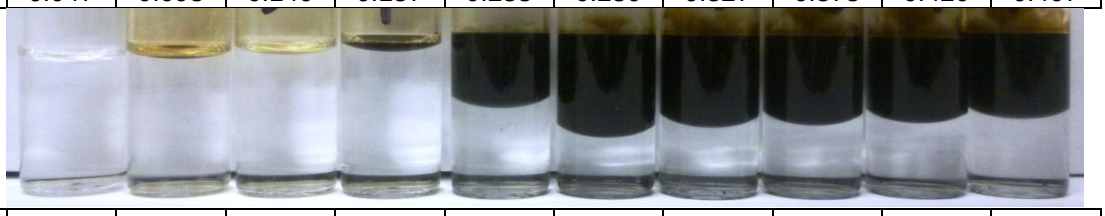

Vial #	11	12	13	14	15	16	17	18	19	20
PV	0.513	0.560	0.607	0.654	0.700	0.747	0.794	0.840	0.887	0.934

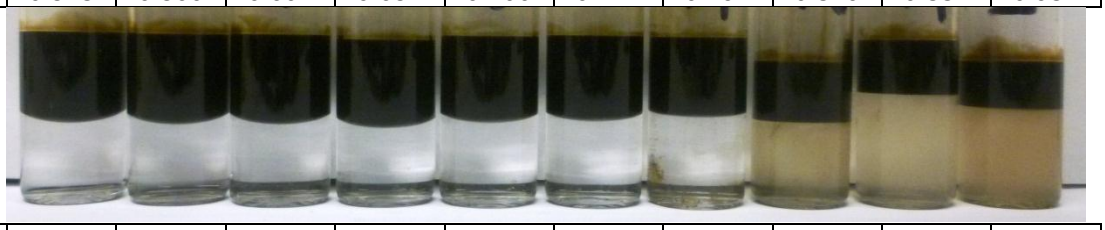

Vial #	21	22	23	24	25	26	27	28	29	30
PV	0.980	1.027	1.074	1.120	1.167	1.214	1.260	1.307	1.354	1.400

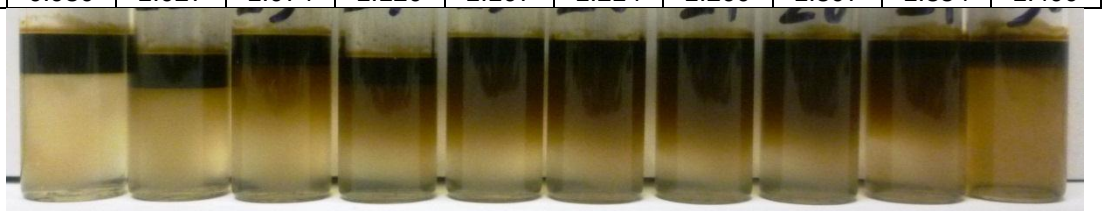

Vial #	31	32	33	34	35	36	37	38	39	40
PV	1.447	1.494	1.540	1.587	1.634	1.680	1.727	1.774	1.821	1.867

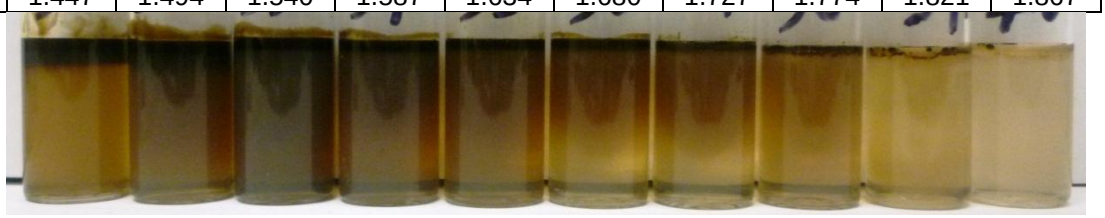

Figure 5.47 CFW#4 (Core#14) photos of chemical flood effluent after equilibrating at reservoir temperature, 43 ℃ for 6 days.

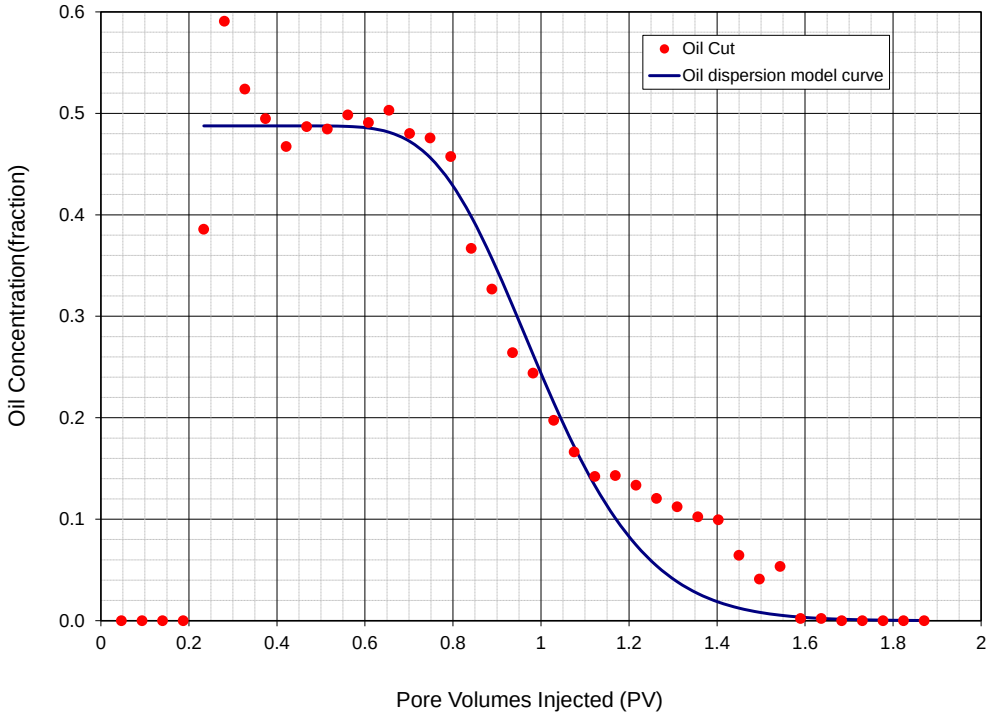

Figure 5.48 CFW#4 (Core#14) oil cut dispersion model

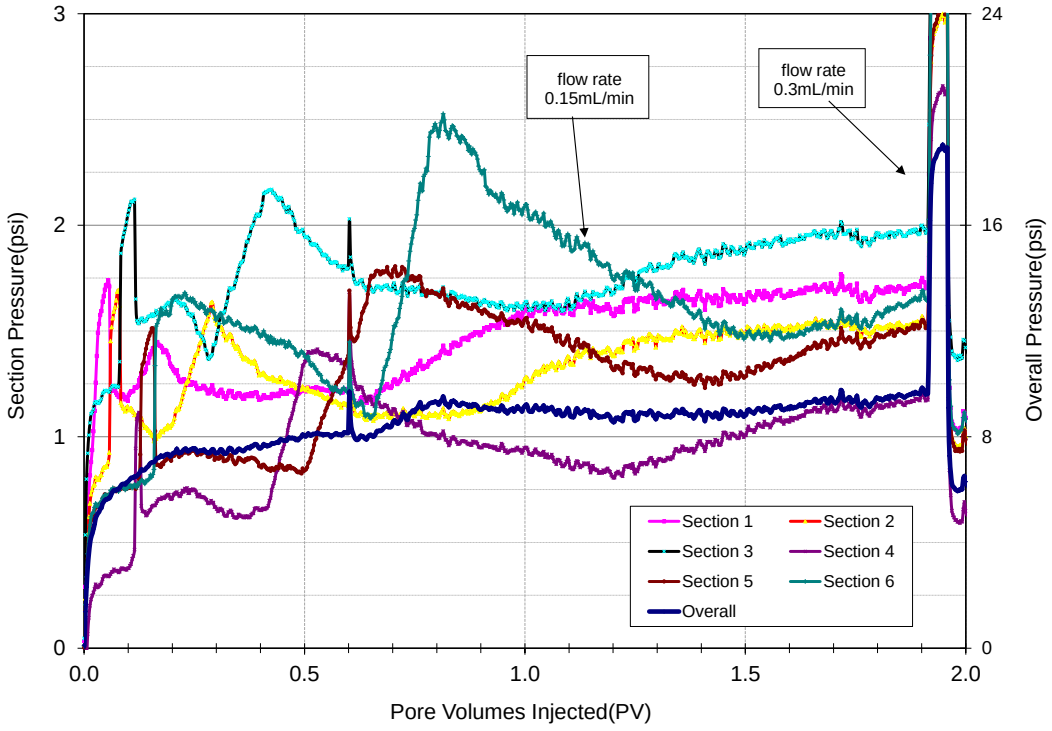

Figure 5.49 CFW#4(Core#14) pressure profile during chemical flood at 43 ℃

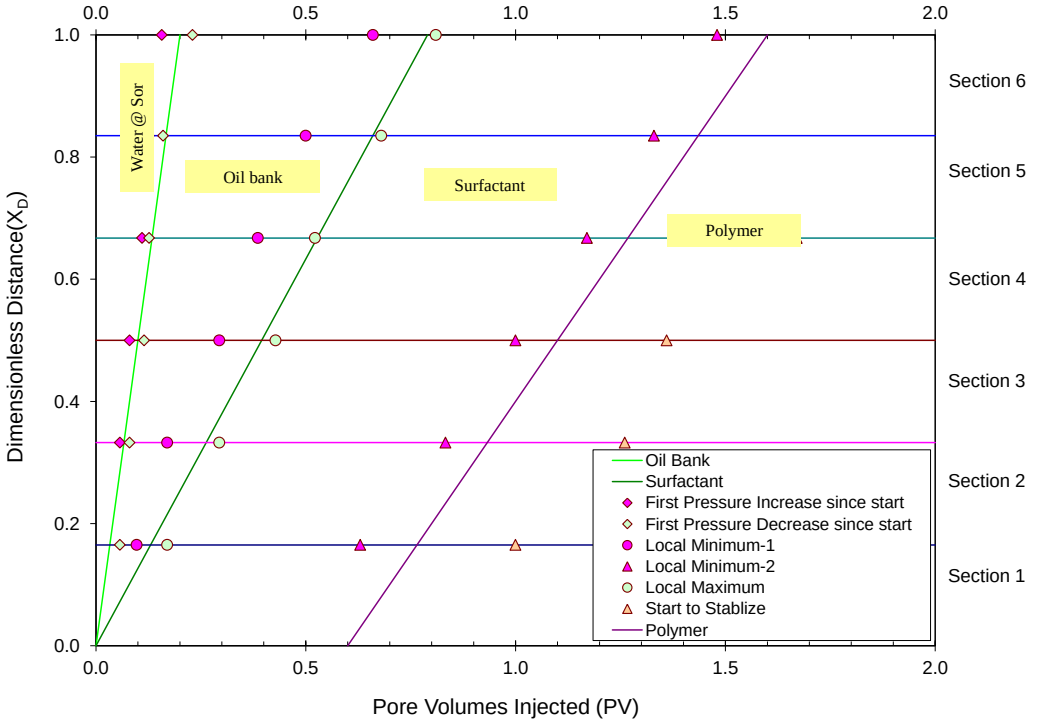

Figure 5.50 CFW#4(Core#14) oil/surfactant/polymer bank front velocity profile during chemical flood at 43 ℃

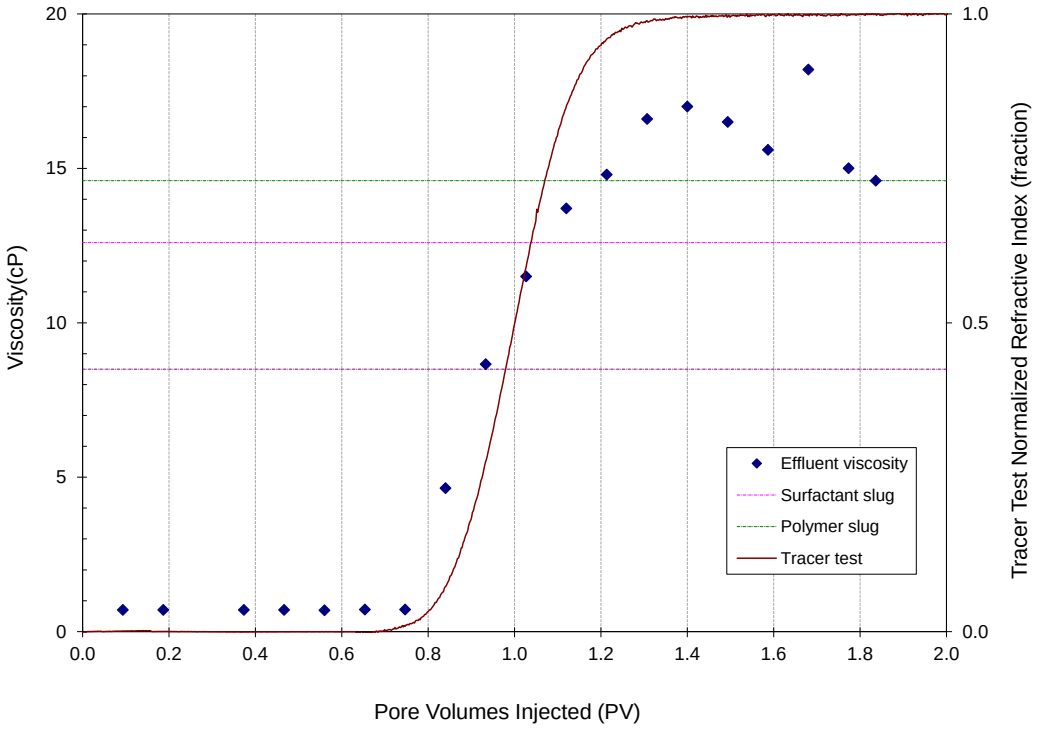

Figure 5.51 CFW#4 (Core#14) chemical flood effluent viscosity (at 30 s^{-1}) profile at 43 ℃

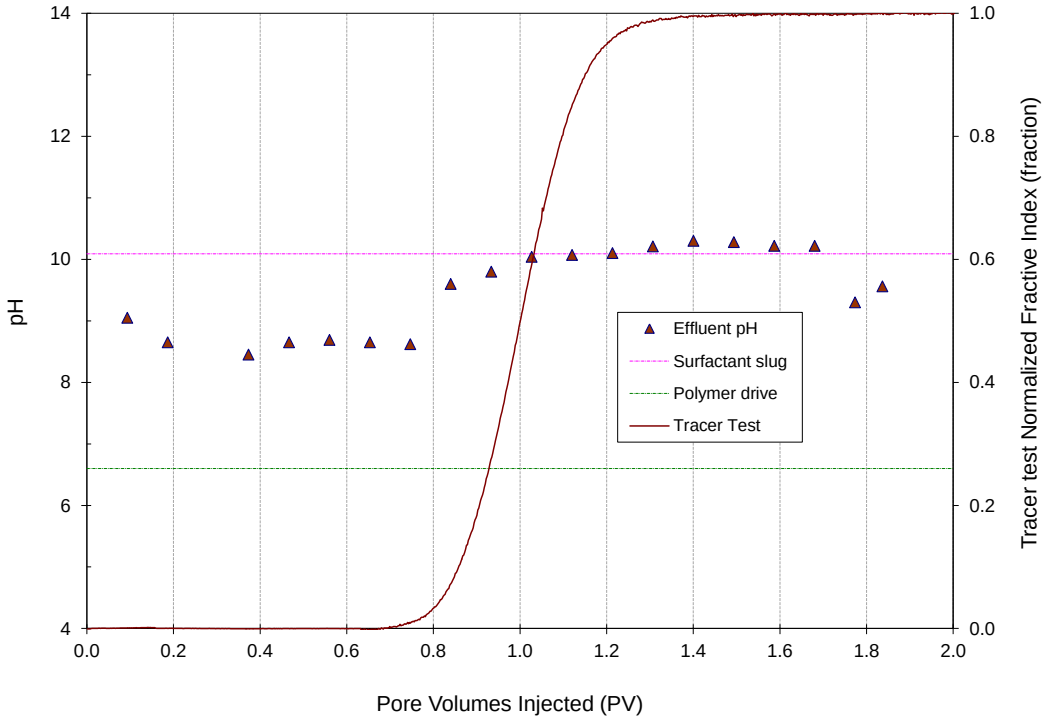

Figure 5.52 CFW#4 (Core#14) chemical flood effluent pH profile

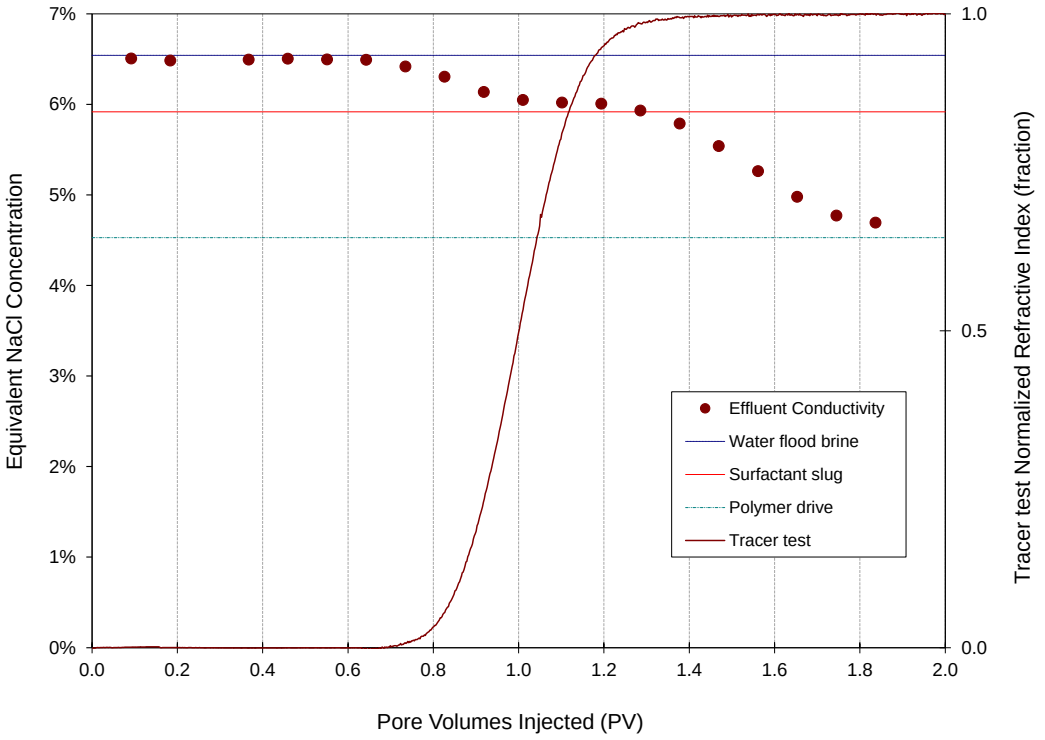

Figure 5.53 CFW#4 (Core#14) chemical flood effluent equivalent profile

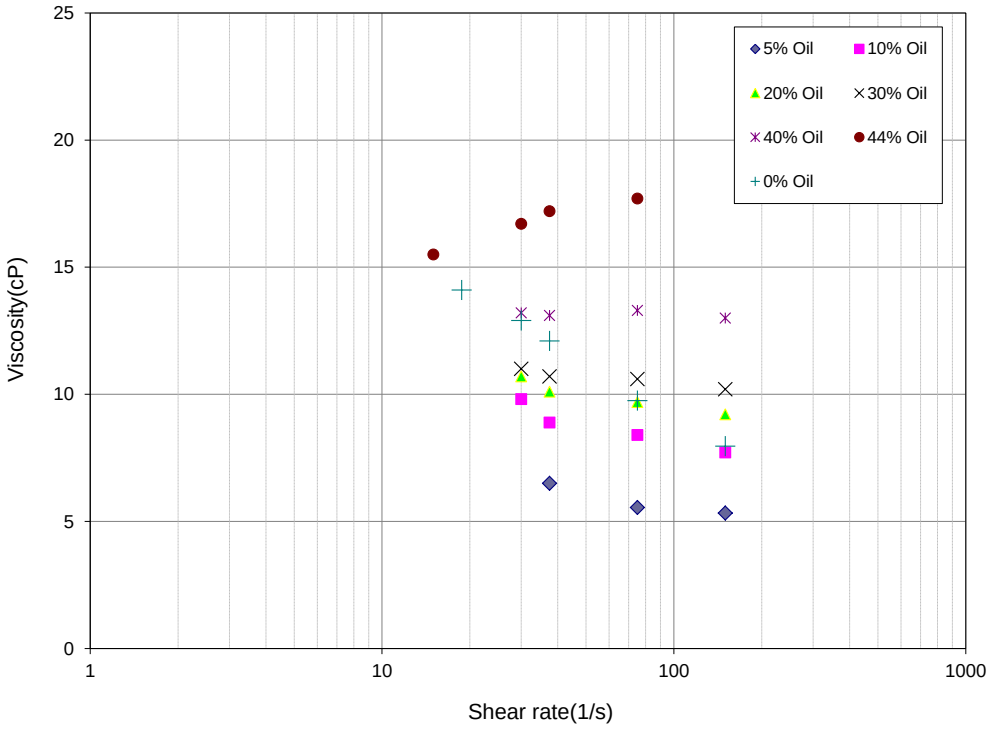

Figure 5.54 Viscosity of microemulsion phase formed by mixing CFW#4 surfactant slug with Wahrman crude oil and equilibrating for 4 days at 43 ℃.

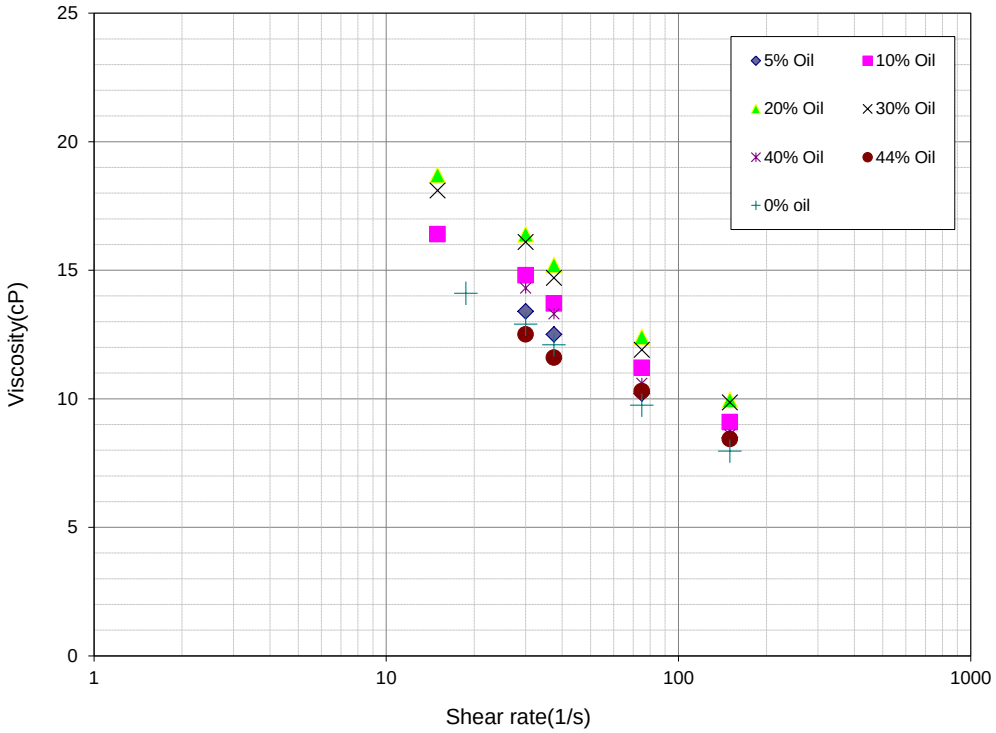

Figure 5.55 Viscosity of mixture formed by mixing CFW#4 surfactant slug with Wahrman crude oil and equilibrating at 43 ℃ for 2 hours.

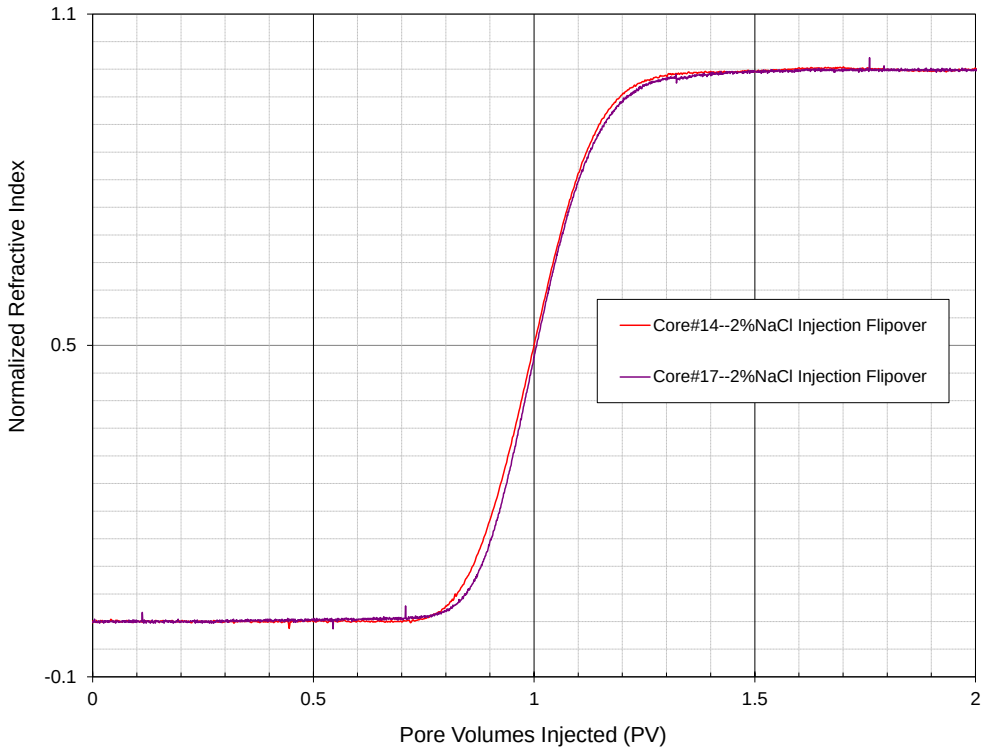

Figure 5.56 CFW#5(Core#17) and CFW#4(Core#14) tracer test results comparison

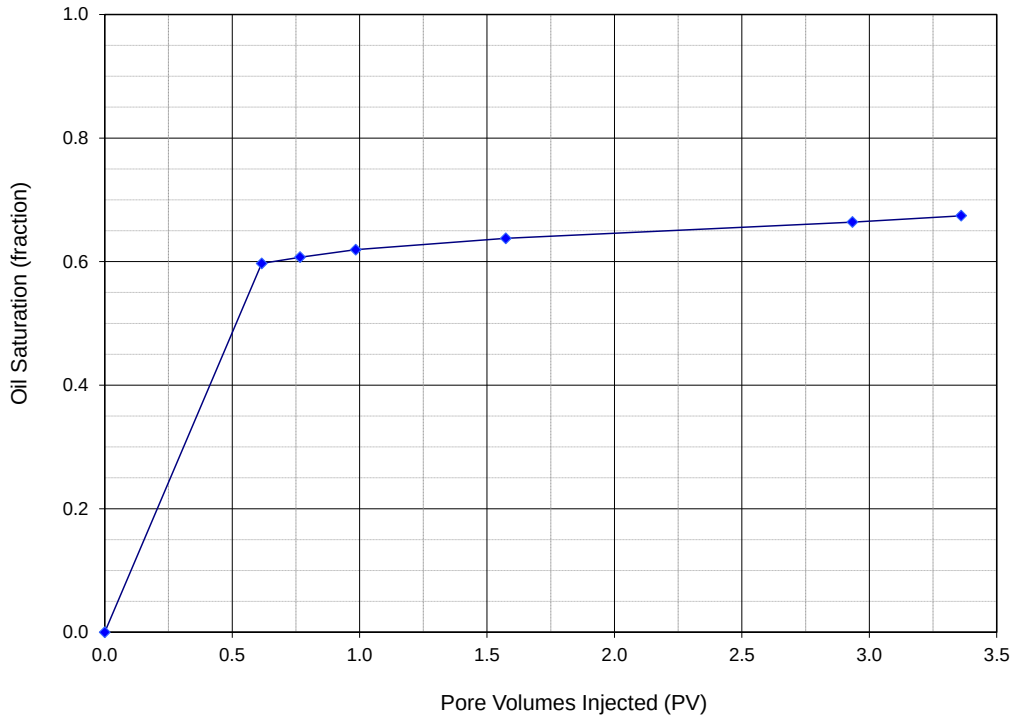

Figure 5.57 CFW#5(Core#17) oil saturation profile during oil flood at 43 ℃

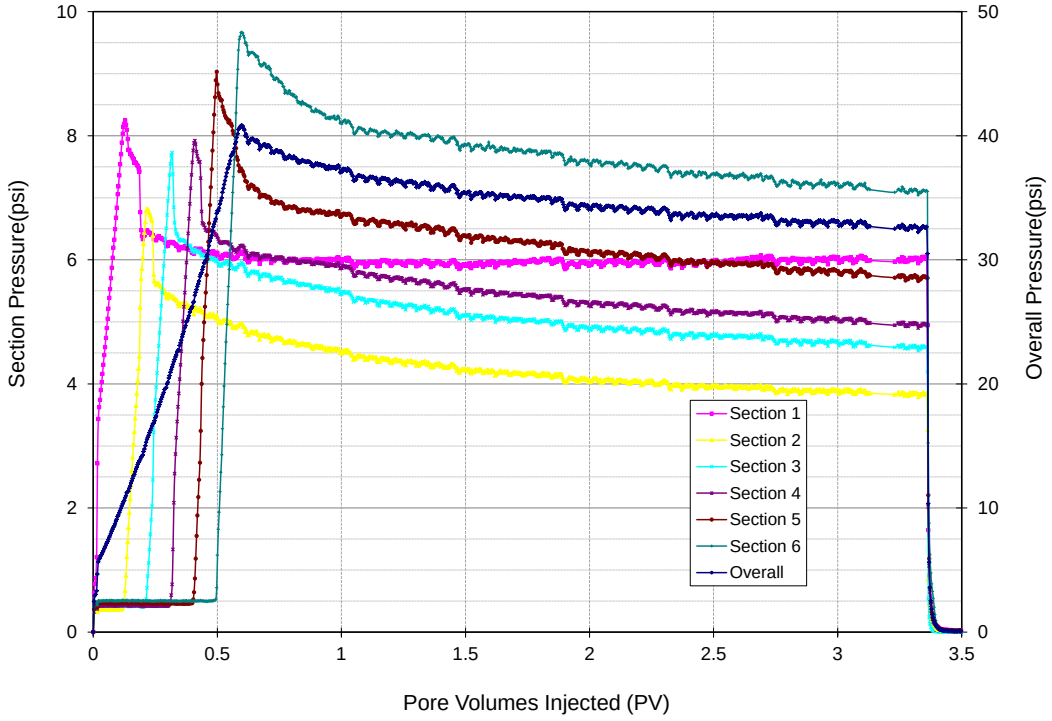

Figure 5.58 CFW#5(Core#17) pressure profile during oil flood at 43 ℃

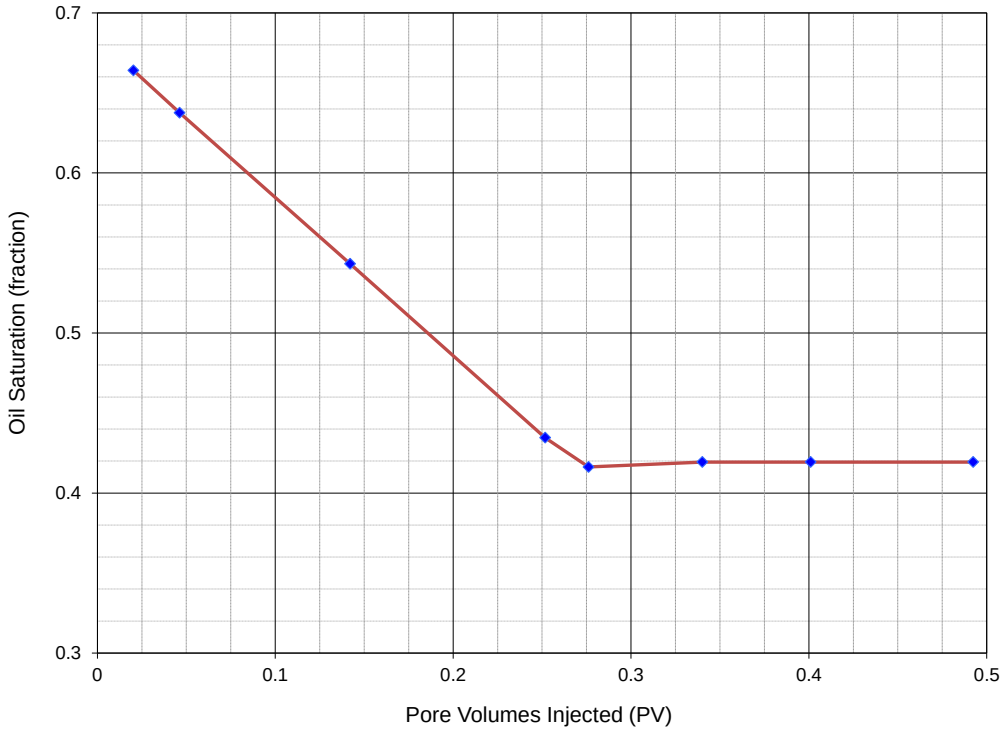

Figure 5.59 CFW#5 (Core#17) oil saturation during water flood at 43 ℃

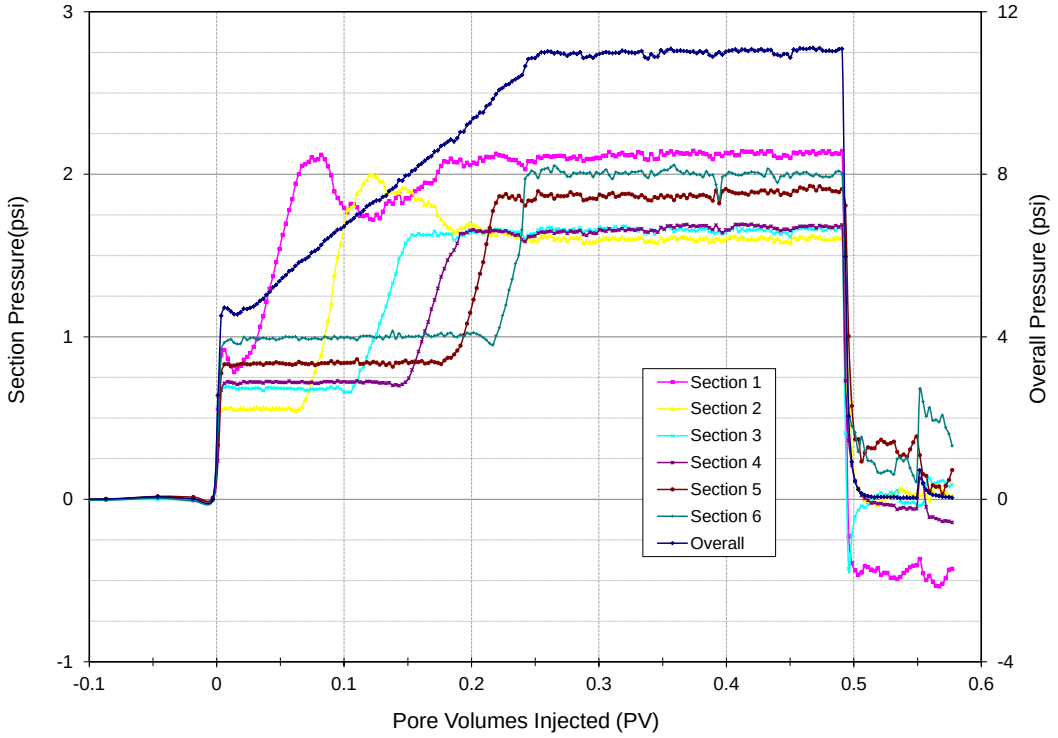

Figure 5.60 CFW#5 (Core#17) pressure profile during water flood at 43 ℃

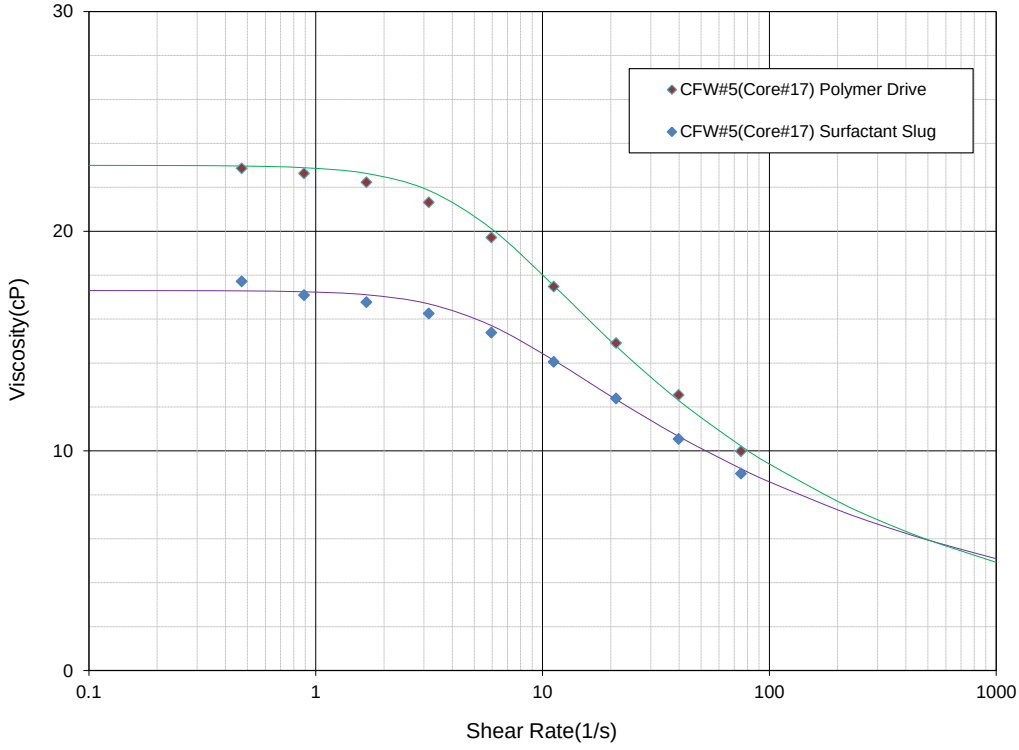

Figure 5.61 CFW#5(Core#17) rheology diagram of surfactant slug and polymer drive at 43 ℃

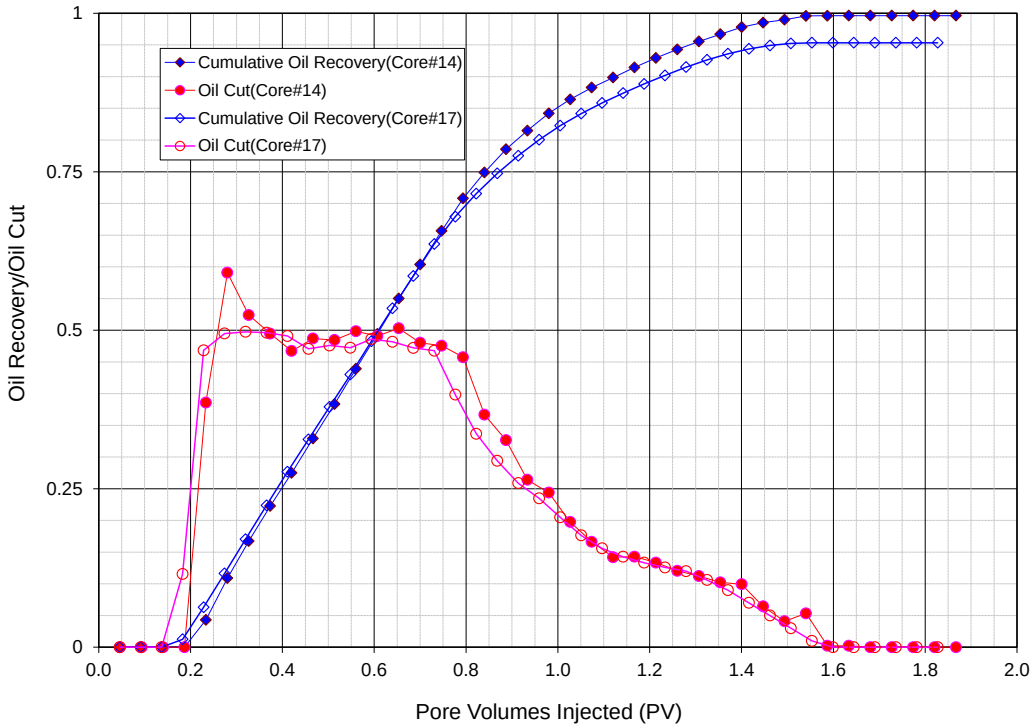

Figure 5.62 CFW#5(Core#17) chemical flood oil recovery and oil cut comparing to CFW#4 (Core#14)

Vial#	1	2	3	4	5	6	7	8	9	10
PV	0.046	0.091	0.137	0.183	0.228	0.274	0.320	0.365	0.411	0.457

Vial#	11	12	13	14	15	16	17	18	19	20
PV	0.503	0.548	0.594	0.640	0.685	0.731	0.777	0.822	0.868	0.914

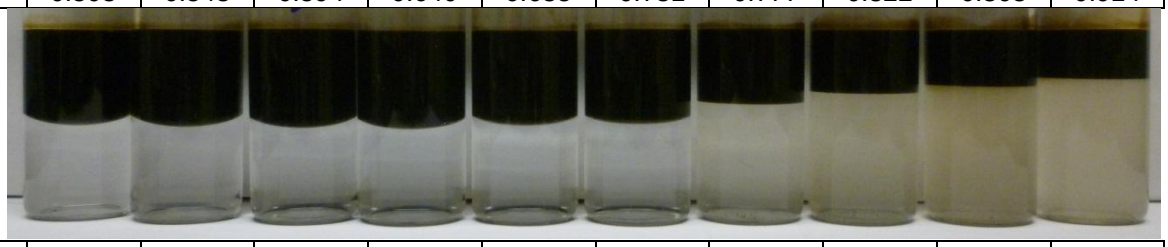

Vial#	21	22	23	24	25	26	27	28	29	30
PV	0.959	1.005	1.051	1.096	1.142	1.188	1.234	1.279	1.325	1.371

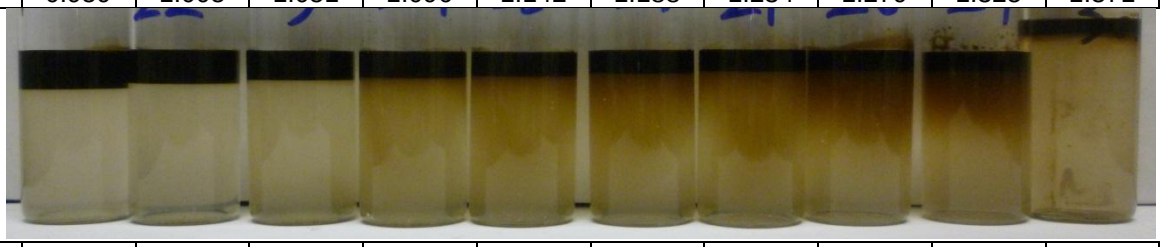

Vial#	31	32	33	34	35	36	37	38	39	40
PV	1.416	1.462	1.508	1.553	1.599	1.645	1.690	1.736	1.782	1.827

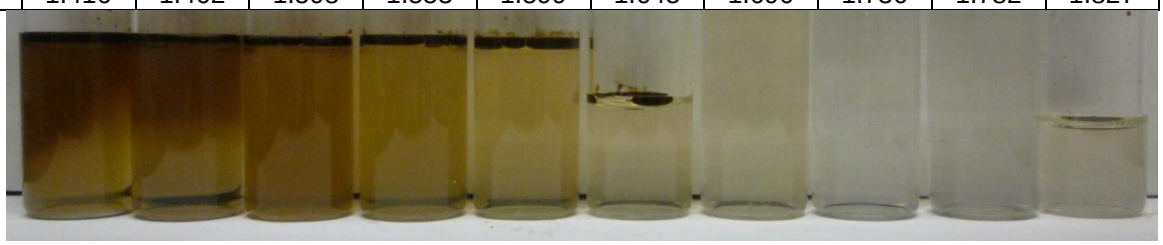

Figure 5.63 Photos of CFW#5 (Core#17) flood effluent vials after equilibration at reservoir temperature (43 ℃) for 5 days

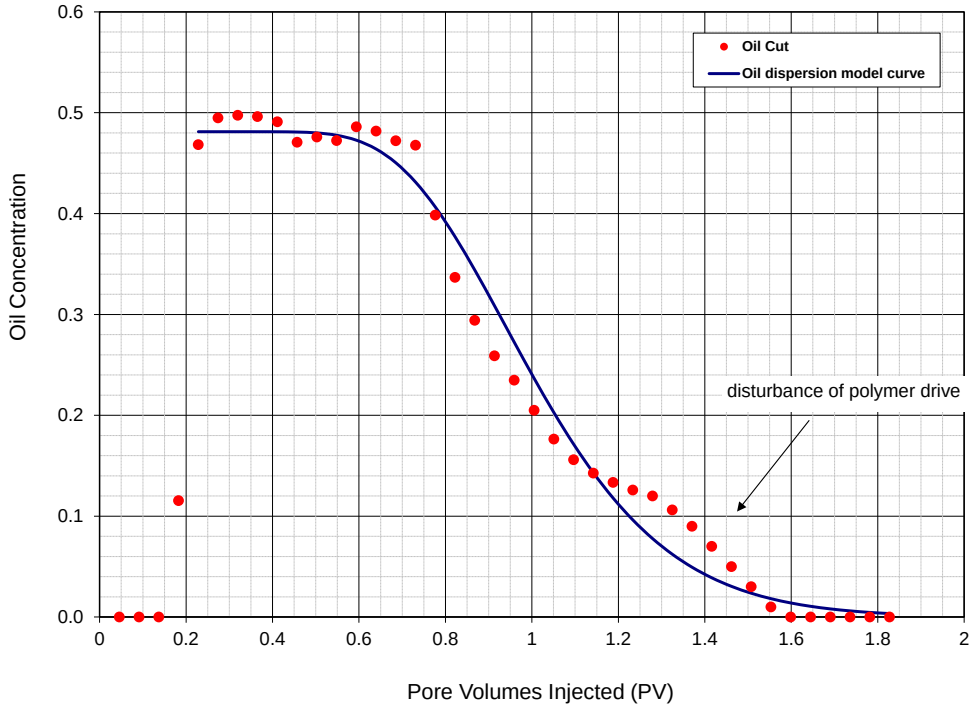

Figure 5.64 CFW#5 (Core#17) oil cut dispersion model

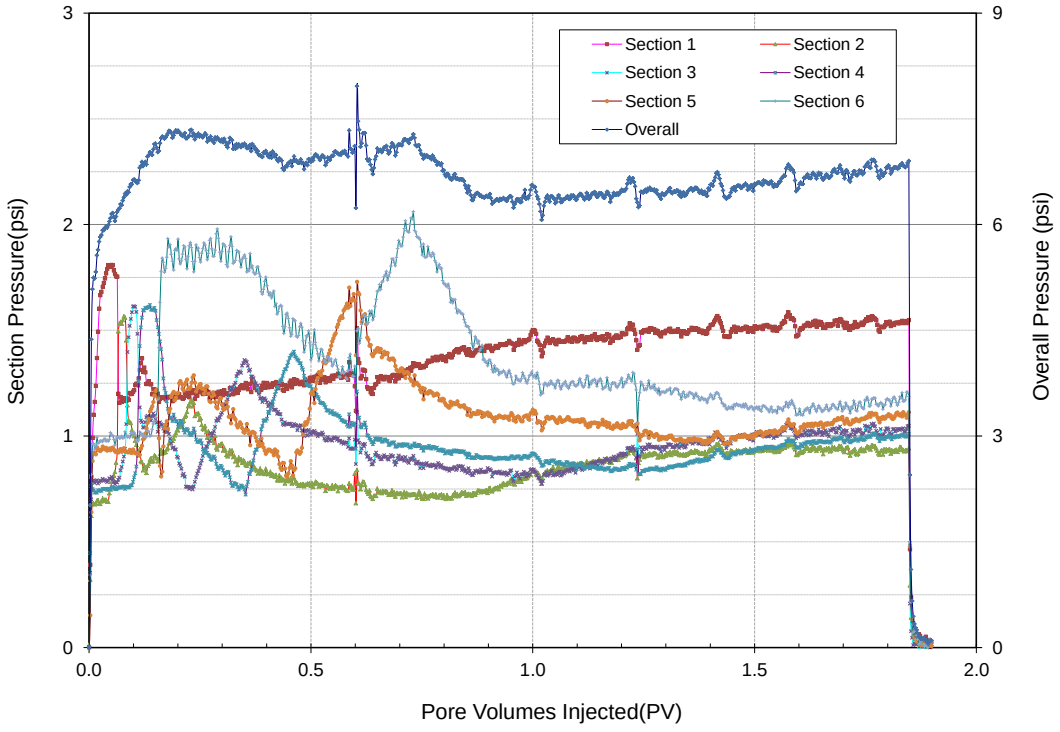

Figure 5.65 CFW#5 (Core#17) pressure profile during chemical flood at 43 ℃

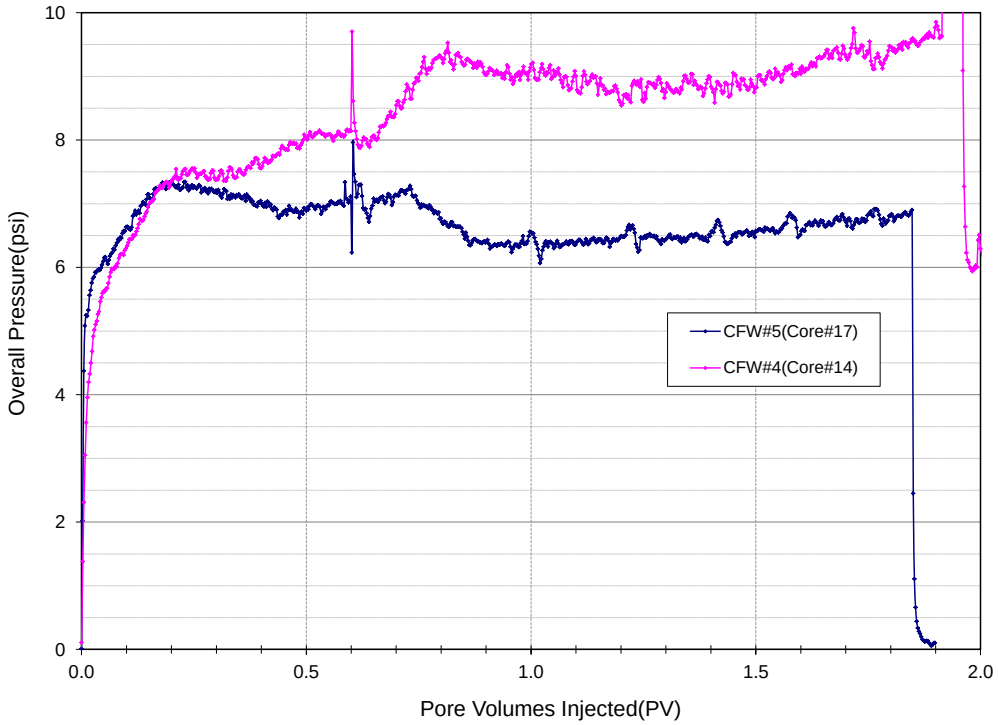

Figure 5.66 Overall pressure comparison between Coer#14 and Core#17.

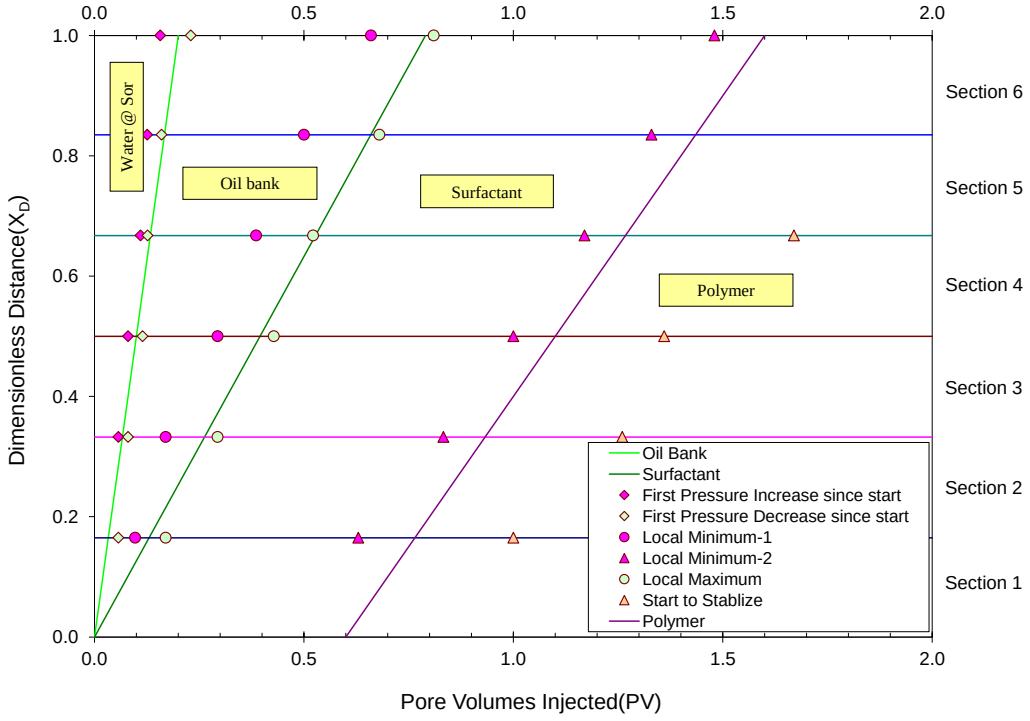

Figure 5.67 CFW#5(Core#17) oil/surfactant/polymer bank front velocity profile during chemical flood at 43 ℃

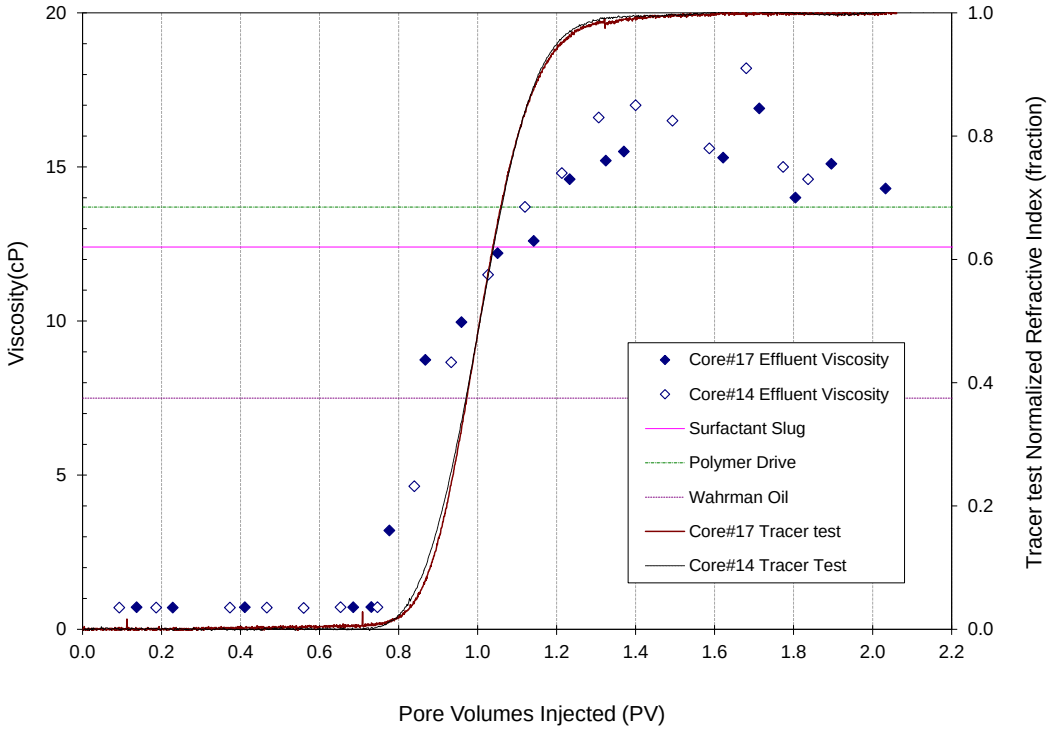

Figure 5.68 CFW#5(Core#17) viscosity (at 30 s^{-1}) at 43 ℃ profile during chemical flood comparing to CFW#4 (Core#14)

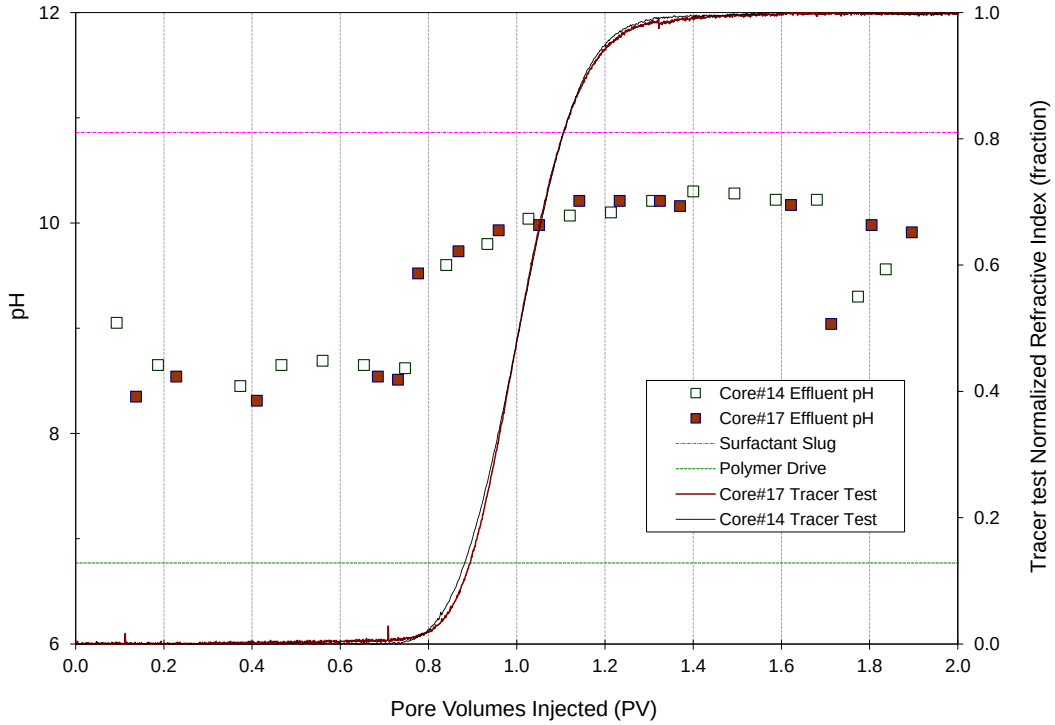

Figure 5.69 CFW#5 (Core#17) pH profile during chemical flood comparing to CFW#4 (Core#14)

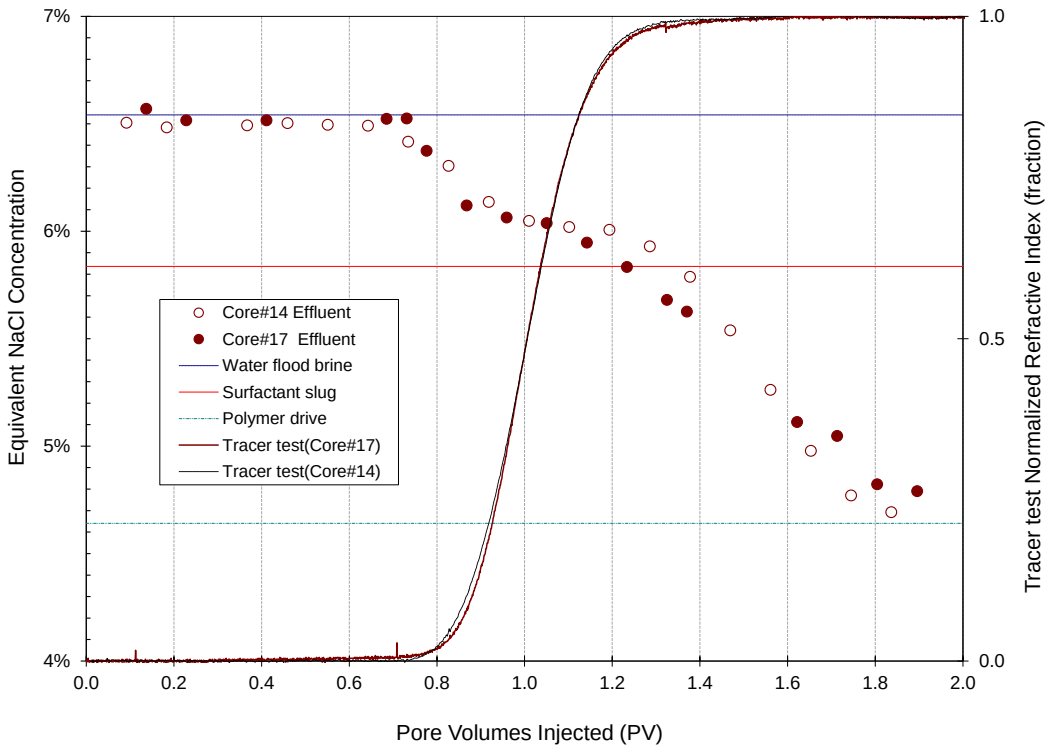

Figure 5.70 CFW#5 (Core#17) equivalent salinity profile comparing to CFW#4 (Core#14)

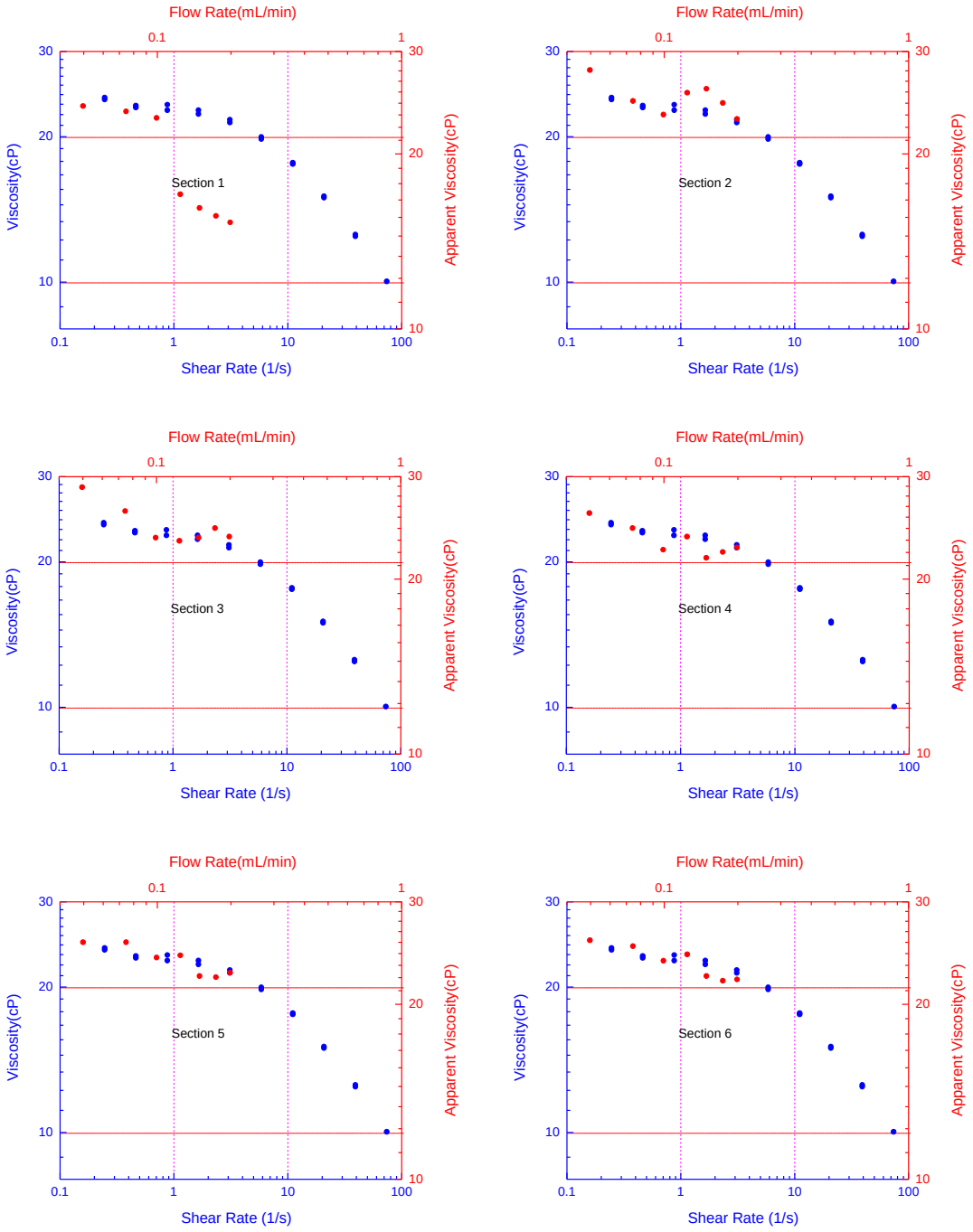

Figure 5.71 CFW#5 (Core#17) post ASP polymer flow analysis, viscosities measured by Bohlin CS rheometer at 43 ℃

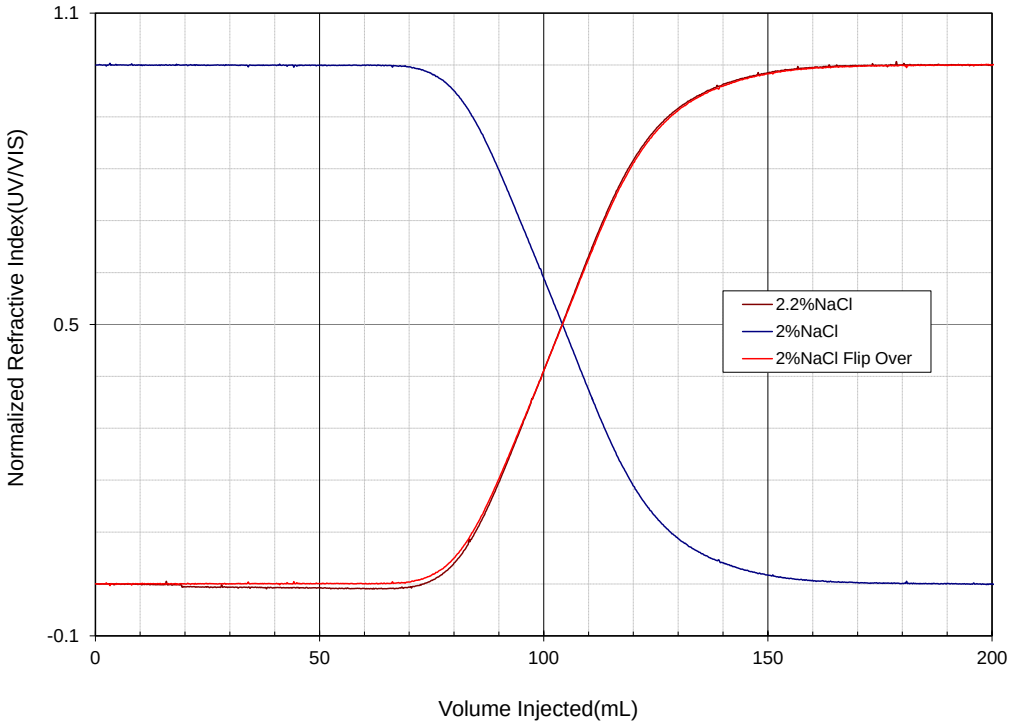

Figure 5.72 CFW#6 (Core#22) tracer test results

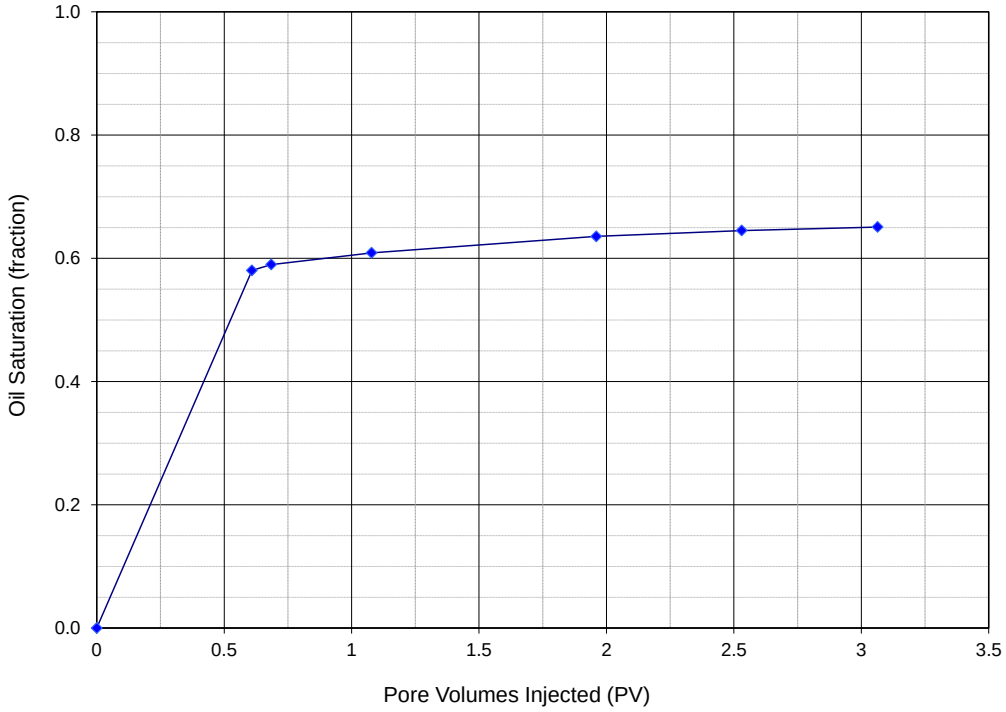

Figure 5.73 CFW#6(Core#22) oil saturation profile during oil flood at 43 ℃

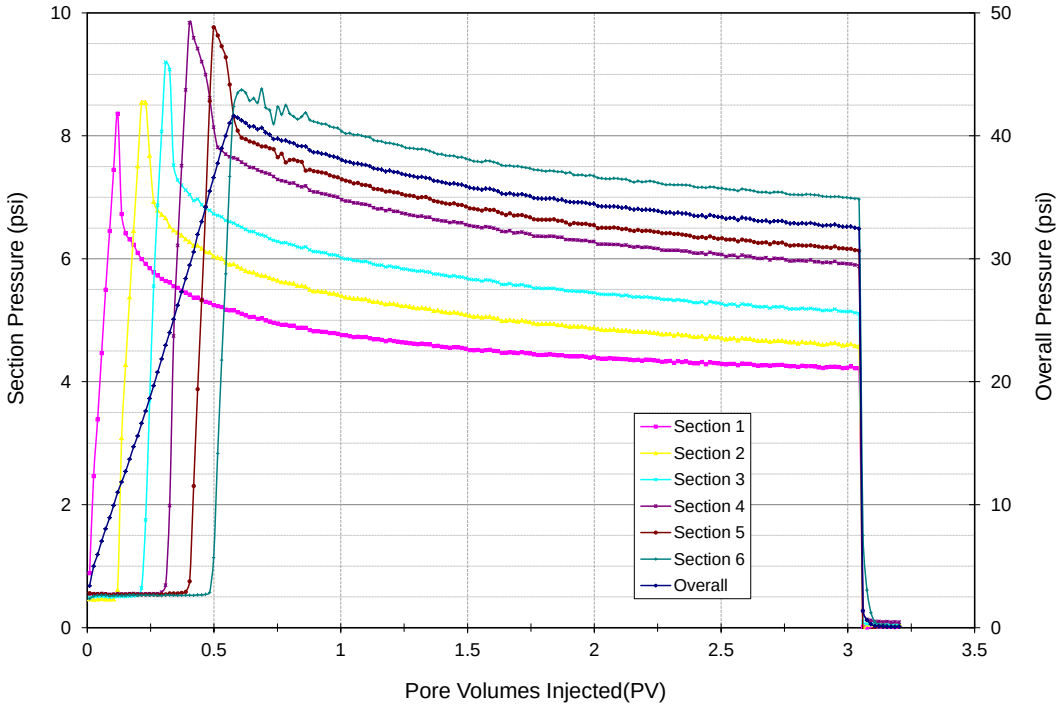

Figure 5.74 CFW#6 (Core#22) pressure profile during oil flood at 43 ℃

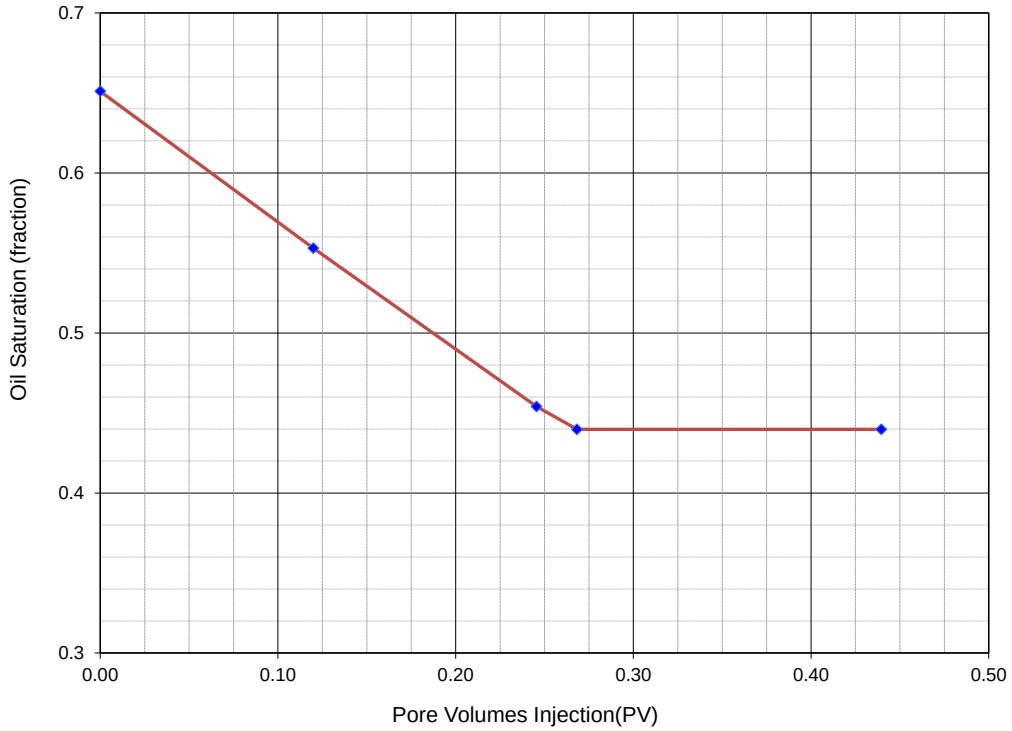

Figure 5.75 CFW#6 (Core#22) oil saturation profile during water flood at 43 ℃

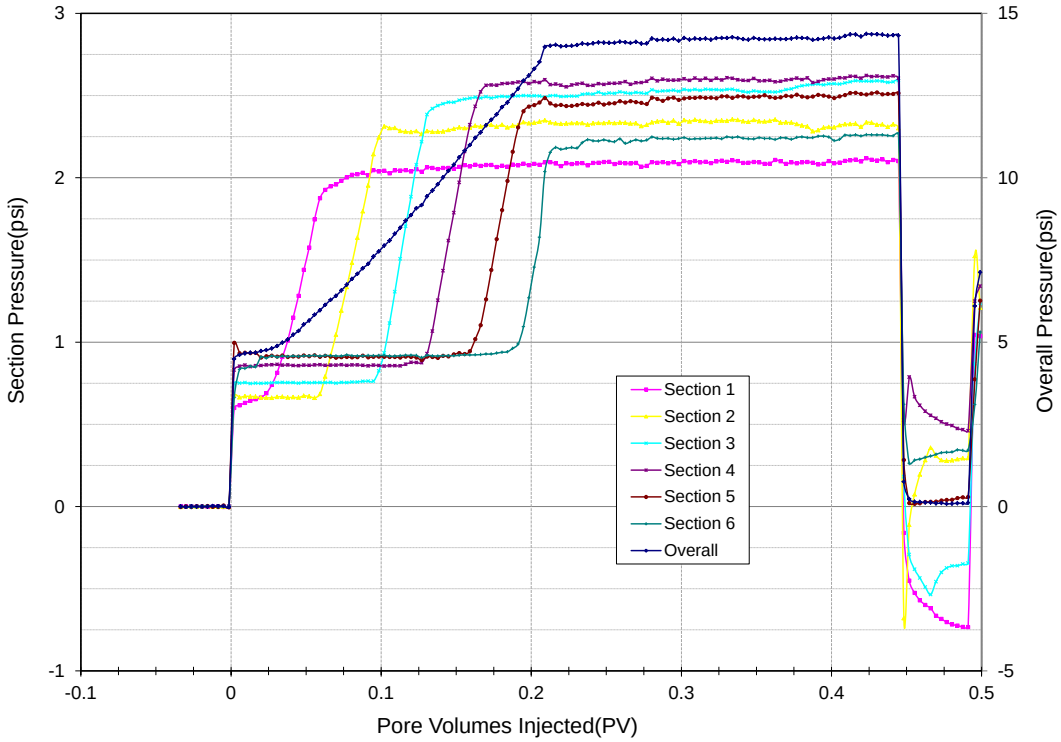

Figure 5.76 CFW#6(Core#22) pressure profile during water flood at 43 ℃

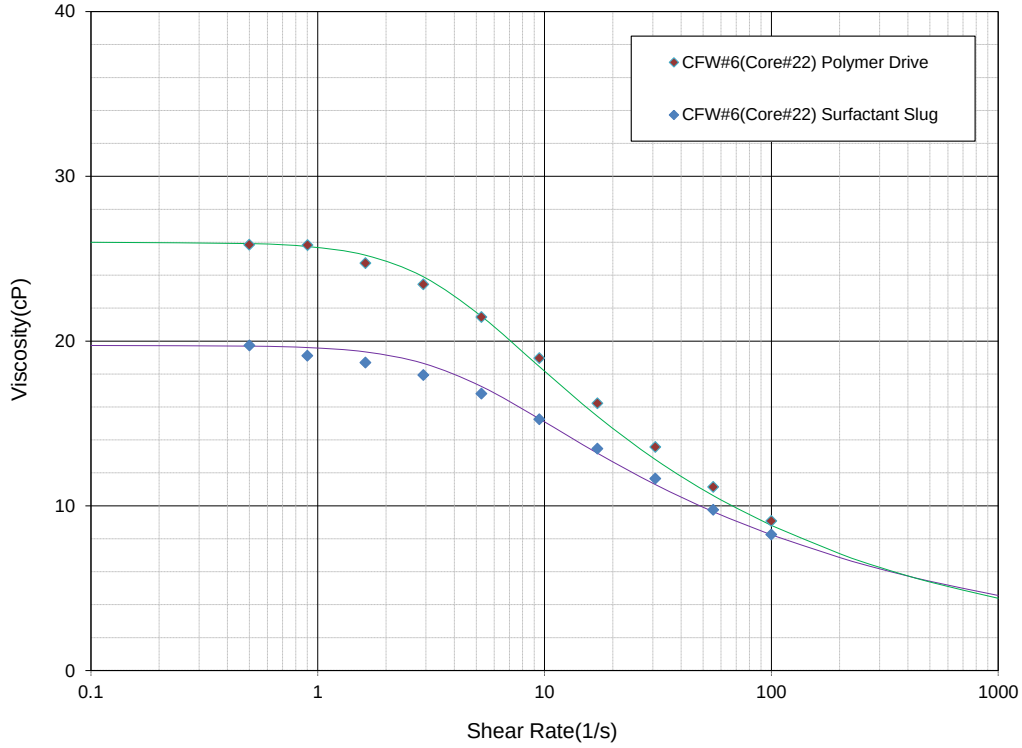

Figure 5.77 CFW#6(Core#22) viscosity of surfactant slug and polymer drive at 43 ℃

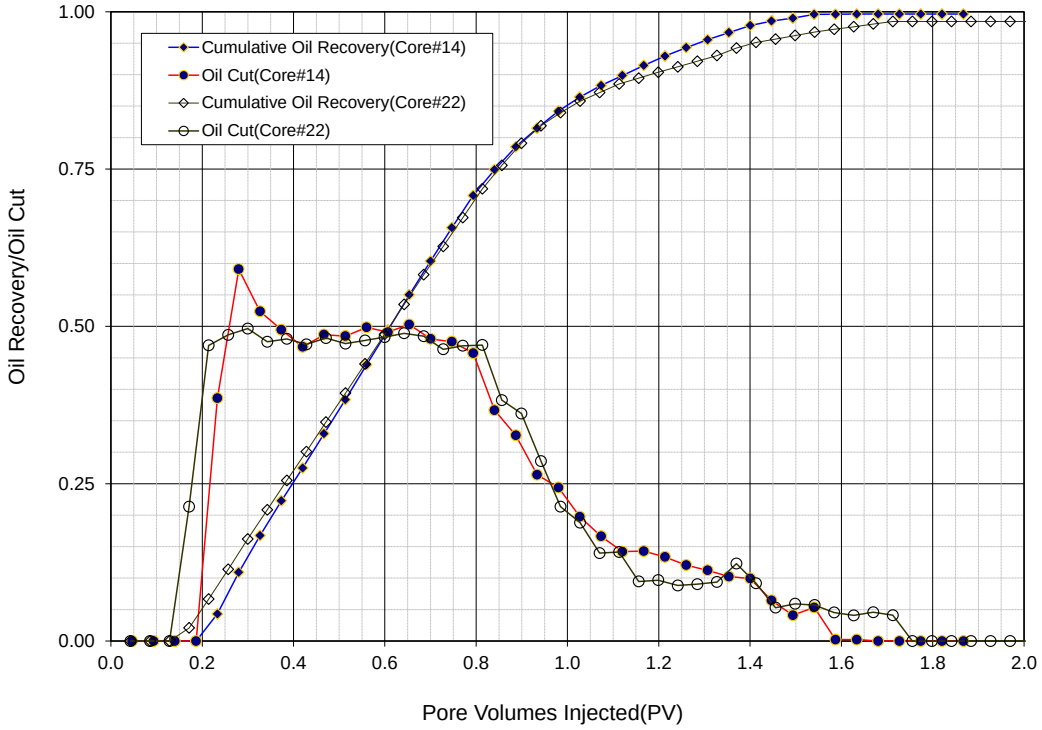

Figure 5.78 CFW#6(Core#22) oil recovery comparison with CFW#4 (Core#14)

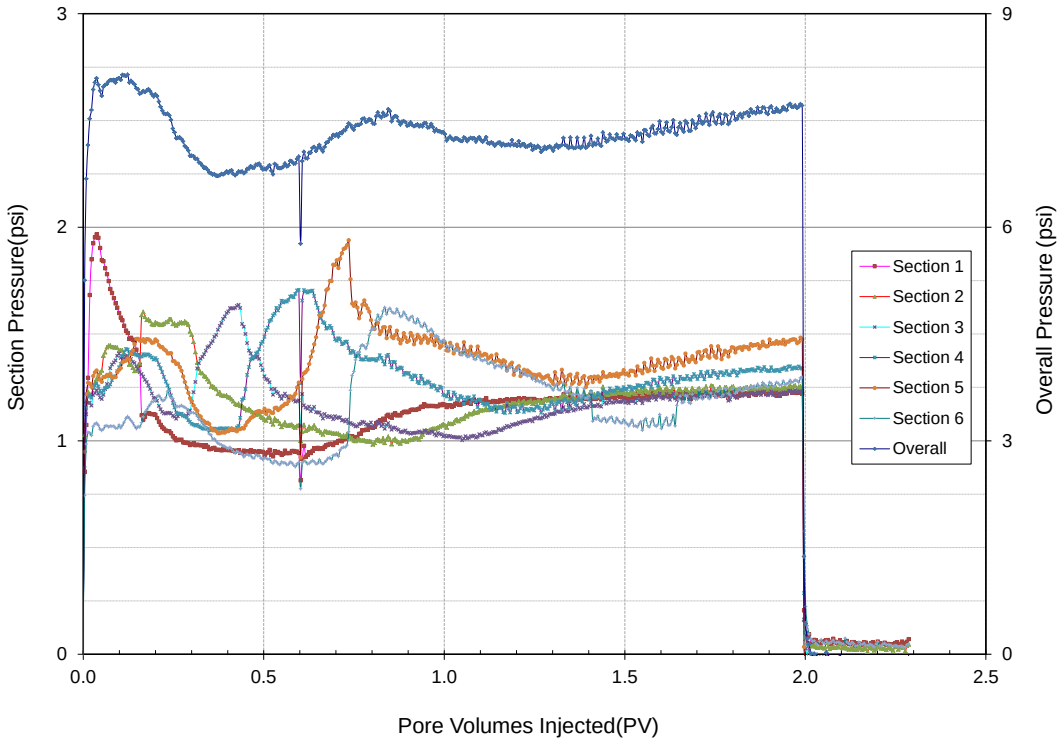

Figure 5.79 CFW#6(Core#22) pressure profile during chemical flood at 43 ℃

Vial #	1	2	3	4	5	6	7	8	9	10
PV	0.043	0.086	0.128	0.171	0.214	0.257	0.300	0.343	0.385	0.428

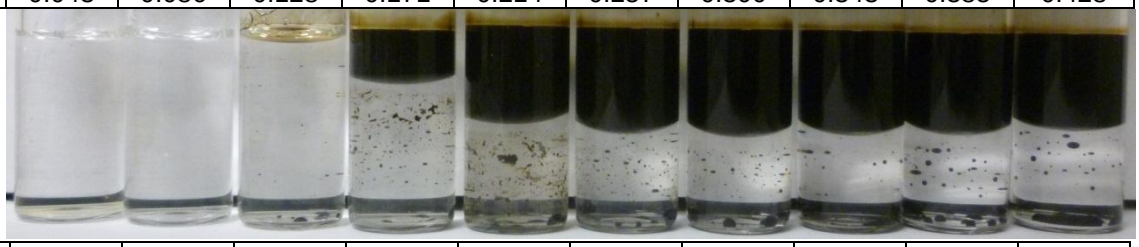

Vial #	11	12	13	14	15	16	17	18	19	20
PV	0.471	0.514	0.557	0.599	0.642	0.685	0.728	0.771	0.814	0.856

Vial #	21	22	23	24	25	26	27	28	29	30
PV	0.899	0.942	0.985	1.028	1.070	1.113	1.156	1.199	1.242	1.284

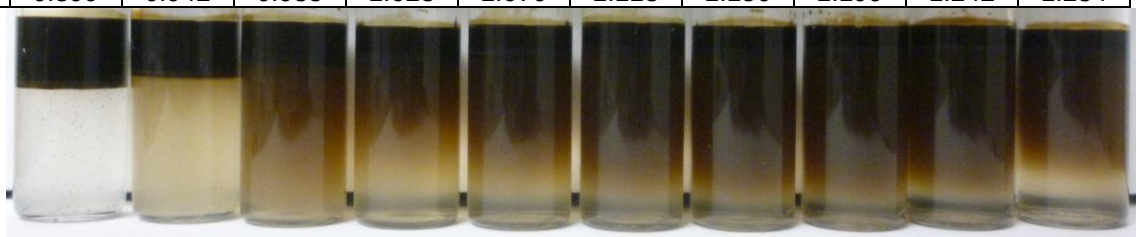

Vial #	31	32	33	34	35	36	37	38	39	40
PV	1.327	1.370	1.413	1.456	1.499	1.541	1.584	1.627	1.670	1.713

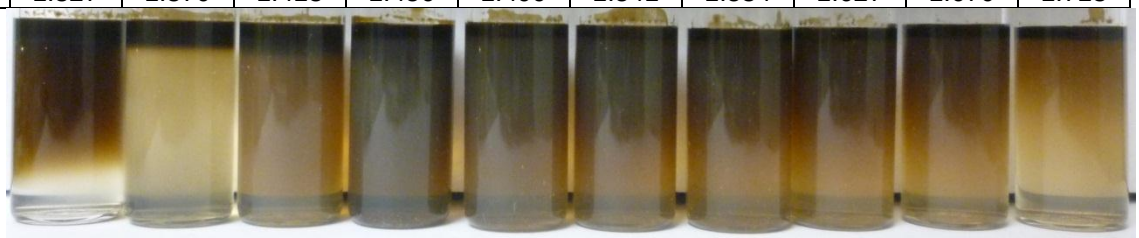

Vial #	41	42	43	44	45	46	47	38	39	40
PV	1.755	1.798	1.841	1.884	1.927	1.970	2.012	1.627	1.670	1.713

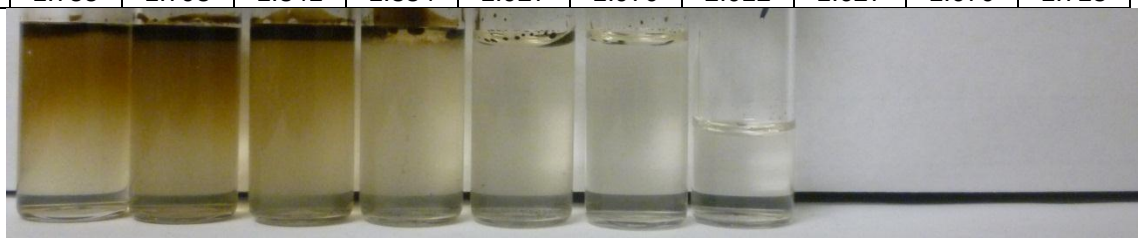

Figure 5.80 Photos of CFW#6 (Core#22) flood effluent vials equilibration at reservoir temperature 43 ℃ for 2 days

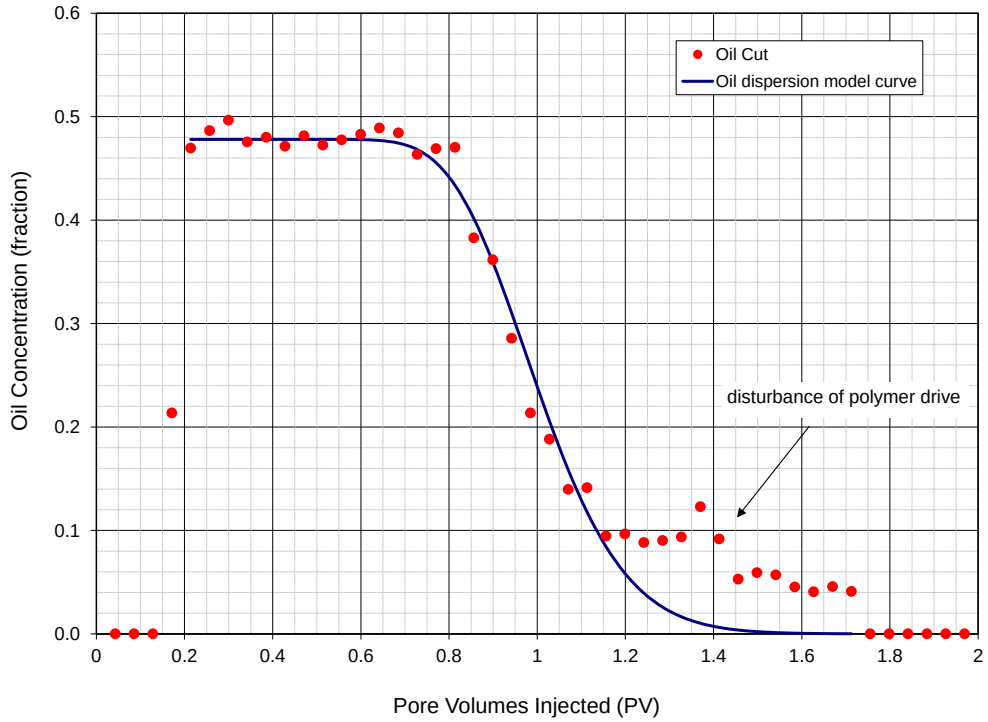

Figure 5.81 CFW#6(Core#22) oil cut dispersion model

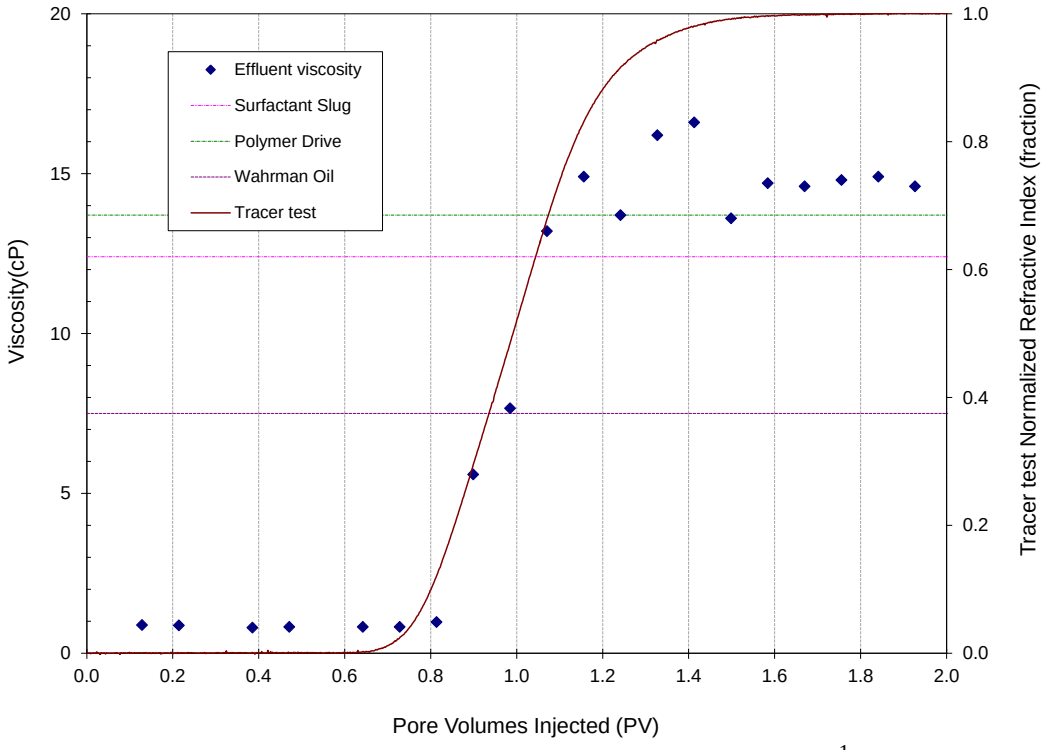

Figure 5.82 CFW#6 (Core#22) chemical flood effluent viscosity (at 30 s^{-1}) profile at 43 ℃

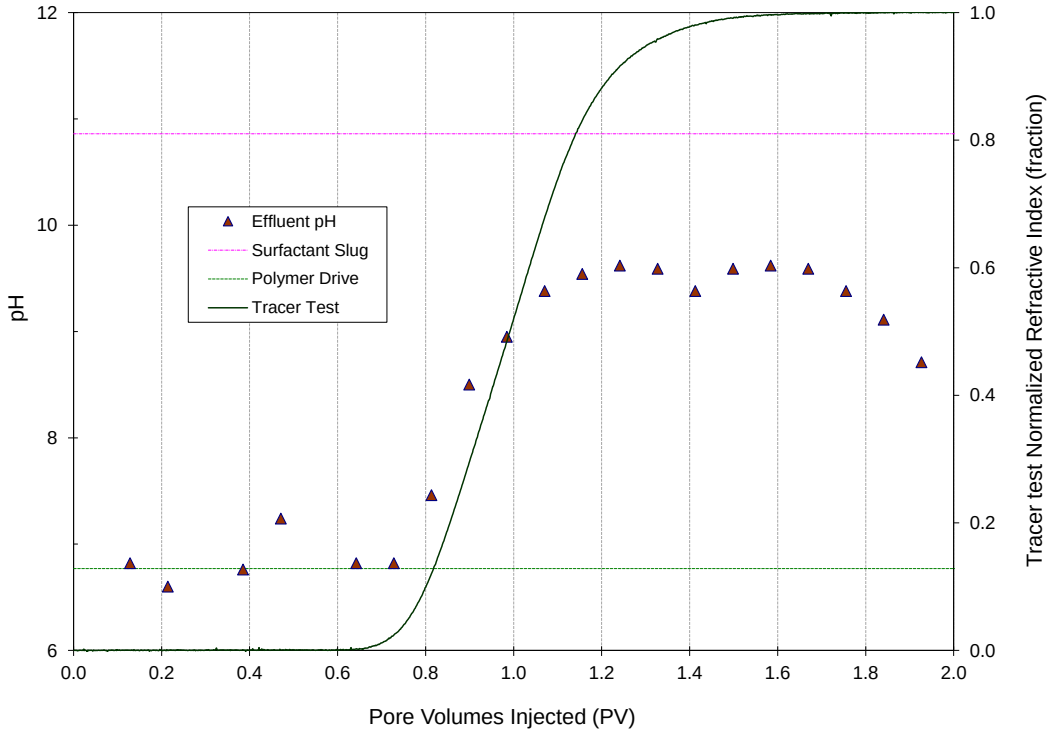

Figure 5.83 CDW#6 (Core#22) chemical flood effluent pH profile

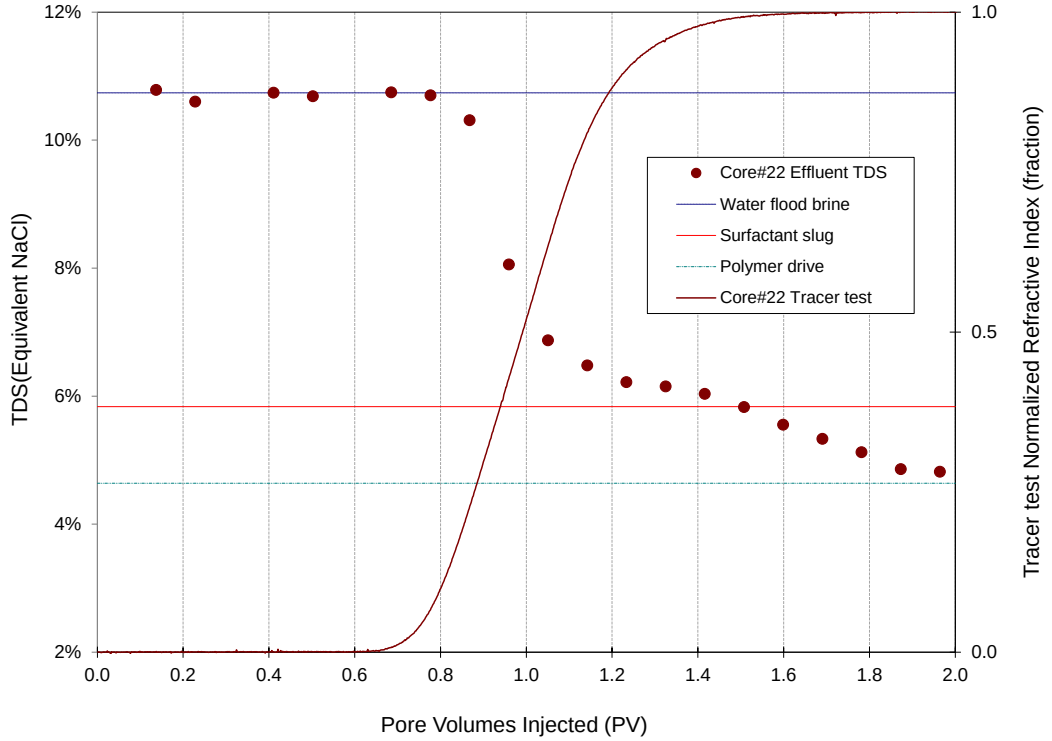

Figure 5.84 CFW#6 (Core#22) chemical flood effluent TDS profile

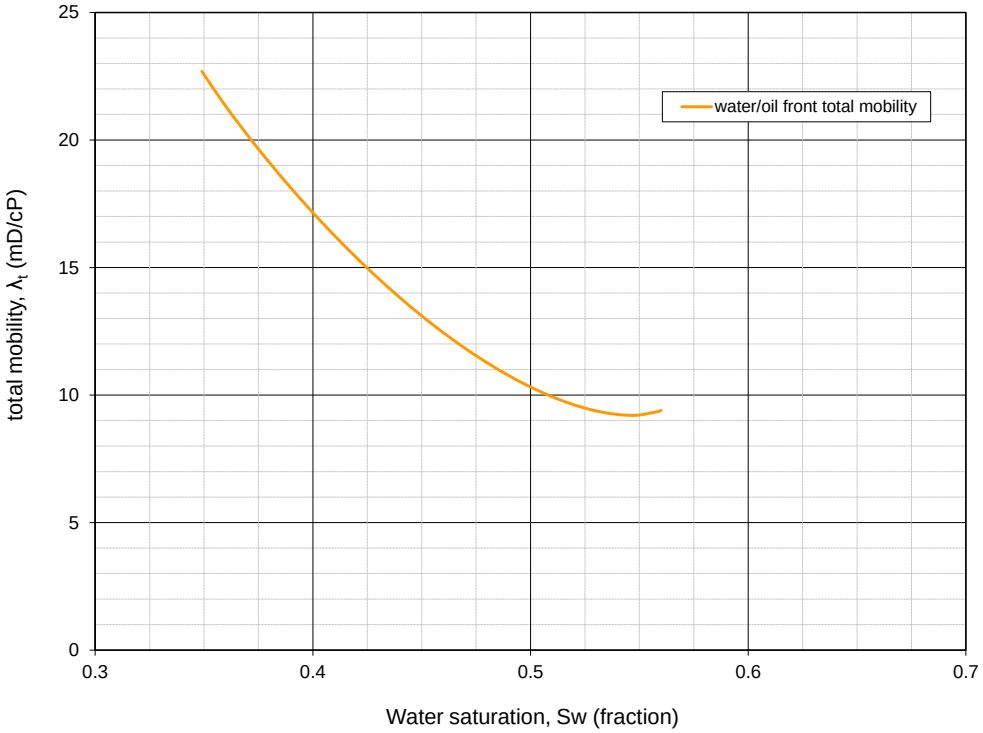

Figure 5.85 CFW#6 (Core#22) mobility design with model proposed by Gogarty (1968)

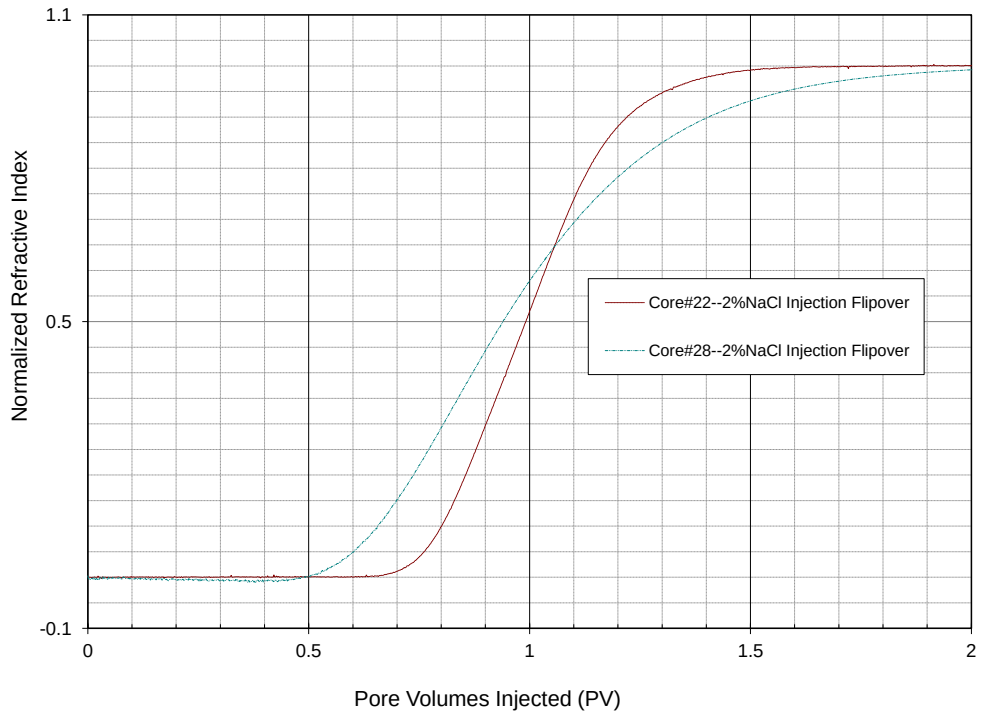

Figure 5.86 CFW#7 (Core#28) and CFW#6 (Core#22) tracer test results comparison

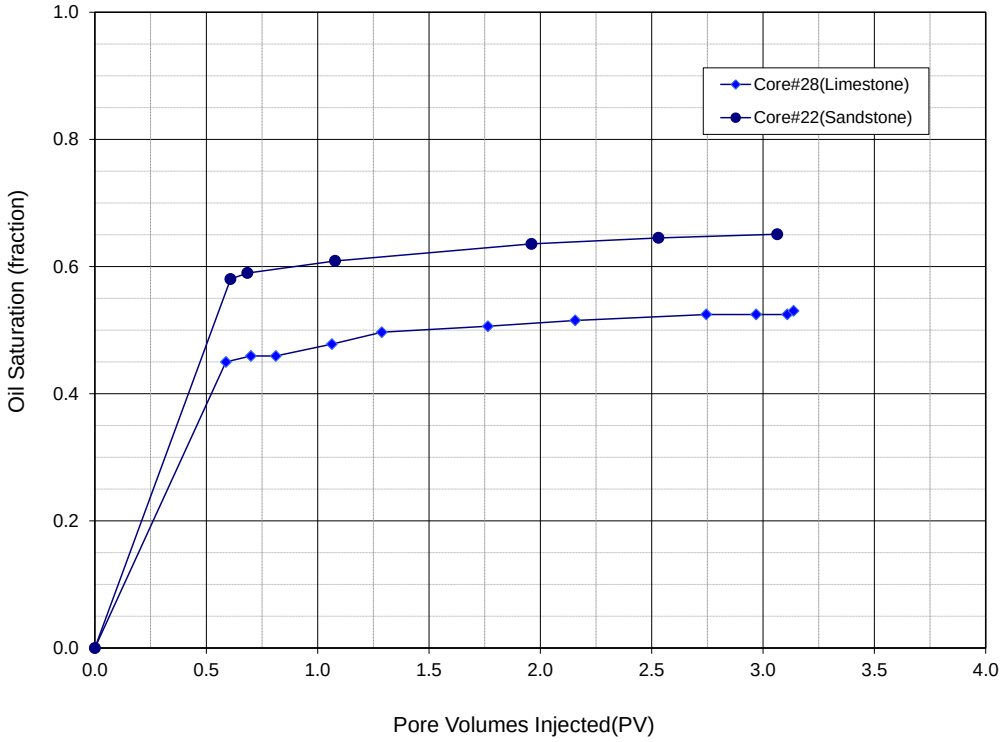

Figure 5.87 CFW#7(Core#28) oil saturation during oil flood at 43 ℃ comparing to CFW#6(Core#22)

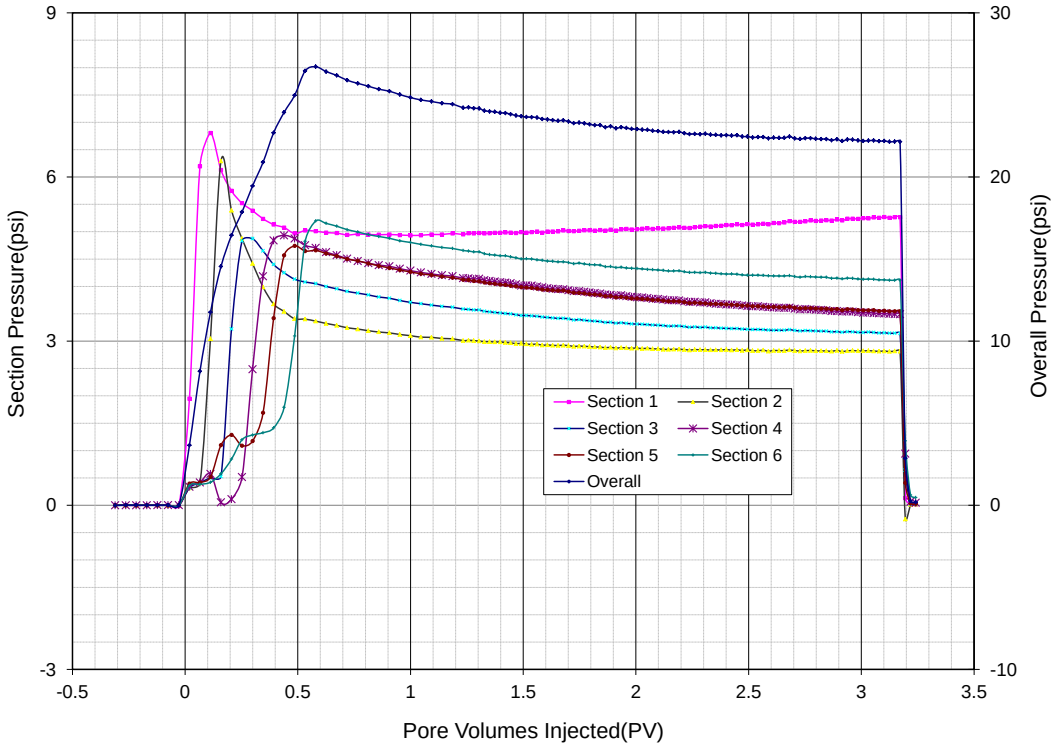

Figure 5.88 CFW#7(Core#28) pressure profile during oil flood at 43 ℃

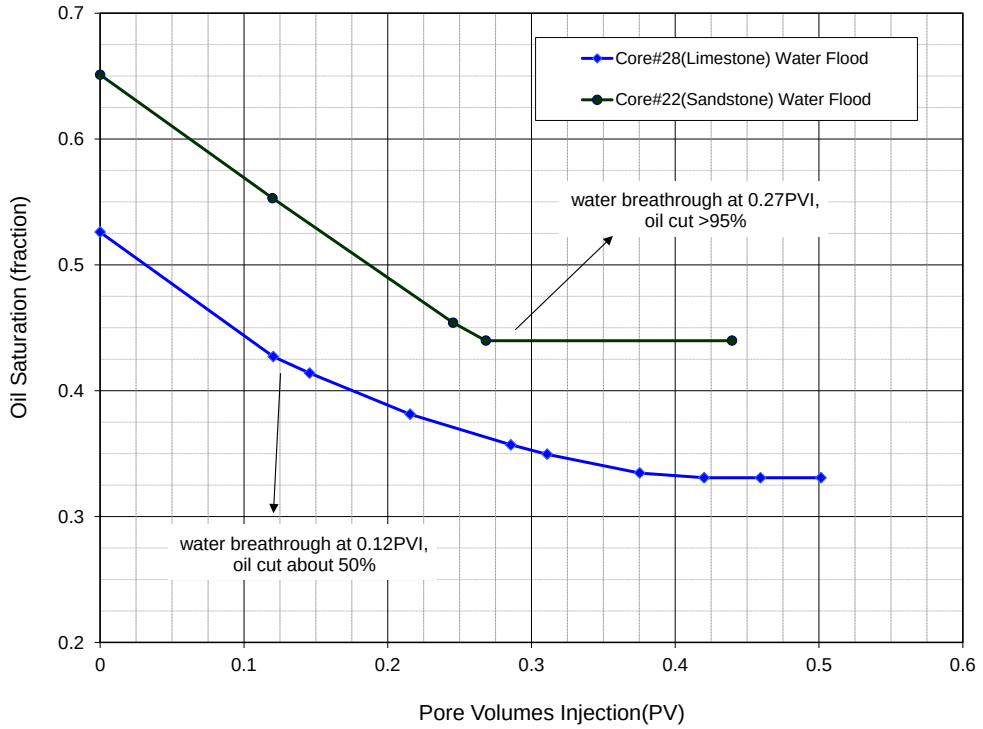

Figure 5.89 CFW#7 (Core#28) oil saturation during water flood at 43 ℃

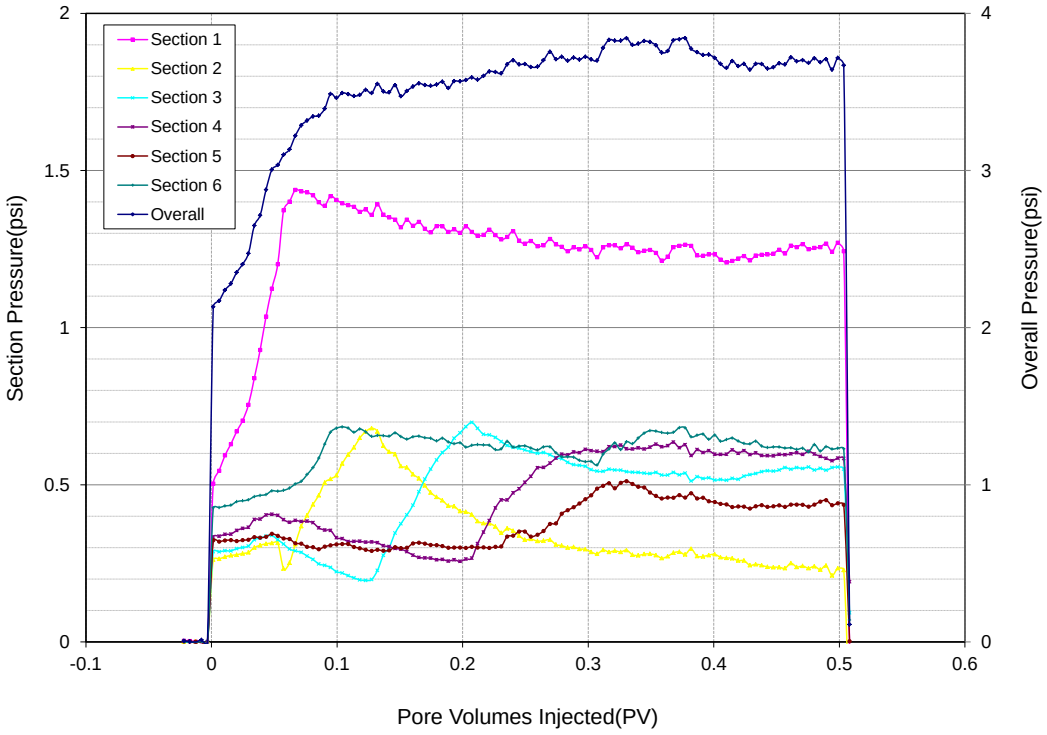

Figure 5.90 CFW#7 (Core#28) differential pressure during water flood at 43 ℃

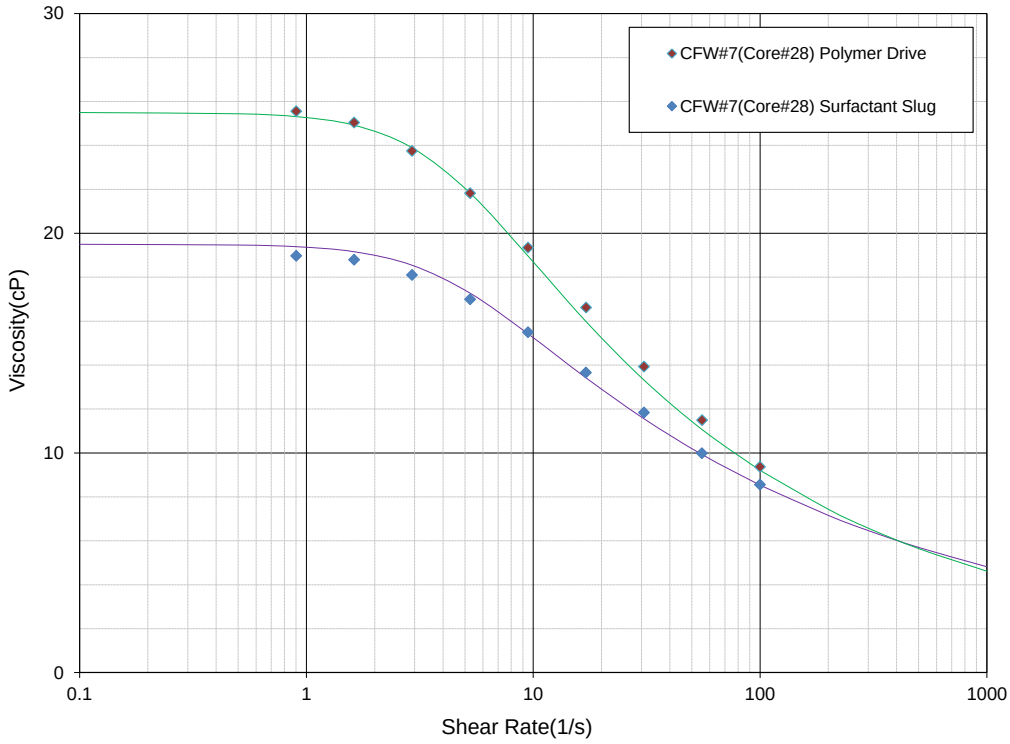

Figure 5.91 CFW#7(Core#28) rheology of surfactant slug and polymer drive at 43 ℃

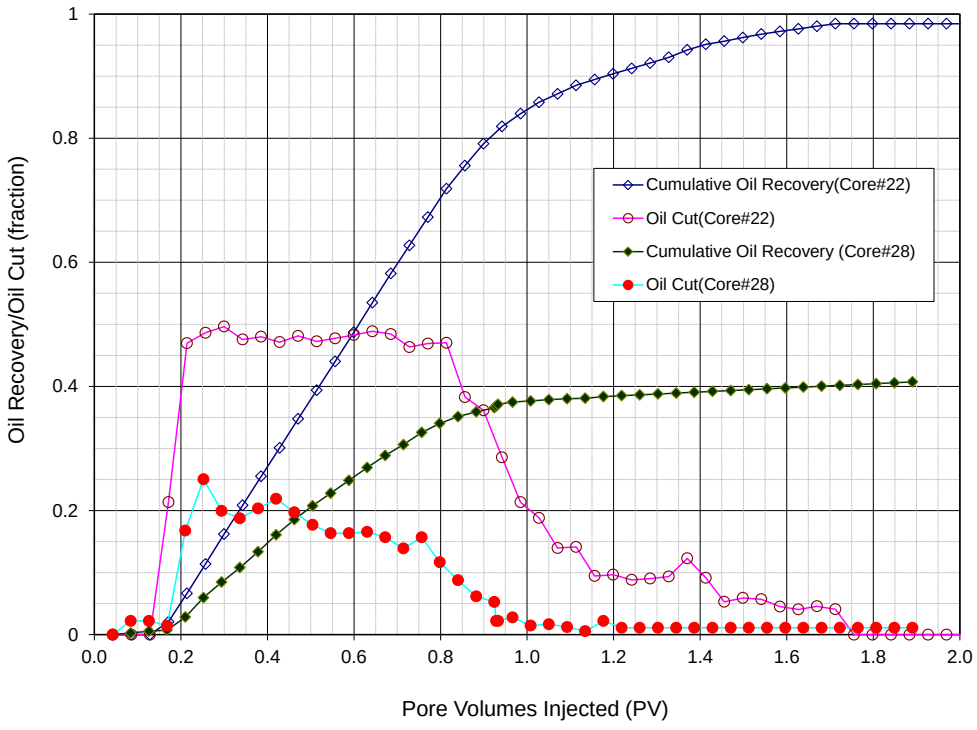

Figure 5.92 CFW#7 (Core#28) oil recovery comparing to CFW#6 (Core#22)

Vial #	1	2	3	4	5	6	7	8	9	10
PV	0.042	0.084	0.126	0.168	0.210	0.252	0.294	0.336	0.378	0.420

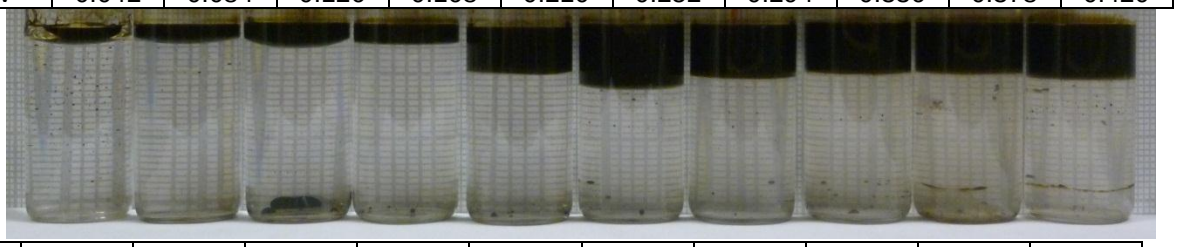

Vial #	11	12	13	14	15	16	17	18	19	20
PV	0.462	0.504	0.546	0.588	0.630	0.672	0.714	0.756	0.798	0.840

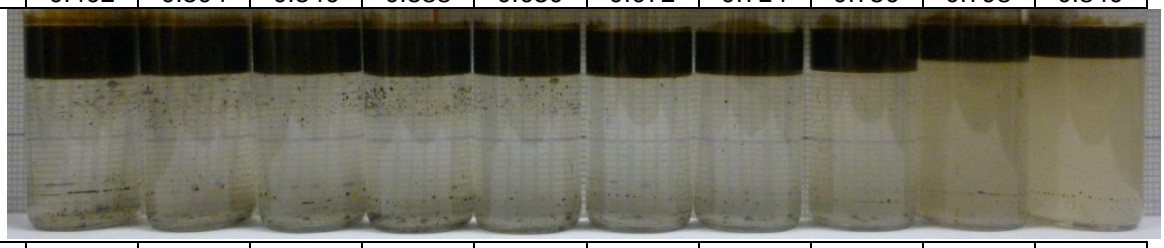

Vial #	21	22	23	24	25	26	27	28	29	30
PV	0.882	0.924	0.929	0.933	0.966	1.008	1.050	1.092	1.134	1.176

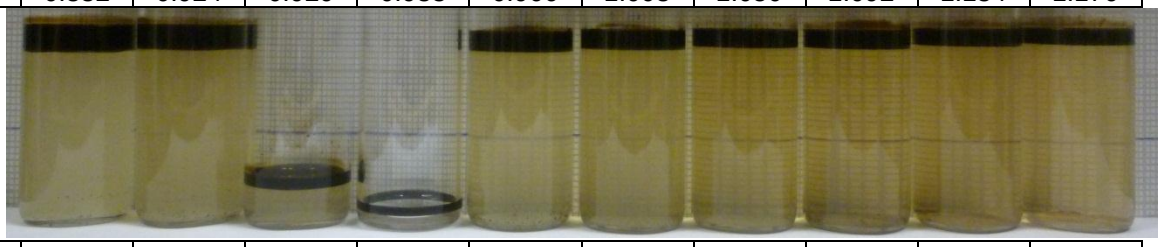

Vial #	31	32	33	34	35	36	37	38	39	40
PV	1.218	1.261	1.303	1.345	1.387	1.429	1.471	1.513	1.555	1.597

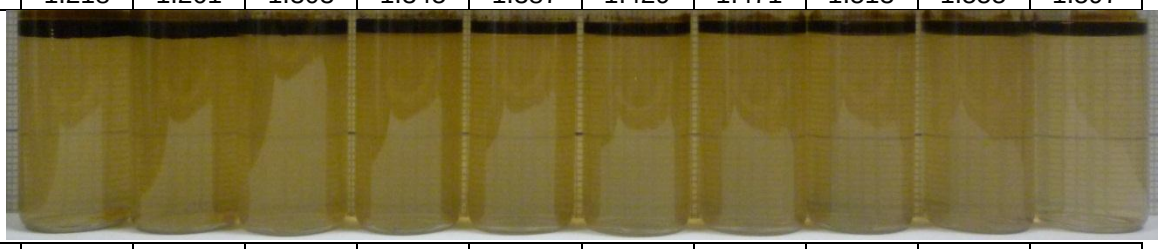

Vial #	41	42	43	44	45	46	47	48	49	50
PV	1.639	1.681	1.723	1.765	1.807	1.849	1.891	1.933	1.975	2.017

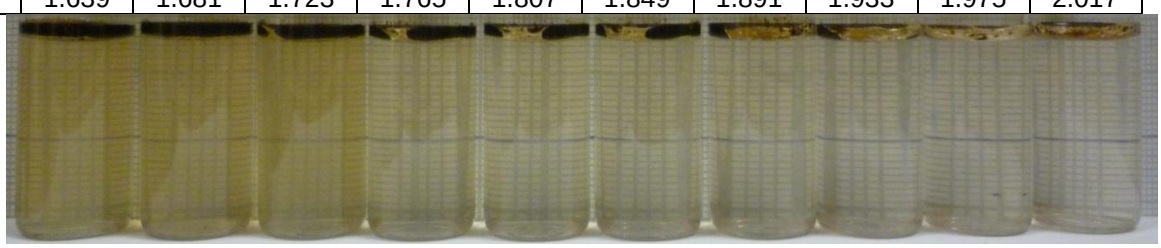

Figure 5.93 Photos of CFW#7 (Core#28) flood effluent vials after 4 days of equilibration at reservoir temp (43 ℃) and 1 day at room temperature (~23 ℃)

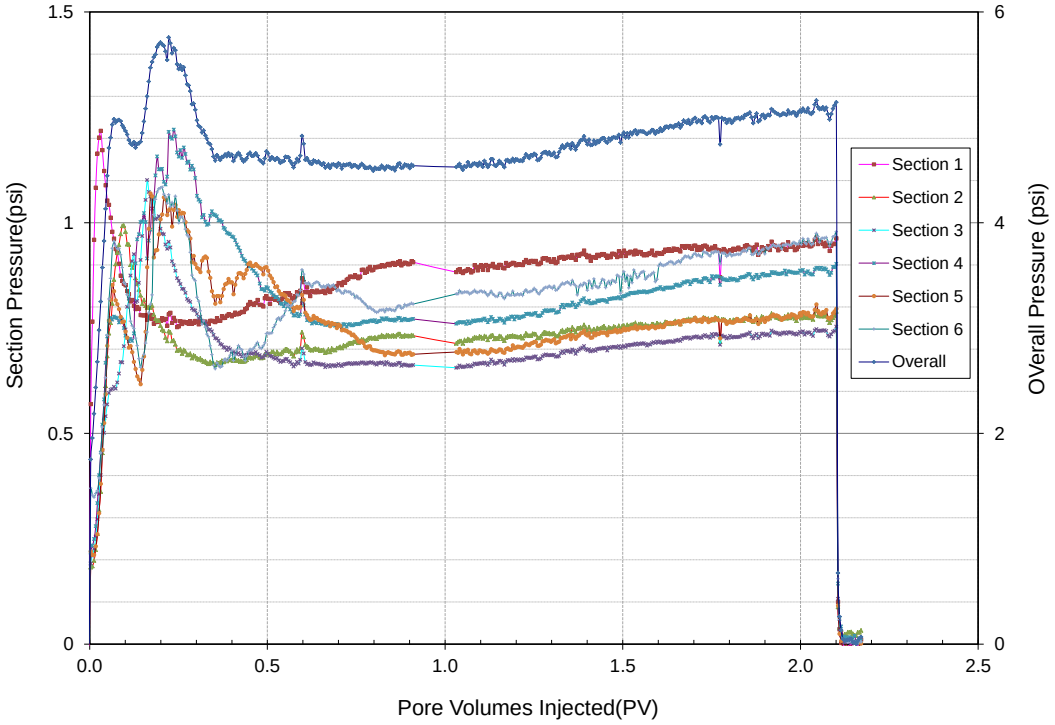

Figure 5.94 CFW#7(Core#28) pressure profile during chemical flood at 43 ℃

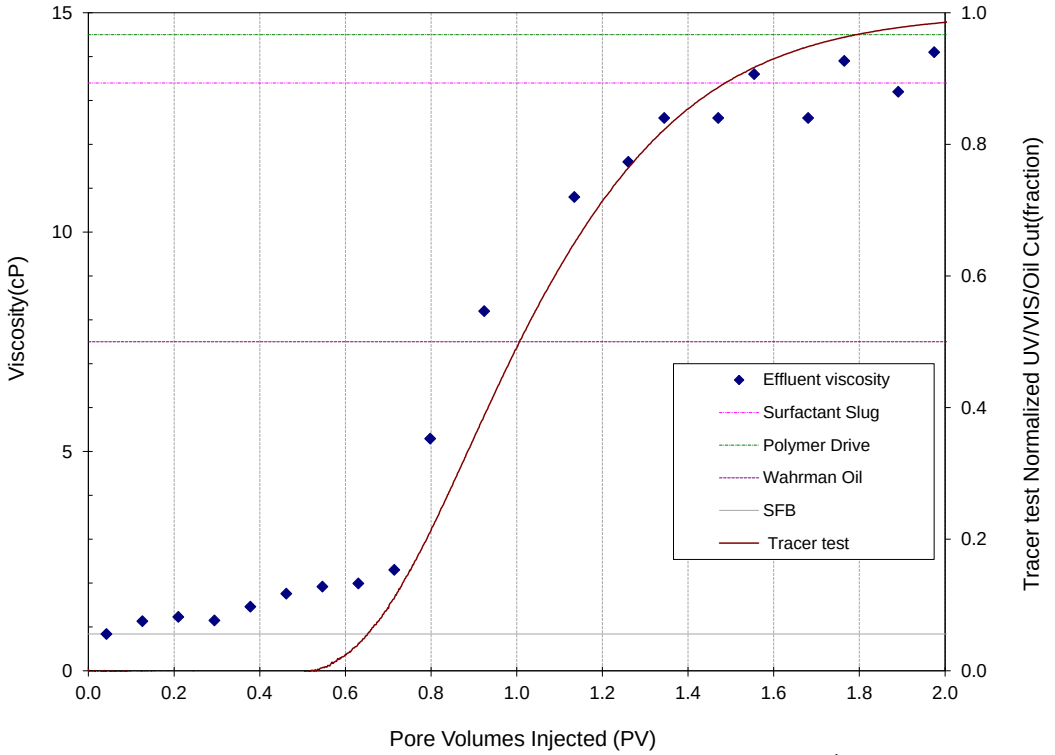

Figure 5.95 CFW#7(Core#28) chemical flood effluent viscosity (at 30 s^{-1}) at 43 ℃ profile comparing to CFW#6(Core#22)

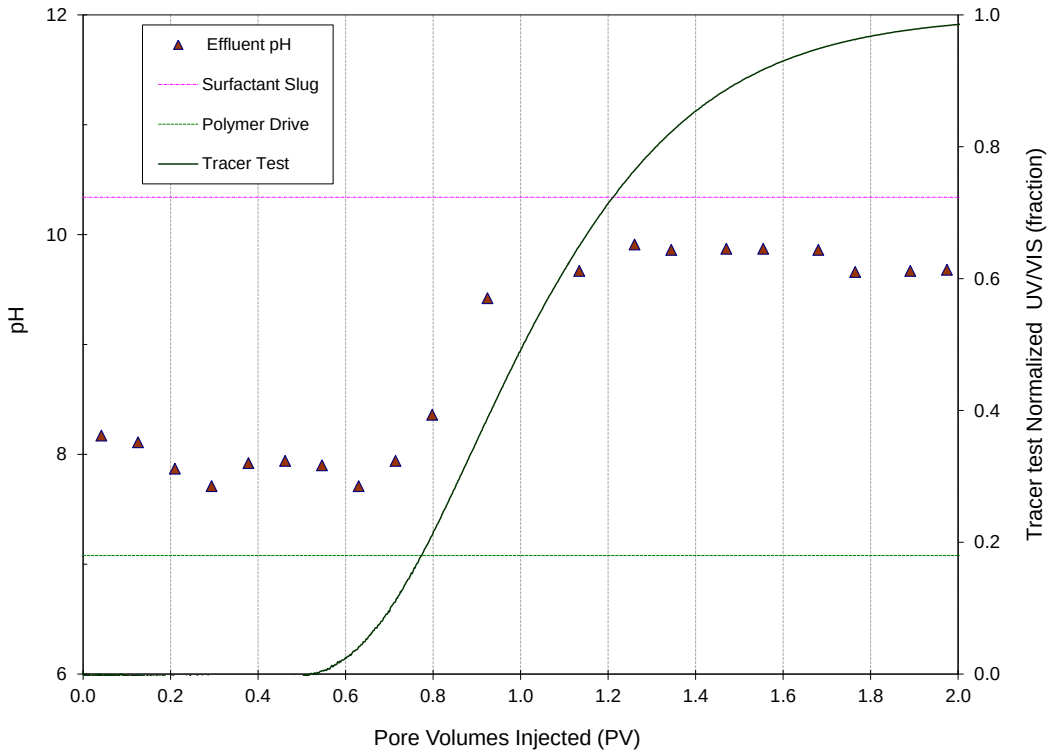

Figure 5.96 CFW#7(Core#28) chemical flood effluent pH profile comparing to CFW#6(Core#22)

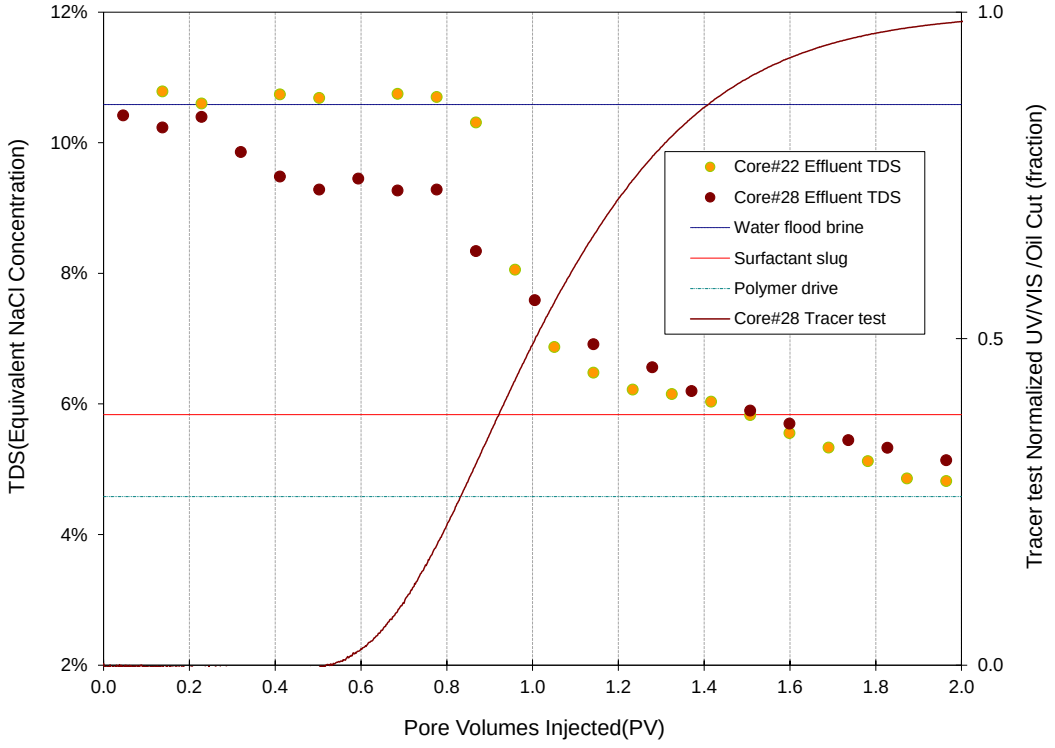

Figure 5.97 CFW#7(Core#28) chemical flood effluent TDS comparing to CFW#6 (Core#22)

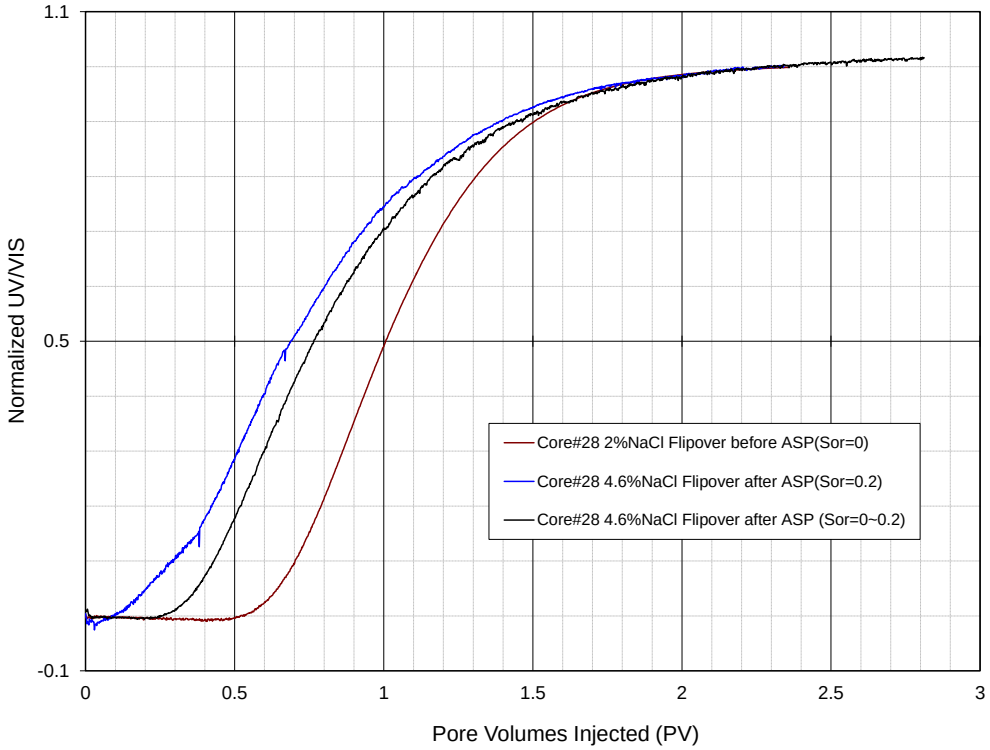

Figure 5.98 CFW#7 (Core#28) tracer test before and after chemical flood

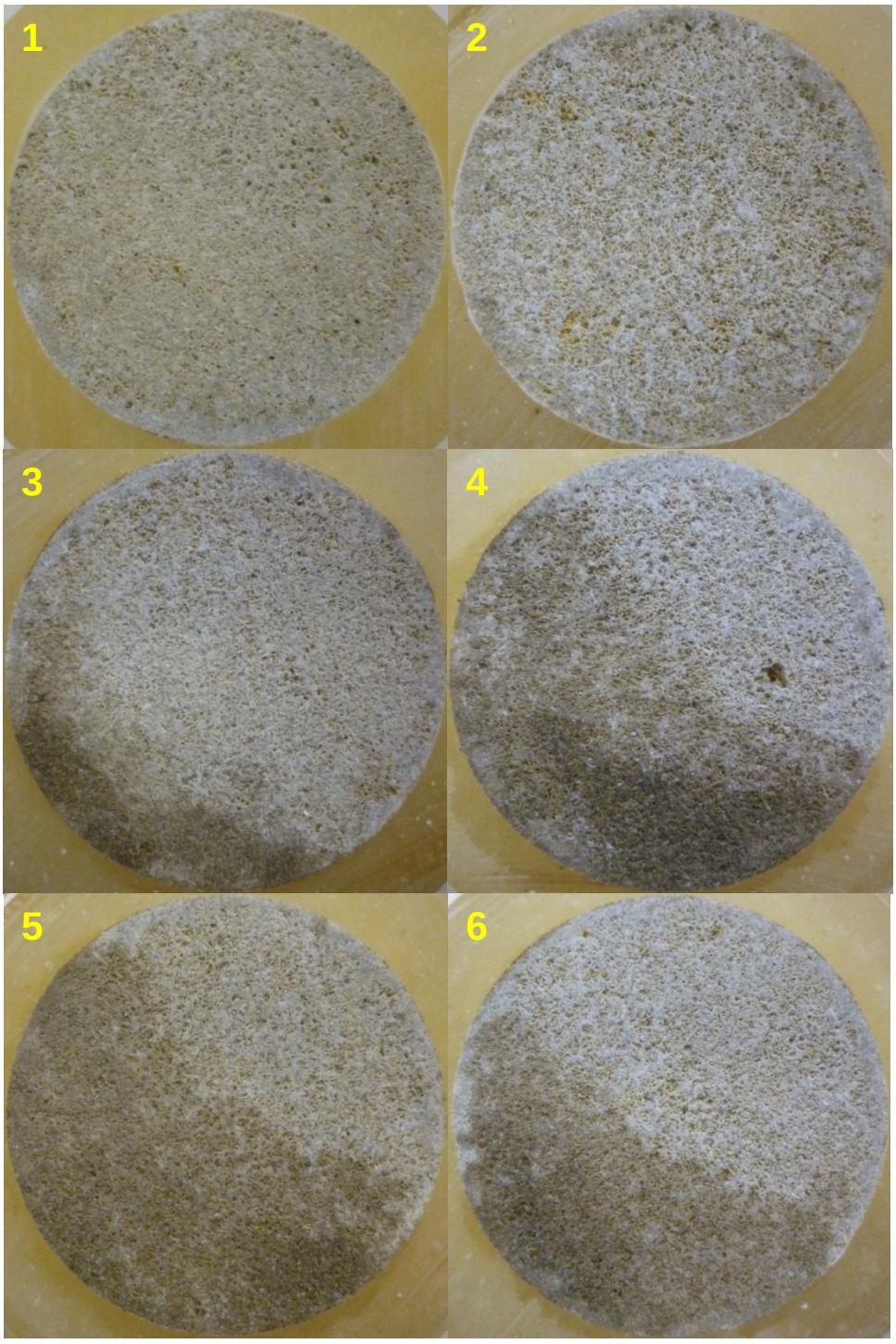

Figure 5.99 Core#28 cross sections after chemical flood

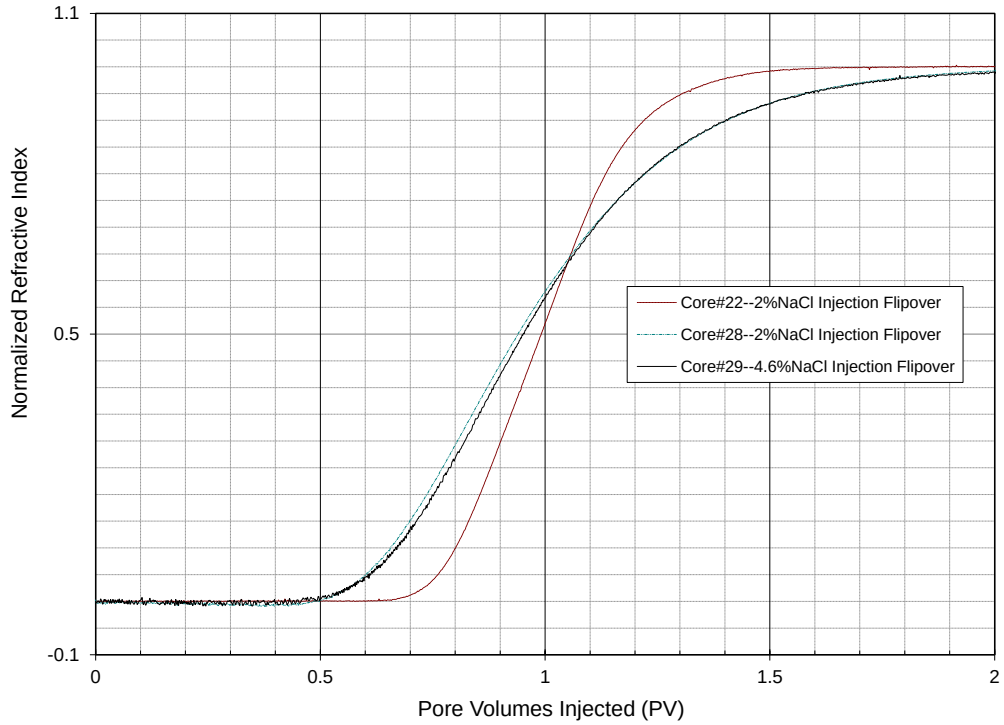

Figure 5.100 CFW#8 (Core#29), CFW#7 (Core#22) and CFW#6(Core#22) tracer test results comparison

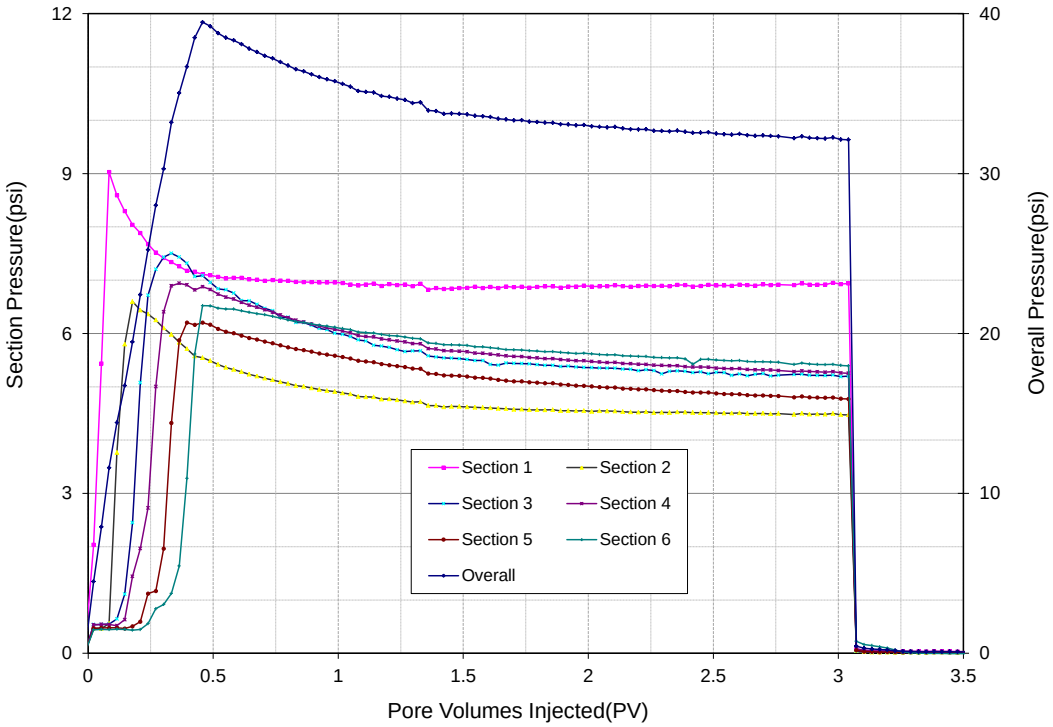

Figure 5.101 CFW#8 (Core#29) pressure profile during first oil flood at 43 ℃

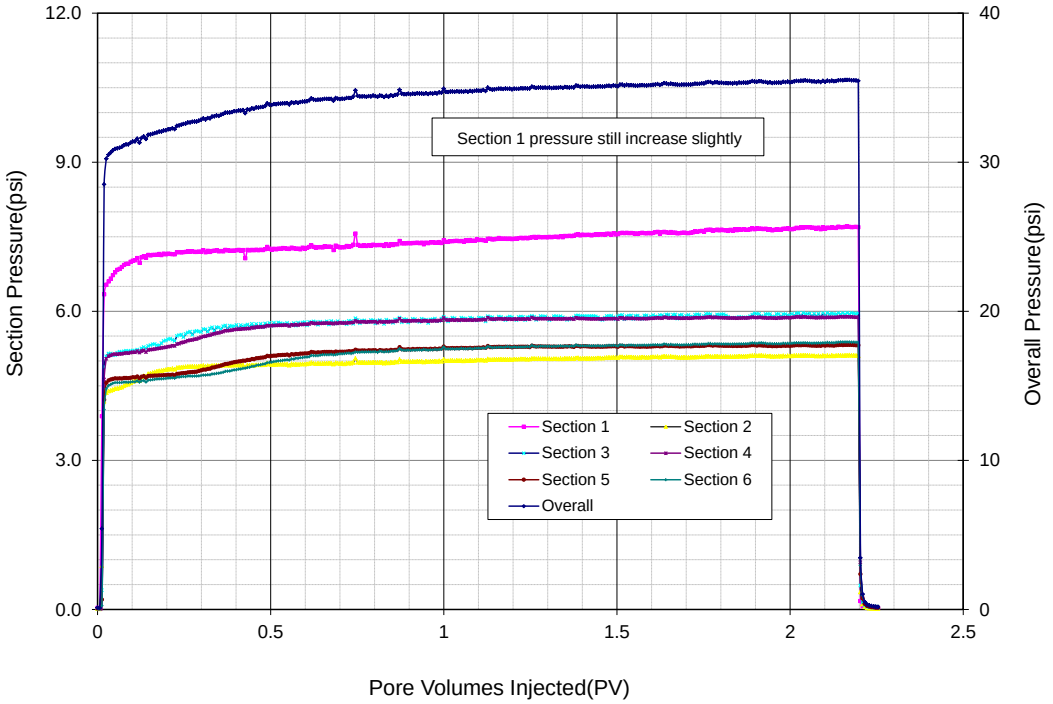

Figure 5.102 CFW#8 (Core#29) pressure profile during second oil flood at 43 ℃

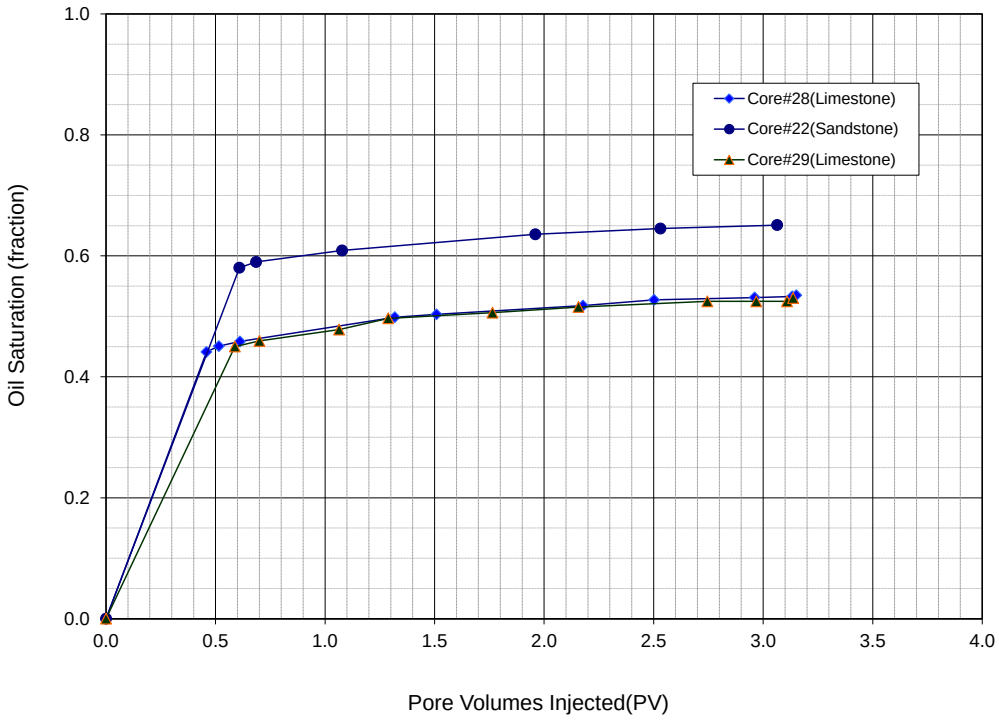

Figure 5.103 CFW#8 (Core#29) oil saturation during oil flood at 43 ℃

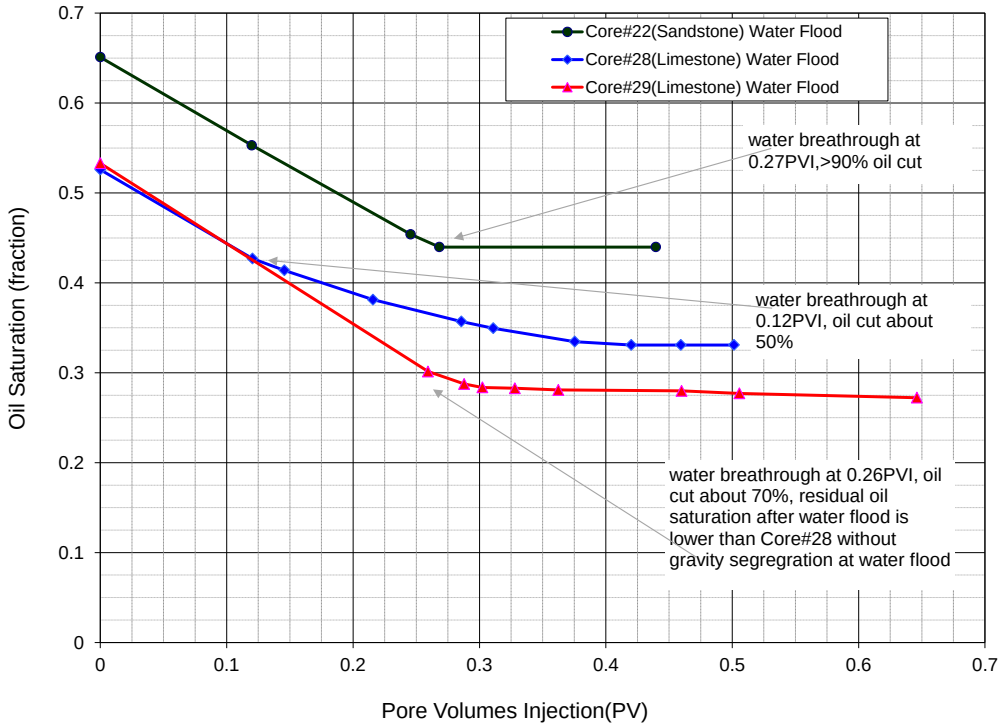

Figure 5.104 CFW#8(Core#29) oil saturation during water flood at 43 ℃

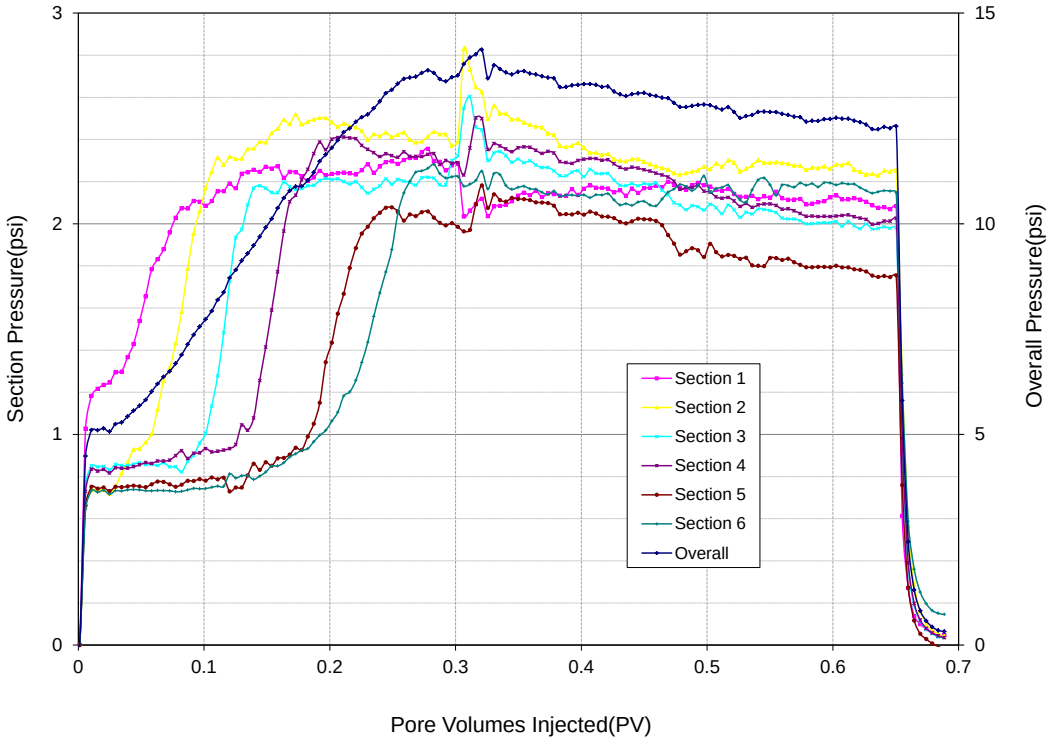

Figure 5.105 CFW#8(Core#29) pressure profile during water flood at 43 ℃

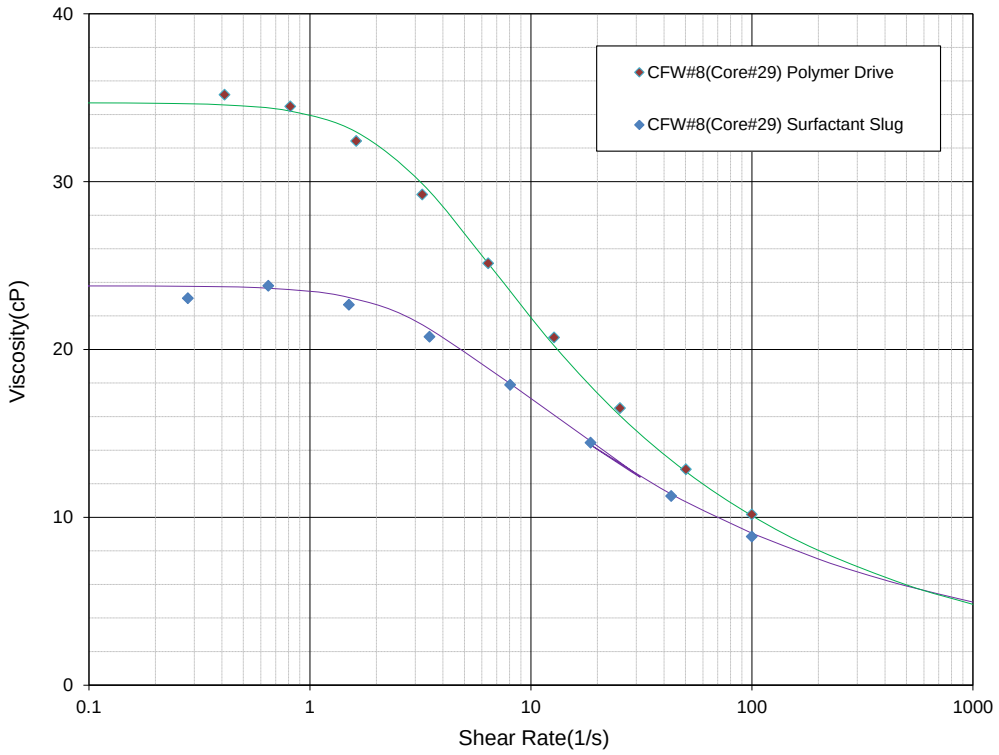

Figure 5.106 CFW#8(Core#29) rheology of surfactant slug and polymer drive at 43 ℃

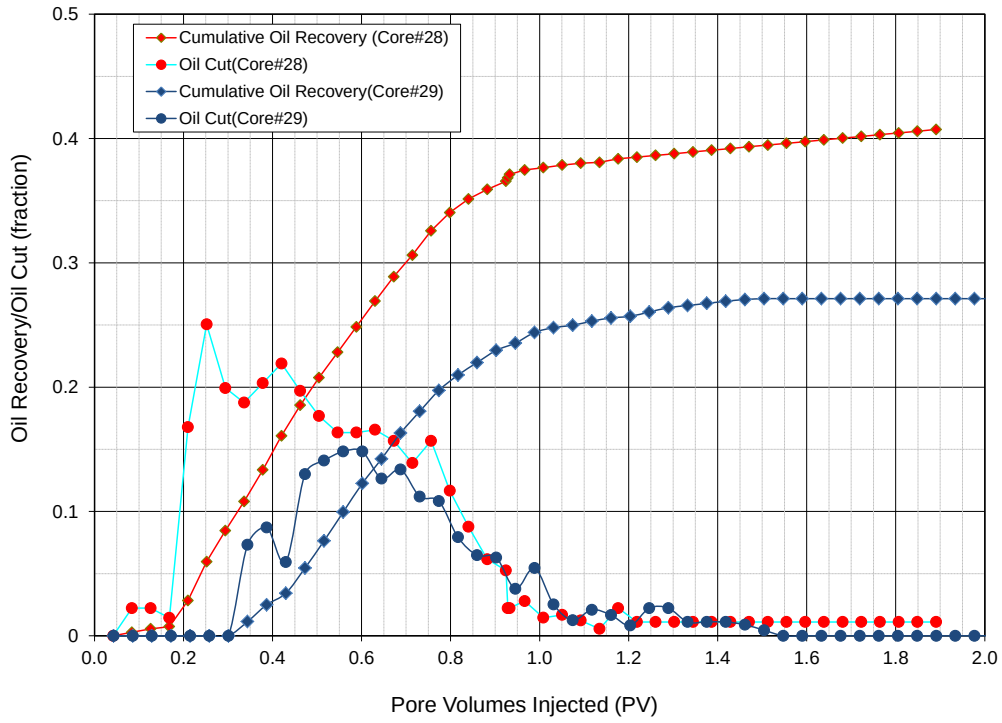

Figure 5.107 CFW#8(Core#29) oil recovery comparing to CFW#7 (Core#28)

Vial #	1	2	3	4	5	6	7	8	9	10
PV	0.043	0.086	0.129	0.172	0.215	0.258	0.301	0.344	0.387	0.430

Vial #	11	12	13	14	15	16	17	18	19	20
PV	0.473	0.516	0.559	0.602	0.645	0.688	0.731	0.774	0.817	0.860

Vial #	21	22	23	24	25	26	27	28	29	30
PV	0.903	0.946	0.989	1.032	1.074	1.117	1.160	1.203	1.246	1.289

Vial #	31	32	33	34	35	36	37	38	39	40
PV	1.332	1.375	1.418	1.461	1.504	1.547	1.590	1.633	1.676	1.719

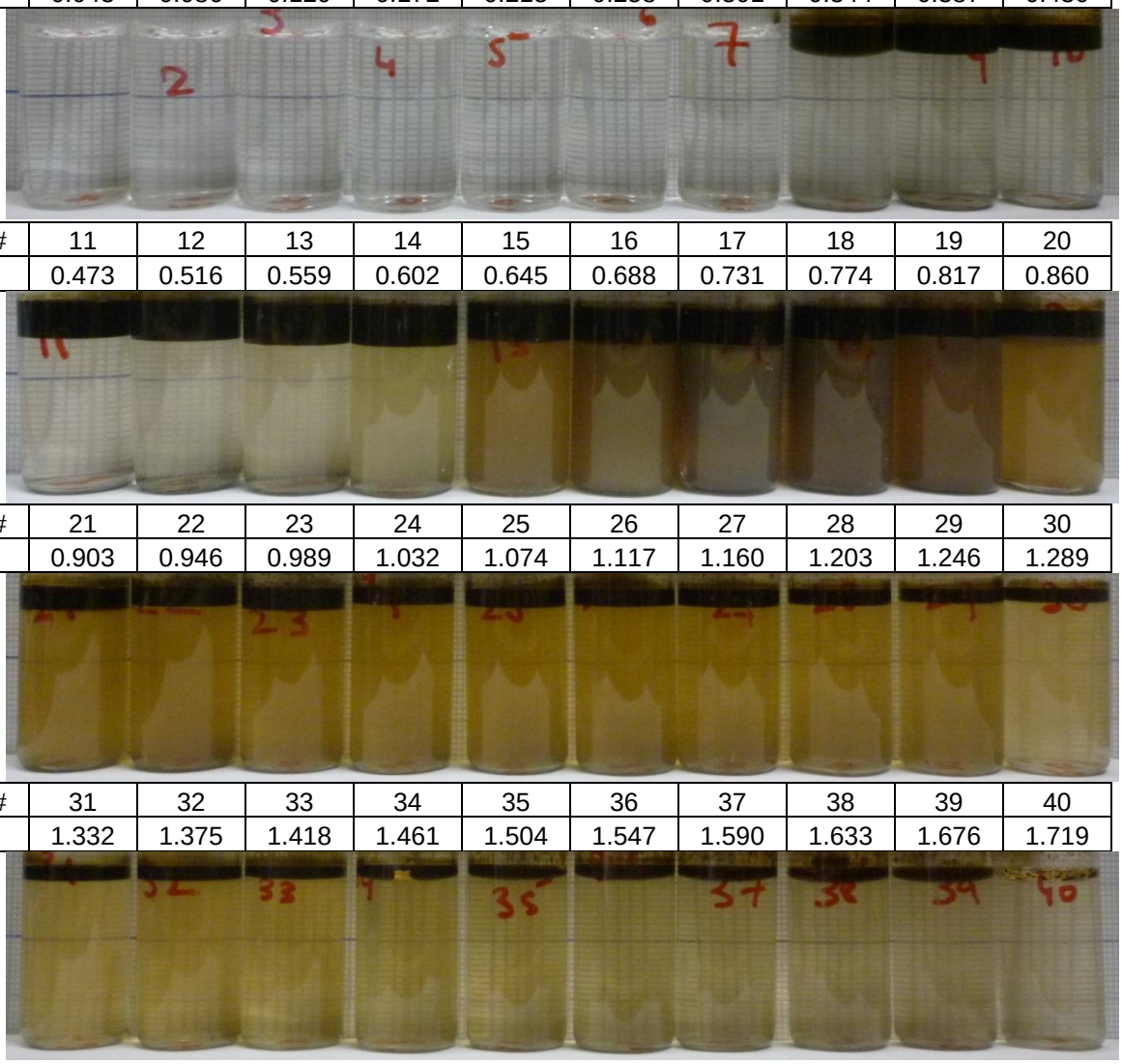

Figure 5.108 Photos of CFW#8(Core#29) effluent vials after 1 days of equilibration at reservoir temp (43 ℃).

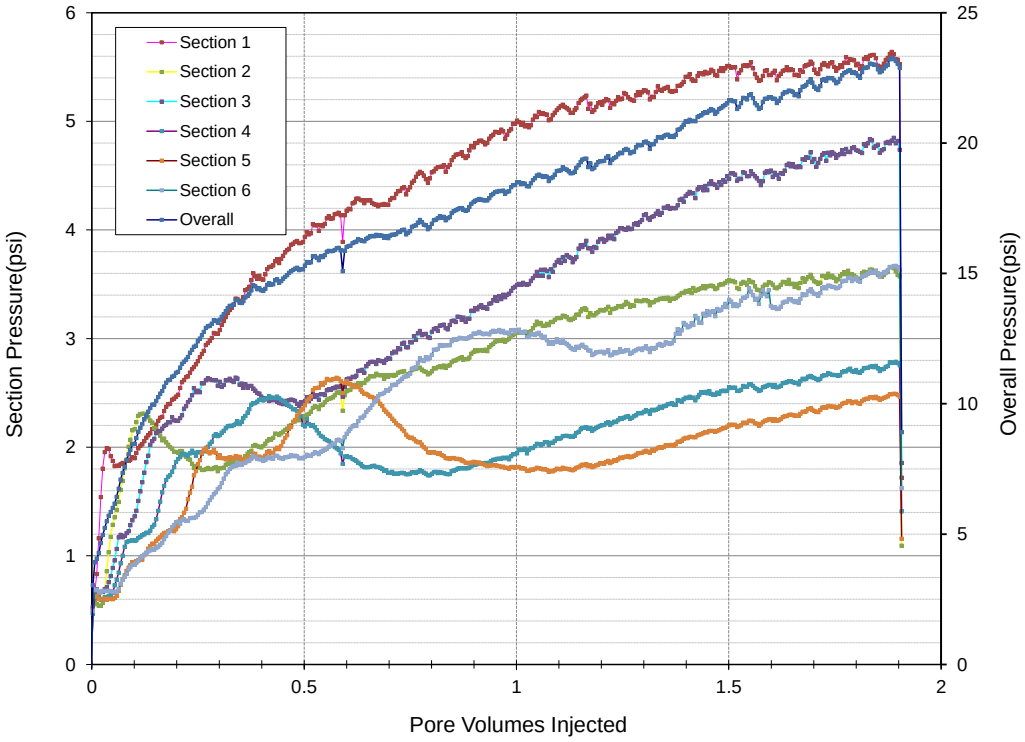

Figure 5.109 CFW#8(Core#29) pressure profile during chemical flood at 43 ℃

Figure 5.110 Core#29 cross sections after chemical flood

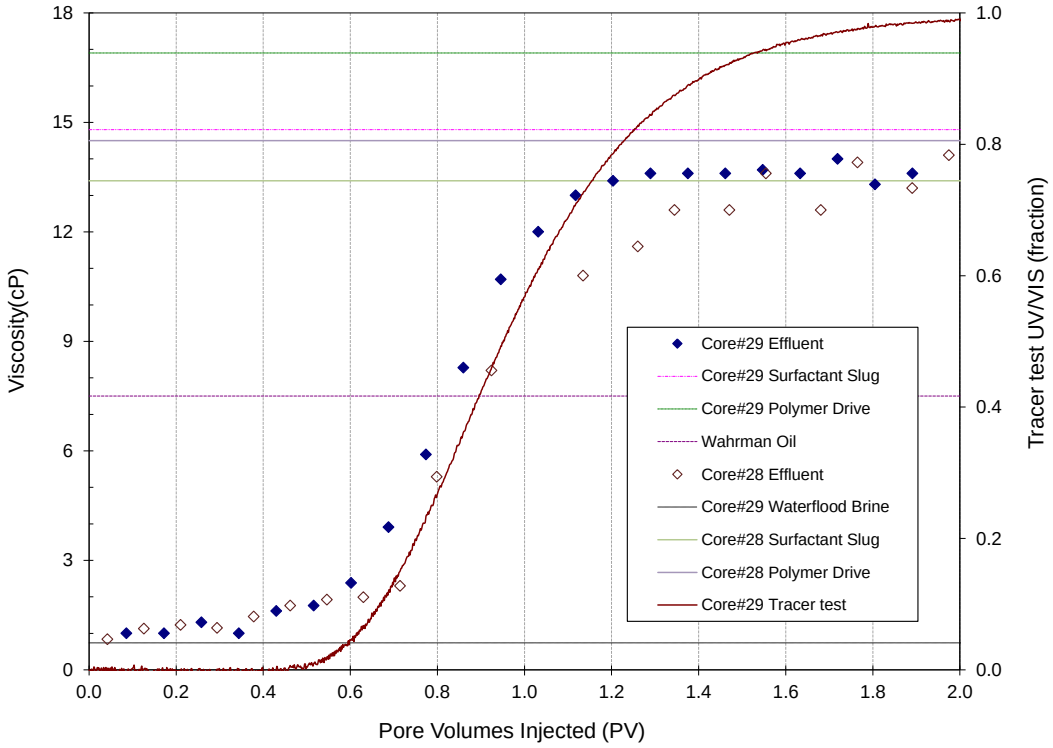

Figure 5.111 CFW#8(Core#29) chemical flood effluent viscosity (30 s^{-1}) profile comparing to viscosity profile of CFW#7(Core#28) at 43 ℃

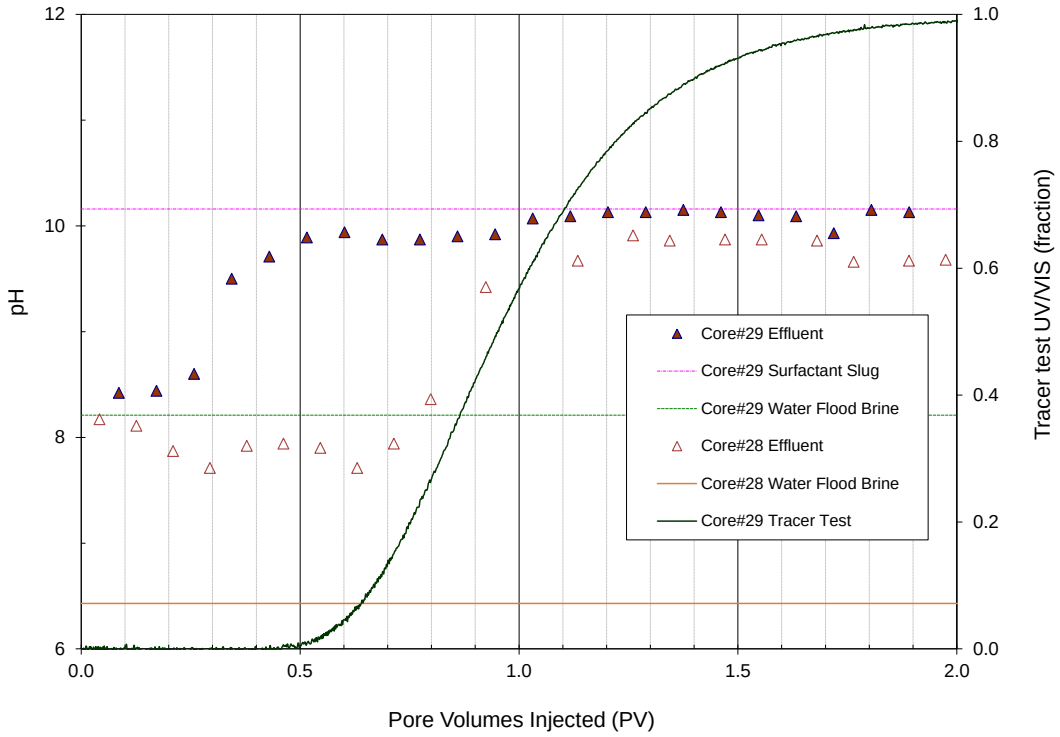

Figure 5.112 CFW#8(Core#29) chemical flood effluent pH profile comparing to pH profile of CFW#7(Core#28)

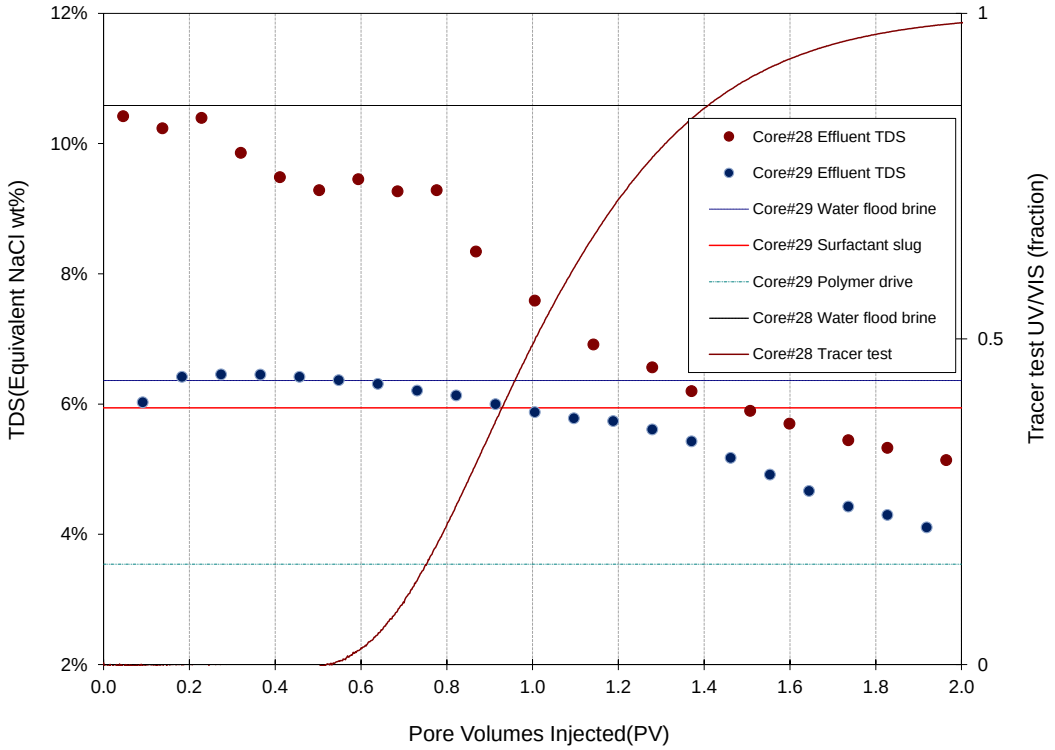

Figure 5.113 CFW#8 (Core#29) chemical flood effluent TDS profile comparing to TDS profile of CFW#7(Core#28)

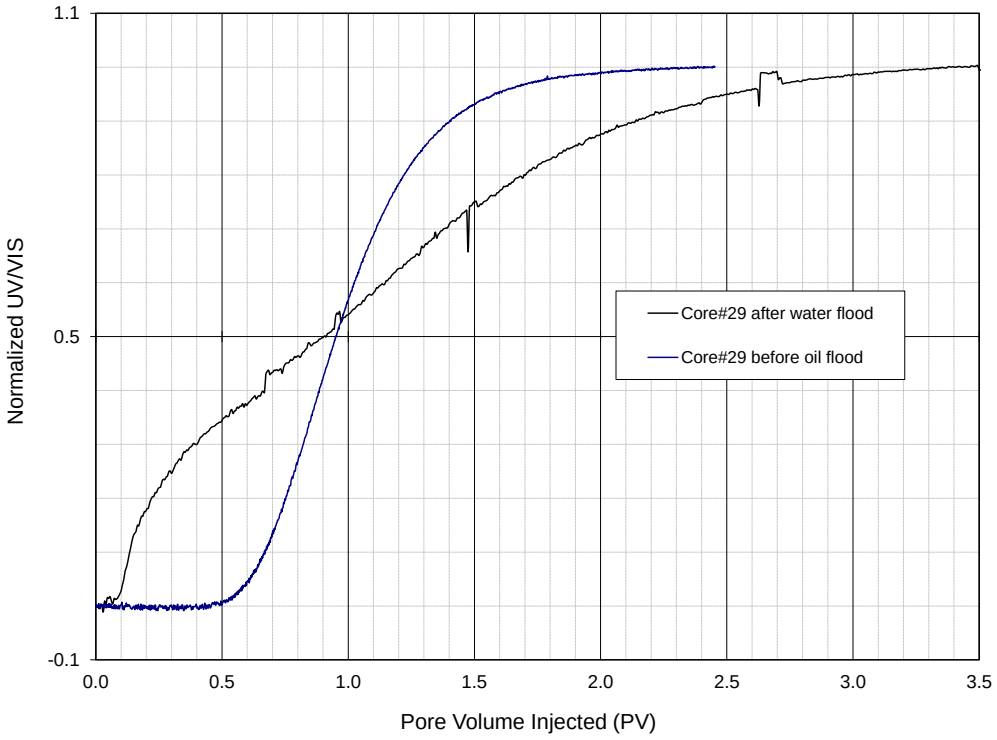

Figure 5.114 CFW#8(Core#29) tracer tests comparison before oil flood and after water flood

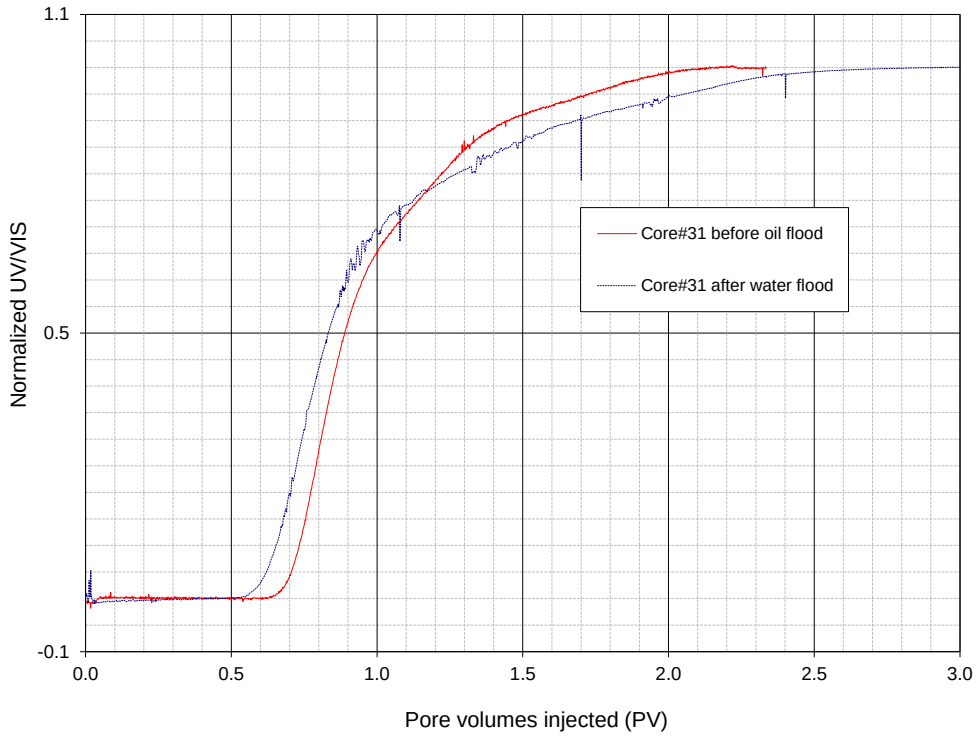

Figure 5.115 Berea sandstone Core#31 tracer tests comparison before oil flood and after water flood

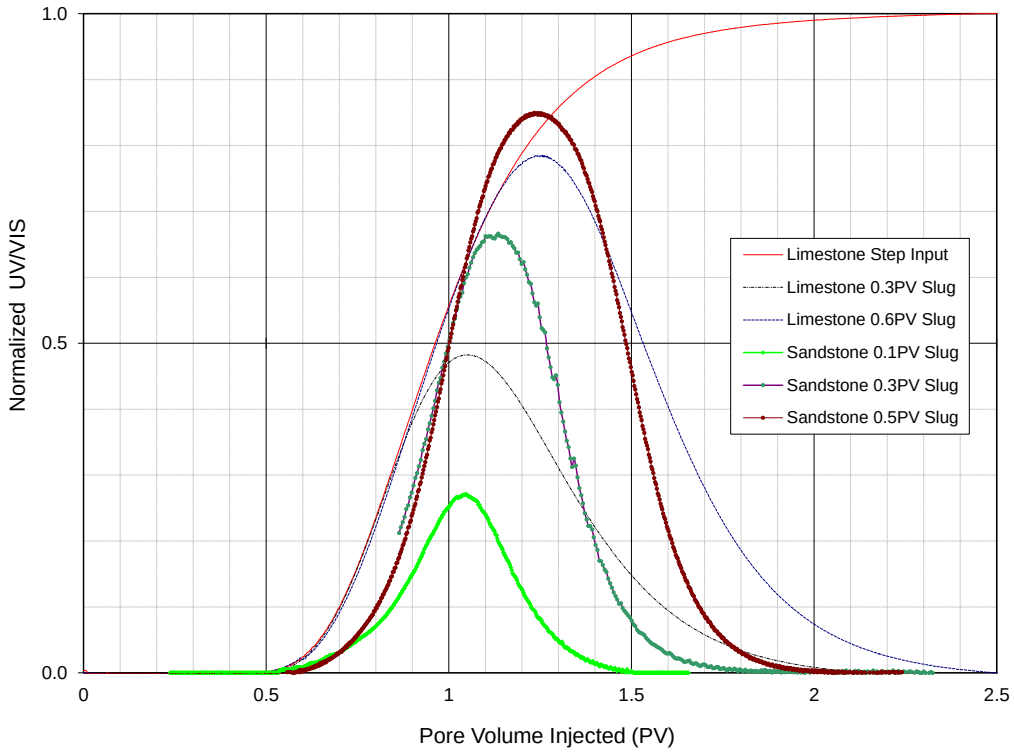

Figure 5.116 Comparison of tracer tests between limestone and sandstone with different tracer slug sizes.

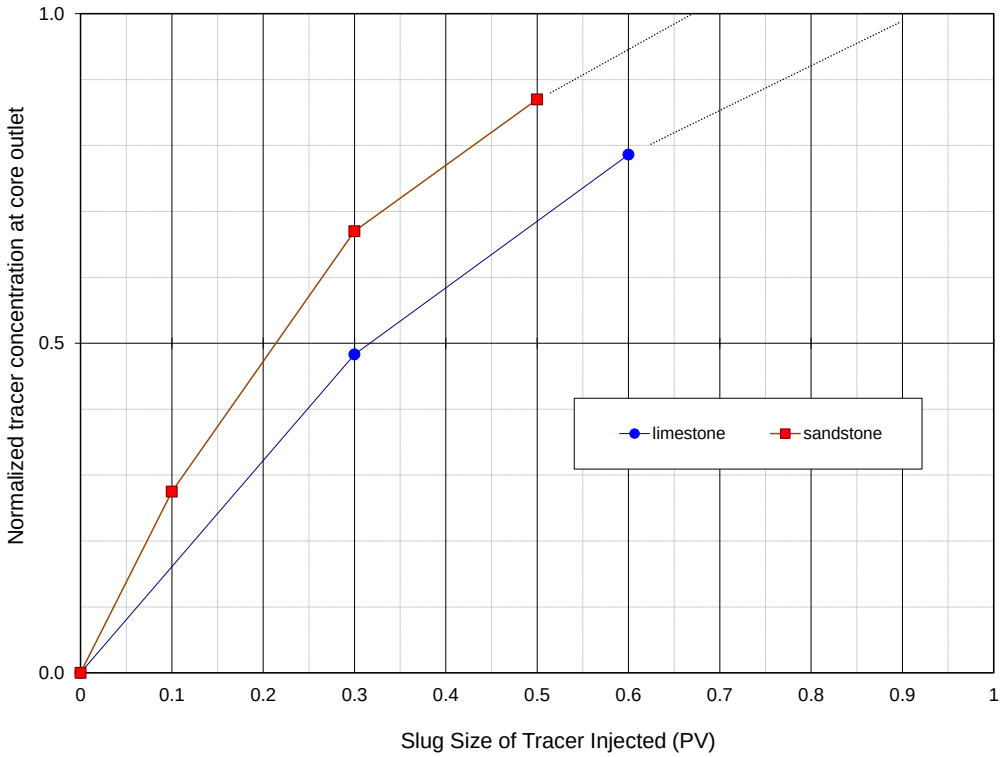

Figure 5.117 Comparison of normalized tracer concentrations at core outlet between limestone and sandstone with different tracer slug size.

Table 5.1 Wahrman Crude Oil Chemical Flood Results Summary

Flood#	W-1	W-2	W-3	W-4	W-5	W-6	W-7	W-8
Core #	5	8	12	14	17	22	28	29
Rock Type	Sandstone						Limestone	
PV(mL)	99	100.2	98	96.4	98.4	105.1	107.1	104.7
Porosity(Φ)	0.175	0.175	0.166	0.163	0.167	0.178	0.173	0.171
k_{br} (md)	223	131	190	178	186	190	374	163
k_{ro}^{o}	0.969	1.00	1.00	0.99	1	0.956	1	0.95
k_{rw}^{o}	0.093	0.053	0.032	0.035	0.036	0.033	0.062	0.063
S_{oi}	0.686	0.66	0.663	0.582	0.664	0.651	0.526	0.533
S_{or}	0.302	0.395	0.414	0.418	0.423	0.44	0.336	0.276
Saturation Brine	5.65%NaCl, 1%Na2CO3	6.55%NaCl	6.55% NaCl	6.55%NaCl	6.55%NaCl	SFB	SFB	6.55%NaCl
Surfactant Slug								
C_{surf} (wt%)	0.36% $C_{16\text{-}17}$-7PO-SO_4^- , 0.14% $C_{15\text{-}18}$ IOS							
$C_{Co\text{-}Solvent}$(wt%)	1.75% DGBE							
$C_{polymer}$ (ppm)	2300 FP3530S	3000 FP3530S	3000 FP3530S	1800 FP3530S	1800 FP3530S	1800 FP3530S	1800 FP3530S	1800 FP3530S
Salinity(ppm)	55500 NaCl	56500 NaCl	56500 NaCl	56500 NaCl	56500 NaCl	56500 NaCl	56500 NaCl	56500 NaCl
	10000 Na_2CO_3							
PV Injected	0.3	0.6	0.3	0.6	0.6	0.6	0.6	0.6
μ_{slug} (cp)	11.3 @ 37.5 s^{-1}	28 @37.5 s^{-1}	29.7 @30 s^{-1}	19.3 @ 1 s^{-1}	17.3 @ 1 s^{-1}	19.7 @ 1 s^{-1}	19.7 @ 1 s^{-1}	23.8 @ 1 s^{-1}
Polymer Drive								
$C_{polymer}$ (ppm)	3000 FP3530S	3300 FP3530S	3300 FP3530S	2100 FP3530S	2100 FP3530S	2100 FP3530S	2100 FP3530S	2100 FP3530S
Salinity (ppm)	39000 NaCl	46000 NaCl	46000 NaCl	46000 NaCl	46000 NaCl	46000 NaCl	46000 NaCl	46000 NaCl
μ_{drive}(cp)	17.6 @ 37.5 s^{-1}	25 @37.5 s^{-1}	30 @ 1 s^{-1}	27 @ 1 s^{-1}	23.2 @ 1 s^{-1}	26.9 @ 1 s^{-1}	26.2 @ 1 s^{-1}	35.2 @ 1 s^{-1}
Oil Recovery Results								
S_{orc}	0.090	0.012	0.060	0.002	0.020	0.007	0.202	0.201
% Recovery	70.2	97.0	87.3	99.6	95.3	98.4	40.7	27.6
Oil BT (PV)	0.41	0.21	0.16	0.2	0.18	0.13	0.08	0.3
Surf. BT (PV)	1.05	0.71	0.8	0.77	0.74	0.83	0.3	0.5
Flood Date	6/15/2010	10/1/2010	10/29/2010	11/18/2010	1/23/2011	2/18/2011	3/21/2011	4/14/2011

Table 5.2 Phase behavior results summary for formulations that passed all the criteria for lab screening and were used for chemical flooding, oil conc.=33%.

	Formulation	Solubilization ratio (mL/mL)	Time to equilibrate (days)	Optimal salinity (wt% NaCl)	APSL* (wt% NaCl) @ 43°C
F-4A	0.36% Petrostep® S1 0.14% Petrostep® S2 1.75% DGBE 1% Na_2CO_3 2300ppm FP3530S	11	6	5.5	5.85
F-4B	0.36% Petrostep® S1 0.14% Petrostep® S2 1.75% DGBE 1% Na_2CO_3 3000ppm FP3530S	11	6	5.5	5.75
F-4C	0.36% Petrostep® S1 0.14% Petrostep® S2 1.75% DGBE 1% Na_2CO_3 1800ppm FP3530S	12	<7	5.55	>6.0

Table 5.3 CFW#1(Core#5) Oil/Surfactant/Polymer bank mobility during chemical flood

	Oil Bank			Surfactant Slug			Polymer Slug		
	PV	λ_t (mD/cP)	u_{app} (cP)	PV	λ_t (mD/cP)	u_{app} (cP)	PV	λ_t (mD/cP)	u_{app} (cP)
Section 1	0.052	N/A	N/A	0.075	13.3	18	1.600	8.6	28
Section 2	0.121	13.7	23	0.175	10.5	30	1.600	8.1	39
Section 3	0.190	14.9	20	0.275	8.7	35	1.600	8.4	36
Section 4	0.259	16.2	17	0.375	8.2	33	1.600	8.1	34
Section 5	0.328	12.7	20	0.475	7.7	33	1.600	7.1	35
Section 6	0.380	14.5	16	0.550	10.1	23	1.600	8.5	27
Average		14.4	19		9.7	31		8.1	34

Table 5.4 CFW#2(Core#8) Oil/Surfactant/Polymer bank mobility during chemical flood

	Oil Bank			Surfactant Slug			Polymer Slug		
	PV	λ_t (mD/cP)	u_{app} (cP)	PV	λ_t (mD/cP)	u_{app} (cP)	PV	λ_t (mD/cP)	u_{app} (cP)
Section 1	0.035	N/A	N/A	0.117	3.97	30	1.600	3.35	35
Section 2	0.070	7.17	20	0.236	5.49	27	1.600	5.33	27
Section 3	0.105	5.22	28	0.355	3.84	38	1.600	3.95	36
Section 4	0.140	8.25	20	0.474	4.62	35	1.600	4.60	35
Section 5	0.175	8.25	21	0.593	4.69	37	1.600	5.09	34
Section 6	0.210	6.99	13	0.710	3.27	28	1.600	4.21	22
Average		7.18	20		4.31	32		4.4	32

Table 5.5 CFW#3(Core#12) Oil/Surfactant/Polymer bank mobility during chemical flood

	Oil Bank			Surfactant Bank			Polymer Bank		
	PV	λ_t (mD/cP)	u_{app} (cP)	PV	λ_t (mD/cP)	u_{app} (cP)	PV	λ_t (mD/cP)	u_{app} (cP)
Section 1	0.026	N/A	N/A	0.132	3.070	50	1.600	2.456	63
Section 2	0.053	8.33	24	0.266	2.99	67	1.600	2.98	67
Section 3	0.080	7.98	24	0.400	2.76	68	1.600	2.87	66
Section 4	0.107	7.80	28	0.534	2.56	87	1.600	3.01	74
Section 5	0.134	6.42	35	0.668	1.50	151	1.600	2.65	85
Section 6	0.160	7.35	26	0.800	0.81	234	1.600	1.37	138
Average		7.58	27		2.12	121		2.58	86

Figure 5.6 CFW#4(Core#14) oil/surfactant/polymer bank mobility during chemical flood

	Oil Bank			Surfactant Slug			Polymer Slug		
	PV	λ_t (mD/cP)	u_{app} (cP)	PV	λ_t (mD/cP)	u_{app} (cP)	PV	λ_t (mD/cP)	u_{app} (cP)
Section 1	0.050	N/A	N/A	0.130	7.9	22	1.60	5.7	30
Section 2	0.090	8.7	22	0.263	8.1	24	1.60	6.5	30
Section 3	0.120	6.5	28	0.395	5.6	32	1.60	5.1	35
Section 4	0.140	14.9	13	0.527	9.4	20	1.60	8.9	22
Section 5	0.167	11.4	16	0.660	6.4	29	1.60	7.0	26
Section 6	0.190	5.9	28	0.790	5.0	33	1.60	6.4	26
Average		9.5	21	0.5	7.1	27	1.6	6.6	28

Table 5.7 Properties (Permeability, length) of overall and each section of cores used for chemical flood.

Core #	Properties	Units	Overall	Section 1	Section 2	Section 3	Section 4	Section 5	Section 6
5	Length	(cm)	27.9	3.8	5.1	5.1	5.1	5.1	3.8
	Permeability	(mD)	223	211	281	267	230	202	168
8	Length	(cm)	30.3	5.0	5.1	5.1	5.1	5.1	5.0
	Permeability	(mD)	131	118	146	144	161	171	92
12	Length	(cm)	30.3	5.0	5.1	5.1	5.1	5.1	5.0
	Permeability	(mD)	190	154	199	189	222	226	189
14	Length	(cm)	30.3	5.0	5.1	5.1	5.1	5.1	5.0
	Permeability	(mD)	178	173	193	178	191	183	166
17	Length	(cm)	30.3	5.0	5.1	5.1	5.1	5.1	5.0
	Permeability	(mD)	186	127	249	215	213	193	174
22	Length	(cm)	30.3	5.0	5.1	5.1	5.1	5.1	5.0
	Permeability	(mD)	190	202	216	200	187	183	189
28	Length	(cm)	30.3	5.0	5.1	5.1	5.1	5.1	5.0
	Permeability	(mD)	374	266	575	518	460	365	524
29	Length	(cm)	30.3	5.0	5.1	5.1	5.1	5.1	5.0
	Permeability	(mD)	163	117	197	162	163	177	193

Table 5.8 Synthetic Wahrman oil formation brine composition.

Mineral			**Ions**		
	Meq/L	ppm		Meq/L	ppm
Sodium Chloride(NaCl)	1884.11	110220	Chloride(Cl-)	2166.3	71894
Magnesium Chloride($MgCl_2$)	42.12	2001	Sulfate(SO_4^{2-})	55.7	2674
Calcium Chloride($CaCl_2$)	98.95	5492	Sodium(Na^+)	1995.5	44616
Sodium Sulfate(Na_2SO_4)	55.71	3955	Magnesium(Mg^{2+})	42.1	505
			Calcium(Ca^{2+})	99.0	1979
Total	*6439.45*	*121668*		*4358.6*	121668

Table 5.9 Core#28 effluent ion analysis

Test ID	Solution	Divalent Ions			Source
		Mg(mg/L)	Ca(mg/L)	S (mg/L)	
A	SFB	480	2000	1160	injected solution
	SFB	460	2000	1180	effluent solution
B	4.6%NaCl	0.12	0.44	3.4	injected solution
	4.6%NaCl	5.8	13.8	9.6	Effluent solution

Chapter 6 Conclusions

1. A surfactant formulation based on phase behavior studies containing 0.36% C_{16-17}-7PO-SO_4^-, 0.14% C_{15-18} IOS, 1.75% DGBE, and 1% Na_2CO_3 was developed for the Wahrman crude oil that satisfied the following criteria :
    a. The formulation was single phase at reservoir temperature and a salinity of 6.1%;
    b. Solubilization ratio was 11;
    c. Equilibration time was less than 7 days at reservoir temperature;
    d. No viscous phases were observed in phase behavior experiments;
2. Berea sandstone cores containing waterflood residual oil saturations were flooded at reservoir temperature with 0.6PV surfactant slugs containing 1800ppm and 3000 ppm FP3530S, recovering more than 95-97% of the residual oil.
3. A Berea sandstone core containing waterflood residual oil saturation was flooded at reservoir temperature with 0.3 PV surfactant slug containing 3000ppm FP3530S, recovering 87% of the residual oil.
4. Therefore surfactant slug size between 0.3-0.6 PV was recommended for high oil recovery on sandstone cores.
5. The residual brine before chemical flood was soft brine with equivalent salinity to surfactant slug in all previous sandstone core floods. A Berea sandstone core with synthetic formation brine as residual brine before chemical flood was flooded with 0.6 PV surfactant slug containing 1800ppm FP3539S, recovering 98% of the residual oil. The

synthetic formation brine, which has high salinity and moderate hardness, did not comprise high oil recovery on sandstone core. This proved the robustness of the surfactant formulation.

6. Two core floods were conducted in Indiana limestone cores using the formulation developed and tested in Berea sandstone cores. Results of these floods were not satisfactory, possibly due to excessive heterogeneity in the cores which caused extensive mixing between the surfactant slug and residual brine.

Chapter 7 References

Abrams, A. (1975). "The Influence of Fluid Viscosity, Interfacial Tension, and Flow Velocity on Residual Oil Saturation Left by Waterflood." SPE Journal **15**(5): 437-447.

Adkins, S., P. J. Liyanage, et al. (2010). A New Process for Manufacturing and Stabilizing High-Performance EOR Surfactants at Low Cost for High-Temperature, High-Salinity Oil Reservoirs. SPE Improved Oil Recovery Symposium. Tulsa, OK.

Bourrel, M. and R. S. Schechter (1988). Microemulsions and Related Systems. New York, Marcel Dekker.

Castor, T. P., W. H. Somerton, et al. (1981). Recovery Mechanism of Alkaline Flooding. Surface Phenomena in Enhanced Oil Recovery. D. O. Shah. New York Plenum Press.

Churcher, P. L., P. R. French, et al. (1991). Rock Properties of Berea Sandstone, Baker Dolomite, and Indiana Limestone. SPE International Symposium on Oilfield Chemistry. Anaheim, CA.

Delshad, M., D. DBhuyan, et al. (1986). Effect of Cappillary Number on the Residual Saturation of a Three-Phase Micellar Solution. SPE Enhanced Oil Recovery Symposium. Tulsa, OK.

Dwarakanath, V., T. Chaturvedi, et al. (2008). Using Co-Solvents to Provide Gradients and Improve Oil Recovery During Chemical Flooding in a Light Oil Reservoir. SPE/DOE Symposium on Improved Oil Recovery. Tulsa, OK.

Flaaten, A. K. (2007). Experimental Study of Microemulsion Characterization and Optimization in Enhanced Oil Recovery: A Design Approach for Reservoir with High Salinity and Hardness, The University of Texas at Austin.

Gogarty, W. B. and W. C. Tosch (1968). "Miscible-Type Waterflooding: Oil Recovery with Micellar Solutions." Journal of Petroleum Technology **20**(12): 1407-1414.

Green, D. W. and G. P. Willhite (1998). Enhanced Oil Recovery. Richardson Texas, Henry L. Doherty Memorial Fund of AIME, Society of Petroleum Engineers.

Healy, R. N. and R. L. Reed (1974). "Physicochemical Aspects of Microemulsion Flooding." SPE Journal **14**(5): 491-501.

Hirasaki, G. and D. L. Zhang (2004). "Surface Chemistry of Oil Recovery From Fractured, Oil-Wet, Carbonate Formations." SPE Journal **9**(2): 151-162.

Hsieh, W. C. and D. O. Shah (1977). The Effect of Chain Length of Oil and Alcohol As Well as Surfactant to Alcohol Ratio on the Solubilization, Phase Behavior and Interfacial Tension of

Oil/Brine/Surfactant/Alcohol Systems. SPE International Oilfield and Geothermal Chemistry Symposium. San Diego, CA.

Huh, C. (1979). "Interfacial Tensions and Solubilizing Ability of a Microemulsion Phase that Coexists with Oil and Brine." Journal of Colloid and Interface Science **71**(2): 408-426.

Jackson, A. C. (2006). Experimental Study of the Benefits of Sodium Carbonate on Surfactants for Enhanced Oil Recovery, The University of Texas at Austin. **M.S. Thesis**.

Kamath, J. and R. F. Meyer (2001). Understanding Waterflood Residual Oil Saturation of Four Carbonate Rock Types. SPE Annual Technical Conference and Exhibition. New Orleans, Louisiana.

Levitt, D. B. (2006). Experimental Evaluation of High Performance EOR Surfactants for a Dolomite Oil Reservoir, University of Texas at Austin. **M.S. Thesis**.

Liu, Q., M. Dong, et al. (2007). "Surfactant Enhanced Alkaline Flooding for Western Canadian Heavy Oil Recovery." Colloids and Surfaces A: Physicochemical and Engineering Aspects **293**(1-3): 63-71.

Milton, J. R. (2004). Surfactants and Interfacial Phenomena. New Jersey, Wiley-Interscience.

Moradi-Araghi and Peter H. Doe (1987). "Hydrolysis and Precipitation of Polyacrylamides in Hard Brines at Elevated Temperatures." SPE Reservoir Engineering **2**(2): 189-198.

Nelson, R. C., J. B. Lawson, et al. (1984). Cosurfactant-Enhanced Alkaline Flooding. SPE Enhanced Oil Recovery Symposium. Tulsa, OK.

Nelson, R. C. and G. A. Pope (1978). "Phase Relationships in Chemical Flooding." SPE Journal **18**(5): 325-338.

Pope, G. A., K. Tsaur, et al. (1982). "The Effect of Several Polymers on the Phase Behavior of Micellar Fluids." SPE Journal **22**(6): 816-830.

Pope, G. A., B. Wang, et al. (1979). "A Sensitivity Study of Micellar/Polymer Flooding." SPE Journal **19**(6): 357-368.

Pope, G. A., W. Wu, et al. (2000). "Modeling Relative Permeability Effects in Gas-Condensate Reservoirs with a New Trapping Model." SPE Reservoir Evaluation and Engineering **3**(2): 171-178.

Sahni, V., R. M. Dean, et al. (2010). The Role of Co-Solvents and Co-Surfactants in Making Chemical Floods Robust. SPE Improved Oil Recovery Symposium. Tulsa, OK.

Salter, S. J. (1977). The Influence of Type and Amount of Alcohol on Surfactant-Oil-Brine Phase Behavior and Porperties. SPE Annual Fall Technical Conference and Exhibition. Denver, CO.

Sanz, C. A. and G. A. Pope (1995). Alcohol-Free Chemical Flooding: From Surfactant Screening to Coreflood Design. SPE Symposium on Oilfield Chemistry. San Antonio, TX.

Shupe, R. D. (1981). "Chemical Stability of Polyacrylamide Polymers." Journal of Petroleum Technology **33**(8): 1513-1529.

Sorbie, K. (1991). Polymer Improved Oil Recovery. Glasgow, Blackie and Son Ltd.

W., S. L. and E. A. R. (1997). "Low Surfactant Concentration Enhanced Waterflooding." SPE Journal **2**(4): 389-405.

Wessen, L. L. and J. H. Harwell (2000). Dilute Surfactant Adsorption in Porous Media. Surfactants: Fundamentals And Applications In The Petroleum Industry. Cambridge, UK, Cambridge University Press.

Winsor, P. A. (1954). Solvent Properties of Amphiphilic Compounds. London, Butterworths

Yang, H., C. Britton, et al. (2010). Low-Cost, High-Performance Chemicals for Enhanced Oil Recovery. SPE Improved Oil Recovery Symposium. Tulsa, OK.

Zhang, R. and P. Somasundaran (2006). "Advances in Adsorption of Surfactants and Their Mixtures at Solid/Solution Interfaces." Advances in Colloid and Interface Science **123-126**: 213-229.